Mineral Processing and Coal Preparation
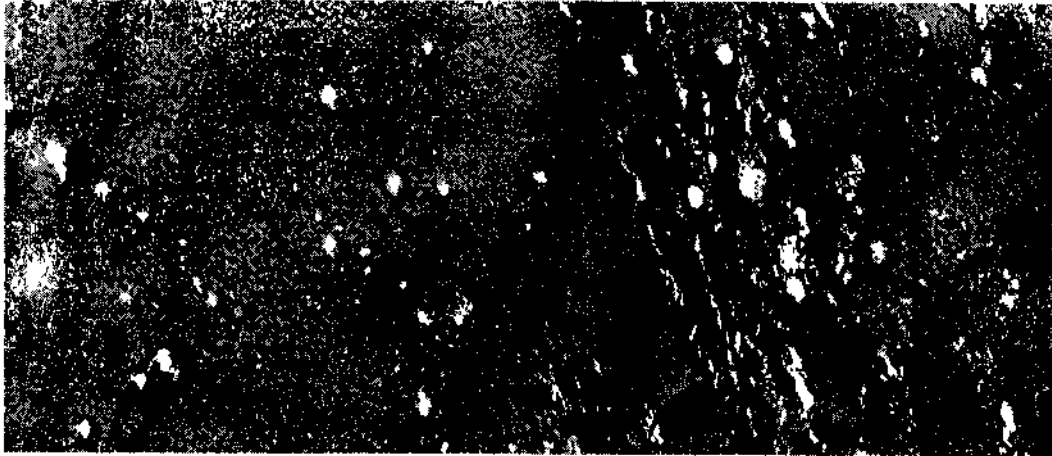
Figure 3 Syngenetic occurrence of pyrite in coal

On the upper photo a typical example of microcrystalhne (syngenetic) occurrence of pyrite ıs shown. This is washed clean coal of a density of 1,3 - 1,4 g/cm³. The pyrite particles (white spots on dark background) are very finely distributed and embedded in the coal. On the lower photo a coal grain of a density of 1,4 -1,5 g/cm³ is shown. Here pyrite particles are finely distributed as well, but they are also a bit more concentrated than in the photo above. It is obvious that pyrite particles settlement is concentrated near small fractures in the coal grain. If the size of the coal grain is reduced, i.e. using mechanical crushing, the gram would break at the various tractures and so pyrite particles

would also be liberated, which cannot be expected in the case of the photo above.

Figure 4 shows macrocrystalline (epıgenetıc) occurrence ot pyrite in coal grains. The photo above shows a coal particle, i.e. middlings of a density of 1,6 - 1,7 g/cm³. The concentration of pyrite particles at the fractures of the coals grain is obvious. A defined impact crushing would liberate the pyrite particles. The lower photo shows a middlings grain with a density of 1,7 - 1,8 g/cm³ with gross pyrite particles which are surrounded by natural fractures. These pyrite particles could easily be liberated by crushing.
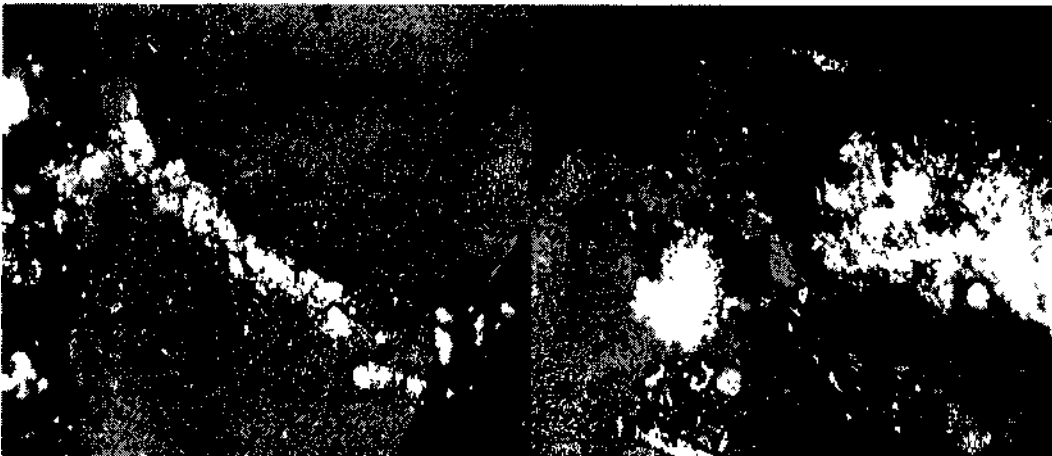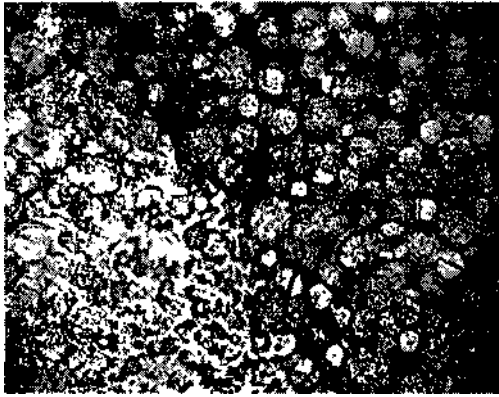

Figure 4 Epigenelic occurence of pyrite in coa

Figure 5. Pyrite in rejects

Figure 5 shows the formation of gross pynle particles in rejects of a density of more than 1,8 g/cm^3. These panicles can usually be separated already in a standard processing route.
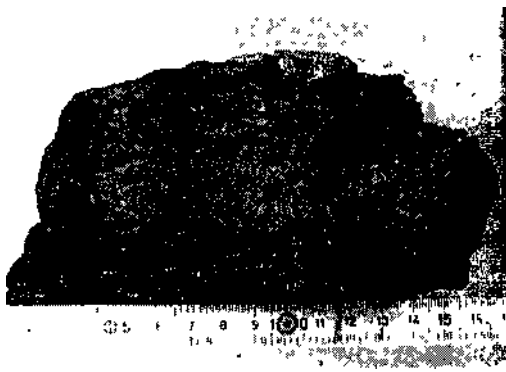

Figure 6 Largei particle of pyrite in coal

Figure 6 shows a piece of coal from Shanxi province in China. The pyrite occurs in a separate layer embedded in the coal structure.

In any case, it a reduction of the sulfur content of raw coals is targeted at, first of all the pyrite particles will

3 MECHANICAL PROCESSING METHODS OF SULFUROUS RAW COALS

It is been common practice in the most industrialised countries to operate flue gas desulfunsation plants in coal-fired power stations in order to avoid high sulfur dioxide emissions. But these measures require high capital and operating expenditures.

There is another method to reduce the sulfur content which can be applied even before coal firing in the power stations: the mechanical liberation and subsequent separation of sulfur components by using specialised processing methods. The success of this way of sulfur reduction depends above all on the sulfur distribution in raw coals.

There is a large number of different coal processing methods at the current state of technological development, depending on the particle size distribution, distribution of density and particle form. It depends on the individual raw coal properties which of these methods or which combinations can be chosen for classification, size reduction, separation and dewatering.

In order to develop a adequate flow sheet for sulfur reduction which is favourable under technical as well as under economical aspects, before planning a processing plant one should carry out laboratory tests particularly tailored to the possible processing combinations.

In the last decades RAG and DMT carried out extensive tests in laboratories and technical schools with a large number of different raw coal qualities. A pilot plant with a feeding capacity of 70 t/h was built.
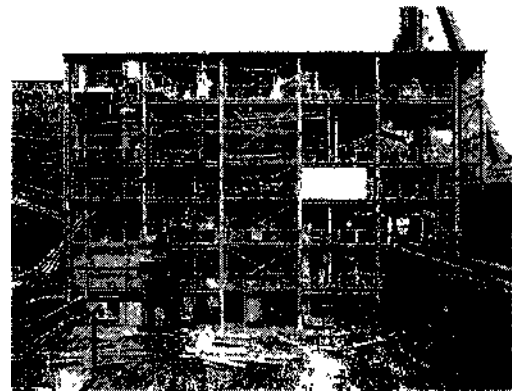

Figure 7. Pilot plant for the desulfurisation ot coal

Figure 7 shows this pilot plant shortly before the end of the installation works. It comprises of all relevant processing installations and allows operation of many different processing combinations.

Under the assistance of DMT another pilot plant for the desulfurisation of high-sulfur containing

356

Figure 9 shows the solid pyrite inclusion of washed clean coal of the density range 1,3 - 1,5 g/cm^3 in the particle size traction 10-3 mm before size reduction

Figure 10 Pyrite inclusion of washed pure coal after size reduction

	pure coal size 10 3mm before size reduction				pure coal ize < 3mm after size reduction				pure coal after desulphunsation by cutting of density traction +1 8g/cm^3		
	mass content		sulphur content		mass content		sulphur content				
$\hat{\underline{}}$.	fraction %	cum %	fraction %	cum %	fraction %	cum %	fraction %	cum %			
1 3	81	81	1 14	1 14	75	75	1 10	1 10	Masse	sulphur	
13 15	15	96	2 14	1 30	19	94	1 26	1 13	%	cum %	
15 16	2	98	3 18	1 33	2	96	2 42	1 16			
16 18	1	99	3 43	1 35	1	97	2 48	1 17	97	1 17	
+ 18	1	100	2 70	1 37	3	100	7~5 "	1 37			X
	100		1 37		100		1 37				

Washed pure coal of particle size 10-3mm contains a total sulphur content of 1,37% where 1,0% is organic sulphur and 0,37% is pyritic sulphur After size reduction < 3mm and cutting of density fraction +1,8g/cm^3 the total sulphur is 1,17%.

Figure 11 Density structure of washed puie coal before and after size reduction

Figure 10 shows the same coal of figure 9 but alter size leduction to less than 3 mm It is quite obvious heie that there aie pyrite particles which have been liberated from the coal grain

Figure 11 shows the density distribution of the washed clean coal shown in figure 10, particle size i ange of 10-3 mm (the pait on the left of the table) There are details on quantities and sulfur contents of the respective density ranges and of the combined density ranges As you can see here, the total sultur content of all density tractions is I 37 "A It the size of the coal grain is reduced to below 3 mm the sulfur content in the different density langes changes compaied to the sultui content in uncrushed malenal Attei the size reduction the sulfui content was reduced in all density ranges, up to the density range < 1,8 g/cm^3 The density range > 1,8 g/cm^3 now shows a sultur content of 7,75 % after size reduction whereas before it was 2,7 % It the density lange > 1,8 g/cm^3 is sepaiated from the range below 1,8 g/cm^3 with the adequate equipment, a clean coal pioduct with a sulfui content of 1,17 % will be received In this case the yield is 97 %, i e the losses aie about 3 % But these losses are tailings with a high sultur content In this connection it has to be mentioned that the organic sulfur in this coal product is about 1 1 % so that the clean coal product only contains a propoition ol pyrite which could not be separated of about 0 07 %

No.	Country	Colliery	Raw coal feed	Total sulphur content		Yield ' pure coal	Reduction in t/a	
				raw coal	pure coal,		Sulphur	SO$_2$
1	Polen	Janina	4 250 000	' 1,78*	<1,0*	ca. 70	46 500	93 000
2	Polen	Jaworzno	3 250 000	2,39*	<1,0*	ca. 70	55 400	110 800
3	Polen	Jan Kanty	1 900 000*	1,91*	<1,0*	ca. 70	I 23 300	46 600
4	Deutschland	Monopol	3 250 000	1,37'*	1,1"	ca. 50	26 700	53 400

Remark: Organic sulphur in total *0,9%
                                                   *" 1,0%

Efficiency of pyrite reduction   No.   7

                                                   1   92%
                                                   2   95%
                                                   3   93%
                                                   4   86%

Figure 12. Examples for the operating results of mechanical desulfurisation of raw coals in preparation plants

Figure 12 shows examples for the operating results of mechanical desulfurisation of raw coals in different European preparation plants. The design concept of this desulfurisation method has been developed by DMT-Montan Consulting engineers. The plants 1, 2 and 3 are in operation in Poland since several years. Annual capacities are 1.9 million tonnes, 3.25 and 4.25 million tonnes. The sulfur contents of the ROM of 1.78 %, 2.39 % and 1.91 % can be regarded as high. The content of organic-sulfur which cannot be separated from the coal is in average of about 0.9 %. As a result of the preparation a clean coal product with a total sulfur content of 1 % and clean coal yield was about 70 % is produced. In the past, coal quantities which where as high as the annual capacities of the three plants, were burnt in power stations without being washed. After the preparation plants had started operation, sulfur dioxide emissions of the power plants were considerably reduced, as can be seen in the very right column. In the 3 Polish plants, sulfur reduction was relatively easy because of the properties of the raw material.

Plant No. 4 was a preparation plant in Germany with an annual capacity is 3.25 million tonnes. The total sulfur content was 1.37 %, of which approximately I % used to be organic sulfur. Pyrite here was more finely intergrown and its dissociation was more difficult, therefore the total pyrite content in the washed coal product was 1.1 %.

Its remarkable to mention that in case of the Polish coals, more than 90 % of the pyrite was removed (92 %, 95 % and 93 %). In case of the German coals, the efficiency of the separation was 86 %, which resulted a reduction of sulfur dioxide emissions by 53,400 tonnes per year.

The figures demonstate that mechanical separation of pyrite from raw coals by means of mechanical processing, can give a significant contribution to the reduction of sulfur dioxide emissions into the atmosphere.

5 PROCESS TECHNOLOGIES FOR MECHANICAL REDUCTION OF SULFUR IN RAW COALS

In the following, two examples of many possibilities for mechanical desulfurisation will be described.

Example 1 shows the float &sink analysis of a raw coal, particle size range 100 - 0.1 mm, which represents inclusions of high sulfur contents within the middlings range of 1.45 to 2.20 g/cm^3. The organic sulfur content in this materials is more or less 0.7 %. The sulfur contents of more than 0.7 7< are epigenetic pyrite inclusions. The rejects of > 2.20 g/cm^3 contains already liberatet pyrite.

To fulfill the required quality of a maximum of 0.8 % sulfur in the saleable product with the highest economical yield, the middlings part of the density range between 1.45 and 2.00 g/cm^3 has to be desulfurised by mechanical processing. The next figure shows a simplified flowsheet as an example for the liberation and separation of pyrite through middlings treatment.

358

The selected process comprises of different separation steps for three particle .size ranges. Due to the fact, that the amount of in the area of near-gravity material is relatively low, the jigging processes for cleaning of the fractions 100-20 mm and 2 0 - 2 mm has been chosen. The size 2 - 0.1 mm will be cleaned on spiral concentrators. The particle size fraction below 0.1 mm is high in ash content and will be rejected after thickening and press-filtration.

Table I. Gravity distribution

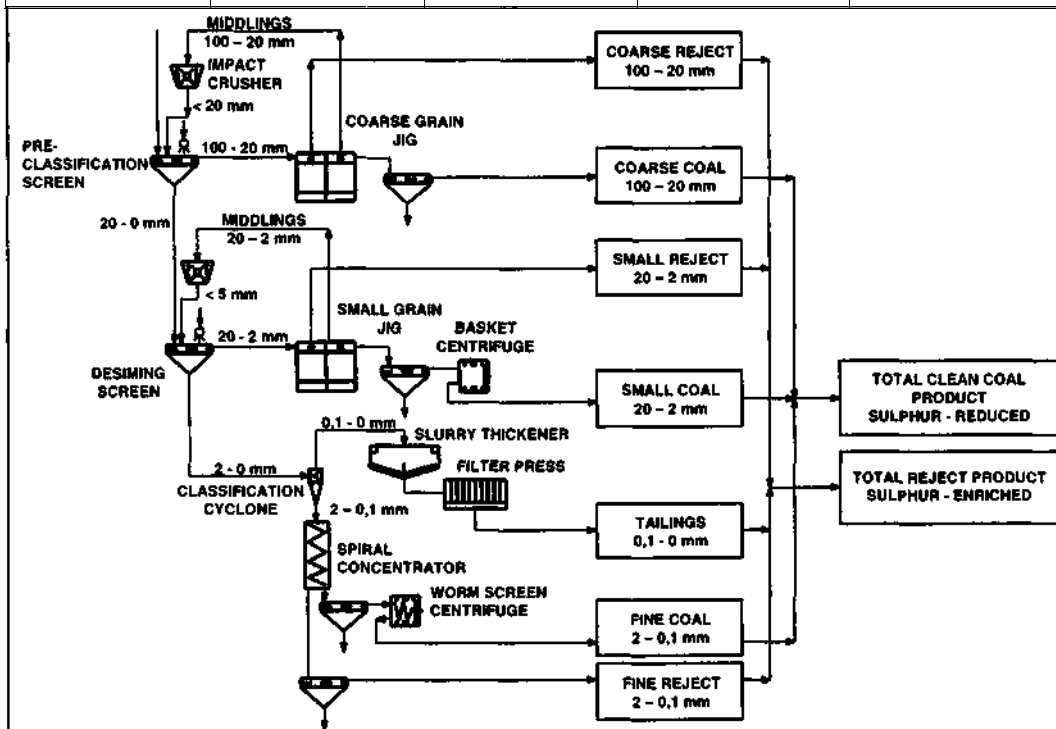| Specific Gravity g / cm³	Weight - %	Ash - %	Sulfur • %	Cum. Sulfur - %
-1.35	67.72	8.54	0.74	0.74
1.35-1.45	3.77	13.40	1.20	0.76
1.45- 160	5.15	26.83	1.82	0.84
1 60 - 1.80	3.48	40.76	3.26	0 94
1.80-2.00	3.22	53.98	4.19	1.07
2.00-2.20	0.87	55.99	5.47	1.11
+ 2.20	15.79	73.00	9.66	2.46
	100.00	22.84	2.46	

Figure 13. Example 1, Liberalisation & separation of pyrite through middlings treatment

After the jigging process of size 100 - 20 mm there are three products as follows:

Clean coal as part of the saleable product containing a sulfur content of around 0.76 - 0.7S g/cm³.

Reject containing some free pyrite, total sulfur content ol around 9.5 %.

Middlings containing inclusions of pyrite pieces, total sulfur content is around 3.5 %

There is normally no sales market for the middlings. Dumping of those material can create problems due to self-ignition. As a result the treatment of the middlings with the objective to liberate and separate the pyrite becomes necessary. For this purpose the middlings fraction 100 - 20 mm will be crushed to < 20 mm by impact crushing. The crushed material will be classified by wet sreening at 2 mm. The screen overflow, size 2 0 - 2 mm is processed together with the original ROM fraction 2 0 - 2 mm on the small grain jig.

By the latter jigging process three products are produced - clean coal, reject and middlings - in similar qualities as the above mentioned coarse products. Clean coal and rejects are final products. The middlings size 20 - 2 mm will be crushed again by impact crushing to < 5 mm. The crushed material will be classified by wet screening at 2 mm. The fraction 5 - 2 mm flows for rewashing back to the feed *jof* the small grain jig. All original raw coal and crushed middlings < 2 mm will be deslimed at 0.1 mm and than cleaned in spiral separators. Products of the spiral separators are desulfered clean coal and sulfur-enriched rejects.

At the end of (he process all the clean coal products together will be in a saleable quality of the required sulfur content of < 0.8 %.

Example 2 shows the float &sink analysis of a raw coal, particle size range 100 - 0.1 mm, which represents inclusions of high sulfur contents within the middlings range of 1.45 to 2.20 g/cm³ and in the clean coal range of 1.35 to 1.45 g/cm³. The organic-sulfur content in this materials is more or less 0.8 %. The sulfur contents of more than 0.8 % are epigenetic pyrite inclusions. The rejects of > 2.20 g/cm³ contain already liberated pyrite.

Table 2 Gravity distribution 2

Specific Gravity g/ cm³	Weight - %	Ash - %	Sulfur - %	Cum. Sulfur - %
- 1.35	35.88	7.29	0.88	0.88
1.35 - 1.45	33.69	9.06	1.01	0.95
1.45 - 1.60	3.77	29.37	3.20	1.06
1.60- 1.80	5.05	44.11	4.14	1.26
1.80-2.00	2.86	52.66	7.64	1.48
2.00 - 2.20	1.6l	53.03	6.83	1.59
+ 2.20	17.14	76.06	8.81	2.83
	100.00	**24.40**	**2.83**	

To lulfill the required quality of a maximum of 0.95 %c sulfur content in the saleable coal product with the highest economical yield, the middlings between 1.45 and 2.00 g/cm³ including the clean coal part of 1.35 to 1.45 g/cm³ has to be desult'urised by mechanical treatment. The next figure shows a simplified flowsheet as an example for the liberation and separation of pyrite through treatment of this material.

The selected process comprises again of different separation steps for three particle size ranges. The first step of the raw coal treatment of size 100 - 0 mm is the classification by screening at 40 mm. The coarse raw coal, size 100-40 mm contains the major part of the subsequently produced rejects. In a deshaling plant, consisting of a dense medium bath separator, rejects and coarse pyrite will be separated. The coal and middlings with pyrite inclusions will be cmshed to < 40 mm by impact crushing. These crushed material and the original raw coal size 40 - 0 mm runs to deshming screening for classification at 2 mm.
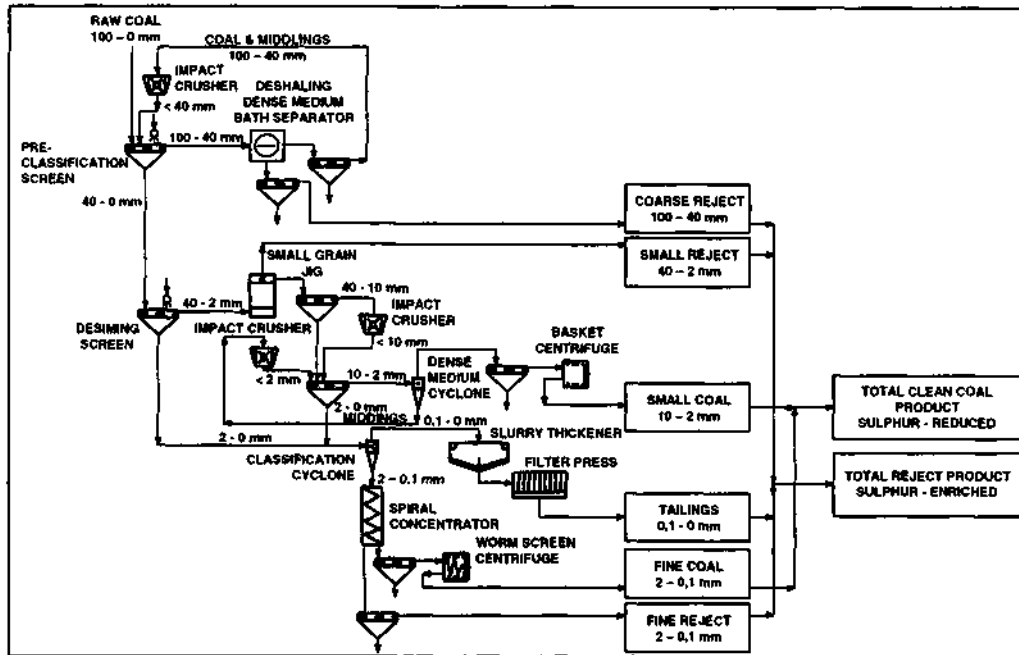
Figure 14. Example 2, Liberalisation & separation of pyrite through middlings & partly coal treatment

Size 40-2 mm will be washed in a two-product jig, tor separation of reject. The jig overflow, coal and middlings with pyrite inclusions will be sreen-dewatered and subsequently crushed to < 10 mm by impact crushing. These crushed material 10-0 mm runs to dcsliming screening for classification at 2 mm.

Due to the fact, that the coal contains a lot of near-gravity material the grain size range of 10-2 mm will be washed in two-product dense medium cyclones, for separation of low-sulfur clean coal with a density < 1.35 g/cm^3. This material is part of the saleable coal product. Cyclone underflows are middlings and clean coal with densities higher than 1.15 g/cm^3. containing inclusions of pyrite. The underflows will be crushed as well to < 2 imn by impact crushing. These crushed material and the original raw coal size 2-0 mm will be deslimed at the same time at 0.1 mm in classification cyclones. The garın size fraction 2-0.1 mm will be washed on spiral concentrators. Products of the spiral sepatators are desulphered clean coal and sulfur-enriched reject.

Size lower 0.1 mm is high in ash content and will be ıejected after thickening and press-filtration

At the end ot the process all the produced clean coal sizes together will be in a saleable quality of the required sulfur content of lower than 0.95 %.

Figure 15. Preparation plant for sulfur reduction

Figure 15 shows a preparation plant for sulfur reduction of Lignite in Spain. This plant was erected

361

lignite has been build and operated lor the Energy-Supphei ENDESA in Spain. The results of all the test and investigations have formed the basis for the design and construction of several industrial scale preparation plants for the mechanical desulfunsation

Figure 8. Pilot plant for the desulfurisation of lignite

On Figure 8 the pilot plant which was designed and operated solely for sulfur reduction *of* extremely high-sulfurous lignites in Spain is shown. The preparation plant is in the right part of the photo and in the background you see a coal-fired power station. This adjacency gave the opportunity to test the coal products of the pilot plant in the power plant and to test their impact on the combustion process.

Our engineers were not only involved and played a significant role in the design, development and construction of those plants, but also during the performance of the individual test series. The know-how and experience gained in these projects today contribute very much to construction planning and remodelling designs of preparation plants aimed at reducing sulfur contents.

4 RESULTS OF SULFUR REDUCTION IN COAL PREPARATION PLANTS

A few preliminary remarks:
The reduction of sulfur content by means of mechanical processing can only be realised by eliminating pyrite. The degree of pyrite separation which is possible depends on:
- the particle size and density distribution of the pyrite and the degree of intergrowth

of raw coal in Germany, Spain and Poland. Specially in the newer plants in Poland, more than 90 % of the pyrite contained in the raw material could have been removed.

- the occurrence of pyrite which is usually macrocrystalline (epigenetic) or microcrystalline (syngenetic)
- the crushing equipment applied
- the separation density and efficiency of the separating equipment.

The processing costs rise more than proportionally with decreasing particle size because of
- increasing financial costs
- increasing yield losses
- additional expenditure for dewatering and thermal drying, it necessary

Figure 9. Pyrite inclusion of washed pure coal before size reduction

What is important for the degree of liberation of pyrite is the sulfur distribution in the different density ranges before and after size reduction of the coal. Have a look at this example:

next to a power plant (capacity 3 x 350 MW), as the raw Lignite come from different mines with different production capacities.

Last but not least it should be mentioned that the separated pynte can be upgraded mechanically and seive as an important secondary raw material for the production of sulfuric acid. According to Chinese experts there is a need for this product in the Chinese industry.

Apart from the mechanical sulfur reduction, the processing in preparation plants lead to a reduction in ash content by separating the waste rock, which originally is the aim of such a plant. This results in a reduced energy consumption for the transport ol coals to the power station and in a higher combustion clficiency, which all in all reduces carbon dioxide emissions as well. Statements about the quantity cannot be made until we know something about the coal qualities used in the power stations and about the distances between preparation plant and power station.

Flotation of A Sulphide Ore Using High Velocity Water Jets

P. Carbini. R. Ciccu, M. Ghiani & C. Tilocca
DIGIT A. - Department of Geoengineering and Environmental Technologies University of Cagliari, Italy

F. Satta
IGAG - Institute of Environmental Geology and Geoengineering of the CNR Department of'Cagliari c/o University of Cagliari, Italy

ABSTRACT: A jet of water issued at high velocity from a calibrated nozzle can be used in a variety ot application owing to its unique capability of carrying a high power concentrated in a vary small space. Although this technology is still applied in many fields of rock and stone engineering (excavation, slotting, cutting, drilling, surface finishing) no commercial instances can be found in the area of mineral separation. The paper highlights a new approach followed in the design and the development of a flotation cell in which conventional impeller is replaced by high velocity water jets generated through a suitable nozzle configuration. The features of the prototype installed at the DIGITA Department of the University of Cagliari are illustrates and the results obtained in the flotation with such technology of a sulphide ore are reported. In particular the influence on metallurgical results of various operation variables like water pressure and flow rate, air flow rate, collector and frother dosage and residence time, is illustrated and discussed in comparison with a similar cell equipped with conventional impeller. Experimental results show that specific energy consumption of the waterjet cell is noticeably lower than that of the conventionally agitated cell.

1 INTRODUCTION

A jet of water issued at high velocity from a calibrated nozzle can be used in a variety of applications owing to its unique capability of carrying a high power concentrated in a very small space. Although this technology is still used in many fields of rock and stone engineering (excavation, slotting, cutting, drilling, surface finishing) no instances of commercial application can be found in the area of mineral separation.

However waterjet can offer new opportunities for designing new machines or improving the performance of conventional equipment (Chudachek et al. 1997).

For proving the concept a prototype of a waterjet-agitated cell (Hydrojet) has been designed and built at the DIGITA Laboratories of the University of Cagliari (Carbini el al. 1998).

2 FEATURES OF THE HYDROJET CONCEPT

2./ Apparatus

The prototype of the Hydrojet cell consists of a cylindrical vessel, 200 mm in diameter and 400 mm high (total free volume 10.2 litres), provided with a hemispherical bottom screen for the discharge of the reject through a central outlet. Froths are skimmed out through a chute in the upper section of the cylindrical body.

2.2 Plant

The laboratory plant is composed by an agitated conditioning tank, a feeding system via a peristaltic pump, the Hydrojet cell itself, a high pressure plunger pump connected to the waterjet lance for the generation of high velocity jets which produce the agitation and bubble dispersion into the vessel, two peristaltic pumps for collector and Irother addition, a pulp aeration system. The liquid level is controlled by acting on the tailings discharge pump speed.

A schematic view of the experimental setup is given in Figure I.

2.3 Past experience

In the past the Hydrojet cell has been tested successfully on coal and on a barite ore.

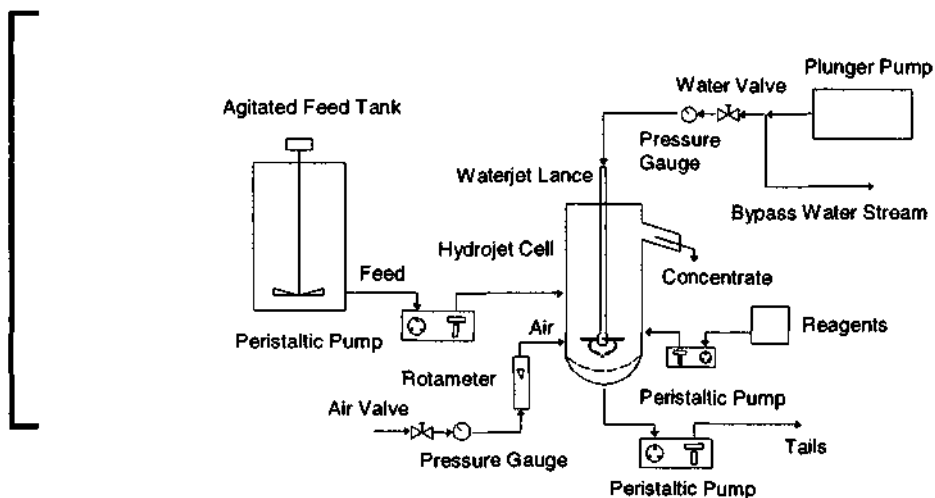Regarding coal, the following aspects are worth underlining (Agus et al. 1998):

Figure I - Laboratory plan! used in flotation tests it *ilh the Hydrojet cell.*

- In all experimental conditions fuel recovery increased gradually with residence time, accompanied by a parallel increase in ash content for both the product and the reject;
- recovery with waterjet was considerably higher than that achieved with mechanical agitation;
- results were better using only two jets since both recovery and ash in the reject were higher than with four jets, although the quality of the product was slightly worse;
- an increase in pressure from 9 to 15.5 MPa at equal hydraulic power using two 0.2 mm nozzles (resulting water tlowrate: 0.48 I/min) did not bring any improvement.

A further advantage offered by the waterjet cell was a considerable reduction in energy consumption. In fact, specific energy with two 0.3 mm jets was less than half compared with conventional cell of equal size and shape.

Concerning the barite ore, results were substantially similar (Carbini et al., 1998). In fact:
- BaSQj recovery with waterjet was somewhat higher than that achieved with mechanical agitation at any dosage of collector, although with lesser evidence than for coal (Carbini et al. 1998; Agus et al. 1998);
- BaSOj content in the concentrate was slightly higher with waterjet in spite of using half the power;
- again results did not improve by doubling the jet flow rate using four 0.3 mm nozzles instead of two at equal pressure.

The above findings are of great interest for the future development of the concept and the improvement in the design and operation of a waterjet cell.

3 FLOTATION TESTS

3.1 Characteristics of the ore sample

The zinc sulphide ore used for the new series of experiments originates from the Sos Enattos mine (Lula, Italy), and averages about 9.5 % Zn. The orebody consists of a number of veins with different economic interest but in recent times only the "Tupeddu" vein was kept in production. The valuable mineral is sphalerite with minor presence of galena and iron sulphides. The main gangue mineral is quartz and the embedding rocks are medium-grained shales.

A sample of the ore was dry ground to below 0.2 mm and the top size was controlled by sieving. The resulting particle size distribution is represented in the following Table 1.

Table I - Sus Eitattm zmc »re. Sue analysis <>/flotation feed

Size Class (nun)	We i Kİıt 1%)	Cum. Weight (%)
-0.200 + 0.150	19.01	19.01
-0.150+0.075	31.04	50.05
-0 075+0.0.175	IS.45	6H.50
-0.0375	31.50	
Feed	100.00	

366

. *

Preliminary batch tests have been carried out using a 2 litre Minemet laboratory cell aiming at identifying the optimum dosage of modulating agent, collector and frother.

In order to put into a better evidence the expected advantages achievable by using water jets, two parallel series of flotation tests have been carried out using the same cylindrical vessel, hosting the waterjet nozzle head (Hydrojet cell) or the conventional impeller (Minemet), respectively.

Common experimental conditions were:
- Volume of the vessel: 10.2 I
- Mass concentration of solids: 25 % by weight
- Modulating agent (CuSO$_4$): 200 g/t
- Collector dosage (Sodium Isopropyl Xanthate): 15 g/t
- Frother (Dowfroth 1012): 30 g/t
- Conditioning time: 5 min
- Solids feed rate: 0.9 kg/min
- Residence time: 3.5 min
- Air flow rate : variable from 2.55 to 10.2 Nl/min.

Rotation velocity of the impeller in the mechanical cell was 2,000 rpm, waterjet nozzle diameter was 0.3 mm.

Further separation tests were carried out with the Hydrojet cell in order to put into evidence the influence on metallurgical results of various operational variables like water pressure, air How rate, residence time and collector dosage.

The experimental conditions were similar to those reported in the above except for :

Collector dosage (Sodium Isopropyl Xanthate): variable from 15 g/t to

- 30 g/t;
- Solids feed rate: variable from 0.7 to 1.5 kg/min (Residence time: from 2 to 4.5 min);
- Pressure at the pump: variable from 5 to 14 MPa (flow rate: variable from 0.615 to 0.825 1/min);
- Air rate: variable from 2.55 to 10.2 Nl/min.

3.2 Experimental procedure

Under the above setting conditions flotation tests were carried out according to the following standard procedure:

- the pulp was fed at constant rate and the froth/slurry interface in the cell (about 5 cm below the discarding edge corresponding to the thickness of the froth layer) was maintained steady by adjusting the speed of the bottom discharge peristaltic pump;
- after a waiting time necessary for the achievement of a steady state (at least twice the residence time), two samples of the froths and of the discharge slurry were drawn in sequence.

The above sampling procedure resulted to be accurate enough and the differences between samples were within tolerable limits. Excluding the rare anomalous results data were averaged.

4 RESULTS

4.1 Waterjet versus impeller

Results of the comparative tests between Minemet and Hydrojet cell carried out according to the above described procedure are summarised in Figure 2, where Zn recovery and Zn grade of the rougher concentrated are plotted against air rate.

It is worth underlining that both Zn recovery and Zn concentrate grade with the Hydrojet cell are well higher (by more than 10 percent points, and by about 2-3 points, respectively) than those achieved with mechanical agitation at any pulp aeration conditions, while the metal loss in the tailings is significantly lower (by at least 2 points).
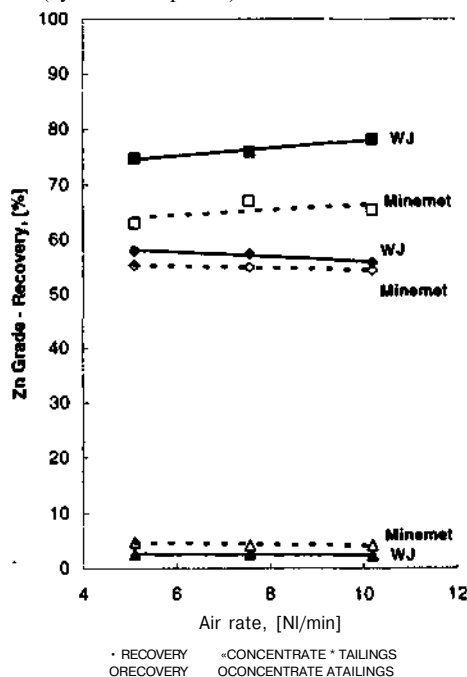

· RECOVERY   «CONCENTRATE * TAILINGS
ORECOVERY   OCONCENTRATE ATAILINGS

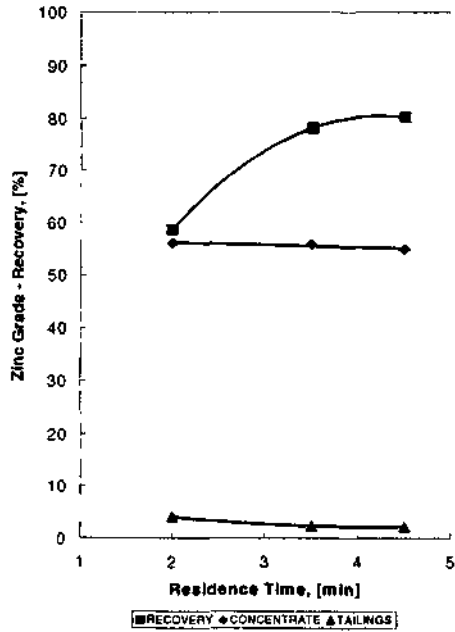*Figure 2 - Influent e ut tur rale tm floiatıtm remits.*

Figure . 1 - Hvilro/et Cell - Influent e of résilient e lime on flotation results.
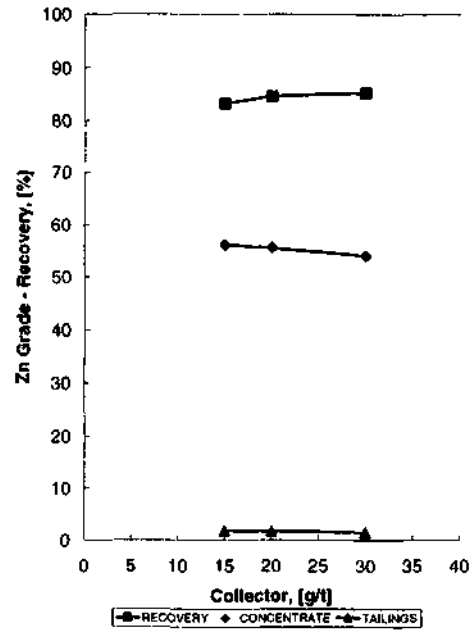

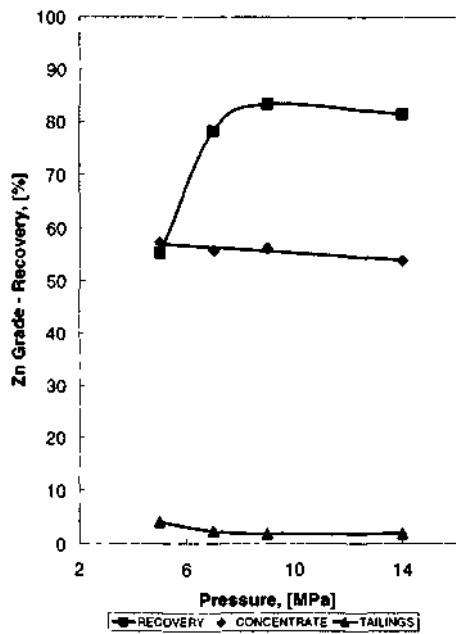Figure 5- Hvtlroiet Cell - Influence of collet lor on flotation results

Figure 4- Hytliojet Cell • Influente of pleasure on flotation results.

Regarding the air rate Figure 2 shows that in the range examined this variable has only a slight influence on separation results producing, as expected, a worsening of concentrate grade at increasing aeration of the pulp.

As represented in Figure 3 residence time has an important influence on the tailings grade while leaving almost unchanged the concentrate grade, thus producing a rapid increase in recovery when passing from 2 to 4.5 min.

Concerning the watcrjet features, tests have been carried out with a collector addition of 15 g/t aiming at singling out the optimum value of pressure. Results are represented by the curves of Figure 4 where Zn recovery and grade of the concentrate and Zn grade of the reject are shown as a function of pressure at the plunger pump. Mass flowrate of solids was 0.9 kg/min (residence time 3.5 min) and solids concentration in the pulp 25% by mass.

It is worth noting that:
- Zn grade of the froth product decreases almost linearly with pressure;
- Zn recovery increases considerably if pressure is raised from 5 to 9 MPa; a further increase in pressure beyond 9 MPa does not bring any improvement whereas flotation tends to deteriorate meaning that optimum pressure is around 9 MPa;

368

- Zn grade of tails decreases noticeably when pressure increases from 5 to 9 MPa then diminishes less markedly.

As shown in Figure 5, the metal grade and recovery follow the general trend of typical flotation tests. In tact at increasing collector dosage both concentrate and reject grade decrease while recovery increases.

5 DISCUSSION

The standpoint underlying the new concept based on the use of water jets in flotation appears corroborated by the experimental tests also in the case of sulphide ores, in addition to coal and industrial minerals. This represents a clear confirmation of the theoretical predictions based on the effect of high shear velocity on the process of bubble formation into the pulp (Klassen & Mokrousov 1963).

It is worth underlining that an intense shear action is necessary only at the bottom section of the cell where bubbles arc generated and dispersed into the pulp, whereas in the upper region only a moderate agitation is advisable in order to avoid the disruption of the collection froths.

In fact, results with only two water jets bearing half power, aimed right at the outlet points of air-nozzles, are much better that those with four jets since the two additional jets having no influence in the process of bubble generation produce an unfavourable stirring, eventually leading to a loss in recovery and a decrease in selectivity. Moreover this would be a great advantage from the economic point of view since energy represents an important cost item in flotation.

It seems that optimum operating pressure is around 8-10 MPa, giving a jet velocity at the nozzle of about 100 m/s. An increase in pressure beyond that level at equal hydraulic power using smaller nozzles does not appear very profitable. However it is likely that higher pressure will be needed in the scale-up of the system.

6 CONCLUSIONS

The use of water jets generated at moderate pressure can be considered as a suitable way for improving the required conditions for the full development of flotation mechanisms, especially in the case *of* very line fractions of the ore.

Separation results are always considerably better than those achieved with conventional mechanically agitated cells at equal conditions.

The following advantages can be predicted with the further improvement and the industrial scale-up of the technology, compared to conventional methods:
- more favourable bubble features;
- efficient control of the agitation pattern by optimising the nozzle arrangement and using fan jets;
- higher recovery and better separation selectivity;
- increased energy efficiency.

REFERENCES

Agus M.. Carbini P.. Ciccu R.. Ghiani M.. Satla F. and Tilocca C. 1998. Flotation of coal fines using high shear water jets. *XIII International Oml Preparation Congress.* Publ. by Australian Coal Preparation Society. Brisbane. Australia. 4-10 October. Paper 13. 358.

Carhini P.. Ciccu R.. Ghiani M.. Satla F. and C. Tilocca C. 1998. Flotation of barile fines with the new Hydrojet cell. *Innovations in Mineral and Coal Processing.* A. A Balkema Publ.. Rotterdam. Netherlands. 219.

Carbini P.. Ciccu R.. Ghiani M.. Salta F. and Tilocca C. 1998. A new concept in flotation technology. *5''' Pacific Rim International Conforme on Water Jet Technology.* New Delili. India, publ. by Allied Publishers Ltd. New Delhi, 295.

Chudacek M.W., Marshall S.H.. Fichera M.A.. Burgess .1. and Burgess F.L.. 1997. Super-scavenging of zinc from tailings by the FASTFLOT piocess. *XX Int. Mineral Processing Cultures*..* Aachen. Germany, publ. by GDMB. Clauslhai-Zellerfeld. Germany. Vol. 3. 275.

Klassen V.l. and Mokrousov V.A... 1963. Formation of air bubbles. *An Introduction to the Theory of flotation.* Butterworlhs. London. 443.

A Novel Collector for Flotation of Phosphate Minerals

R. Asmatulu
FEORC, 106 Plantation Road, Blac-kshtirg, VA 24061 - USA

ABSTRACT: Flotation of fine phosphate particles is one of the most difficult parts of line particle processing in preparation plants. One of the main difficulties is due to the fact thai the recycled water is used in the flotation circuit, which has high dosages of suspended particles and harmful ions. For this reason, currently used flotation reagents (i.e., fatty acid and diesel) cannot produce desired grade and recoveries on fine phosphate particles. In the present investigation, a novel collector was developed and used for the purpose of improving the grade and recovery of phosphate particles. The test results showed that at least 10% recovery with higher grade could be achieved on phosphate samples. As a result, it is concluded that in the present of the new collector phosphate companies could have higher benefits from the ore.

1 INTRODUCTION

Phosphate is mainly used as a fertilizer in agricultural industries. It is reported that more than 95% of phosphate rock produced in the world is utilized for the phosphoric acid production. With one-thirds of the world phosphate production, the USA (Florida, North Carolina and Idaho) is the largest pioducer of the world, and more than 80%' of the US production comes trom Florida itself. When the phosphate is mined, it does not meet requirements for the phosphate industry due to the higher gangue mineral contents (i.e., dolomite, silica sand, clay, clay-sized minerals, etc.), and necessary to improve the content of phosphate (PiOO in the final product. Flotation that has been applied for the separation of phosphate fines since late 1920s seems to be the best separation method (Miller *et.al..* 2000 and 2001).

Nowadays, double flotation process is mostly preleired one for the separation of a phosphate from the gangue minerals. This process includes an anionic flotation (fatty acid + fuel oil) of the phosphate minerals at alkaline pH, and then cationic flotation (amme) of fine silica minerals (presented during the anionic flotation) at neutral or acidic pH. The second step is conducted after the concentrate is de-otled with diluted sulfuric acid. This double flotation process is extensively applied to sedimentary phosphate minerals in the USA (Miller *et.al.,* 2000 and 2001; and El Shall *et.al..* 1999).

Recently, plant-recycling water is used to float the phosphate lines in several flotation circuits due to the environmental concerns in the world. However,

it is found that the plant water contains several nanosize suspended particles and different harmful ions including Ca, Mg, AI, Fe, Na, K, CI, F, S₁, $S0_4$ and P, which increase the plant water hardness and decrease flotation recovery and phosphate grad (Weiss, 1985; and Summers *et.al.,* 2002). Among these ions, the phosphorus ion seems to be one of the worst ions affecting the flotation process in the plant. Thus, to eliminate these effects the reagent consumption is increased to receive the higher recovery and grade but this also increases overall flotation costs. For a while, a number of research programs have been performed on the phosphate flotation using plant water, and it was seen that recovery results were still far from the expected one (approximately 10% lower than tap water) (Miller *et.al.,* 2000 and 2001; and El Shall *et.al.,* 1999). In order to solve to problem associated with the phosphate flotation using the plant water, a novel flotation reagent (dissolved in appropriate carrier solvent before use) has been developed and successfully conducted on phosphate samples. The chemical seems to be the most promising option for the phosphate industry to recover fine phosphate in the flotation circuits.

2 EXPERIMENTAL

The deslimed phosphate samples from the USA were screened in two sizes (-2+0.075 mm and -1+0.075 mm), and then representative samples were poured into a conventional 4-liter stainless steel Denver

flotation cell. It is known that the desliming improves the flotation recovery and grade due to the removal of ultrafine dolomite and clay-sized particles, which can also eliminate the cationic flotation step [Miller *et.al.,* 2000; and Weiss, 1985). A hydrophobic surfactant - called Reagent PI23 and saponified fatty acid (crude tall oil) were employed for the flotation tests at 1600 rpm and 17% solid content. Before the tests, the phosphate samples were conditioned with fuel oil and the chemicals at 70% solid content for two minutes, and then flotation tests were performed for two minutes at pH 7.4-8.1 using plant recycling water. The ratio of fuel oil to fatty acid (or new flotation reagent) was 0.6. The purpose of these tests is to compare the efficiency of the new collector with fatty acid under plant water conditions.

3 RESULTS AND DISCUSSION

Figures 1 and 2 show the results obtained on the phosphate sample (-1 mm + 0.075 mm) using plant-recycling water. The test results with a single stage flotation step showed that a 1000 g/ton of Fatty acid and Reagent PI23 gave 27.30% P-,0, and 27.81% $P_2 0$, grades and 89.68% and 97.89% recoveries, respectively. This indicated that the hydrophobizing agent could improve the force of attachment between bubbles and hydrophobized particles (selectivity), which in turn affected the recovery and grade of the phosphate fines. However, the traditional fatty acid/fuel oil combination did not provide such a high selectivity in the harsh water conditions. In addition, it was also observed that in the presence of the new reagent flotation kinetic was also improved at least 50%, which might be due to the same reason.

In order to compare the efficiency of the new collector on coarse particles (-2+0.075 mm), a series of flotation tests were also conducted using the same plant water. The flotation recovery/collector dosages and recovery/grade curves of the tests are shown in Figures 3 and 4, respectively. Based on the flotation test results, it is seen that using a 1000 g/ton of the new collector a single stage flotation recovery of 86.76% is possible on the coarse phosphate particles with a concentrate grade of 24.64% PiO,. The higher recovery (i.e., more than 11%) as compared to the conventional reagent could be attributed to the fact that the new reagent specifically adsorbed on the phosphate particles, and made those particles hydrophobic enough for better flotation in the plant conditions. Additionally, the improvement of the flotation kinetics was also seen in all the tests.
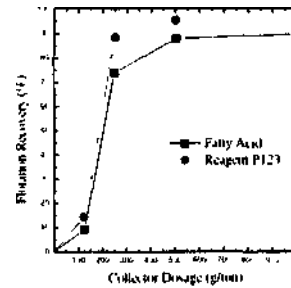

Figuie I Flotation leeovciy ol phosphate sample (-1+0 075 mm) as a function ol fatty And *MI<1* Reagent PI23 with plant watci
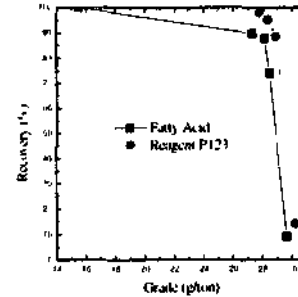

Figure 2 Comparison of recovery/grade curves obtained using Fatly Acid and Reagent P12.1 for the phosphate sample (-1+0.075 mm) with plant water
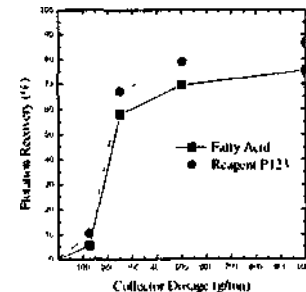

Figuie 3 Flotation recoseiy ot phosphate sample (-2+0 075 mm) as a function ol Fatty Acid and Reagent PI23 Willi planı watei.
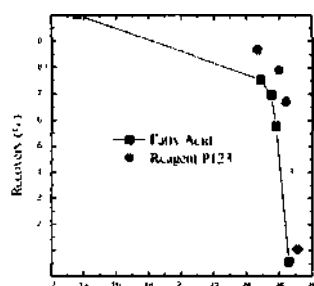
372

Figure 4 Comparison »I recovery/grade cmves obtained using Fatty Aud and Reagent PI2^ for the phosphate sample (-2+0 07^ mm) with plant water

4 CONCLUSIONS

A newly developed hydrophobic reagent was tested on flotation of a phosphate sample at neutral pH to be able to improve recovery and grade of the phosphate samples. All the tests were conducted in the laboratory condition using plant water supplied from a phosphate company. The test results showed that flotation performances of fine phosphate samples, including recovery, grade and flotation kinetics

could be significantly enhanced. This can be attributed to the fact that the novel reagent improved the hydrophobicity of the fine particles to be efficiently floated in the flotation circuit.

REFERENCES

El Shall. H.. Khalek. A . Svoionos. S.. Shamia. R and Gupta. S 1999 Column Flotation of Florida Phosphate An Optimisation Sludy *SME Animal Meeting,* Mai. 1-3. Denvei Coloi ado.

El Shall. H . Yous.sef. A and Khalek. A 2002. Recoveiy of Phosphate Values fioin Benefication Waste *SME Annual Meeting.* Fch 25-27. Phoenix. Anzona.

Mılleı. D J.. Wang. X . and Li. M. 2000 Recent Development of Advanced Flotation Stıategıes tor Florida Phosphate Resouices. *SME Annual Meeting.* Feb 28-Mar I. Salt Lake City. Utah.

Miller. DJ.. Wang, X. and Li. M. 2001 A New Collect™ Chemisliy loi Phosphate Flotation *SME Annual Meeting.* Feb 26-2X, Denvei. Colorado

Summers. C Dahim. D. Sis H and Charnier. S 2002 Selective Flocculation of Fine Phosphate Matenals *SME Annual Meeting.* Feb 25-27 Phoenix. Anzona.

Weiss. N.L. 1985. *SME Mmeial Proie.siint: Handbook- Volume 2.* New Yoik.

Rio Tinto Borax's Initiative on Sustainable Development in Mining Operations

T. S. Griffin
U.S. Borax Inc., Valencia, California, USA

ABSTRACT: Sustainable Development is defined as "Development that meets the needs of the present without compromising the ability of future generations to meet their own needs." In late 1998, Rio Tinto joined with a number of the world's largest mining companies to develop the Global Mining Initiative to ensure that the mining, metals, and minerals industry addressed global needs and challenges. Early in 2000, Rio Tinto Borax was selected as the pilot project within Rio Tinto to develop and lest the concepts of sustainable development. As a result, Rio Tinto Borax embarked on a major project with a mission to ensure that the company's operations and products contribute to the three pillars of Sustainable Development: economic, environmental, and social. A global team has developed live primary objectives to support the project mission, and each objective is further supported by indicators, metrics and targets. Examples will be taken from Rio Tinto Borax's global operations as well as from its world class mine and processing facility in Boron, California. USA.

1 BACKGROUND AND INTRODUCTION

Early in 2000, Rio Tinto Borax embarked on a major initiative with a mission to ensure that its operations and products contribute to sustainable development. Borax was selected as the pilot company to carry out a case study of the role of sustainable development in the daily operations of one of Rio Tinto's major business units. The outcome of this pioneering case study would then be a valuable guide to other Rio Tinto business units also launching sustainable development projects. Rio Tinto is one of the leaders in the group of the world's largest mining companies who in 1998 joined together in the Global Mining Initiative (GMI) to ensure that the mining, metals, and minerals industry faced global needs and challenges. The GMI was formed to address the question: how best can the mining and minerals industry contribute to the transition (o sustainable development? The GMI has been successfully concluded at the global conference in Toronto on 15 May 2002 with structures and relationships in place to help answer this question (www.ulobalmining.com, see also, www.icmm.com).

Sustainable development is defined in the Brundtland report as "development that meets the needs of the present generation without compromising the ability of future generations to meet their needs." The Borax team developed a definition of sustainable development, which applies to the day-to-day decision making of Borax management. It includes an integrated consideration of economic performance, environmental management, and social responsibility. This is underpinned by ethical, transparent, and accountable business practices. In practical terms, it means that all business decisions involve trade-offs in which the three pillars of sustainable development, economic, environmental, and social, must be considered. Under the leadership of Dr. Elaine Dorward-King, Borax's Global Executive Environment, Health and Safety, a cross-functional and multi-cultural team developed the mission, objectives, measurements, and initial projects to drive Borax to achieve tangible results in sustainable development in 2001 (Rio Tinto Borax 2001 Social and Environmental Report). Dr. Dorward-King is now Head of Health, Safety and Environment for Rio Tinto Ltd, London, and leadership of Borax sustainable development teams has been continued by the Borax Chief Executive, Preston Chiaro, and the Borax Executive Team. In 2003, as sustainable development is transitioning to full integration into day-to-day Borax operations, leadership of the initiative has been assigned to an Executive triumvirate representing the three pillars of sustainable development-Jeff Olsen, Chief Financial Officer, Jim Qin, Chief Health, Safety, and Environmental Officer, and Alexis Fernandez, Chief Communications Officer (also responsible for community relations).

375

2 BENEFITS TO BORAX

Early in the initiative, it was recognized that the business benefits of sustainable development had to be identified and understood. Thus a concerted effort was undertaken to quantify these benefits, which were termed "success factors" in recognition of their importance. The success factors emerged during the numerous projects that were undertaken as the indicators of progress toward reaching the objectives of sustainable development. Overall, it was recognized the sustainable development program differentiated Borax in the mining industry as an innovator and leader in the marketplace by managing risk, improving efficiency, stimulating innovation, bringing value to customers, and by managing reputation. The latter is critical to the success of any natural resource company, where the agreement of the outside community and appointed regulators is necessary for continued operations (effectively a license to operate).

3 OBJECTIVES

Rather than dealing only with abstract concepts, the Borax sustainable development effort has evolved through the completion of numerous projects, headed by team members with assistance from employees. This process can best be illustrated by the *measurement pyramid,* shown in Figure I. The pyramid illustrates with an example from the health and safety objective how the Borax sustainable development mission-"Rio Tinto Borax Operations and Products Contribute to Sustainable Development"-is supported by objectives, indicators or suc-

cess factors, metrics for measurement, targets, and supporting projects. Since 2000, over 80 projects have been carried out by Borax teams in support of Borax's objectives in sustainable development. Details of the 2002 projects are available in the "2002 Progress Report, Borax and Sustainable Development," a copy of which can be obtained by contacting Borax through its web site at www.boraK.com. Borax's objectives cover each of the key areas of sustainable development and are listed below:

- To protect the safety and health of employees, contractors, neighboring communities, and the public.
- The enhance the human potential and well-being of communities and employees.
- To maximize efficient utilization of resources while minimizing environmental impacts of our operations.
- To optimize our economic contribution to society.
- To expand how our products contribute to sustainable development.

4 HEALTH AND SAFETY

Safety is the top priority at Borax, and very early in the program the sustainable development team recognized "number of injuries" as a key success factor. There were no fatal accidents in 2001 and 2002. Borax also achieved an 83 percent decrease in serious injuries, as measured by Lost Time Injuries (LTI's) and LTI Frequency Rale, and the All Injury Rate, which includes minor injuries, decreased by 25%. A summary of the results is shown in the following Table   I.

Table 1 A summary of results

(a) Injury Measure	2001	2002	% Chaiitfe	2002 Goal
Fatalities	0	0	0	0
Lost Tune iniune.s	18	3	-83.3	-50%
Medical Treatment Cases	20	24	20.0	
LTI Frequency Rate	0.92	0.16	-82.6	-50%
Total Injuries	.18	27	-28.9	
All Injury Rate	1.94	1.45	-25.3	
Seventy (Shifts Lost)	502	278	-44.6	
Severity Rate	25.6	15	-41.4	

The excellent performance-the best in Borax's history and the best among Rio Tinto operating companies-confirms the effectiveness of Borax's safety program which emphasizes preventing injuries by focusing on unsafe behaviors and conditions, identified by the implementation of Safety Management Audit Training (SMAT) at all sites including offices. Another important initiative towards the goal of reducing injuries is the near miss reporting system.

started in January 2001. In a near miss, the injury or equipment damage is averted but other risks are in place that could result in an accident. Near misses are investigated including a root cause determination just like actual accidents, and thus near misses are valuable learning tools to prevent an actual related accident from occurring. In 2001, 54 near misses were reported, and 64 in 2002, for a combined ratio of reported near misses to all injuries of 4:1. The

target in 2003 is a reported near misses to all injuries ratio of 7:1, which is fell to be a level where significant impacts on reducing accidents will be seen. This target is to include increased emphasis on analysis of "recovery actions" that employees took to prevent an actual accident from occurring.

5 COMMUNICATION AND COMMUNITIES

The key focus of Objective 2, the human potential and communities objective, was to increase internal and external consultation and mutual understanding of sustainable development principles. Results of a 2000 survey of employees and external opinion leaders showed they knew little about sustainable development, but they wanted to know more. In response to these results, information about sustainable development was provided to employees in a number of forms including a series of workshops held in 2002 at most global sites. Opinion leaders received the 2001 Social and Environmental Report and throughout the year Borax representatives presented the sustainable development project to external audiences which included colleagues in the mining industry, community leaders, customers, trade associations, governmental officials and NGO's. In addition, a community needs assessment (CNA) was carried out in the community immediately adjacent to our Boron operation. The CNA, which was conducted in partnership with local government and the community, identified drug and alcohol abuse, attracting new business, youth activities, and unemployment as the four critical issues facing the community. Working groups have been organized to address these issues and move ahead with solutions in 2003. As a follow up to this action plan, the Borax Communities Department has set a target for 2003 of aligning 75% of the Borax-supported community programs with needs identified in the CNA.

6 MINING, REFINING, AND ENVIRONMENTAL PERFORMANCE

Efficiency in mining, refining, and environmental performance is a key objective of sustainable development-and the benefits are multiple-economic through high efficiency and low risk operations and social in the public's expectation that mining businesses operate in a way that doesn't harm the environment or people. Projects geared towards improving performance at Borax"s operating sites in operating and environmental efficiency fall into the following categories: mining efficiency, refining ef-

ficiency, global supply chain, and environmental improvements.

6./ Mining Efficiency

2002 Borax set aggressive targets for improving its energy, water, and fuel use. While in 2001 a significant reduction in water usage in the mine was seen, 2002 water usage (used for dust control on haul roads) was not improved due primarily to changes in hauling patterns. Fuel usage was almost fiat from 2001 to 2002 as part of the haul truck fleet was put on standby. Two areas where efficiency targets were exceeded were in fuel usage by auxiliary equipment such as graders and in the amount of blasting powder used.

6.2 Refining Efficiency

In our Boron operation. Borax met the recovery target in the primary process (sodium borate) plant and reduced effluents to the ponds by nine percent from 2001, however water usage increased. The boric acid plant did not meet recovery or water usage targets, however production was at record levels with longer intervals between equipment maintenance. Condensate return and plant availability were below target in the primary process, and the cogeneration plant exceeded the plant on-stream target. Overall refinery scheduled and predictive maintenance performance was slightly below target. The Coudekerque plant (France) met targets to reduce waste and improve efficiency in the borax decahydraie plant, and in Borax Argentina, both process plants were on target for recovery. At the Wilmington plant in the Los Angeles harbor, throughput targets for zinc borate and spray dry were not met and improvement projects will continue, however the plant set aggressive targets to reduce water usage and volume of waste to the sewer system, and both targets were achieved (Figures 2 and 3).

6.3 New Primary Crusher

At Boron, the Jeffrey impact primary ore crusher, which had been in service since 1960, was replaced in 2000 by a new crushing system employing MMD toothed double roll sizers in two reduction stages. Benefits included an increase in processing rate, imprqved particle size distribution with less fines and surges of coarse lumps, and reduced maintenance-all part of sustainable development (Mineral Processing on the Verge of the 21" Century, Ozbayoglu, et al., eds, 2000 Balkema. Rotterdam, ISBN 90 5809 172 4).

Table 2

MINE EFFICIENCY FACTOR	2001 Performance	2002Target	2002 Performance
Fresh water use m Boion mine	38% reduction	Additional 28% reduc-tion fiom 2001	5%> increase from 2001
Fuel use tor haul ti ticks	0.0152 gallons/mile/avg. truckload	Maintain 2001 levels	0.0159 gallons/mile/average truckload
Blasting efficiency (powder factor)	0.35 lbs of ammonium mti ate/ton	0.33 lbs/ton	0.30 lbs/ton
RBFIN1NG/PROCESSI NG EFFICIENCY FACTOR	2001 Performance	2002 Target	2002 Performance
Watei use in Primary Process and Boric Acid Plant (Boion)	4'/,-1 eduction from 2000 - P P 17, reduction fiom 2000 - B A P	11% reduction from 2001 - P P 7% reduction from 2001 - B A P	12% over target- PP 13%. over lai ge1- BAP
Effluent to Primary Process R-Ponds (Bo-1011)	17% reduction fiom 2000 - PP	89Ì reduction from 2001 - P P	9%) reduction from target - PP
Recovery in Primai y Process and Boric Acid Plant (Boron)	1.1% dec. from 2000 - PP 1.6% dec. from 2000 - BAP	New target sei - PP 4.6% inc. over 2001- BAP	On large! - PP 4%. under target - BAP
Condensate return and plant availability (Boron lefinery and co-generaiion plant)	Target set - PP 76% on-siream - PP	11% over 2001 taiget - PP 85% on-slream - PP 93.4% on-stream - co-gen	Same as 2001 pel l'orinance - PP 82.3%. onstrm - PP 96.1 % onstream - cogen
% scheduled & pic-dıctıve maintenance compliance (Boron)	Target set in 2002	Scheduled: 65% Predictive: 85%	Scheduled: 63% Predictive: 82%
Throughput effi-ciency (Wilmington - ZB. sprav dry)	Target set in 2002	Taiget set - ZB Target se t - S D	18% under target - ZB 7.5% under target-S D
Wilmington plant water usage and waste-waier discharge to sewer	Program initiated in 2002	Baselines measured and water usage and waslewater discharge to sewer reduc-tion initiated	35% reduction in water usage and 55% reduction in wastewater dis-charged to sewer
Recovery, water and natural gas usage (Ar-gentina)	13% dec. from 2000 - H;0 3% dec. from 2000 - gas	Target sel - Tl recov. Target set - CQ recov. 1,7%> reduction from 2001 - H_2O 2.0%' reduction from 2001 -gas	1 % undei largel - TI recov. On target - CQ recov 2.5%. ovei target - H;0 2.2%. under target - gas

6.4 Environmental Improvements

An extensive plant dust reduction program was un-dertaken at Borax's Rotterdam bulk terminal port fa-cility. The project included replacement of old prod-uct-handling equipmenl such as open conveyors with chain conveyors and installation of a pneumatic product transfer system and vacuum clean-up sys-terns for product spillage. The result was a dramatic decrease in dust emissions (< 10 mg/m at each filter outlet), reduced product spillage, and an improve-ment in the attitude of management and employees towards plant housekeeping. A similar effort is un-derway at the Boron refinery in an area where old equipmenl results in excessive product spillage. At Coudekerque, improved cooling systems resulted in a 50% reduction in boron discharged to the nearby canal, well below permit requirements. Remediation of the Coudekerque gypsum waste pile is well un-derway, and at Boron, with help from local horti-

378

culture students, rehabilitation of mining waste overburden piles increased to 60 acres per year, which puts it on track to reach a target of rehabilitating 100 acres per year by 2007. At Borax Argentina, water usage was flat from 2001 to 2002, but gas reduction targets have been achieved for two years in a row. There were zero environmental incidents of any significance in 2002 across all Borax global sites.

6.5 Oil Recycling

Oil recycling units are in place on Boron's fleet of haul trucks. The units, which burn used oil in the fuel, reduce engine maintenance, extend engine life, reduce deterioration of the crankcase oil in service, and eliminate the generation of waste oil. Additionally, these units allow the trucks to increase production hours, as they are not taken out of service for oil changes. Over the life of a truck, use of the fuel recycling units significantly reduces costs and eliminates the requirement to haul waste oil to off-site treatment facilities.

7 BORAX PRODUCTS AND SUSTAINABLE DEVELOPMENT

Borax produces five major refined products at its facility near Boron, California: Borax Decahydrate ($Na.B_4O_7.IOH_2O$), Borax Pentahydrate *(Neobor®,* $Na_2~B_4O_7.5H_2d$), Anhydrous Borax *(Dehxbor®,* $Na_2B_4O_7$), Boric Acid *(Optibor®,* $H.,BO,$), and Boric-Oxide (B_2O0. Smaller volume specialty products are produced at its refineries in Wilmington, California and in Coudekerque, France. Borax ensures that people and the environment are protected from any significant exposure risks through its product stewardship policy. In 2001. Borax revised the policy to incorporate all aspects of sustainable development, and in 2002 communicate that policy to customers and employees. This communication effort will continue in 2003. The five major products produced at Boron were subjected to cradle to gate life cycle assessments (LCAs) in 2002. These LCAs measure the amount of energy and natural resources used, the amount of waste produced, and all environmental impacts in making each product. LCAs will be completed for Wilmington specialty products in 2003. Sustainable development principles are incorporated in the "stage gale process" as one of the hurdles new applications and products for the market must pass through. A sustainable development checklist ensures that all new applications and products are consistent with Borax's sustainable development principles and objectives. A "leading edge" project underway in collaboration with business, academic, and government partners is the development of long-term replacement of fossil fuel energy sources with hydrogen-powered fuel cells for vehicular and stationary applications. The objective is to utilize the hydrogen storage capabilities of sodium borohydride and related hydroborates as safe and environmentally benign sources of hydrogen to power fuel cells. This is a long-term development process with enormous potential to benefit society.

8 WHAT'S NEXT FOR BORAX

In 2003, Borax is progressing in the completion of its goal to integrate the principles of sustainable development into daily decision-making at every level and in every department within Borax. A number of cross-cutting projects were completed in 2002 to achieve this goal. These included incorporation of sustainable development principles into the capital expenditure approval process, application of the principles to procurement decisions from vendors and suppliers, and increased partnerships with customers in key areas with sustainable development components, for example, recycling and re-use of borate feedstocks, and control of borates in wastewater. A logistics and distribution team has been set up to consider applications of sustainable development principles to the Borax global supply chain. The target is to model alternative transportation scenarios, which could potentially reduce emissions and increase transport efficiencies. Employee workshops were held in 2002 and in 2003 to increase employee awareness of the principles and benefits of sustainable development. Projects undertaken by employees were highlighted in these workshops. In 2003, the core sustainable development teams, which have been a mainstay of the project since 2000, have been replaced by a "transition team" lead by an executive triumvirate, consisting of the Chief Financial Officer, the Chief Communications Officer, and the Chief Health, Safety and Environment Officer. Under this new team, Borax is expecting to complete the transition to fully integrating the principles of sustainable development in every aspect of its business and operations (Borax and Sustainable Development. 2002 Progress Report).

Effect of Alkalinity on Flotation Behavior of Quartz

A.Sayılgan & A.İ.Arol

Middle East Technical University, Mining Engineering Department. Ankara, Turkey

ABSTRACT: Alkalinity is defined as the capacity of a water to neutralize strong acids. In natural waters, this capacity is attributable to bases such as HLU,,CO; and OH" as well as to species often present in small concentrations such as silicates, borates, ammonia, phosphates and organic bases. Commonly, alkalinity originates from the total amount of carbonates in water. Since notation is a process dependent on the water chemistry, carbonate alkalinity which may change as a result of the seasonal climatic changes can be a plausible concern in flotation.

Effect of alkalinity on the notability of quartz with an amine type collector and with Na-oleate, in the presence of calcium ions al alkaline pH values were studied. It was observed that as the alkalinity of the process water is increased, the notability of quartz decreased both with an amine type collector and with Na-oleate.

1 INTRODUCTION

Flotation is affected by a number of factors such as the electrical properties of the mineral surface, electrical charge of the collector, molecular weight of the collector, the solubility of the mineral, the interaction between the dissolved species and notation reagents, etc.. Many of these factors are related to the process water chemistry.

Carbonates are always present in natural waters, thus in the process waters in notation. When COi dissolves in water it forms a weak acid. This acid and its salts in solution constitutes the carbonic system which forms a buffer system that resists pH change. The pH of natural waters on land is controlled mainly by this system. Carbonic species in natural waters consist of dissolved CO_2, carbonic acid $1H,CU,j$, bicarbonate (HCO,) and carbonate CO; ions. The predominant carbonic species is pH dependent. Almost all carbonic species exists as H,CU, below pH =b.J. asHLU, between pH=6.3-10~25 and as *CO;* above pH=10.25 (Stumm& Morgan, 1981). Alkalinity is the capacity of a water to neutralize strong acids. Alkalinity in natural waters derives mainly from the carbonate system and total alkalinity can be expressed as HLO, + 2CO; + OH - H . Addition of bicarbonate and carbonate ions, and a strong base increase alkalinity, addition of a strong acid lowers the total alkalinity. Normally, dissolution of CO_2 does not change alkalinity. However, above pH=4.5, pH of the solution is lowered upon CO_2 dissolution. In order to keep the pH at a higher value than pH=4.5, a base has to be added to the solution. As a result in alkaline pH range, carbonate alkalinity of water continuously increases in the presence of CO_2 if the pH is to be kept constant (Snoeyink&Jenkins 1980).

It is known that the solubility of carbon dioxide in water is dependent on the partial pressure of carbon dioxide which is constant in the atmosphere at 10^{-15} atm and the temperature. Solubility increases with the decreasing temperature. For example, the amount of dissolved carbon dioxide in water at 5"C is nearly 2 times that in 25"C. Thus, alkalinity of waters at high pH values will be affected by temperature. Alkalinity of natural waters also varies depending on the ratios of source waters. Natural waters during rainy seasons are dominated by poorly buffered surficial runoff and have low alkalinity; on the contrary, during dry seasons, ground waters rich in weathered bedrock ions are dominant in the natural waters which will have higher alkalinity values (Howlandel.al2000.).

As climatic changes lead to the change in the process water chemistry especially in terms of alkalinity, mineral processing operations in general and notation in particular are expected to be affected by these changes. In fact, it has been reported, without deliniating the reasons, that seasonal climatic changes have a determining effect on grade and recovery (Lin 1988). A clear understanding of the effect of the carbonic system, i.e. alkalinity, on notation would provide a useful tool to improve the process efficiency.

In this study, the effect of alkalinity on notation behavior of quartz in the presence of both a cationic and anionic collector using EMDEE Microllot cell was investigated. Quartz was chosen on the basis of two reasons: Firstly, its flotation behavior is well defined and widely studied. Secondly, the cationic notation and the anionic flotation of quartz with an activator are both carried out at high pH values where the effect of alkalinity is more pronounced.

2 MATERIALS AND METHODS

Quartz sample used in the experiments was obtained from the Kalemaden Industrial Raw Materials Industry&Trade. As received sample was first ground by a roll crusher and then screened to obtain -140+200 mesh fraction for the tests. To remove the impurities from the sample, it was subjected to magnetic separation using a high intensity magnetic separator! Bateman Lab Permroll) followed by leaching with hot IN HCl solution several times. The leached quartz was washed with distilled water until free of chloride ions. The sample had a SiO_2 content of 99.21%.

All ol the flotation experiments were carried out by using the EMDEE Microtlot Agitator. The sample, weighing 0.5 g, was piaced in the flotation cell and filled up to 60 mL with water. After adding the collector and bringing the water level in the tube to 70 mL, the pulp in the tube was conditioned for 10 minutes using a two blade mixer tightly fitted to the tube by a stopper to prevent the interaction of the pulp with air. After conditioning, frother was added and the test tube was placed in the EMDEE Micro-Hot Agitator. Air pressure was adjusted to 250 kPa. The test tube was agitated for 20 cycles and then allowed a few seconds for drainage prior to froth removal with vacuum suction. All float and sink fractions were collected separately and filtered on tared filter papers which were dried at I05°C for 4 hours and weighed to determine the recovery.

Waters with different alkalinities at different pH values were prepared by dissolving $NaHCO_3$ in CO_2 free water (obtained by nitrogen Hushing at pH 4).As collectors, Flotigam Eda which is alkyl ether amine and Na-oleate were used for the notation tests. Flotanol D-14 which has a composition of alkyl polyglycol ether was used as a frother. NaOH and HCl were used for pH adjustment. $CaCl_2$ was used as an activator for quartz when Na-oleate was used as the colleclor.NaHCO,,, HCl. NaOH and CaCI; used in the tests were all reagent grade

3 RESULTS AND DISCUSSION

In order to investigate the effect of alkalinity on the flotation of quartz, the optimum flotation conditions

with both the cationic collector and the anionic collector with no carbonate alkalinity were determined first. As shown in Figures 1 and 2, the optimum collector concentrations and pH value for the cationic and the anionic notation were found to be 50 mg/L amine at pH 10 and $4*10^a$ M Na-oleate in the presence of $4*10^*$ M Ca^{2+} at pH=!2, respectively.
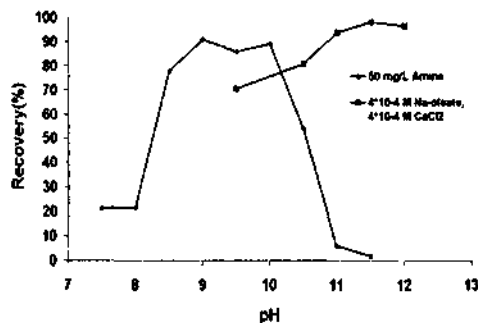

Figure I Flotation of quaitz with amine and Na-oleate as a function of pH at *lem* carbonate alkalinity; 100 ppm frotlier.
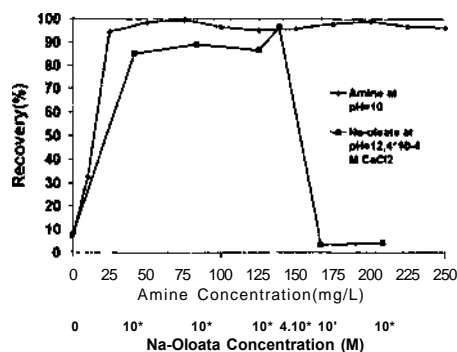

Figure 2. Flotation of quartz with amme and Na-oleate as a function of collector concentiation; 100 ppm frother.

The flotation mechanism of quartz with cationic and anionic collectors in the presence of an inorganic salt is well established and documented (Fuerstenau l976,Uwadiale l992.Takedae4.Usui 1988, Iskra 1997a). In summary, the pzc of quartz occurs at pH 2. Therefore, quartz is negatively charged above this pH. Collector adsorption is due to the electrostatic interaction in cationic flotation and to chemisorption of oleate on calcium adsorbed on quartz (Iskra I997b, Sirkeci 2000,Ye&Matsuoka 1993). Ionization, micelle formation and hydrolysis of the collectors and activator ions play an important role in a successful notation operation. In addition, presence of other species may affect flotation. For example, Ba^{2+}, Ca^{2+}, Mg^{2+}, Na^+ and K^+ ions have been reported to cause depression in the cationic flotation of quartz (Scott&Smith 1992.1993, Somasundaran 1974).

Flotation tests were carried out to determine the effect of carbonate alkalinity on the flotation of quartz. Alkalinity was adjusted by adding NaHCOj to the water. The carbonate alkalinity in waters equilibrated with atmosphere at or above pH 10 is in the form of (JO* and can exceed 10''' M (Stumin&Morgan 1981). Therefore, alkalinity of the test waters varied from zero to K)''' M CO; alkalinity. The flotation recoveries in the cationic and the anionic flotation as a function of alkalinity are given in Figure 3.
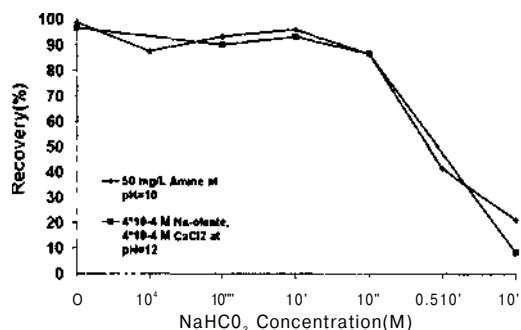
Figuie 3 Ettect of carbonate alkalinity on the flotation lecoveiy ot quartz with amine and Na-oleale: 100 ppm frother.

It is clear from the figure that as alkalinity increases from zero to 10''' M $W\backslash$, quartz is depressed as flotation recoveries sharply decrease from over 90% to 10% in both the calionic flotation using amine and in the anionic flotation using Na-oleale and Ca^{2+} as activators. In the case of cationic flotation, the depression of quartz might be related to the compression of the double layer caused by the higher ionic strength upon NaHCO^ addition(Vidyadhar et.al. 2002) or competetive adsorption of Na^+ and amine ions preventing the amine adsorption as reported earlier (Onada&Fucrstenau 1964, Iwasaki 2000). Another mechanism might be a reaction between amine and carbonate in the solution which would consume the collector and hinder flotation.

In the case of anionic flotation with Na-oleate, the mechanism of depression could be the replacement of $Ca(OH)^+$ ions on the quartz surface with Na^+ ions introduced by NaHCOi addition and pH adjustment with NaOH(Cooke&Digre 1949,Cooke 1949). $Ca(OH)^+$ ions which is thought to be responsible (Clark&Cooke 1968) for activation may react with CO; and precipitate on the quartz surface as CaCOi according to equation 1 :

$$CaOH + CO_3^- \rightarrow CaCO_3 + OH \qquad K = 10^{...} \qquad (1)$$
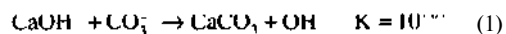
From the equilibrium constant of the reaction above, it is seen that CaCCh precipitation will strongly be favored at high pH values ihermodynamically. This

occurrence has been exploited in the precipitation of calcium ions in the selective floceulation of iron oxide from silica(Manukonda&lwasaki 1987). It can be speculated that in the anionic flotation of quartz, too, the activator calcium ions will react with the carbonate ions and precipitate. This freshly precipitated amorphous CaCO, is likely to be negatively charged at pH 12 (Rao&Forssberg 1991). The precipitates covering the surface of quartz will hinder the flotation of quartz with Na-oleate at high pH values in a similar manner to earlier studies (Aplan&Fuerstenau 1962). This phenomenon is probably more complex and requires further investigation.

Another series of flotation tests were conducted in order to investigate the effect of collector concentration on the flotation recovery at zero and 10''' M carbonate alkalinity. The latter value was chosen because of the noted effect. The results for amine and oleate are given in Figures 4 and 5, respectively.
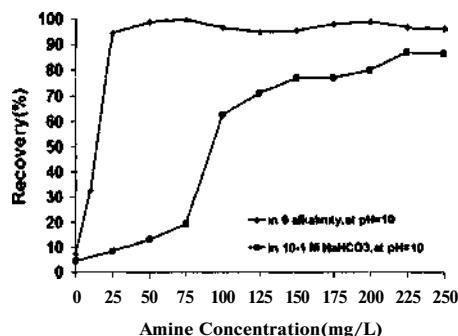

Figure 4. Effect of amine concentration on the flotation recovery of quartz at zero and l()''' M carbonate alkalinity; I00 ppm frother

It appears that increasing the amine concentration restored the recovery at I0''' M alkalinity tested. This behavior is in good agreement with earlier studies (Scott&Smith 1992,1993) where the effect of high ionic strength and calcium ions were reported to be remedied in the same way, that is by increasing the amine concentration. As the adsorption mechanism of amine on quartz is known to be electrostatic, adsorption equilibrium should be established as a result of ion exchange reaction according to equation 2:

Quartz'' - Amine* + Na* -> Quartz' - Na* + Amine* (2)
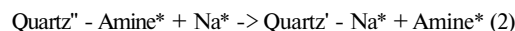
The equilibrium will shift in either direction depending on the relative abundance of Na^+ or amine in the solution. Excess amine ions will favor amine adsorption on quartz and vice versa. A similar cation exchange mechanism has been reported for the clay-amine adsorption system (Iwasaki 2000).

In the case of oleate, a different flotation behavior was observed. Quartz, initially activated with calcium and then depressed with 10^{-3} M carbonate alkalinity can not be floated effectively by increasing the oleate concentration, Figure 5.
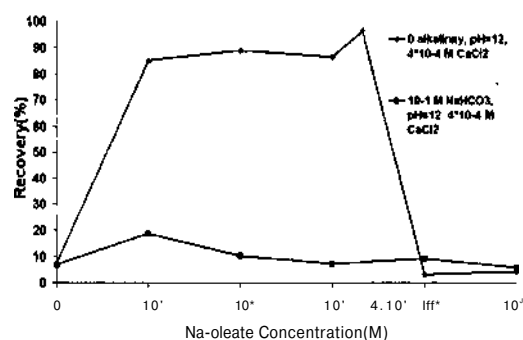

Figure 5. Na-oleate Concentration versus Recovery in different alkalinity values

This fact supports the postulation that Ca^{2+} ions precipitate on quartz and alter the nature of the surface. As an increase in the collector concentration does not effect the surface properties, in contrast with the cationic flotation explained above, quartz remain unfloatable. In this figure, the nonflotability of quartz with no added alkalinity beyond 10^{-3} M oleate concentration is related to the micelle formation (Antti&Forssberg 1989).

4 CONCLUSION

Carbonate alkalinity is an important characteristics of process waters open to atmosphere and can be as high as 10^{-3} M. At this alkalinity level, both cationic and anionic flotation of quartz is adversely affected. Cationic flotation of quartz in the presence of 10^{-3} M alkalinity can be improved upon increasing the amine addition. However, no improvements can be attained in the oleate flotation of quartz activated with calcium at the same alkalinity. As the carbonate alkalinity of the process water originates from either the dissolution of carbon dioxide in water or dissolution of carbonate minerals care must be taken to control both, so that flotation performance is not impaired.

REFERENCES

Anttı.-B.M and Forssberg, K.S.E.. 1989. Pulp Chemistry in Calcite Flotation Modelling of Oleate Adsorption using Theoretical Equilibrium Calculations. *Minemi.', Engineering.* Vol 2, No I. pp. 93-109.

Aplau. FF. and Fuersteiiau. D.W.. 1962. Principles of Nonmetallic Mineral Flotation. In Fuersteiiau, D.W.(ed.), *Froth Flotation.*

Clark, S.W and Cooke. S.R.B.. 1968. Adsorption of Calcium. Magnesium and Sodium Ion by Quartz. *Tram. AIME,* Vol 241. pp. 334-341.

Cooke. S.R.B.. 1949. The Flotation of Quartz using Calcium Ion as an Activator. *Trans. AIME.* Vol 184. pp. 306-309

Cooke. S.R.B. and Digre. M.. 1949. Studies on the Activation of Quartz with Calcium Ion. *Trans. AIME.* Vol 184. pp 299-305.

Fuersteiiau. M.C..I976. *Flotation, A.M. Gandin Memorial Volume.*

Howland. R..1.M.. Tappin. A.D.. Uncles. R.J.. Plummer. D.H. and Bloomer. N.J.. 2000. Distributions and Seasonal Variability of pH and Alkalinity in the tweed Estuary. U.K.. *The Si ience {if Total Environment,* Vol 25 I, pp. 125-138

Iskra. J.. 1997.a. Flotation Properties of Silicon Carbide with Anionic and Cationic Collecolor. *Ceramics International.* Vol 23. pp. 337-342.

Iskra. J.. I997.b. Flotation Properties of Silicon Carbide: II. On the Influence of Multivalent Cations on the Flotation ot Silicon Carbide with Sodium Oleate. *Ceramics International.* Vol 23. pp. 343-348.

Iwasaki. I.. 2000. Iron Ore Benetkiation in the USA: Past and Future. *Pioceedings of the <S" International Mineral Processing Symposium,* pp. 271-281.

Lin. 1.1. 1988. The Effect of Seasonal Variations in Temperature on the Performance of Mineral Processing Plants *Proceedings of the II. International Mineral Proi essing Symposium,* pp. 107-116.

Manukonda. V.R. and Iwasaki. I.. 1987. Control of Calcium Ion via Chemical Precipitation-Ultrasonic Treatment in Selective Flocculation. *Minerals and Metallurgical prot - essing,* Vol 4. No 4. pp. 217-222.

Onada. G.V. and Fuersteiiau. D.W., 1964. Amine Flotation of Quartz in the presence of Inorganic Electrolytes* *International Mineral Processing Congress Technical Papers.* Vol 7, pp. 301-306.

Rao. K.H. and Forssberg. E.. I991. Mechanism of Fatty Acid Adsorption in Salt-type Mineral Flotation. *Minerals Engineering.* Vol 4. No 7-11, pp. 879-890.

Scott. J.L. and Smith. R.W., 1992,. Ionic Strength Effects in Diamine Flotation of Quartz and Magnetite. *Minerals Engineering.* Vol 5. No 10-12. pp. 1287-1294.

Scott. J.L. and Smith. R.W.. 1993. Calcium Ion Effects in Amine Flotation of Quartz and Magnetite. Minerals Engineering. Vol 6. No 12. pp. 1245-1255.

Sirkeci. A.A.. 2000. Electrokinetic properties of Pyrite. Arsenopyrite and Quartz in the Absence and Presence of Cationic Collectors and Their Flotation Behavior. *Minerals Engineering.* Vol 13, No 10-11, pp. 1037-1048.

Snoeyink, V.L. and Jenkins. D.. 1980. *Water Chemistry.*

Somasundaran, P., 1974. Cationic Depression of Amine Flotation of Quartz. *Trans. AIME.* Vol 256. pp. 64-71.

Stumm. W. And Morgan. J.J.. *[9$\.Aquıtiı Chemistix.*

Takeda. S. And Usui. S.. 1988. Canonic Flotation of Quartz from An Artificial Mixture with Hematite Using Hexylamine. *Colloids and Surfaces.* Vol 29, pp. 221-232.

Uwadiale. G.G.O.O.. 1992. Flotation of Iron Oxides and Quaitz-A Review. *Mineral Processing and Ext rut live Metallurgy Review,* Vol 11, pp. 129-161.

Vidyadhar. A.. Rao. K.H. and Forssberg. K.S.E.. 2002. Adsorption of N-Tallow 1.3-Propanediamine-Dioleate Collector on Albite and Quartz Minerals, and Selective Flotation of Albite from Greek Stefania Feldspar Ore. *Journal of Colloid and Inleifai e Science,* Vol 248, pp. 19-29.

Ye, H. And Matsuoka, I., 1993. Reverse Flotation of Fine Quartz from Dickite with Oleate. *International Journal of Mineral Processing.* Vol 40. pp. 123-136.

Briquetting of Afsin/Elbistan and Sorgun/Yozgat Lignites without Adding a Binder

M. Yıldırım
Department of Mining Engineering, Çukurova University, Adana, Turkey

ABSTRACT: In this study, results of the cleaning and briquetting experiments of the lignite samples were presented. Basic aim of the work was to determine the binding effects of the humic acid contents of these lignite samples in the briquetting. Ash contents of the Afsin/Elbistan and Sorgun/Yozgat lignites were reduced to 29.8% and 14.8% respectively by the shaking table and flotation methods. The products cleaned were oxidized in atmospheric conditions in an oven at 90° C for the period of 48-192 hours. The oxidized samples were reacted with ammonium hydroxide (NH4OH) solution at again 90"C in a 2L laboratory reactor for one hour to generate ammonium humate, which was responsible for binding the coal particles into agglomerate. The green briquettes were heated from 135 to 175*C for one hour. The briquetting pressure was changed from 460 to 1565 kg/cm". In the end, although satisfactory mechanical resistances to the breakage were reached for both of the samples, water resistances of the briquettes obtained from the Afsin/Elbistan lignite were poor.

1 INTRODUCTION

There has been a long-felt need for a suitable, inexpensive and environmentally sound binder to consolidate the coal particles into weather- resistant agglomerates of convenient size for solid fuel use. Coal briquetting has generally been considered uneconomical for commercial-scale application. One of the impediments to coal agglomeration is the high cost of available hinders. Because coal is a relatively low-cost commodity, the binder must be low in cost and readily available to produce briquettes that are durable, moisture- resistant and should cause no hazardous environmental emissions during the combustion.

Many different binding materials have been used to facilitate the briquetting process in which it is responsible for increasing of cohesion forces between the particles of the briquetted materials. Conventional binders such as coal tar pitch provide strong briquettes. However, their use has been restricted due to their carcinogenic effects on human health and their contribution to air pollution. On the other hand some organic binders such as molasses, starch etc. provide poor moisture-resistant briquettes, and often subject to bacterial and fungal attack and may require the addition of environmentally 'unfriendly' biocides (Thomas et.al.. 1999).

Afsin/Elbistan and Sorgun/Yozgat lignites contain about 48%> and 16% humic acids respectively in organic base. It can easily be extracted after oxidation and alkali treatment operations. Binding property of ammonium humâtes has already been known (Wen, 1980; Yildirim and Ozbayoglu, 1995).

This work is basically considered with understanding the binding effect of the ammonium hydroxide soluble humic acid contents of these samples cleaned, which can be formed in the coal particles after the controlled aerial oxidation and ammoniation treatments. The nitric acid (HNOj) ajid alkali permanganate (KMnO.4) oxidation are much more rapid than the aerial oxidation, but the air as the agent is the cheapest and most widely available.

2 MATERIAL AND METHODS

2.1 Material

One of the samples used in the experimental works was taken from the size reduction input line of the Afsin/Elbistan power plant. The other sample was taken from the lump coal product of the Ayridam/Sorgun/Yozgat lignite deposit. Properties of the samples are shown in Table I.

Table 1. Proximate analyses of the R.O.M Atsın/Elbistan and Ayridani/Sorgun/Yozgat lignites

Contents	Elbistan lıenıte		Soreun leinte	
	Org" (%)	DB-(%)	Org¹ (%)	DB"(%)
Moisture	48 80	–	6.80	–
Ash	20.20	39.40	27 90	29.94
VM'	21 50	42.00	28.75	30 65
FC⁴	9.50	18.60	36.55	39.41
TS'	1.60	3.10	145	1.58 '
NCV"	940	1394	4380	4600

Original   ⁴Fixed caibon
~Diy basis   Total sulphui
Volatile matter   "Net calorific value (kcal/kg)

2.2 Methods

2.2.1 Removal of ash

Inorganic mineral particles in the samples, which have higher specific gravities than the lignite particles were cleaned by a laboratory scale-shaking table. For this purpose, Afsin/Elbistan and Sorgun/Yozgat lignites were crushed and classified into -1.400+ 0.250 mm and -1.000+0.500 mm respectively. These fractions were fed to the table in the pulp form (12-15 lt./min. water flowrate) and the products were taken separately.

The -0.250 mm sized fraction obtained from the Afsin/Elbistan lignite was mixed with the table tailing and pulverized by wet grinding conditions in a ball mill to provide further liberation of the mineral matters (Figure I). Then, the ash making material in -0.074 mm sized product was cleaned by the agglo-flotation method. Here, fuel oil (No.6) containing *20'/i* kerosene was used as the agglomérant. For each agglomeration test lOOgr. of the sample and 900 ml. tap water was placed in a 1000 ml. Denver Cell. Then, 35% fuel oil /kerosene emulsion [emulsion% = wt. of emulsion xlOO/ feed wt.x(100-%ash)/100] was added. 0.5 ml. of Na_2SiO_3 (10%) and a few drops of pine oil were added to depress siliceous and pyrite minerals and to improve the frothing. The results obtained for the agglo-flotation are shown in Table 2.

-0.5 mm sized Sorgun/Yozgat lignite fraction was directly fed to the flotation cell. I ml. of NajSiO.i (10%) and 6 ml. of pine oil/kerosene (IV/5V) emulsion were added to the pulp containing 10% solids. After obtaining the concentrate cleaned it was dcwatered and analyzed (Figure 2). The results are shown in Tables 2, and 3.

2.2.2 *The aerial oxidation and ammoniation*

Oxidation experiments were conducted on the cleaned samples. In each case, about 100 gr. of the sample was spreaded on the tlat bottom of an aluminum pan that has 200 mm diameter to provide air lo the particle surfaces completely, and placed in an oven. After heating the sample in atmospheric conditions at 90"C for the periods from 48 to 192 hours, it was cooled.

Then certain amount of oxidized sample was placed in an autoclave and predetermined amount of ammonium hydroxide solution (NHi(g)/coal (g): 0.2 and solid (g)/liquid (g): 1.3-1.7) was added. The mixture was stirred at 90"C tor about one hour. Alter this period, it was observed that it was in muddy form and dark brown colored ammonium humate generated and covered the whole surfaces of the particles. This muddy mixture was taken out of the vessel and dried until to reach 10.50% moisture content.

2.2.3 Briqitetting

In the pressing experiments, 30 g. of the sample obtained from the ammoniation treatment was transferred to a cylindrical steel mould (Figure 3). The sample in the mould was heated up to 80"C externally and pressed between the bottom and top steel discs by the steel pressing piston to which an adjusted pressure was provided from an oil-hydraulic type press. The briquetting pressure was changed from 460 to 1565 kg/cm". After the pressing, the briquette sample was taken out of the mould and placed in a drying oven already heated to 80" C. Heating temperature was then increased from 135 to 175" C for 60 minutes to see the effects of heat treatment or on the strength and moisture resistance properly of the briquettes cylindrical in shape. After this period it was gradually cooled to room temperature and conserved for the analyses and quality tests. The results are shown in Tables 4, 5,6 and7.
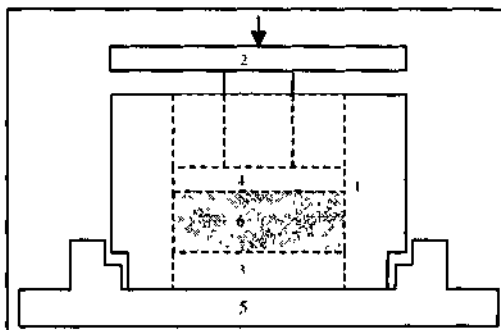

Figure .3 Schematic view of the pressing mould.

1 Sieel mould (46x65 mm)
2. Steel pressing piston (40x 100 mm)
3 Sleel disc-bottom (15-45 mm)
4 Sleel disc-top (15x45 mm)
5. Sleel down plate (stable)
6 Sample placed

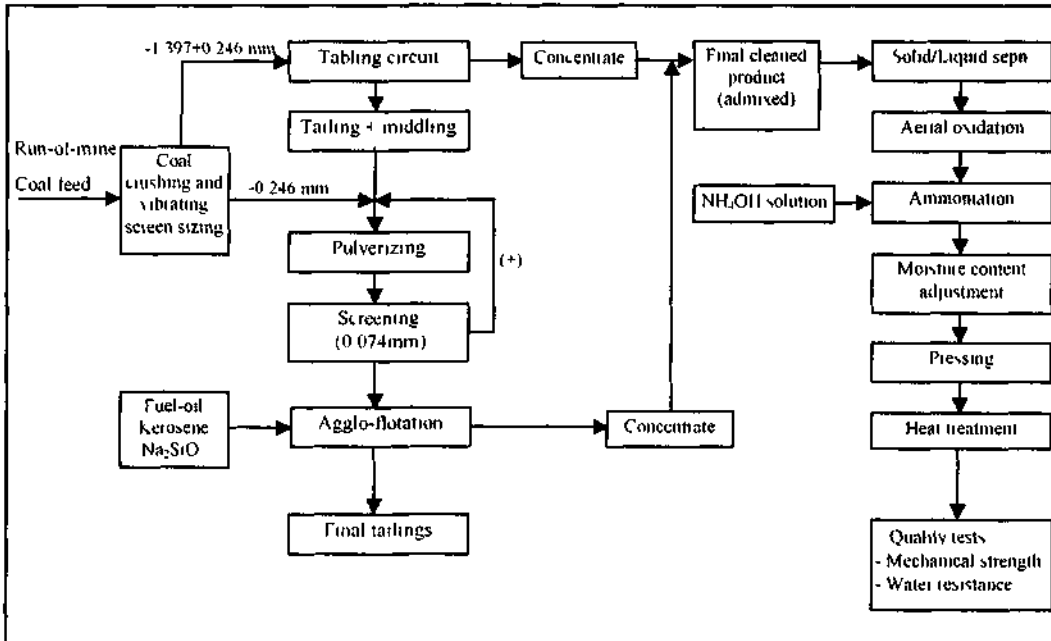**Figure 1**

-1 397+0 246 mm → Tabling circuit → Concentrate → Final cleaned product (admixed) → Solid/Liquid sepn

Run-of-mine Coal feed → Coal crushing and vibrating screen sizing

Tailing + middling

-0 246 mm

Pulverizing (+)

Screening (0 074mm)

Aerial oxidation

NH₄OH solution → Ammoniation

Moisture content adjustment

Pressing

Heat treatment

Fuel-oil Kerosene Na₂SiO → Agglo-flotation → Concentrate

Final tailings

Quality tests
- Mechanical strength
- Water resistance

Figure 1 Simplified schematic diagram of the experimental works for the Afsin/Elbistan lignite at laboratory scale

---

Figure 2

-1 00 + 0 5 mm → Tabling circuit → Concentrate → Final cleaned product (admixed) → Solid/Liquid sepn

Run-of-mine Coal feed → Coal crushing and vibrating screen sizing

Tailing + middling

Pulverizing (+)

Screening (0 5mm)

Aerial oxidation

NH₄OH solution → Ammoniation

Moisture content adjustment

Pressing

Heat treatment

Pine-oil Kerosene Na₂SiO₃ → Flotation → Concentrate

Final tailings

Quality tests
- Mechanical strength
- Water resistance

Figure 2 Simplified schematic diagram of the experimental works for the Sorgun/Yozgat lignite at laboratory scale

2.2.4 Quality tests

In order to determine the axial-compressive strength obtained by applying compression through the flat surfaces of the tablet like briquettes.an ELE 3000KN compression-testing device was used. After placing the briquettes on the compression unit of the device, pressure was applied through the surfaces and the load required to crush the briquette under compression was recorded. This load was divided by the area of the flat surfaces of the briquettes (15.89 cm") and the axial strength was obtained as kg/cm.

There has been no standard leading method to measure the water resistance of the coal briquettes. In this work, 5 of the briquettes that each has about 40 cm' volume were immersed in 600 ml of water for 24 hours and after that period the briquettes were dried and screened with a 10 mm sieve. The weight percent of the fines passed through the sieve was found as the water disintegration index. Water resistance of the briquette was calculated by subtracting the water disintegration index from 100.

3 RESULTS AND DISCUSSION

3.1 Cleaning

Table 2. Results of the cleaning operations on the Afsin/Elbistan lignite.

Cleaning Operation	Concent rate		Tailme+ middling		AR (%)	RC (7r)
	Wt. (%)	Aslı (%)	Wt.	Ash		
Tabling	58.1	27.1	41.9	56.4	60.0	69.9
Agglo-flotation	65.4	32.4	34.6	74.6	54.9	83.4

Table 3. Results of the cleaning operations on the Sorgun/Yozgat lignite

Cleaning Operation	Concentrate		Tailina+middling		AR (%)	RC CA)
	Wt. (%) ex)	Ash (%)	Wt. (%)	Ash (%>		
Tabling	58.0	15.0	42.0	47.1	69.5	68.9
Agglo-flotation	58.7	14.6	41.3	48.7	70.1	70.3

Percentage of ash rejection (AR) and percentage of recovery of combustibles (RC) were calculated by the following approach, e.g. AR for the tailing and RC for the concentrate (Suresh and Arnold, 1995).

AR(%) = [tails wt. x *1* ash of tails]xlO0 /

[tails wt x *9r* ash of tails) + (cone wl x % ash of cone.)]

RC('/r) = [cone. wl. x (100 - »ash of cone.)] x I (X) /

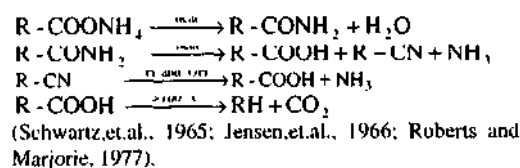[conc.wt.x (100- %ash of cone.) + (tails wt.x (100- %ash of tails)]

As shown in Table 2, the ash content was reduced from 39.4% to 27.1% by the tabling circuit and at the end a final product containing 32.4% ash was obtained. It is indicated from these results that liberated inorganic mineral particles that have higher specific gravities than the lignite particles were successfully separated due to the gravity differences. Nevertheless, fairly high percentage of recovery of combustibles (RC) was achieved. The percentage of ash rejection (AR) obtained was not high for the flotation circuit. This was possibly due to the insufficient liberation of clay type mineral matter in the Elbistan lignite. On the other hand it is shown from Table 3, that a clean product containing 14.6% ash was obtained by the flotation, which was the final stage in the cleaning operation of the Sorgun/Yozgat lignite. Hence, the AR and RC values reached were high enough and a low ash-bearing product was obtained.

3.2 Effects of the heat treatment

Table 4. Effect of the heat treatment on the durability of the briquettes (briquetting pressure: 1280 kg/cm"; the oxidation period: 144 hours).

Heal ("O	Elbistan Li'.;nıte		Soreun Lignite	
	Axial Comp. Sır. (ke/enr)	Water Resistance (%)	Axial Comp. Str. (kg/cm^2)	Water Resistance (%)
135	117.7	0	104.0	0
145	12X.1	0	118.1	0
155	133.4	0	126.4	0
165	176.5	0	151.0	100
175	152.3	0	138.2	100

Heal treatment temperature to improve the water resistance of the briquettes was the most critical parameter. The best results for both of the samples were obtained at the temperature 165"C. This result was in agreement with the results obtained by the previous workers (Driskell, 1961; Wen, 1980). The possible reactions took place during the heating operation on the ammonium humate binder could be given as:

$$R\text{-}COONH_4 \longrightarrow R\text{-}CONH_2 + H_2O$$
$$R\text{-}CONH_2 \longrightarrow R\text{-}COOH + R\text{-}CN + NH_3$$
$$R\text{-}CN \longrightarrow R\text{-}COOH + NH_3$$
$$R\text{-}COOH \longrightarrow RH + CO_2$$

(Schwartz,et.al., 1965; Jensen,et.al., 1966; Roberts and Marjorie, 1977).

The results shown in Table 4, mentions that although acceptable level of the axial compressive strength of the briquettes produced from both of the samples was achieved, no water resistant briquet was obtained from the Afsin/Elbistan lignite sample. It was most probably due to the finely dissemination

of the clay mineral particles in the sample. Whereas, water resistant and durable briquettes were produced at 165"C temperature from the Sorgun/Yozgat lignite sample.

3.3 Effects of the oxidation period

Table 5. Effect of the oxidation period on the durability of the briquettes (briquetting pressure 1280 kg/cm"; heat treatment temp. 165"C).

| | Elbistan Liamte | | Sorsun Lianite | |
Oxidation Period (hours)	Axial Comp. Str. (kg/cm"!1	Water Resistance (%)	Axial Comp. Str. <kg/cnr)	Water Resistance (%)
48	137 1	0	65.6	0
96	147.0	0	93.1	54
144	173.2	0	154.1	100
192	166.0	0	167.1	100

It is shown in Table 5, that as the oxidation period was increased stronger briquettes were obtained. The possible reason was that amount of the alkali soluble humic acid binder which was basically ammonium humate (R-COONH4) salt increased between the particles to be agglomerated (Yildirim and Ozbayoglu, 1997). In order to obtain durable briquettes from both of the samples it was definitely necessary to prolong the oxidation period up to at least 144 hours.

3.4 Effects of the pressure

Table 6. Effect of the briquetting pressure on the durability of the briquettes (oxidation period: 144 hours; heat treatment temperature: 165"C).

| | Elbistan Lianite | | Soi 2l1ll Lianite | |
Enqueuing Piessure (ke/cnr)	Axial Comp. Sır. (kg/cm²)	Water Resistance W	Axial Comp. Str. (ka/cıır)	Water Resistance (%)
460	112.4	0	105.0	84
711	135.5	0	128.4	90
995	148.2	0	137.2	91
1280	171.0	0	161.4	100
1565	184.3	0	180.1	100

Briquetting pressure was effective on the axial compressive strength of the briquettes. As it was increased the strength of the briquettes improved. As it is shown in Table 6, when the pressure was 1280 kg/cm² l00'% water resistance and 161.4 kg/cm" axial compressive strength were achieved for the Sorgun/Yozgat lignite sample. The pressure was not effective on the water resistance of the Afsin/Elbistan lignite briquettes.

Table 7. Results of proximate, sulphur and calorific value analyses of the briquettes obtained from the cleaned products.

Contents	Elbistan Lignite (% dry basis)	Sorgun Lignite (% dry basis)
Moisture		
Ash	29.8	14.8
Volatile matter	34.1	37.5
Fixed carbon	36.1	47.7
Total sulphur	2.5	1.2
Net calorific value	3688	5880

4 CONCLUSIONS

1. In order to decrease ash content of the Afsin/Elbistan lignite sample to lower levels it should definitely be ground into finer size intervals, and an ash removal technique that is efficient in processing finely sized lignite particles such as column dotation may be chosen. There was not any problem in cleaning of the Sorgun/Yozgat lignite by the shaking table and conventional flotation methods.

2. When Afsin/Elbistan and Sorgun/Yozgat lignites are oxidized in air at 90"C for more than 144 hours, ammonium hydroxide soluble humic acids are formed, and it can be extracted in liquid form at 90"C.

3. When the briquettes are heated at temperatures lower than 165"C poor water resistance property are achieved. If the temperature is higher than 165"C water resistant but weak briquettes will be obtained. So, the heat treatment temperature is critical parameter and it is around I65"C in this method.

4. The ammonia gas (NH3) released during the heat treatment can easily be converted into ammonium hydroxide, which can be recycled and used for the extraction of ammonium humate. This will lower the cost of the method.

5. The briquettes having enough mechanical strength but not water-resistant can be produced from Afsin/Elbistan lignite. This method is promising in producing briquettes from lignites containing more than 15% alkali soluble humic acids in organic base and ash that does not consist mainly of clay type mineral matter liberating at very fine sizes.

REFERENCES

Alonso, M.I.. Values. A.F.. Martinez-Tarazona. R.M. and Garcia. A.B.. 1999. Coal recovery from coal tines cleaning wastes by agglomeration with vegetable oils: effects of oil type and concentration. *Fuel.* Vol.78, pp.753-759.

Dnskell. J.C.. 1961. Coal-a source of humic acids, humâtes, and humamides. *Literature Survey, Tennessee Valley Authority Division of Chemkal Development Applied Research Branch.*

Jensen. E.J.. el., al.. 1996. The dry oxidation of subhituminous coal. *Coal Science.* Vol. 55, pp. 621-642.

Roberts. D.J.. and Marjorie. C.C., 1977. *Basic Principles- of Organic Chemistry.* 2"¹ Edition, W.A. Benjamin Inc..

Saracogullan. M. and Gencer. Z.. 1990. Bnquetting of Soma and Tuncbilek lignites with various kinds of stalks and an investigation of their combustion properties. *Proi. of the III. International Mineral Processing Symposium.* Istanbul. 305-113.

Schwartz, D.. Asfeld. L.. and Green. R.. 1965. The chemical nature of the carboxyl groups of humic acids and conversion of humic acids to ammonium nitrohumates. *Fuel.* Vol.44, pp. 417-424.

Suresh. M.S.. and Arnold, D.W.. 1995. Recovery of waste line coal by oil agglomeration. *Fuel.* Vol.74. No.3. pp.459-465.

Thomas. L.J.. Snupe CE. and Taylor. D.. 1999. Physical characteristics of cold cured anthracite/coke breeze briquettes prepared from a coal tar acid. *Fuel.* No. 78. pp. 1961-1965.

Wen. W.W.. 19X0. A humic acid binder for pellelizing of fine coal. *Wilt International Coal Preparation Congress.* Pittsburgh Energy Technology Center. U.S. DOE. Pittsburgh, pp. 120-131.

Yildinm. M. and Ozbayoglu. G.. 1997. Production of ammonium nitrohumate from Elbistan lignite and its use as a coal binder. *Fuel.* Vol.93. No. I045.pp.l()3-I06.

Yildinm. M. 1995. *Production of Water Resistant Coal Briquettes hv the Use ofHumii Acid Binder.* Ph. D. Thesis. Middle East Technical University. Ankara.

390

Selective Separation of Na-K Feldspar in Nepheline Syenite

C. Karagiizel
Department of Mining Engineering, Osmungazi University, Eskişehir, Tıırkev
C. Demir
Department of Mining Engineering, Karadeniz Technical University, Trabzon, Turkey
I. Gülgönül
Department of Mining Engineering, Balıkesir University, Balıkesir, Turkey
İ. Bentli
Department of Mining Engineering, Dumliipinar University, Kütahya, Turkey
M.S. Çelik
Department of Mining Engineering. Istanbul Technical University, Istanbul, Turkey

ABSTRACT: Differential flotation of albile and microcline in a synthetic feldspar mixture with amine (G-TAP) at natural pH is accomplished with monovalent inorganics at an optimum salt concentration of $5 \times 10^{"2}$ M. Testing of this concept on a nepheline syenite ore using magnetic separation followed by flotation resulted in a major increase in the total alkali content along with a significant removal of colored impurities. Particularly, the remarkable effect of slime coating on flotation recoveries is intriguing. Application of differential flotation using monovalent inorganics on a nepheline syenite ores has shown that perthitic texture of the ore hinders the selective separation of Na and K feldspars.

1 INTRODUCTION

Albite (NaAISUOx) and microcline and/or orthocla.se (KAlShOs), are the most important commercial feldspar minerals. They are generally found together with quartz, mica and colored impurities. Beneficiation of feldspar minerals is mainly performed by separation methods including gravity, magnetic separation, and flotation. Although the concentration scheme is usually dependent upon the quality ot the end product, flotation is the most widely used beneficiation method for the separation of quartz, mica and sometime of colored impurities. The main application of flotation is in the treatment ol typical feldspar containing rocks such of pegmatites, nepheline syenites and granites. Among the impurities the mica is normally removed first followed by flotation of ferruginous impurities. Once the mica and ferruginous impurities have been removed, the feldspar is then floated from the quartz.

In feldspar rocks where Na- and K-Feldspar minerals are found together, it is important to separate feldspar into individual phases of Na and K. In a typical rock, Na and K-mincrals exhibit NaiO or K;0 values in the range of 3 to 5 %. The aim for a practical application is often to raise one of the values of NaiO or KiO above 8 % while keeping the other below 3 %.

The floatability of individual feldspar minerals has not been well studied in the literature (Demir et al. 2001). Thus, their separation remains as a controversial subject. Our earlier micro flotation study revealed that the separation of albite from microcline is possible with cationic collectors at natural pH in the presence of monovalent inorganic electrolytes.

In this study, the applicability of this concept has been first tested on a set of synthetic feldspar minerals and then extended to an actual ore, nepheline syenite. The problems associated with this concept are elaborated on the basis of flotation data.

2 EXPERIMENTAL

Albite and microcline samples of high purity used in these experiments were obtained from Aydin-Cinc region of Turkey. The chemical analysis of the samples shown in Table 1 together with the XRD analysis (Figure 1) reveals that the samples are albite, and microcline with albite impurity. The lump sized materials were crushed by a hammer and ground in an agate mortar followed by wet screening to produce a sample of - 150 microns in size.

Mineralogical investigations on the feed sample were carried out through microscopic examinations. The chemical analysis of the feldspar ore used in this study is presented in Table 1. The chemical and microscopic analysis coupled with XRD determinations reveals that the ore contains albite, microcline, biotite, nepheline, chlorite, epidote, rutile, and opac minerals (magnetit, pyrite).

Table I. Complete chemical analysis of feldspars.

hem	Nepheline syenite %/<	Albite*	Mieiochne %
SiO:	5X %	66.02	65.30
A1,0,	18.34	19.92	18.72
Fe₂0,	5.4	0.04	0.05
TiO	0.73	0.04	0.01
Na 0	4.22	10.68	2.84
K₂0	6.3	0.42	11.81 •
CaO	2.3	1.74	0.24
M.aO	1.4	0.04	0.01
LOI	105	0.50	0.60

The ore sample received from the Sorgun-Yozgat region of Turkey was reduced down to 1 mm in size by a combination of jaw, cone and roll crusher. The sample was divided into three size fraction as - 1+0.6, -0.6+0.3, and -0.3+0.2 mm and used for magnetic separation. The minus 0.2 mm size fraction was kept aside. The non-magnetic product was further ground to obtain a product of -0.2 mm in size. The grinding tests were carried out in a ceramic mill to prevent iron contamination. The grinding tests were conducted for 12, 15 and 20 minutes of which the 20-minute test result was selected because of its appropriate size distribution and also relatively less slime formation.

Magnetic separation tests were carried out by a rare-earth permanent magnetic roll separator abbreviated as the REMS. All REMS tests were carried out in a single-stage. In all experiments, the sample weight used for an each size fraction was 300 grams. The resultant magnetic and nonmagnetic fractions were collected and analyzed for TiO:, Fe^O.i, and K:0 using X-ray Flourescence (XRF). The effects of front splitter angle, back splitter angle, roll speed, and feed rate parameters were optimized.

Flotation tests for nepheline syenite were performed in a Denver cell equipped with a 1.5 I cell. A sample of 300 g was mixed with 1200 ml tap water at 1250-rpm impeller speed. Both conditioning and notation were carried out at the same impeller speed and percent solids by weight. Desliming was made prior to flotation. No desliming and no frother were used in the case of synthetic sample. Conditioning period of 5 min. for the first-stage conditioning and 3 min for the subsequent stages of collector addition was utilized. Percent solids by weight and natural pH of 7.7 were kept constant in most experiments unless otherwise specified. Aerofroth 88 was used as a frother. The float and unfloat fractions were analyzed for KjO by X-Ray fluorescence spectrometer (XRF) and Na^O by atomic absorption. All other chemical analyses were performed by wet chemistry and XRF methods. The cationic collector (Genamin-TAP) is a commercial

reagent manufactured by Clariant of Germany. The reagent is in the solid form and was prepared at pH 3 as recommended by the manufacturer. The pH was adjusted by HCl and NaOH.

3 RESULTS AND DISCUSSION

Nepheline syenite, similar to feldspar, is an igneous rock composed of aluminum silicates together with an alkali ion such as Na and K. It is a light-colored, quartz-deficient feldspathic rock made up of mostly albite, microcline and nepheline, a mineral with the composition of (Na, K) AISİO4 (Burger, 1990: Kendall, 1993). The nepheline mineral which imparts industrial features to the rock is $Na_3KAI_4Si_4Oi6$ with a ratio of 3/I=Na/K.

Nepheline syenite is a raw material alternative to feldspars. While about 85 % of it is used in ceramic and glass industries, 15 % of it is used in the production of a variety of products including paints, fillers, and insulators. However, nepheline syenite has a higher alkali/alumina ratio than feldspar, and, thus a good fluxing effect. In glass nepheline syenite improves the workability and lowers the melting temperature and also supplies alumina, which provides increased resistance to scratching and breaking, improved endurance, and increased chemical durability (Potter, M J Min yearbook 1994). For colorless glass, the nepheline syenite like feldspar should not contain more than 0.1% Fe?Oi. Iron content may be up to 0.5% FeiOj in colored glass.

3.1 Magnetic Separation Texts

Magnetic separation tests were carried out by a dry rare-earth permanent magnetic roll separator (REMS). The results conducted in different size fractions as -1+0.6, -0.6+0.3, and -0.3+0.2 mm are shown in Table 2. Some parameters were fixed based on the previous studies (Çelik et al., 1999). The roll speed of 45 rpm, right splitter angle of 80° and left splitter angle of 140" were used in magnetic separation experiments (Yılmaz. 2001). The results were evaluated on the basis of TiOş, FeiCh, and KjO grades in the nepheline syenite concentrate.

The combined results of different size fractions are shown in Table 2. It can be seen that nepheline syenite concentrate (non-magnetic product) containing 0.76% Fc₂0?, 0.82 Ti0₂, and 7.69% K 0 is obtained.

Table 2. Magnetic Separation Test Results

Size (mm.)	Products	Weight (%)	Fe,0., (%)	Ti0$_2$ (%)	K$_2$0 (%)
-1+0.6 (40.7%)	Cone.	45.8	0.78	0.76	7.96
	Middlings	43.3	4 49	0 42	5.87
	Tailings	10.9	10.54	0 02	4.61
-0.6+0.3 (27.3%)	Cone.	61.0	0.80	0 82	7.54
	Middlings	31.4	5.40	0.11	4.72
	Tailings	7.6	13.07	0 19	4.07
-0.3+0.2 (10.8% l	Cone.	67.7	0 62	0 99	7.36
	Middlings	25 0	5 17	0.26	5 16
	Tailings	7.3	17 15	0 01	2 97
Combined Cone. -l+0.2mm		100 0	0.76	0 82	7.69

Figure I Floatabilny of feldspar minerals versus NaCl concentration.

3.2 Flotation Tests

Figure I shows that the flotation profile of syntehie sample composed of albite and microcline at lOOg/ton constant amine concentration as a function of NaCl concentration at natural pH. It can be seen that the selectivity between Na-feldspar and K-feldspar is improved upon increasing NaCl concentration. The most effective selectivity occurs between albite and microcline at amine solutions of 0.83 mg/l at the expense of recoveries. The reason for the depression of albite can be ascribed to the inability of albite to undergo an effective ion exchange process with NaCl and thereby remain less negatively charged surface unto which the adsorption of calionic collector is relatively hindered (Demir et al. 2001).

In this study, the nepheline syenite ore was first subjected to magnetic separation and the concentrate was treated by flotation to test the possibility of sodium-potassium feldspar separation using G-TAP as collector and NaCl as depressant. Flotation tests were conducted at 20 wt. "/<• solids. The effect of G-TAP concentration on grades (KjO) and recoveries is presented in Figure 2. A small amount of Aerofroth 88 (20 g/t) as frother was added. A series of experiments performed to determine an optimum flotation time resulted in a froth removal time of 60 sec.

The results do not show any significant trend to demonstrate an optimum amine dosage (Figure 2). The reasons for this could be attributed to the non-systematic desliming during flotation tests. A value of 150g/t G-TAP dosage given in previous works was used for optimization of desliming studies.
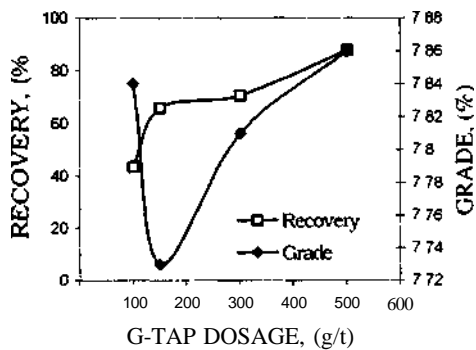
Figure 2 Effect of G-TAP Dosage on K.0 grade and recoveiy for nepheline syenite.

3.2 Effect of Slime in Flotation Tests

A series of desliming tests were designed to determine the effect of slime coating on flotation. The desliming tests were conducted in a 2 l graduated cylinder. The suspension of 1800 in volume was stirred and a portion of the upper part was removed and the particle size distribution and corresponding weight % was recorded. A separate test was performed for each desliming stage followed by a separate flotation experiment. The

results shown in Table 3 and Figure 3 indicate that while desliming less than 12 % of the total material resulted in zero recovery, only at and above 24 % desliming was the nepheline syenite flotation restored. These results are unique as they demonstrate that even a portion of -0,074+0.038 mm size fraction had to be removed in order to avoid slime coating effect.

Tatile 3. Liberation of slime

Slime (%)	Particle Size (mm.)	Weight (%)
4	-0.038	100.0
8	-0.038	100.0
12	-0.038	100.0
16	-0.074+0.038	44.7
	-0,038	56.3
24	-0.074+0.038	38.2
	-0.038	61.8
32	+0.074	7.9
	-0.074+0.038	27.3
	-0.038	64.8
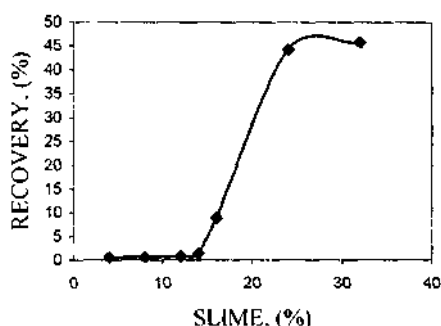
Figure 3 Effect of Slime coating on flotation recoveries of nepheline syenite.

3.4. Effect of NaCl and KCl Addition in Flotation Separation

The effect of NaCl and KCl dosage on the separation of sodium and potash feldspars was investigated with 150 g/t G-TAP (150 g/t) as collector at natural pH. Tables 4 and 5 present the effect of NaCl and KCl additions on separation. Figure 4 illustrates the combined results. The results are evaluated on the basis of NanO and KiO grades in the nepheline syenite concentrate.

It is evident from Tables 4 and 5 together with Figure 4 that feldspar recoveries are substantially decreased with increasing both NaCl and KCl dosages. But depression is more pronounced with NaCl addition. These results are in line with our

earlier reports (Demir et al., 2001). The absence of change in Na:0 and KiO grades is intriguing. Optical microscopic analysis indicates that in nepheline syenite (NatKAl$_4$SijOir.) potassium ions are not in the form of individual microcline or orthoclase but rather imbedded in the nepheline syenite matrix. This perthitic texture identified as potash rich feldspar containing intergrown plagioclase is probably crystallized as a product of exsolution. In other words, because potassium ions are largely part of nepheline structure, it is not possible to induce a selective separation between Na and K at natural pH of 7.7. It is believed that it might be possible to obtain a better separation in HF medium.

Table 4 Effect of NaCl on Flotation Recovery

NaCl conc (M)	Products	Weight (%)	K$_2$O (%)	Na$_2$O (%)	Rec. (%)
5.10-	Cone.	42.9	7.81	-	43.4
	Tailing	57.1	7.61.	-	56.6
	Feed	100.0	7.70	-	100
1.10'''	Cone.	80.0	7.95	5.47	82.4
	Tailing	20.0	7.27	5.36	17.6
	Feed	100.0	7.81	5.41	100
2.10^1	Cone.	81.5	7.83	4.48	82.6
	Tailing	18.5	6.62	4.52	17.4
	Feed	100.0	7.59	5.41	100
S.1O'	Cone.	50.8	7.88	-	51.8
	Tailing	49.2	7.75	-	48.2
	Feed	100.0	7.82	-	100
1	Cone.	13.6	7.78	4.52	13.7
	Tailing	86.4	8.39	4.91	86.3
	Feed	100.0	8.30	5.41	100

Table 5 Effect of KCl on Flotation Recovery

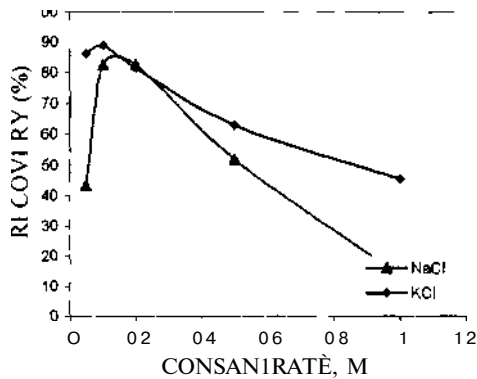| NaCl cone (M)	Products	Weight (%)	K$_2$0 (ft)	Na$_3$0 (%)	Ree. (%)
S.10^{-2}	Cone.	86.1	1.14	-	86.4
	Tailing	13.9	7.19	-	1.3.6
	Feed	100.0	7.66	-	100
U O^1	Cone.	86.8	7.90	-	88.8
	Tailing	13.2	7.30	-	11.2
	Feed	100.0	7.82	5.41	100
2.iCT	Cone.	80.0	7.87	4.89	81.5
	Tailing	20.0	7.15	-	18.5
	Feed	100.0	7.37	5.41	100
5.10''	Cone.	62.9	7.72	-	62.9
	Tailing	37.1	7.54	-	37 1
	Feed	100.0	7.65	5.41	100
1	Cone.	45.2	7.76	4.92	45.4
	Tailing	54.8	7.45	5.14	54.6
	Feed	100.0	7.59	5.41	100

394

Fıgıııe 4 Combined Test Results on the effect ol inorganic electiolytes

4 CONCLUSIONS

Selective flotation of albite and microcline in a synthetic mixture with amine (G-TAP) at natural pH is achieved in the solutions of NaCI and KCl salts

Benefiuation of a nepheline syenite ore using magnetic sepaiation followed by flotation lesulted in a majoi unpiovement in the total alkali content with a significant ıemoval of coloied impurities The remaikable effect of slime coating on flotation tecovenes demonstrates the crucial eltecl of desliming

Application ot dılfeıentıal flotation using monovalent inorganics on a nepheline syenite oies

has shown that perthitic textuie of the ore has detenoratcd the selective sepaiation of Na and K feldspars

ACKNOWLEDGEMENTS

REFERENCES

Buıgeı I I990 Feldspai and nephclme syenite at the meicy ol glass maikets *tntliisliial mmaals* 2! 26

Çelik MS Fren RH Uztek G Gürcuoglıı Doğan M Z 1999 Benefiuation ot Nepheline Syenite by Magnetic Sepaıalıon and Flotation Techniques *Pioiiitlintfs ol VIII Balkım Mııcıal Pıoı ıssııii, Conltiinii* Heiceg Novi Sepl 14 IX

Deınıı C Abiamov A A And Çelik MS 2001 Flotation sepaiation of na teldspai tiom k-leldspai by monovalent salts *Minimis enziminin,* 14 7"?^ 740

Kendall T 1991 Feldspai and nepheline syenite the alumina pıovıdeıs *IM Glass anil Ciiamits Sums* 17 19

Potteı M I 1994 Feldspai and Nepheline Syenite *US Geiihtiiial Stu\i\ Mini nils Yearbook* 26 126 7

Yılmaz III 2001 Recoverv ol Na-K I eldspar in Nepheline Syenite *Gıtuluattım lhı\ı\ Mumu; Itııult\ Istanbul Tti/i/muf Uimn\l* Istanbul Tuikey

Microwave Heating Characteristics and Microwave Assisted Magnetic Enhancement of Pyrite

T.Uslu
Department of Mining Engineering, Black Sea Technical University, Trabzon, Turkey

Ü.Atalay
Department oj Mining Engineering, Middle East Technical University, Ankara. Turkey

ABSTRACT: In this study, microwave heating characteristics and microwave assisted magnetic enhancement of pyrite were investigated. Studies include the microwave heating of pyrite samples having size fractions of -1680+1200 urn, -1200+ 850um , -850+420um , and -420 urn in a microwave oven at 850 W, 680 W and 510 W power levels and 2.45 Ghz frequency. The microwave treated pyrite samples of -420 |im particle size, was subjected to magnetic separation process at magnetic field intensities of 0.1, 0.3 and 0.5 Tesla. It was observed that heating rate and maximum attained temperature of pyrite samples increased with increasing power levels and decreasing particle size. Of all heatings, highest attained temperature and heating rate were observed for -420|im size fraction and at 850 Watt. Temperature raised to 860°C in 495 seconds. Magnetic-separation tests showed that amount of magnetic product recovery increased with increasing temperature, and magnetic field intensity. Following the 120 seconds heating at 825 °C, 97 % of the pyrite was removed as magnetic product by magnetic separation at 0.5 Tesla.

1 INTRODUCTION

Microwave energy is nonionizing electromagnetic radiation with frequencies that range from 300 MHz to 300 GHz or wavelength that range from 1 mm to 300 mm. Microwaves can be transmitted, absorbed or reflected. Insulators are transparent to the microwaves and. thus, do not store any of energy in the form of heat. Metals with high conductivities, reflect the microwaves which provide no significant heating effects. Materials such as semiconductors, with medium conductivities, typically from 1 to 10 Sm"¹, can be effectively heated with microwaves. (Xia & Pickles 1997). The materials which absorb the microwave contain dipoles. When microwaves are applied to the material, the dipoles align and Hip around, as the applied field is alternating. Materials heat when the stored internal energy is lost to friction. (Kelly & Rowson 1995; Kingman et al. 1999; Haque 1999). The advantages of microwave heating are rapid and selective heating, uniform heal distribution,flexiblemoduler design, environmentally friendly application, fast switch-on and switch-off. and high efficiency. Cooking food, drying, pasteurising, curing, thawing and tempering, waste control, denaturing proteins, deinfestation are some ot the examples of microwave processing (Matthes et al. 1983: Vasilakos & Magalnaes 1984).

In recent years there has been a growing interest of microwave heating in mineral treatment and a number of potential application of microwave processing have been investigated. These include microwave assisted ore grinding, microwave assisted carbolhermic reduction of metal oxides, microwave assisted drying and anhydration, microwave assisted mineral leaching, microwave assisted roasting and smelting of sulphide concentrate, microwave assisted pretrcatment of refractory gold concentrate, microwave assisted spent carbon regeneration and microwave assisted waste management.

One of the most important possible application of microwave heating is coal desulphurization. The inorganic sulphur occurs in raw coal mainly in pyritic and sulfate form. The separation of fine pyrite from coal is difficult by conventional magnetic separation methods. The performance of magnetic separation in removing mineral pyrite from coal can be improved by increasing the pyrite's magnetic susceptibility. Several studies have shown that magnetic susceptibility of pyrite can be enhanced by heating (Ergun &Bean 1968). However, the problem of heating pyrite in coal is that energy is wasted by also heating the coal. (Fanslow et al. 1980). A selective method of heating is to use microwaves at sufficiently high energy density to heat quickly for

minimum heat loss to the coal (Fanslow et al. 1980; Kelland et al. 1988)

2 EXPERIMENTAL

2. / *Mineral Sample*

Different size fractions of test .samples were prepared from pyrite crystals by comminution and sieving. These fractions were -1680+1200u.m, -1200+850um . -850+420um . and -420 urn. Samples were further purified through microscopic examination and cleaning.

2.2 Microwave Treatment

A variable power (maximum output 850 watt) and 2.45 GHz microwave oven was used for microwave heating. 10 grams of representative samples of different size fractions were heated at 850 W, 680 W and 510 W applied power levels. Each sample for every run was loaded into microwave transparent porcelain crucible. A stainless steel-sheathed, K type thermocouple which was inserted through the roof of oven and hole of crucible cover was used for measuring and continuously monitoring sample temperature. The accuracy of the thermocouple data was with in + 2 °C from measurements made on boiling water. Healing was continued until the maximum temperatures was attained. Microwave treatment was also applied under inert nitrogen atmosphere. Thermocouple data were recorded during irradiation in both air and nitrogen atmosphere. To minimize the effect ot field pattern variations within the oven, the curicible was always located in the same central position.

2.3 *Magnetic Separation*

Alter determining the healing characteristics of different size fractions of pyrite samples, samples of finest fraction namely -420 \im were subjected to microwave irradiation for 120 seconds at attained temperatures of 325 °C, 475 °C, 625 °C, 725 °C, and 825 °C. A switch off equipment was connected to microwave oven to keep the temperatures constant during the microwave irradiation. Then, treated samples were subjected to magnetic separation by using high intensity dry test magnet, at 0.1.0.3 , and 0.5 Tesla magnetic field intensities.

3 RESULTS AND DISCUSSIONS

Microwave heating characteristics of different size Iractions of pyrite sample for different power levels arc given in Figures 1 to 6. Detailed results have

been presented elsewhere (Uslu, 2002). As seen from the figures, heating rale and maximum attained temperature of pyrite samples increased with increasing power and decreasing particle size. Heating rates decreased when the temperatures approached to maximum. Of all heatings, highest attained temperature and healing rate were observed for -420 urn size fraction at 850 watt. Temperature raised to 860 °C in 495 seconds. The increase in heating rales with increasing microwave power results from the increase in the absorbtion of microwave energy.
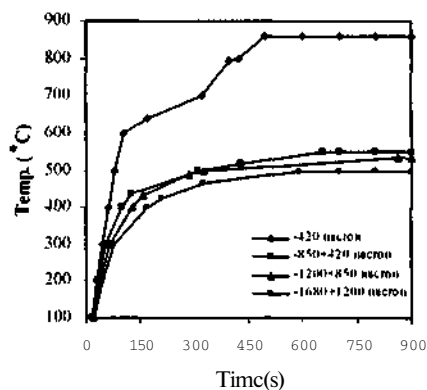
Figure I. Heat treatment of pyrite under air for different size fractions at 850 Watt
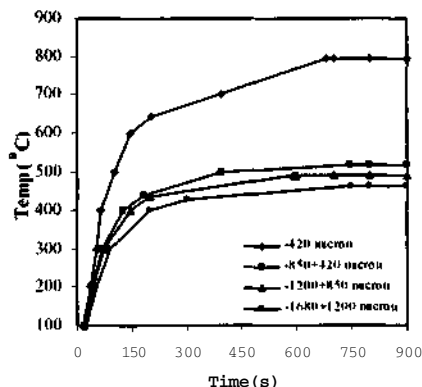
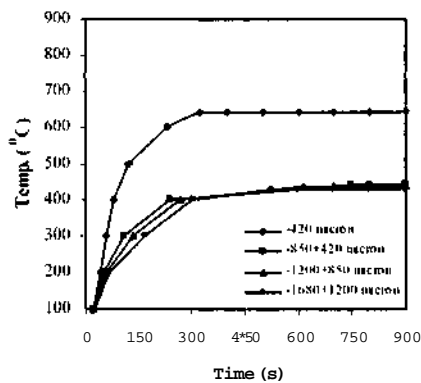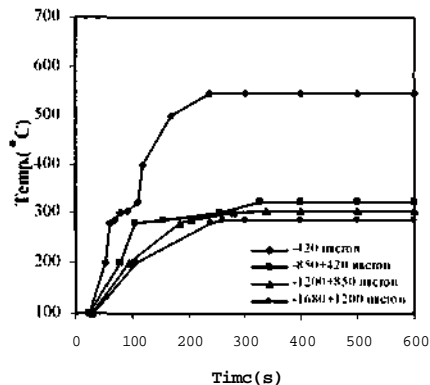Figure 2. Heat treatment of pyrite under air for different size fractions at 680 Watt .

398

Figure 3. Heat treatment of pyrite under air for different size fractions at 510 Watt

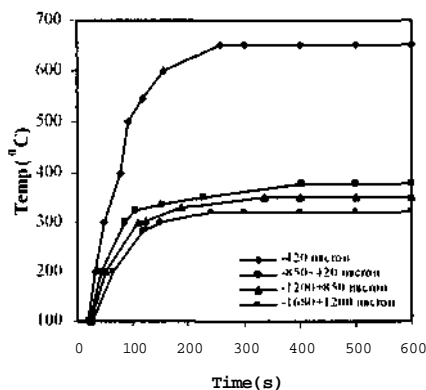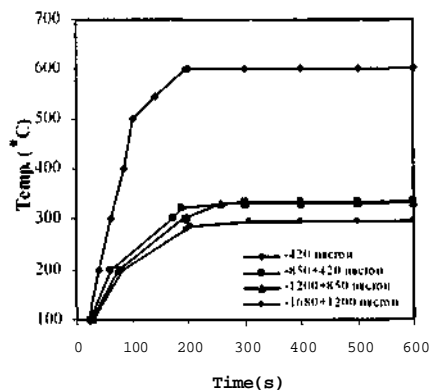Figure 6. Heat treatment of pyrite under nitrogen for different size fractions at 510 Watt

Experimental results also demonstrated that the heating of pyrite particles is indeed influenced by particle size; the observed behaviour was rationalized from heat transfer effects. Maximum attained temperature and heating rate were lower in heatings under nitrogen. Nitrogen decreased the heating by hindering the contact of pyrite with oxygen in the air. The maximum attained temperature and heating rate under nitrogen were observed for -420 ujn size fraction at 850 watt. Temperature raised to 651 °C in 258 seconds.

Results of magnetic separation tests are given in Figures 7-8. As seen from figures, amount of magnetic product recovered increases with increased attained temperature and magnetic field intensity. Maximum magnetic product recovery was obtained for pyrite particles with maximum temperature of 825 °C in 0.5 tesla magnetic field intensity. Magnetic separation of microwave treated samples in nitrogen atmosphere resulted lower magnetic product recovery. The XRD analysis and microscopical examination of microwave treated samples showed that the pyrite (FeS_2) is converted to new phases like pyrrhotite (Fe $|_{-x}$ S, ($0 < x < 0.125$)), troilite (FeS), a-hematite (a-Fe_2O_3) and y-hematite (y-Fe_2O_3). Due to thermodecomposition of pyrite (weakly paramagnetic) to pyrrhotite (ferromagnetic), 7- hematite (ferromagnetic) and troilite (moderately paramagnetic) magnetic separation of sample is facilated at low magnetic-field intensities. The increase in magnetic susceptibility of pyrite can be attributed to the fact that as the mineral heats up, the atoms re-align making the structure of the lattice more ordered. This alignment of atoms increases the magnetic-susceptibility of the mineral overall.

Figure 4. Heat treatment of pyrite under nitrogen for different size fractions at 850 Watt

Figure 5 Heat treatment of pyrite under nitrogen for different size fractions at 680 Watt

399
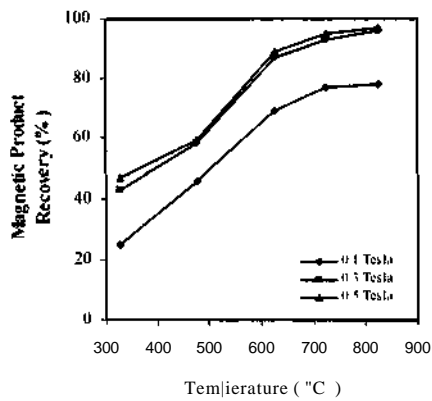
Figure 7. Magnetic separation of microwave pyrite samples heated under air
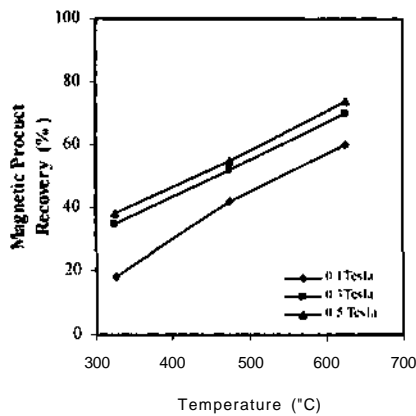

Figure 8. Magnetic separaten of pyrite samples heated under nitrogen

4 CONCLUSIONS

The results of this study show that microwave treatment has a considerable effect on the mineralogy,

heating characteristics and magnetic processing of pyrite mineral. Heating rate and maximum attained temperature of pyrite samples increased with increasing power and decreasing particle size. The maximum attained temperature of 860 °C was obtained for the -420 um size pyrite particle at 850 watt in 495 seconds. It was also shown that the magnetic susceptibility of the pyrite could be increased by a considerable amount due to decomposition of pyrite to a strongly magnetic phases. Use of microwave radiation for the removal of pyritic sulphur from the coal may soon be commercial reality. Therefore, it is necessary to establish a multidisciplinary research team for the commercial development of microwave technology in mineral processing.

REFERENCES

Ergun. S. and Bean. E.H. 1968. Magnetic Separation of Pyrites from Coals. *Bureau of Mines Report of Investigations.* No:7181

Fanslow. G.E.. Bluhm. D.D. and Nelson. S.O. 1980. Dielectric Healing of Mixtures Containing Coal and Pyrite. *Jornal of Microwave Power* 15 (3): 187-190.

Haque. K.E. 1999. Microwave Energy for Mineral Treatment Processes- a brief review. *International Journal of Mineral Processing* 57: 1-24.

Kelly. R.M. and Rowson. N.A. 1995. Microwave Reduction of Oxidized Mineral Concentrates. *Minerals Engineering* 18(11): 1427-1438.

Kelland.D.R.. Lai-Fook.M., Maxwell.E. and Takayasu.M. 1988. HGMS Coal Desulplumzatioii with Microwave Magnetization Enhancement. *IEEE Transactiom on Magnetics* 24 (6): 2434-2436

Kingman . S.W.. Cortield. CM. and Rowson, N.A. 1999 Effect of Microwave Radiation upon the Mineralogy and Magnetic Processing of a Massive Norwegian llmentte Ore. *Magnetic and Electric al Separation.* 9: 131-138.

Matthes. S.A.. Fan-ell. R.F. and Mackie. A.J. 1983. A Microwave System for the Dissolution of Metal and Mineral Samples. *Tecimimi Progress Report 120, US Bureau of Mine.r.9* pp.

Vasilakos, N.P. and Magalhaes. F. 1984. Microwave Drying of Polimers. *Journal of Microwave Power* 19(2): 135-144.

Xia. D.K.and Pickles. C.A. 1997. Application of microwave Energy in Extractive Metallurgy, a review. *CIM Bulletin* 90(I):99-I07

Uslu, T. 2002. Microwave Heating Characteristics of Pyrite and Microwave Assisted Coal Desulphunzation. *Ph.D.Thesis.* Middle East Technical University, Mining Eng. Dept. Ankara. Turkey.

Comparison of the Combustion Characteristics of Three Different Fossil Fuels from Turkey

C.Hiçyılmaz & N.E.AItun
Department of Mining Engineering, Middle East Technical University, 06531, Ankara, Turkey

ABSTRACT: In this study, thermal features and reaction kinetics of the raw Çorum-Alpagut Lignite, Zoıguldak-Üzülmez Bituminous Coal and Şırnak-Avgamasya Asphaltite were investigated through a qualitative and quantitative comparison via Thermogravimetric Analysis (TG/DTG) and an Arrhenius Type Kinetic Model, in order to determine the liability to ignite and effectiveness of the combustion of the concerned fuels as well as the critical points during their reaction periods. At the end of experiments, Alpagut Lignite, Üzülmez Bituminous Coal and Avgamasya Asphaltite resulted in different combustion features in terms of residue left, peak temperatures and activation energies from which the combustion behaviour of these fuels can be interpreted in details. In this study, thermal features and reaction kinetics of the raw Çorum-Alpagut Lignite. Zonguldak-Üzülmez Bituminous Coal and Şırnak-Avgamasya Asphaltite were investigated through a qualitative and quantitative comparison via Thermogravimetric Analysis (TG/DTG) and an Arrhenius Type Kinetic Model, in order to determine the liability to ignite and effectiveness of the combustion of the concerned fuels as well as the critical points during their reaction periods. At the end of experiments, Alpagut Lignite, Üzülmez Bituminous Coal and Avgamasya Asphaltite resulted in different combustion features in terms of residue left, peak temperatures and activation energies from which the combustion behaviour of these fuels can be interpreted in details.

1 INTRODUCTION

Rather than oil, lignite, bituminous coal and asphaltite are the most important fossil fuel types in Turkey with considerable reserves all around the country. These energy sources are utilized extensively for electricity production and heating purposes. For the determination of the appropriate fuel among the alternatives for specific purposes and the design of the combustor facilities, it is essential to have considerable information related to the thermal behaviour of such fuels. Ignition and proceeding combustion reactions of fossil fuels are accompanied by weight loss, thermal decomposition of the mineral matrix, diffusion and heat transfer to the surroundings. These subsequent phases are excessively influenced by various parameters such as the reactivity of the fuel, its liability to react with Oj, as well as physical features arising in accordance to the origin *of* the fuel. Thermal analysis methods proved to be a sucessful tool in the investigation of the combustion behaviour of the fossil fuels (Kanikowski and Stenberg, 1988), especially in the previous two decades. The reliability of the process in reflecting the consecutive thermal processes (i.e. loss of moisture, devolatilization, oxidation of fixed carbon, pyrolysis reactions, etc.) and the flexibility in the application of various temperature regimes attracted great interest to thermal analysis methods like DSC (differential scanning calorimetry), DTA (differential thermal analysis) TGA/DTG (thermogravimetric analysis/differential thermogravimetry) DSC and TGA techniques were effectively utilized for the characterization of Ohio Bituminous Coals by Rosenvold et al. (1981). Twentyone coal samples from Ohio were analyzed for the determination of the distinct volatilization and oxidation regions as well as endothermic and exothermic peak points. Chemical reactions corresponding to the related individual temperature values which have dictated the on-going combustion process were dealt and compared in details with respect to the coal type. Khulbe et al. (1984) performed pyrolysis studies with the asphaltene fraction derived from Cold-Lake (Canada) bitumen by using TGA and the kinetics of the conversion process was determined via an Arrhenius type kinetic model. Combustion behaviour of 10 different coals of lignite, sub-bituminous and bituminous type was compared qualitatively through DSC and TGA by Janikowski and Stenberg (1988). For all the coals studied, two definite regions of chemical reactivity were

401

Table 1. Proximate Analysis and Sulphur Content of the Samples (original basis)

	Alpagut Lignite	Avgamasya Asphallite	Üzülmez Bituminous Coal
Moisture *(%)*	7.56	0.66	0.36
Volatile Matter (7r)	II 09	33.25	25.75
Fixed Carbon (%)	35.20	21.23	58.71
Ash(%)	46.15	44 86	15.18
Sulphur (tf)	1.80	5.53	0.35
Calorific Value (Kcal/Kg)	4300	4515	6754

determined, but at varying temperature ranges. All these and parallel studies claimed that thermogravimetric methods were very well adopted to researches concerning fossil fuels This study deals with the comparison of three most important energy sources in Turkey of different type, lignite, bituminous coal and asphaltite. In this respect, the combustion behaviour of these solid fossil fuels were investigated by means of non-isothermal TG/DTG analyses. Both quantitative and qualitative determined, but at varying temperature ranges. All these and parallel studies claimed that thermogravimetric methods were very well adopted to researches concerning fossil fuels This study deals with the comparison of three most important energy sources in Turkey of different type, lignite, bituminous coal and asphaltite. In this respect, the combustion behaviour of these solid fossil fuels were investigated by means of non-isothermal TG/DTG analyses. Both quantitative and qualitative evaluations were made and the results related to the thermal features of the competing fuels were complemented by a successive reaction kinetics approach.

2 EXPERIMENTAL

For the study, Alpagut Lignite (Çorum), Üzülmez Bituminous Coal (Zonguldak) and Avgamasya Asphaltite (Sımak) were used whose proximate analyses are given in Table 1. At this point, it should be noted that, Avgamasya asphaltite consists of considerably high sulphur amount when compared with the lignite and bituminous coal, which is one of its distinct characteristics.

The calorific values of the samples were measured with a Parr Oxygen Bomb Calorimeter For commencing the thermogravimetric analyses, firstly, the bulks were crushed to -100 mesh and then represantative samples were taken to be combusted in a Polymer Laboratories PL TGA-1500 analyzer (Fig. 1). Non-isothermal TG method enables the observation of the weight loss of a sample as a function temperature and time through a pre-determined temperature regime and/or period. In addition, it is possible to obtain and collect series of numerical data of weight, temperature and time changes at any desired interval. For each experiment, samples of approximately 25 mg were placed in a platinum crucible and installed to the furnace of the TG unit. The initial temperature was set to ambient and it was continuously increased upto 900 "C with a constant heating rate of 10 "C/min through a full controlled temperature programme. A uniform airflow of 15 mL/min was supplied to the combustion cell during the whole experiment. Prior to the experiments, the TGA instrument was calibrated for reliable results. At the end of each session, data required for the determination of the thermal characteristics and application of the kinetic analyses were obtained by means of thermogravimetric and differential weight loss curves of the realized combustion reactions.

3 RESULTS AND DISCUSSION

3. J Thermal Features

Although the combustion profiles of most of the fossil fuels possess a number of common phases such as loss of moisture and volatiles, oxidation of fixed carbon and evolution of heat, the differences related to those dictate the nature and efficiency of the combustion reaction. The temperature ranges of such individual intervals, their effect on the overall combustion period, importance on the whole reaction series and similar phenomena all rely on the composition, origin, mineral matrix, etc. of the concerned fuel type. Owing to these distinct features, various fuels result in considerably different combustion behavior efficiency and consequences.

At the end of experiments, the thermograms of lignite, bituminous coal and asphaltite showed characteristic combustion profiles. These differences were apparently noticed through the complementary DTG curves. The TG/DTG profiles of Alpagut lignite, Avgamasya asphaltite and Üzülmez bituminous coal are shown in Figures 2, 3 and 4, respectively.
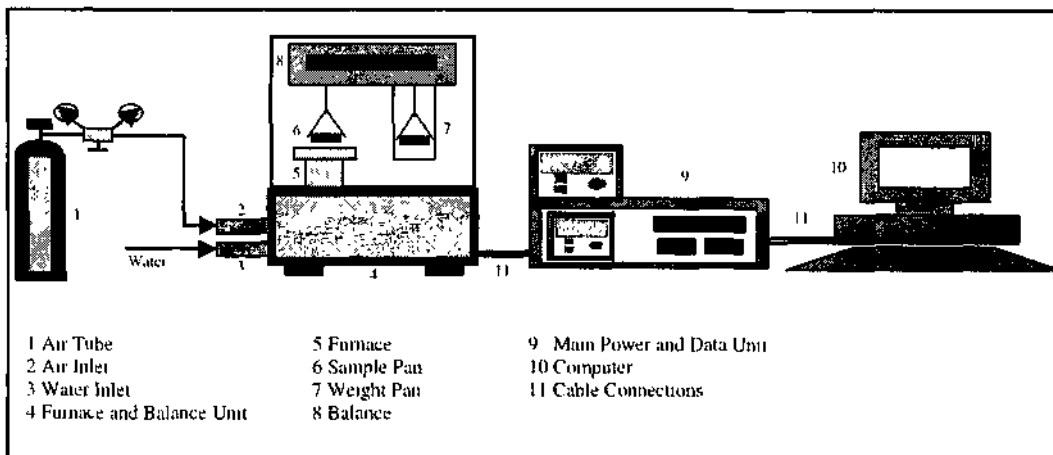
402

1 Air Tube	5 Furnace	9 Main Power and Data Unit
2 Air Inlet	6 Sample Pan	10 Computer
3 Water Inlet	7 Weight Pan	11 Cable Connections
4 Furnace and Balance Unit	8 Balance	

Figure I. Schematic form of the TG/DTG analyzer.

It was seen that Alpagut Lignite lost its moisture and the volatiles in two distinct regions around 35-180 "C and 210-360 "C, respectively (Fig. 2). After these periods, the onset of fixed carbon oxidation was seen aprroximately at 365 "C. It was observed that combustion occurred at two successive regions, between 365-541 "C and 551-787 "C, respectively. However, the weight loss realized during the second region was so slight compared to the primary one, indicating that the reactions dictating the combustion behaviour mainly occurred during the first one (Fig. 2). Like Alpagut lignite, the release of the moisture and the volatiles fraction occurred as particular processes between 60-165 "C and 274-380 "C, respectively for Avgamasya asphaltite. Oxidation reactions were realized at two distinct phases, between 385-558 "C and 630-836 "C (Fig. 3). Ft is obviously seen from Figures 2 & 3 that the second oxidation region of asphaltite is broader than lignite's in terms of weight loss. Gorman and Walker (1973) reported that inorganic minerals occunng in fossil fuels such as various clays or carbonates tend to decompose beginning from 600-650 "C upto 800-850 °C. Thus, this distinct second oxidation region may be well attributed to the decomposition of calcitc and dolomite which were reported to exist in considerable amounts in the mineral matrix of Avgamasya asphaltite (Hicyilmaz & Altun, 2002). For the combustion of Üzülmez bituminous coal, it can be claimed that no significant moisture release was observed (Fig. 4). It is seen from the proximate analysis (Table 1) that moisture content of Üzülmez coal is very low. Thus, it is normal not to observe any distinct region corresponding to the loss of moisture in the TG and/or DTG profiles. However, beginning from approximately 180 "C, the weight of the sample happened to increase gradually upto 290 °C. This peculiar segment in the TG/DTG profile of Üzülmez bituminous coal corresponds to the ehemisorption of oxygen to the pores (Crelling et al., 1992) due to which the sample gains weight (Fig. 4). The loss of volatiles was realized between 290-386 "C. The onset of combustion was observed beyond 395 °C and oxidation of the combustible species occurred in one apparent region that lasted around 770 "C.

In thermogravi metric studies, one of the distinctive aspects is the maximum peak temperature which accounts for the point where the rate of weight loss is at its highest level. Relative reactivity of the coal samples may be determined by using these peak temperatures, which can be directly interpreted from the DTG curves, in this respect, Alpagut lignite can be claimed to be more reactive than Üzülmez bituminous coal with a lower maximum peak temperature at 463.80 "C (Table 2). The reactivity order of the coal samples involved in this study may be well attributed with the rank concept. The reactivity order given here is in confirmation with the literature (Ceylan et al., 1999), where young coals (lignite in this study) which are of low rank proved to be more reactive than the old ones of higher rank (bituminous coal in this study). However asphaltite can be narrated with neither the reactivity nor the rank relation owing to its petroleum origin (Orhun, 1969). The residue left after the non-isothermal thermogravimelry runs is also one of the indicators providing clues about the thermal behaviour and combustion quality of the fossil fuels. Although, Üzülmez bituminous coal was found to be the least reactive sample, it proved to result in the most efficient combustion from the view of residue with the lowest residue value of 15.68 %. Furthermore, it was seen that Alpagut lignite involved a high amount of incombustible material which was approximately 45 % (Table 2)
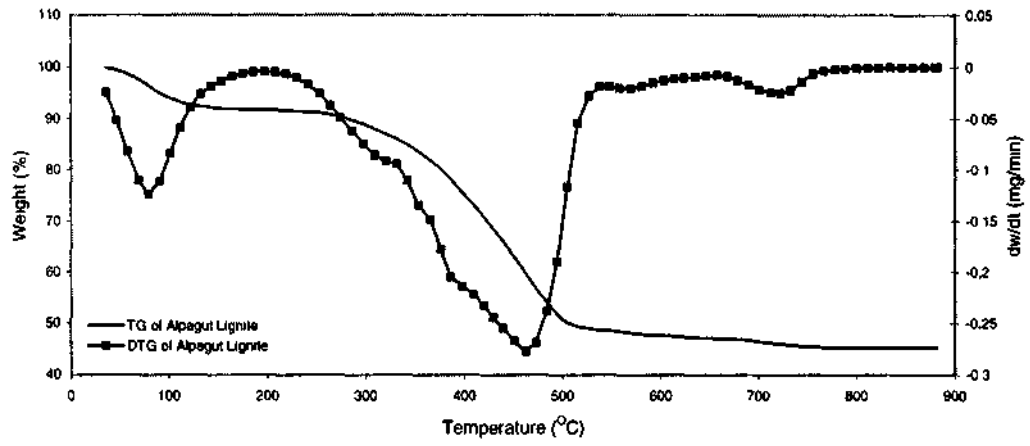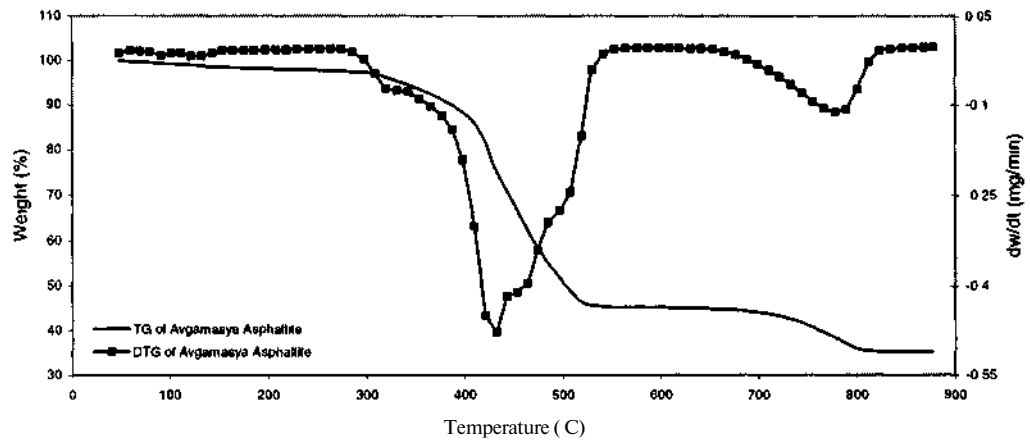
403

Figuie 2 TG/DTG Profiles ot Alpagut Lignite

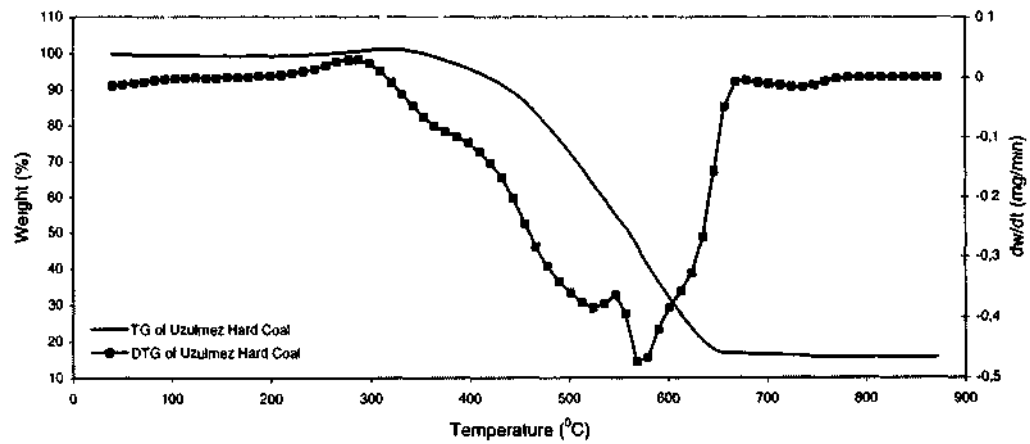Figure 3 TG/DTG Piofiles ot Avgamasya Asphaltite

Figure 4 TG/DTG Piotiles of Üzülmem Bituminous Coal

404

Table 2. Thermal Features of the Samples

	Alpagut Lignite	Avgamasya Asphaltite	Üzülmez Bituminous Coal
Maximum Peak Temperature ("O	463.80	427.55	572.70
Burnout Temperature ("O	786.64	836.01	768.32
Residue (%)	45.26	35.06	15.68

3.2 Kinetic Analysis

As well as thermal features, evaluating the overall combustion process in view of reaction kinetics provides considerable data related to the reactivity degree of the fossil fuels. Kinetic analysis enables the interpretation of the very complex subsequent series of reactions comprising the overall combustion profile in a very rapid, reliable and more understandable way. In this study, the thermal findings of the concerned fossil fuels were complemented with the determination of their activation energies, since activation energy is the measure of the easiness of a sample to begin combusting and complete the reaction. Arrhenius type kinetic model is one of the most appropriate concepts in expressing the reaction kinetics of the samples, which can be successfully adopted and relied to TG/DTG data. Hence, kinetic characteristics of the samples were analysed and investigated by this method

According to the model;

$$\frac{dw}{dt} = kW^n \qquad (1)$$

$$k = Ar \exp(\frac{-E}{RT}) \qquad (2)$$

Combining 1 and 2 gives;

$$\frac{dw}{dt} = Ar \exp(\frac{-E}{RT})W^n \qquad (3)$$

In this equation, dw/dt shows the rate of weight change of the reacting material, Ar is the Arrhenius Constant, E is the activation energy, T is the temperature, R is the gas constant, and n is the reaction order.

For analysing the TG/DTG data, the model assumes that the rate of weight loss of the total sample depends only on the rale constant, the weight of the sample remaining and the temperature with assumed unity reaction order. Thus, the equation takes the following form;

$$\frac{1}{W}\left(\frac{dw}{dt}\right) = Ar \exp\left(\frac{-E}{RT}\right) \qquad (4)$$

Taking the logarithm of both sides provides;

$$\log\left[\frac{1}{W}\left(\frac{dw}{dt}\right)\right] = \log Ar - \frac{E}{2.303\ RT} \qquad (5)$$

TG/DTG data provides directly the variation of weight with respect to temperature (i.e. dw/dt) and weight of the reacting material at each temperature level. Thus, plotting log[l/W(dw/dt)] against 1/T, results in the experimental interpretation of the model. The normalization of this curve results in a straight line whose slope explicitly equals to -E/2.303R(Koketal., 1997).

As has been stated, the overall combustion reaction of fossil fuels is comprised of a number of individual events taking place subsequently. The individual activation energies for each reaction region may rely on and can be notionally attributed to different mechanisms. However, they do not give any indication of the contribution of each region to the overall reactivity of the sample as singular ones. Hence, the Arrhenius type kinetic model is complemented with the concept of weighted mean activation energy, E_{wm} (Cumming 1984), to involve the participation of each individual region so as to determine the overall reactivity of the sample at all;

$$E_{wm} = F_1 E_1 + F_2 E_2 + F_3 E_3 + \ldots + F_N E_N \qquad (6)$$

where Fi, F:........F,, are the mass fractions of the combustible content of the sample oxidized during each region of Arrhenius linearity, and Ei, Ei......, E,, are the individual apparent activation energies corresponding lo each region.

In Table 3, the activation energies of the samples are given. As seen from this table, the activation energy of Üzülmez bituminous coal is twofold of Alpagut lignite and higher than Avgamasya asphaltite. Alpagut lignite resulted in the lowest activation energy value with 17.52 KJ/mol. These results suggested that, Alpagut lignite was the most liable fuel to ignite and combust. The ignition and the on-going combustion reactions became harder and harder as shifted to Avgamasya asphaltite and Üzülmez bituminous coal. Consequently, the

combustion of the lignite sample occurred in the most favorable way when compared to asphaltite and bituminous coal. When the observations about thermal and kinetic features of the fuels are evaluated together, it can be proposed that having a high calorific value and/or a low amount of inorganic constituents are not the determining features for an easy ignition and favorably proceeding combustion when the comparison is among fuels of different types. Despite having the most adverse residue and calorific value, Alpagut lignite was found to be the most reactive fuel, proving this approach.

Table 3. Activation Energies of the Samples

Sample Type	Activation Energy (KJ/mol)
Alpagut Lignite	17.52
Avgamasya Asphaltite	29.56
Üzülmez Bituminous Coal	36.18

4 CONCLUSIONS

In view of the findings of the study, the following conclusions can be derived;

1. It was seen that Alpagut lignite, Avgamasya asphaltite and Uzulmez bituminous coal resulted in significantly different combustion profiles in terms of thermal features and kinetic behaviour.

2. The oxidation of the combustible matter of Alpagut lignite and Avgamasya asphaltite occurred in two succeeding regions. It is noteworthy to mention that the weight loss during the second oxidation region of asphaltite was significantly higher than that of lignite. The combustion profile of Üzülmez bituminous coal resulted in a very characteristic weight gain region corresponding to the oxygen chemisorption.

3. From the view of thermal features, Üzülmez bituminous coal appeared to be the highest quality fuel among the supplements in the study, providing the lowest residue and highest calorific value. However, in terms of reaction kinetics combustion of Üzülmez bituminous coal gave rise to the highest activation energy, indicating that initiating and proceeding the

combustion reactions were considerably harder when compared to lignite and asphaltite.

4. Although, Alpagut lignite was observed to be the most unfavorable fuel with the highest residue and lowest calorific value, it was found to be the most reactive fuel with the earliest combustion onset and the lowest activation energy. Thus, ignition and oxidation of the combustible matter occurred more easily and efficiently when compared to asphaltite and bituminous coal.

5. The thermal and kinetics features of Avgamasya asphaltite were observed somewhere in between lignite and bituminous coal. Hence, it may be accepted as a considerable supplement to lignite and bituminous coal where exists. However, the high sulphur content may be an obstacle, which should be evaluated further.

REFERENCES

Ceylan. K.. Karaca. H. ami Onal. Y. 1999. Thermogravimetnc Analysis of Pıetıeated Turkish Lignites.. *Fuel.* Vol.78: pp. 1109-1116.

Celling. J.C.. Hippo. F.J.. Woerner. B.A. and West. D.P.Ji 1992. Combustion Characteristics Of Selected Whole Coals and Macérais. *Fuel.* Vol.71: pp. 151-158.

dimming. J W. 1984. Reactivity Assessment of Coals via a Weighted Mean Activation Energy. *Fuel.* Vol. 63: pp 1436-1440.

Hieyihnaz. C. and Altını. N.E. 2002. Asfaltitlenn Zenginleştirilmesi ve Termogravımetnk Özelliklerinin Belirlenmesi. *ODTÜ Bilimsel Araştırma Pro/elerı,* BAP-2002-03-05-03 Ara Raporu. Ankara: pp. I -8.

Janikowski. S.K. and Steıberg. V.l. 1989. Thermal Analyses of Coals Using Differential Scanning Calorimetry and Thermogravimetry. *Fuel.* Vol. 68: pp. 95-99.

Kluilbe. K.C.. Sachdev. A.K.. Mann. R.S. and Davis. S. 1984 TGA Studies of Asplialtenes Derived fiom Cold-Lake (Canada) Bitumen. *Fuel Processing Teilmolosx.* Vol. 8: pp. 259-266.

Kök. VM. Ozbaş, E and Hiçyılmaz, C 1997 Effect of Particle Size on the Thermal and Combustion Properties of Coal. *Thermoclum'ua Aaa.* Vol.302: pp. 125-130.

Orhun, F. 1969. The Characteristics. Melamorphism Degrees and Classification Problems ol Asphaltic Materials in Southeastern Turkey. *MTA Jmuiuil.*Vol.72: pp. 146-157.

Rosenvold. R.J.. Dubow. J.B. and Rajeshwar. K. 1982. Thermal Analyses of Ohio Bituminous Coals *Thermm liimiat Ada.* Vol. 53: pp. 321-332.

The Krebs Gmax Cyclone Development In The Coal Industry

Roman van Ommen, MSC, MBA
Krebs Engineers Europe, Manager Applications and Sales Obere Hauptstrasse 27/3/4 Top27

Robert G. Moorehead. MSC
Krebs Engineers USA

ABSTRACT: The gMax[IM] development program for coal illustrated that no single cyclone design is optimal for all applications in all industries. A cyclone designed for one application can not necessarily be directly applied in another industry, because the separation mechanics, feed characteristics, and operating mode of a cyclone is loo complicated for that simplistic an approach. Specific process requirements must always be considered in any cyclone application. The coal gMax development program demonstrated that the unique geometry of the gMax provides a finer separation through increased centrifugal acceleration in the lower sections of the cyclone, along with optimal inlet and vortex-finder geometries. This characteristic makes the gMax most advantageous for coal applications.

1.1 INTRODUCTION

In 2000, Krebs Engineers implemented a program to study the impact of various inlet and cone designs on the performance of hydrocyclones. This program, which featured laboratory testing, plant testing, and Computational Fluid Dynamics studies (CFD) resulted in a new Krebs Engineers cyclone product line called gMax[1w].

This program centered on the performance of the hydrocyclones in closed circuit grinding (CCG) operations for minerals such as iron ore, gold, and copper. The results were impressive (1), as indicated by the comparative classification curves (Figure 1), which shows the 20-in. diameter-gMax[m] configuration to have a D50 size roughly 62 percent of a standard 20-in. cyclone. Similar D50 decreases were seen in other mineral applications as well.

Typically, any design that decreases the D50 cut point of a cyclone occupying the same physical volume and with equal capacity provides customers with an advantage. As showen in Figure 2 The specific design of the gMax[IM] enables it to essentially occupy the same physical volume as Krebs 10.5° Series design (10.5° cone angle), but provide a finer separation.
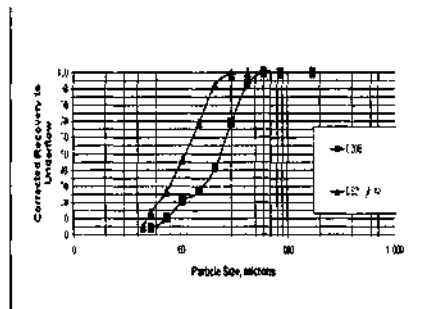
Figure 1 : Corrected Recovery Curce.
Dal;i tor Standard D20B and DS20-gMax Cyclones Wesiern xI'S Copper Concertrator. March 2001
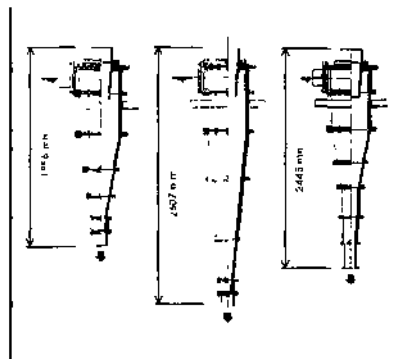
Figure 2 : Comparison of Cyclone Lengths KrebsD15LB, D15LB-T. and D15LB-gMax

Alternately the gMax[IM] design allows a larger-diameter cyclone, with its greater capacity, to be employed to achieve the same separation as a smaller-diameter cyclone. Thus the gMax[IM] design provides the potential advantage of permitting the installation of fewer cyclones to process the same volumetric feed rate at the same separation size.

2. 1 BASIS OFGMAX[IM] IMPROVED PERFORMANCE

In order to determine the basis of the improved gMax[IM] performance, Krebs Engineers investigated computation fluid dynamic studies of cyclone How patterns. Although cyclone flow patterns are extremely difficult to predict, with CFD the
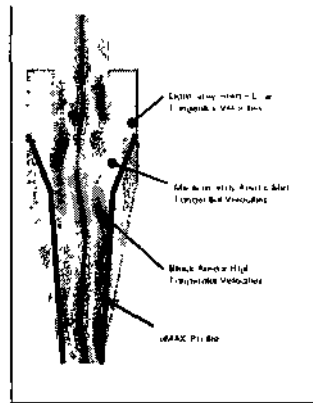
Figure 3 : CFD Image of Tangential Velocities in a Cyclone

modeling has provided evidence of the gMax[IM] improved performance.

Figure 3 illustrates CFD predictions of tangential velocities in a conventional cyclone, along with a superimposed gMax[IM] profile (2). This CFD illustration indicates, as have experimental data, that the highest tangential-velocity regimes reside near the air core. The gMax[IM] profile forces the descending slurry into the higher-tangential velocity region and, by virtue of the higher centrifugal acceleration forces in this region, enhances the migration of particles to the cyclone wall.

Figure 4, which shows the predicted CFD tangential velocities, further supports this theory(3)(4). As shown in Figure 4, the gMax[m] profile allocates a

greater volume of the cyclone to higher tangentially velocities. This results in the descending slurry, in the lower section of the cyclone,
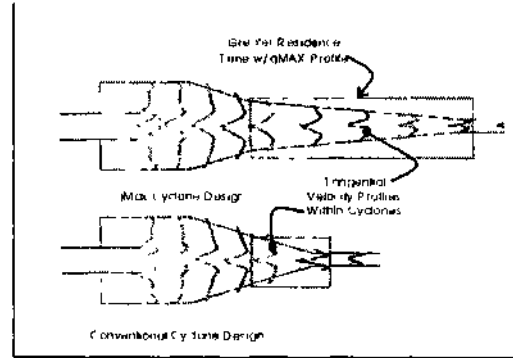
Figure 4: Comparison of Tangential Velocities Between Conventional & gMAX Cyclones

being exposed to greater centrifugal acceleration for a greater period of time than a conventional cyclones. This exposure to greater centrifugal acceleration coupled with greater residence time in this region results in the finer separation achieved by a gMax[IM] cyclone in comparison to a conventional cyclone of the same diameter, in grinding circuits where the solids densities and the flow splits to underflow are much higher than typical coal applications.

Initial gMax[IM] coal testing did not show the same decrease in separation size shown by previous testing in closed circuit grinding applications. It is postulated that the reason for this was tied to two variables:

- Coal typically has densities from 1.25 to 1.60 SG. Lower particle densities result in much lower induced settling velocities in the upper section of the cyclone.

- For typical coal classification applications, flow splits to underflow range from 10 to 20 percent (v/v). A much lower percentage of the feed slurry is exposed to the high tangential velocities region of the gMax[IM] (typical CCG applications have flow splits to underflow of 30 to 60 percent).

In order to apply the gMax[IM] design to coal, a series of lab tests were performed on a 10-in diameter cyclone. These tests featured various combinations of new inlet and vortex-finder designs as well as varying combinations of gMax[IM] cones and apexes.

Initial base-line testing indicated that the critical operating parameters and particle characteristics in coal applications differ enough from CCG that although the "metallurgical" g-Max[IM] did provide a finer D50 than the "T" Series design, the decrease was not as great as that established in CCG commercial and test installations. Figure 5 shows the corrected recovery curves for the baseline testing.
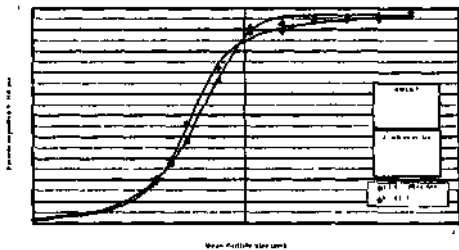
Figure 5 : Connected Recovery Curves for D10LB-T vs Metallurgical "M1" D10LB-gMax Lab-Test Results

Theoretical assessment of the initial lab results, from this testing, led to the conclusion that the following physical characteristics of coal required a modified gMax[m] design different than thai used in minerals:

• Coal size distributions are typically bi-modal with the size distribution comprised primarily *of* coarser, low-density particles and finer, high-density particles, with a low mass percentage of particles occupying the sizes between these two extremes.

• The shape of the lower-density coal particles (non-spherical) make these particles more susceptible to being drawn to the overtlow by drag forces in the upper region of the cyclone.

These physical characteristics require a cyclone design that provides greater residence time to the incoming slurry before accelerating it in the high-centrifugal-force region of the gMax[.M] lower cones.

Figure 6 shows the comparative corrected-recovery curves for the original "metallurgical" gMax[IM]

design (Ml), two variations of the modified gMax[.M] design for coal (CI & C2), and the "T" series design.
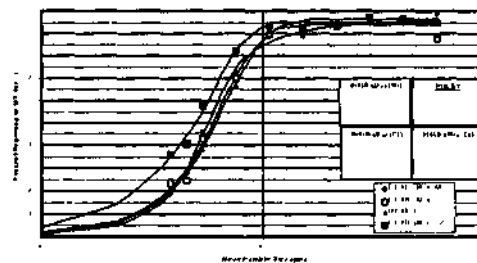
Figure 6 : Connected Recovery Curves for D10LB-T, "M1" "D10LB-gMax, and "C1& C2" DIOLbgMax Lab Test Results

Review of the corrected-classification curves indicates that the initial changes made to the coal gMax[m] design (CI) resulted in slightly lower coarse-particle bypass than the "M1 " design, but with no improvement in D50 size.

Further modifications were made to the Coal gMax[.M] design and subsequent testing of the new "C2" design indicated that coarse-particle bypass was reduced below that of the "T" series. Furthermore, the "C2" D50 size decreased roughly 21 percent below that of the "T" series (49pm versus 62pm).

The results shows that the design modifications embodied in the "C2" design provided the same improvement in performance with a coal feed, that the "M1"
gMax design provides in CCG.

Generally, the changes in the gMax[IM] design for coal uses less radical cone-angle relationships than in minerals. These changes were necessitated because of the physical differences of coal versus minerals, as well as the different operating mode of typical coal cyclones versus cyclones used in closed-circuit grinding.

.2 FINAL RESULTS OF THE COAL GMAX DESIGN

Although Krebs determined the optimum geometry tor the Coal gMax, based on the "C2" design, testing continued in the laboratory to further confirm the performance improvements. Figure 7 shows a comparison of subsequent lab testing for the "Coal" gMax[IM] and the "T" Series design. These tests were performed with the same inlet and vortex size in both the gMax and "T" Series units. These results confirm the original testing results, showing the gMax"[1]' design provided a finer separation and greater recovery than the "T" Series design.
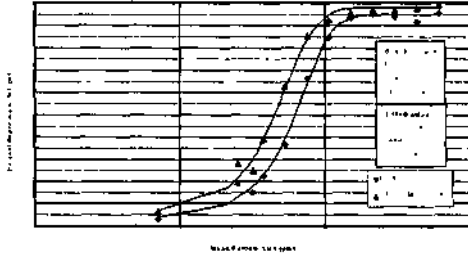
Figure 7 : Actual Recovery Curves for D10Lb-T and D10LB-gMax in Confirmation Lab Tests

Table 1 shows the critical performance results of this comparative test. Most notably is the decrease in separation size (-30% finer than the "T" Series) and greater recovery of plus 75um size particles (97.2 versus 92.6 wt%).

To put this improved performance into perspective: One (1) cyclone, fed 272 gpm of 5 percent solids slurry, results in 3.46 t/h of feed solids. If 19 percent of that feed is plus 75pm, a 5 percent increase in recovery of this size, would result in each cyclone recovering an additional 0.039 st/h of coal. This seems rather minimal, however if that tonnage is calculated for twenty (20) operating units, the improved performance of the gMax would potentially result in an additional recovery of 4,000-5,000 short tons annually.

1.3 GMAX ">" FOR COAL FIELD TEST RESULTS

n i t   Midwestern U.S. Plant Testing

After completing the preliminary lab testing of the revised gMax[IM] design for coal, several field tests were conducted to verify the results determined in the lab. Testing was conducted in a Midwest plant comparing a 15-in. diameter "standard" cyclone and a
15-m. gMax[IM] cyclone in a raw-coal classification application. The results of the testing indicated the gMax[IM] cyclone provided a D50 roughly 20 percent finer than the standard 15-in. model.
This decrease m separation size resulted in a 5.37 percent increase in recovery. Based on these results, the gMax-model cyclones were selected lor commercial installation.

After commissioning, the «Max cyclones were sampled and Figure 8 shows the comparative results of the installed gMax units and the standard D15LB results from testing.

The recovery curves show the gMax units are providing a ~ 26 percent finer separation and ~ 3.69 percent higher recovery.
Of more importance however, is that the gMax underflow ash content is slightly lower than the original D15LB units (29.12 percent ash for the gMax versus 30.14 percent ash for the D15LB).
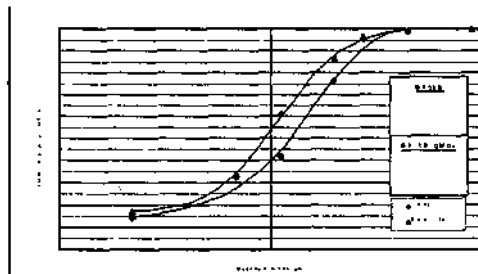

Figure 8 : Actual Recovery Curves for D15LB-20[0] and D15LB-gMax in a Midwestern Coal Application Test.

The reason that the underflow ash decreased is because the gMax recovered additional plus 44pm size fractions without additional fine-particle bypass. Normally, the oversize fractions errantly reporting to overflow contain the lowest-ash coal particles. Since the gMax's additional recovery is concentrated in these sizes, the underflow ash is now lower than

the original DI5LB's. Figure 9 shows the
comparative underflow yields and ash contents for
the gMax and original DI5LB's, with the increased
recovery of the 44pm x 150pm size fractions. Of
course, increasing carbon recovery is of paramount
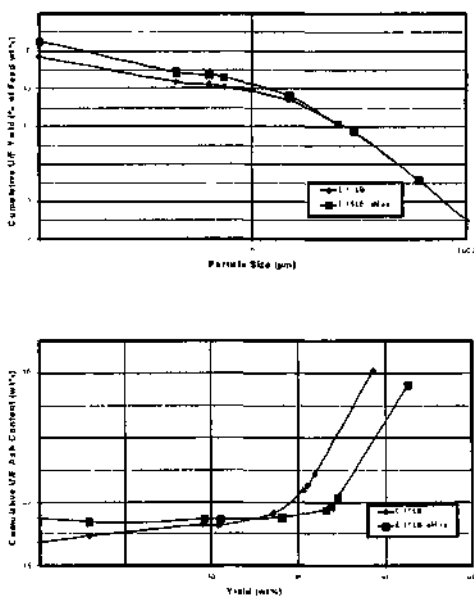importance to the steam-coal producer.

Figure 9 : Conparison of Underflow Yields and Ash
Content for a D15Lband D15LB-gMax in a Midwestern
Coal Application Test.

13 i : Eastern U.S. Plant Testing

Testing of a U6-gMax design (6-in. diameter, all-
polyurethane) was also performed in a eastern *U.S.*
plant. This testing was in a secondary-stage
application where the objectives included maximum
recovery of primary-stage ,raw-coal-classifying
overflow prior to flotation.

Figure 10 shows the actual recovery curve achieved
during testing. The unit achieved a D50 of 29pm.
Although the indicated fine-particle bypass of- 38
percent seems rather high, the underflow solids was
25.7 percent and the water split was 84/16 (DO/Du).
This indicates that the cyclone was creating
centrifugal forces sufficient to affect a separation on
some of the minus 44pm particles.
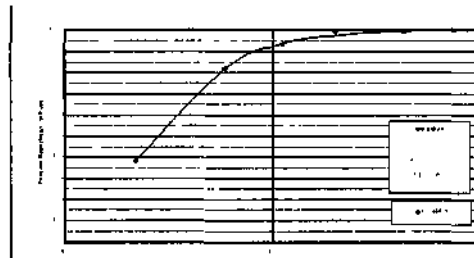
Figure 10 : Actual Recovery Curves for a U6-gMax
in a Eastern U.S. Coal Application Test

These high centrifugal forces resulted in the cyclone
recovery 99 percent of the 250pm x 149pm size, 94
percent of the 149pm x 74pm size, and more
importantly, 82 percent of the 74pm x 44pm size
fraction - those size fractions which normally
contain the highest percentage of carbon.

1.4 CONCLUSIONS

The gMax^m development program for coal
illustrated that no single cyclone design is optimal
for all applications in all industries. A cyclone
designed for one application can not necessarily be
directly applied in another industry, because the
separation mechanics, feed characteristics, and
operating mode of a cyclone is too complicated for
that simplistic an approach. Specific process
requirements must always be considered in any
cyclone application.

The coal gMax development program demonstrated
that the unique geometry of the gMax provides a
finer separation through increased centrifugal
acceleration in (he lower sections of the cyclone,
along with optimal inlet and vortex-finder
geometries. This characteristic makes the gMax
most advantageous for coal applications where the
objective is maximizing solids recovery, such as:

• secondary-stage classification applications up
  stream of notation, and

• raw-coal classification in plants without
  • flotation.

As a major cyclone supplier to both the minerals as
well as the coal industry, we are continually

411

studying the fluid dynamics of free-vortex How regimes to improve cyclone design. Major breakthroughs will likely be tied to greater understanding of the energy profiles in a cyclone and adjusting the geometry to better comply with natural energy distributions.

A perfect example of this was caught by a photograph of a transparent cyclone. The embellished photograph (Figure 1 !) shows the shape of the air core during cyclone shut down, and its similarity to the cone profile of a gMax^{IM} cyclone.

1.5   REFERENCES

(1)   Turner, P., Olson, T., Hoyack, M, "Best Hydrocyclone Operating Practices for Sag Mill Circuits"

(2) Slack. M.D.. Prasad R.O., Bakker A. and Boysan F.. " Advances in Cyclone Modeling using Unstructured Grids", Fluent Europe LTD, 2001

(3)   Petty, CA., S.M. Parks, and T.J. Olson, "Flow Simulations within Hydrocyclone Separators", Symposium on Centrifugal Separation, Minerals Engineering Conference on Solid-Liquid Separation, June 18-20, Falmouth,
   UK.

(4)   Petty. CA.. S.M. Parks, "The Influence of Hydrocyclonc Geometry on Separation Performance", Symposium on Particulates and Multiphase Flows, Annual AlChE Meeting, November 4-9, Reno, NV.

Table 1   Performance Data for D10LB-T and D10LB-gMax-Confirmation Lab Tests

Unit: Test	D10LB-T Lab Test 1	D10LB-gMax Lab Test 11
Capacity		
Flow Rate (gpm)	276	272
Head (PSIG)	20	20
Recovery		
Total Recovery (wt%)	24 2	43 3
Avg Recovery +75p.m (wt%)	92 6	97 2
% Increase in +75nm Rec	Base	4 96
Performance		
D50 (pm)	62 5	45 1
% Decrease in D50	Base	27 85
Bypass (a)	6 0	4 2
Alpha	2 52	2 32
Ep	25 4	193
Recovery Numbers		
(Mean Size (jm)		
600	95 5	99 4
425	91 8	97 8
300	93 8	968
212	95 5	97 1
150	93 5	95 5
106	84 9	92 4
75	66 6	85 4
53	36 7	62 8
38	22 2	39 1
32	14 7	25 0
25	18 7	28 0
20	12 4	36 2
7	3 0	6 4

Effect of Surface Area, Growth Media and Inert Solids on Bioleaching of Complex Zinc/Lead Sulphides

H.Deveci, I.Alp & T.Uslu
Department of Mining Engineering, Karadeniz Technical University, 6J0S0 Trabzon, Turkey

ABSTRACT: The effects of surface area (as a function of particle size and pulp density), growth media and inert solids on the extraction of zinc from the complex sulphide ore/concentrate were evaluated using the mesophilie and moderately thermophilic bacteria. The results have shown that an increase in the available surface area via size reduction improves the dissolution of zinc from the ore at low pulp densities (1-2% w/v). However, excessive increase in the surface area with increasing pulp density was found to adversely influence the dissolution process due to the inability of the bacteria to maintain the oxidising conditions in favour of the mineral sought after. Addition of nutrient salts was found essential to sustain the optimum bioleaching activity and the concentration of nutrient salts to be provided appears to depend on the availability of substrate (i.e. head grade and/or pulp density) for bacterial oxidation. The addition of inert solids (quartz) was shown to have a limited effect on the bioleaching of the concentrate.

1 INTRODUCTION

Complex sulphide ores are difficult to treat by conventional extraction processes mainly due to the extremely fine dissemination of valuable sulphides and their intimate association with gangue minerals in the ore matrix (Barberly et al. 1980, Buchanan 1984, Logan et al. 1993). The benefieiation of complex sulphide ores containing zinc, lead and copper has traditionally used processes such as differential flotation to produce concentrates of sufficient grade to be treated for the recovery of contained values within a pyrometallurgical process route (Barbery et al. 1980, Chadwick 1996). However, the pyrometallurgical processes now endure stringent environmental regulations and high capital costs in addition to the low quality of end product with further refilling being often a necessity (Grant 1994, Gordon 1985)

Biooxidation of refractory gold concentrates have already proved an economically viable and competitive process with reduced environmental impact and low capital costs involved (Dew et al. 1997, Rawlings et al. 2003). This has led to the extension of the technology to the treatment of low grade and/or difficuit-io-treat ores/concentrates in particular, for the recovery of copper, nickel, cobalt and zinc (Miller et al. 1999, Rawlings et al. 2003).
Bioleaching is inherently based on the use of acidophilic bacteria such as *T. ferrooxidans, L. ferrooxi-*
dans (<40°C). *S. tlwrmosulftdooxidans* (45-55°C) and *S. metallic-its* (~70°C) that have the ability to oxidise inorganic substrates such as ferrous iron and/or elemental or reduced sulphur compounds (Norris et al. 2000. Suzuki 2001). The oxidation of ferrous iron (1) and elemental sulphur (2) leads to the formation of ferric iron and sulphuric acid respectively which act as lixiviant for the oxidative dissolution of sulphide minerals (MeS; Me: Metal e.g. Zn) (3) in acidic environments (Sand et al. 2001, Rawlings et al. 2003).

$$2Fe^{2+} + 1/2O_2 + 2H^+ \xrightarrow{\text{bacteria}} 2Fe^{3+} + H_2O \qquad (1)$$

$$S^0 + 3/2O_2 + H_2O \xrightarrow{\text{bacteria}} H_2SO_4 \qquad (2)$$

$$MeS + 2Fe^{3+} \rightarrow Me^{2+} + 2Fe^{2+} + S^0 \qquad (3)$$
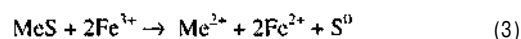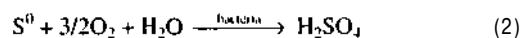
Biolcacliing ol'sulphide minerals is naturally a complex process with chemical and biological reactions occurring concomitantly. The acidophilic bacteria utilised as the mediator of the oxidative reactions (1&2) in bioleaching processes themselves establish the optimum conditions under which they optimally thrive. However, the optimum growth conditions may be adjusted in order to achieve the maximum rate and extraction of contained values (Bosecker 1997). This assumes the primary consideration is the overall chemical and microbiological aspects of the dissolution process.

The factors deemed of fundamental importance for a bioleaching process are temperature, acidity, metal toxicity, availability of oxygen and carbon dioxide, nutrients, and substrate (i.e. mineral surface area) (Bailey & Hansford 1993, Bosecker 1997). A culture medium is essentially a mixture of inorganic chemical compounds mainly to provide NH_4^+, $PO_4^{'\backslash}$, Mg^{2+}, K^+, Ca^{2+} and $SO_4^{;"}$, which are utilised by bacteria for the synthesis of cellular material (Tuovinen & Bhatti 1999). Bacterial oxidation of sulphide minerals occurs through surface chemical reactions via the attachment of bacteria and/or the leaching by bacterially generated ferric iron and/or acid. The increased surface area through size reduction would be expected to lead to a high rate and extent of extraction at low pulp densities (Torma et al. 1970). However, there are certain practical limitations to increasing the pulp density due to the factors including the limitation of O_2 and CO_2 transfer (Bailey & Hansford 1994, Boon "& Heijneri 1998), mechanical damage to bacteria (Deveci 2002), bacteria-to-solid ratio (Komnitsas & Pooley 1991) and the build-up of toxic products (Bailey & Hansford 1993).

In this study the effect of growth medium, particle size and pulp density, and inert solids on the bioleaching of a complex sulphide ore/concentrate was investigated using mesophilic and moderately thermophilic bacteria.

2 EXPERIMENTAL

2. / Mineral Sample

The ore and rougher concentrate samples were obtained respectively from the McArthur River and Elura deposits in Australia (Logan et al. 1993, Anon. 1983). The mineralogical analysis (XRD & SEM) revealed that sphalerite (ZnS), galena (PbS) and pyrite (FeS.) occurred as the major sulphide phases and quartz (SiO.) was the most abundant non-sulphide phase in the ore and concentrate matrix. The chemical composition of both samples is shown in Table 1. The crushed ore sample as received was dry-milled to d_{sl},=-250 urn or -85 urn prior to the experimental use while the concentrate sample was used as received (d_{so}=-28 urn).

Table I. Chemical composition of the ore and concentrate

Sample	% Zn	‹›/‹ Fe	<7hPb	%S	Ag (K/ton)
Ore	162	7.95	5.60	15.2	59
Concentrate	45.4	8.95	2.94	29.1)	66

A number of size fractions (-250+125 pm, -125+90 urn, -90+63 pm, -63+45 um, -45+20 pm and -20 pm) were obtained from the ground ore $(ci_m=-250$

pm) and used to study the particle size effect. High grade quartz material (-75 pm) was used as the inert solids to investigate the effect of solids on the activity of bacteria.

2.2 Bac -teria and gro wth media

DSM 583 (*T. feiTooxideins*) and the designated mixed cultures, mesophilic MES1 and moderately thermophilic MOT6 were used in this study. These cultures were grown and maintained on the ore (1-2% w/v) using orbital shakers at 30°C (DSM 583 and WJM) and 50°C (MOT6). An enriched salt solution with a composition of $MeSO_4.7H^{\wedge}O$ (0.4 g/1), $(NH_4)_2SO_4$ (0.2 g/l), $K_2HPCC3H.0$ (0''.l g/1) and KCl (0.1 g/1) was used as the growth medium. Yeast extract (0.02% w/v) was provided for MOT6 culture to support the growth.

2.3 Bioleaching experiments

Bioleaching experiments were carried out in Erlenmeyer flasks (250 ml) containing 90 ml of enriched salt solution and 10 ml inoculum at the desired pulp density (% w/v). The progress of bioleaching and acid leaching (i.e. control) was followed by analysing the metal content (Zn and Fe) of the samples (1 ml) daily removed using an Atomic Absorption Spectrometer (AAS). pH and redox potential were also monitored and the pH was attempted to control if exceeded the initial pre-set values of 1.7 for the mesophilcs (DSM 583 and MES1) and 1.6 for the moderate thermophile MOT6.

3 RESULTS AND DISCUSSION

3.1 Effect of growth medium on the bioleaching of the ore

The effects of enriched salt solution (ES), double distilled water (DDW) and tap water (TW) as growth medium on the growth of DSM 583 strain are illustrated in Figure I. There was no significant difference in the rate and extent of metal dissolution in the first subculture (as denoted by "1") although a tendency for a decrease in the final extraction of zinc in DDW was noted. However, when the culture was subsequently subcultured onto fresh medium ("2") under the same conditions (i.e. ES->ES, TW->TW and DDW—»DDW) a remarkable deterioration in the dissolution of zinc became evident for the bacteria growing in DDW and TW as growth media. This limitation of the bacterial growth in DDW and TW appeared to be due to the limited availability of the nutrient components of enriched salt solution (ES).
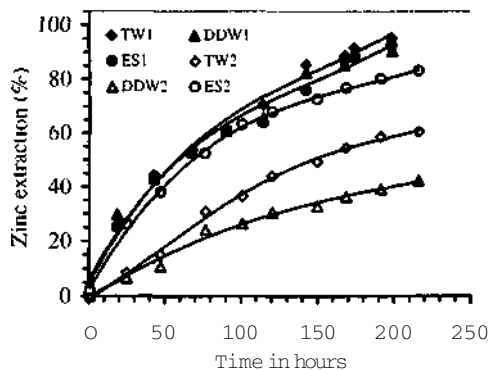
Hguie I Extraction of zinc tioni the oie by DSM 581 culture in the first (denoted by "I") and second ("2") subcultuies using enriched sali solution (ES), tap waiei (TW) and double distilled water (DDW) as the growth medium at 3()°C & Ph I 7

The occurrence of comparably extensive growth (i.e. zinc dissolution) using these three media in the first subculture was most likely owing to the transfer of some salts with the initial inoculum (10% v/v), quantity of which (despite being >I0 times diluted) appeared adequate to support the build-up of biomass and hence to achieve significant dissolution of metals. More extensive extraction of zinc (60%) occurred in TW than in DDW (42%) in the second subculture was most likely due to the presence of anions and cations at relatively high concentrations in TW i.e. Mg^{+} (2.93 ppm cf. <<X001 ppm), PO_4^v (0.31 cf. 0.15 ppm) and NO,' (5.4 cf. 0.1 ppm). These findings suggest that the requirement of growth media i.e. the concentrations of salts to be added would be determined by the quantity of the substrate available (i.e. head grade and/or pulp density) for bacterial oxidation.

Gomez et al. (1999) observed significantly higher extractions of metals (Zn, Cu and Fe) within 9K medium (no Fe^{+}. $(NH_4)_2SO_4$, 3 s/l: $MgSO_4.7H_2O$, 0. 0.5 g/l; KH_2PO_4, 0.5 g/l: KCl. 0.1 g/l; $CafNO^.HjO$, 0.01 g/l) than those within the Norris medium (it has a similar composition to ES medium; the only difference being the concentration of $MgSO_4.7H_2O$ (0.2 g/l compared with 0.4 g/l in ES). In light of the current findings the limitation of the extraction of metals in the Norris medium observed by Gomez et al. (1999) was probably due to the high metal content of the bulk concentrate i.e. 17.1 % Zn, 25.0% Fe and 14.0% Cu and operating pulp density (5% w/v) compared with the ore sample (Table I) (1% w/v) used in the current study. It was suggested that ammonium and phosphate are the most important nutrients for the bacteria with the deficiency of ammonium producing the most depressing effect (Morin et al. 1993, Torma et al. 1970).

3.2 Effect of particle size on the hioleaching of the ore

An increase in the availability of the surface area via size reduction was observed to enhance the dissolution of zinc and iron. The extraction of zinc from the size fractions <-90+63 urn was in the range of 92-97% over the hioleaching period whilst only 77% of the zinc was solubilised from the coarsest fraction (-250+125 urn). Figure 2 illustrates the plot of the dissolution rate of zinc and iron versus the initial surface area per unit volume (the initial surface area was determined using nitrogen adsorption technique). A significant increase in the dissolution rate of zinc and iron was apparent as the surface area per unit volume increased from 26.7 m^2/I (-250+125 urn) to 33.1 nr/l (-63+45 urn).

Torma et al. (1970) found a similar relationship between the metal extraction rate and particle size to that presented in Figure 2. However, Shrihari et al. (1991) observed an increase in the hioleaching rate of copper with increasing the particle size, which was attributed to the increased attachment efficiency of bacteria. Komnitsas & Pooley (1991) indicated that an excessive increase in the reactive surface area by either size reduction or increasing solids concentration per unit volume resulted in the inability of the bacterial culture to maintain high redox conditions i.e. high Fe'''/Fe^{+} ratio to effectively drive the oxidation of pyrite, instead, having led to the enhancement in the selective oxidation of arsenopyrite over pyrite.

Figure 3 shows the positive influence of reducing particle size of the ore (2% w/v) from d_{x0}=-250 urn down to -85 urn on the dissolution of zinc using the mixed mesophilic MES1 and moderately thermophilic MOT6 cultures. The dissolution rate of zinc by MOT6 and MES 1 cultures was found to increase
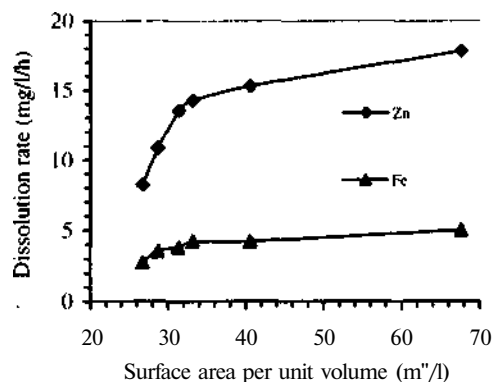

Figure 2. Effect of surface area as a function of particle size on the dissolution rate of zinc and iron from the oie (1%- w/v) using DSM 583 cultuie at 30°C
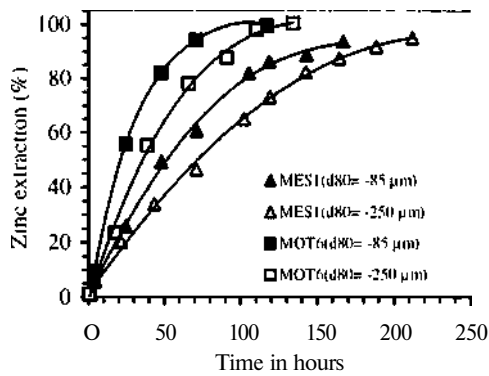
417

Figüre 3. Effect of reducing the particle size of the ore (2% w/v) on the extraction of zinc using MES1 (30°C & pH 1.7) and MOT6 (50°C & pH 1.6 & 0.02% w/v yeast extract)

by 40% and 29% respectively on decreasing the particle size of the ore with a considerable reduction in residence time. Consistently low redox potentials were recorded for the fine sample (d_{80} = -85 urn) e.g. 506 mV at 116 h compared with 631 mV even at 90 h for the coarse sample for MOT6 strain. This may indicate the relatively slow rate of accumulation of ternc iron generated by the strain in accordance with the increased surface area of the ore sample (d_s >= -85 urn). In other words, the extraction of zinc from the coarse sample (d_{80} = -250 pm) was "limited" by the available surface area allowing the accumulation of ferric iron at a faster rate.

The effect of decreasing particle size on the chemical (acid) leaching of the ore sample (in the absence of bacteria) was also evaluated as shown below in Figure 4.
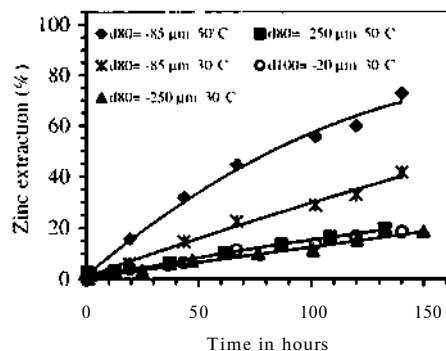
Figure 4. Effect of grinding on the acid leaching of zinc İroni the oie in the absence of bacteria at ^0ᵁC & 50'C

A remarkable enhancement in the chemical dissolution of zinc with decreasing the particle size of

the ore sample from d_m = -250 urn to d_{xo} = -85 urn was noted to occur. However, the extraction of zinc from the -20 pm fraction, which had been obtained from the ore sample (d_s) = -250 pm), was significantly lower than that from the d_{80} = -85 pm sample at 30°C (Fig. 4). The ore samples, d_{s9} = -250 urn and d_sO = -85 pm had been prepared by tema-miliing the crushed ore as received for 10 sec and 30 sec respectively. There fore, the above findings suggest that the tema-milling for a longer period affected the leaching characteristic of the ore in such a way that led to the "activation" of the ore sample as this phenomenon had been reported by Balaz et al. (1994). They postulated that the grinding influenced the solid state properties of the sulphide phases inducing defects in the mineral structure and enhancing the anodic behaviour of sphalerite in mixture with pyrite.

3.3 Effect of pulp density on the bioleaching of ore using inesophilic bacteria at 30°C

Figures 5-6 illustrate the effect of pulp density (2-10% w/v) on the extraction of zinc and iron from the ore using MES1 culture. The dissolution rate (mg/i/h) of zinc was noted to increase with increasing pulp density from 2% w/v to 8% w/v, which was consistent with the increased availability of substrate (sphalerite). Notwithstanding this, the increase in the dissolution rate of zinc was not commensurate with the increase in the pulp density such that the rate increased 1.6 times despite a 2.5 times increase in the pulp density from 2 to 5%) w/v. The time required for >90% zinc extraction increased with pulp density in the range of 2-8%) w/v (Fig. 5). There appeared a "lag" period of 155 h prior to the acceleration of the extraction of zinc at 8% w/v. The release of zinc at 10% w/v though was only slightly better in the bioleaching experiment than that in the abiotic control experiment i.e. chemical leaching.

A significant increase in the dissolution rate of iron at 2-3% w/v (Fig. 6) appeared to coincide with 60-80% zinc extraction (Fig. 5) already occurred. However, the rate and extent of iron extraction (Fig. 6) declined with further increases in the pulp density (5-10% w/v). Despite the high zinc extractions (95-97%) there was no substantial increase in the dissolution of iron at 5-8%> w/v. In fact, a decrease in the concentration of iron at 8% w/v was observed during the final stages, which could be attributed to the precipitation of ferric iron.

The rate and extent of extraction of zinc and iron at 10%> w/v were low, only marginally better than the control (acid leaching) with the implication of a severely limited contribution of bacteria to the dissolution process, which was also consistent with the low redox potentials recorded (<404 mV) (Fig. 7). These low extractions at this pulp density may be attributed
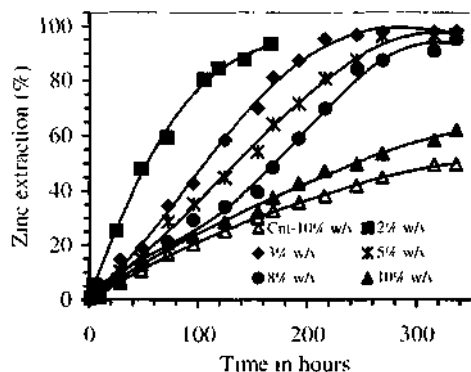
418

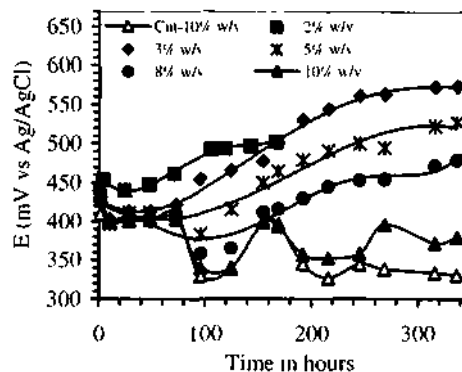Figure 5 Eltect of pulp density on the extraction of zinc from the ore ((^,.=-85 Mm) using MES I tultuie tit 30°C & pH 1 7

Figure 7. Redox potential profiles at different pulp densities duung the bioleaclnng of the oie (d»n=-85 uni) using MES1 culture at 30°C & pH f 7
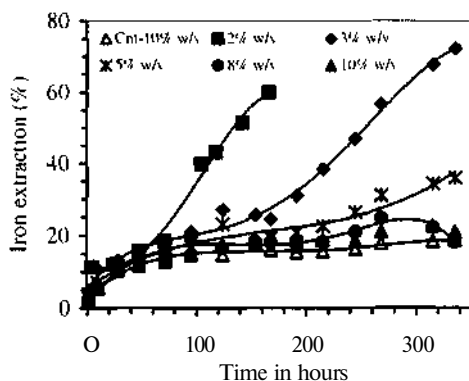

Figure 6 Effect of pulp density on the extraction of iron from the oie (d«n=-H5 pin) using MES1 culture at 30°C & pH 1.7

to a number of reasons. The increase in the residence time required for achieving the desired zinc-extractions (>90%) with increasing pulp density suggests that the bacteria-to-solid ratio at 10% w/v probably became too low lo generate the ferric iron in sufficient quantity and hence to maintain the strong oxidising conditions. A similar (linear) pattern of zinc extraction observed at 8% and 10% w/v during the initial 155 h may well be interpreted as the implication of this phenomenon. Kommtsas & Pooley (1991) had also proposed that the number of free cells in suspension decreases at high pulp densities resulting in the low rate of production of ferric iron in solution compounded with the rapid consumption of ferric iron by the sulphides present due to high surface area per unit volume which would further aggravate the oxidising conditions.

In addition to the low bacteria-to-solid ratio, as the pulp density increased, the concentration of metals in solution also increased e.g. 3.6 g/l zinc at 2% w/v compared with 13.1 g/l zinc at 8% w/v, which could have inhibited the growth and oxidising activity of bacteria. The culture MES1 was found to tolerate zinc concentrations of -10 g/l when grown on ferrous iron (100 mM) and at higher zinc concentrations the adaptation of the strain was necessary. It was also noted that the growth of the strain at high pulp densities (5-10%' w/v) improved, to some extent, with successive subculturing and gradually increasing the pulp density i.e. 5%-*8%->10%-M2% w/v. This improvement in the bioleaching of the ore may therefore be ascribed to the increase in the cell numbers (bacteria-to-solid ratio) within the inoculum as the pulp density incrementally increased and lo the adaptation of bacteria to increasing concentrations of metal ions such as zinc.

The availability of oxygen and carbon dioxide dictates ihe oxidising activity of the bacteria and thus, the bioleaching rate of sulphide minerals would be controlled by the transfer rate of oxygen and carbon dioxide into the bioleaching media (Bailey & Hansford 1993, Boon & Hcijnen 1998). In this context, the time taken for achieving the same level of extraction would increase with increasing pulp density when the system operates under oxygen and carbon dioxide limited conditions, which is consistent with the current findings.

Following the termination of the experiments, the solid residues at 3-8% w/v were separated and examined by XRD. Consistent with ihe extensive dissolution of zinc obtained at 3-8%> w/v (Fig. 6) no sphalerite was detected. The XRD profiles also revealed that the galena present in the ore was extensively converted lo lead-sulphate (anglesitc) since no sialena was found in the residues.

419

3.4 Effect of pulp density on the bioleaching of ore using moderately thermophilic bacteria at 50°C

The extraction of zinc and iron from the ore using MOT6 culture at different pulp densities is presented in Figures 8-9. A consistent delay prior to the onset of the substantial increase in the extraction of zinc occurred with increasing the pulp density from 2% to 8% w/v i.e. only 12% zinc extraction at 8% w/v compared with 51% zinc at 3% w/v over an initial period ot 28 h. In contrast to the observed trend at <8% w/v, a linear trend similar to abiotic control (acid leaching) was observed at 10% w/v indicating the inability of the strain to efficiently drive the oxidation of the ore beyond the acid leaching.
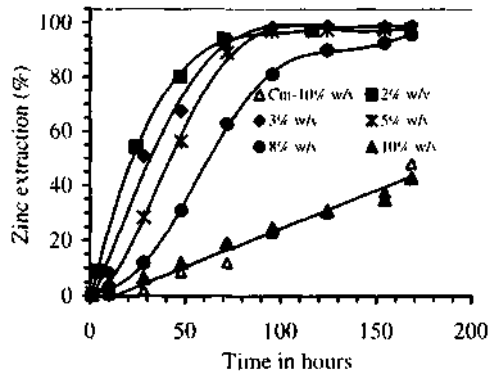
Figure S. Effect of pulp density on the extinction of zinc from the oie (d$_s$„=-X5 MITI) using MOT6 culture ;it 5()°C & pH 1.6 & 0.02V; w/v yeast extract.
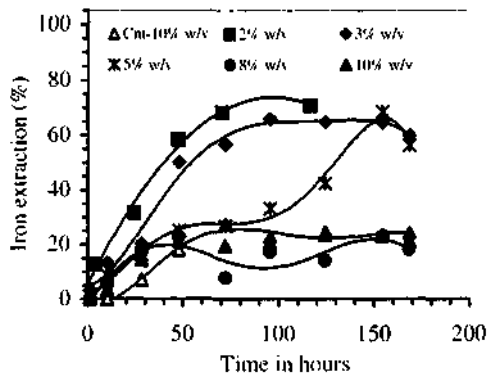
Figure 9. Effect of pulp density on the extraction ot zinc from the oie (d$_w$>=-85 urn) using MOT6 culture at 50°C & pH 1.6 & 0.02"/» w/v yeast extiact.

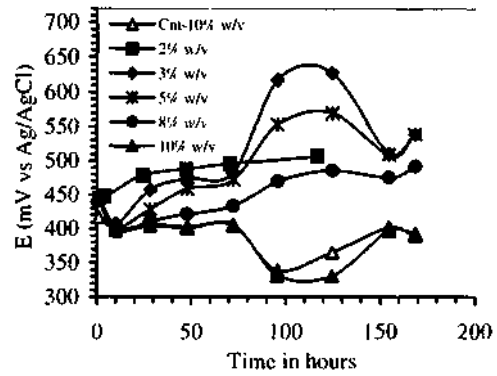Figure 10. Redox potential profiles at different pulp densities during the bioleaching of the ore (d$_s$„=-85 um) MOT6 culture at 50°C & pH 1.6 & 0.02% w/v yeast extract

The loss of some iron from solution occurred at 3-5% w/v following a bioleaching period of 155 h as shown in Figure 9. Similarly, the fluctuations observed in the extraction of iron at 8% w/v suggested the occurrence of the concurrent precipitation of ferric iron. These observations were consistent with the redox potential profiles produced at each pulp density (Fig. 10). The drop in the redox potential at 3-5% w/v after 124 h may indicate the decrease in the Fe^{3+}/Fe^{2+} ratio probably in conjunction with the precipitation of ferric iron from solution.

The XRD analysis of the residues (at 3-8% w/v) revealed the presence of K-jarosite. The only difference in the XRD profiles produced at each pulp density was the absence of pyrite in the residues for 3% w/v, which suggested more extensive dissolution of iron than that observed (60%) in Figure 9. The implication is that the actual extraction of iron could have been masked by the precipitation of ferric iron during the dissolution process. The XRD profiles also affirmed the extensive oxidation of sphalerite and galena present in the ore sample.

After the experiments had been terminated, using the strain grown in the flasks at 8% w/v as the inoculum, further tests were conducted at pulp densities 8% w/v to 12% w/v and the results were compared with the earlier tests as coded (D in Figure 11. A significant improvement in the extraction of zinc in the second subculture at 10% w/v was apparent (i.e. a 2.8-fold increase in the dissolution rate of zinc). Furthermore, an increase in the extraction of zinc even at 12% w/v was also observed during the later stages of the process (>139 h). This enhancement in the extraction of zinc in the second subculture at 10% w/v can be attributed to the utilisation of the inoculum grown at 8% w/v at which the strain had been presumably adapted to the high concentrations
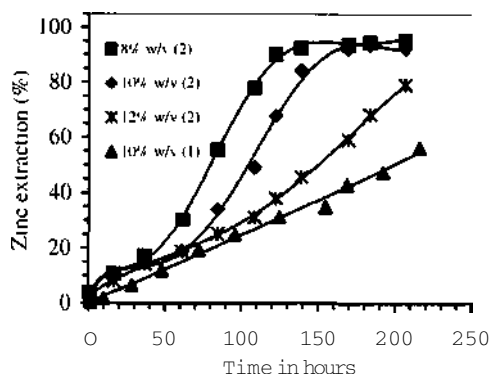
420

Figure 11 Extinction of zinc from the ore (dsu=-8S pin) using MOT6 culture grown at 2% w/v (denoted as "I") and at 8% w/v ("2") as inoculum at 8-12% w/v & 50°C & pH 1 6 & 0 02% w/v yeast extract

of zinc (-13 g/l) and/or the number bacteria was most likely high due to the increased availability of the substrate in comparison with the inoculum used in the first subculture, which had been grown at 2% w/v. These findings accord with the earlier presumptions as regards the adverse effect of low bacteria-to-solid ratio and the inhibitory effect of increasing concentrations of metal ions at high pulp densities.

The moderate thermophile MOT6 appeared to sustain a better growth than the mesophile MES1 in response to the increase in pulp density. This could be attributed, in part, to the supplementary addition of 0.02% w/v yeast extract, which is utilised as a source of cellular carbon by moderate thermophiles. However, the mesophilic MES1 culture is strictly autotrophic and requires atmospheric carbon dioxide to obtain their cellular carbon. Boon & Heijnen (1998) suggested that the decrease in the biooxidation kinetics at high pulp densities was, to a large extent, related to the exhaustion of carbon dioxide in the bioleaching medium. They also estimated that the amount of carbon dioxide available in a shake flask containing 100 ml slurry with 1 g/l pyrite would be consumed within 1 h.

3.5 Effect of (inert) solids on the bioleaching of concentrate

Tonna et al. (1970) had mooted that the decrease in the bioleaching rate at high pulp densities (>20% w/v) could have resulted from the destruction of bacteria by solids attrition. Dispinto et al. (1981) found that the addition of glass beads (0-5% w/v) led to the extension of initial lag period with no growth to occur at 5% w/v beads during the oxidation of ferrous iron by *T. fetroo.xidans* in shake flasks. Similarly, Curutchet et al. (1990) observed

that the bioleaching rate of copper from covellite (0.01% w/v) decreased with increasing the amount of quartz added with a negligible growth at 8% w/v. They interpreted the adverse effect to the attachment of bacteria to quartz particles.

In this study, the addition of inert quartz particles was found to have no apparent effect on the leaching activity of MES I culture up to 13% w/v albeit an increase in the extent of lag period with increasing the concentration of quartz added from I to 8% w/v was observed for MOT6 culture (data not shown). These findings were consistent with the redox profiles (not shown) indicating the inability of MOT6 culture to maintain the oxidising conditions (>400 mV) required to efficiently drive the extraction of zinc over the lag periods observed. Presuming that the capacity of the system for the production of ferric iron would be directly proportional to the number of viable bacteria present, the low redox potentials can be attributed to the low bacterial numbers presumably due to the damage to bacterial cells by the action of solid particles at a particular pulp density.

Further tests using a stronger inoculum even at high concentrations of quartz (13-18% w/v) showed no adverse effect of quartz particles on the rate and extent of extraction of zinc as presented in Figure 12 where the pulp density of the concentrate was kept constant at 2% w/v. Consistently, the bacterial population was able to sustain high redox potentials (>431 mV) over the bioleaching period (Fig. 12).

The current and literature data suggest that solids could cause mechanical damage to the bacterial cells but providing the bacterial population could maintain sufficiently high oxidising conditions, no adverse effect on the metal extraction would probably be experienced.
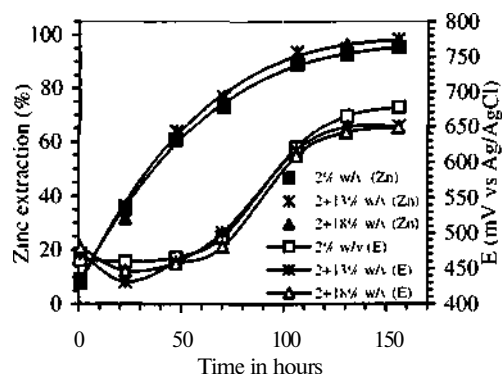

Figure 12. Extraction of zinc from the concentrate (2% w/v) and redox profiles produced using MOT6 culture (50°C & pH 1 6 & 0 02% w/v yeast extract) in the presence of 13-18% w/v quartz

4 CONCLUSIONS

This study has shown that the provision of nutrient salts in the growth medium is essential to sustain optimum bioleaching activity. Quantity of nutrient salts within the growth medium appears to depend on the head grade and/or the pulp density.

The increase in the available surface area via size reduction was found to enhance the dissolution of zinc from the ore at low pulp densities (1-2% w/v) and also the size reduction (i.e. grinding) may "'activate" the sulphide minerals. However, the excessive increase in the surface area with increasing pulp density was shown to adversely influence the dissolution process leading to a prolonged residence time lo achieve the desired zinc extraction. This was consistent with the inability of the bacterial cultures to maintain the oxidising conditions required for the efficient dissolution of zinc (>400 mV). The adverse effect of increasing pulp density can be attributed i) to the decrease in the number of bacteria-to-solid ratio, ii) to the inhibitory effect of increasing concentrations of metal ions in solution, iii) to the limited availability/transfer of oxygen and carbon dioxide (i.e. increasing demand for these gasses) with increasing pulp density, and iv) to the mechanical damage to the bacterial cells by solids.

The moderate thermophile M0T6 culture appeared to sustain a better growth than the mesophile MES1 in response to the increase in pulp density probably due to the supplementary addition of yeast extract (0.02% w/v) as a source of cellular carbon. The use ot strong inoculum i.e. prepared/grown at high pulp densities could, to some extent, alleviate the adverse effect of increasing pulp density probably due to a high cell-to-solid ratio within the system. The addition of inert solids even at high concentrations was found to produce a limited effect on the bioleaching process.

REFERENCES

Anon 1983 The Elura mine. New South Wales. *Mining Meclizine* 149(61: 436-443.

Bailey. A.D and Hansford. G.S. 1993. Factors affecting the biooxidalion of sulphide minerals at high concentrations of solids: A review. *Biotechnology tu«! Bioengineering* 12(10): 1164-1174.

Bailey, A.D. and Hansford. G.S. 1994. Oxygen mass transfer limitation of batch biooxidalion ai high solids concentration. *Minerals Engineering* 7(2-3): 293-303.

Baliiz B.. Kusnierova M.. Varencova V.l. and Misura B. 1994. Mineral properties and bacterial leaching of intensively ground sphalerite and sphalerite-pyrite mixture. *Int. ./. Mineral Processing* 40: 273-285.

Barbery G.. Fletcher A.W. and Sirois L.L. 1980. Exploitation of complex sulphide deposits: A review of processing options from ore to metals. In Complex Sulphide Ores. ed. M.J. Jones. IMM. London: 135-150.

Boon M. and Heijnen J.J. 1998. Gas-liquid mass transfer phenomena in biooxidalion experiments of sulphide minerals: A review of literature dala. *Hvdronietullurgv* 48: 187-204.

Rosecker. K. 1997. Bioleaching: Metal solubilization by microorganisms. *FEMS Microbiology Reviews* 20: 591-604.

Buchanan. D.T. 1984. The McArthur River project. In *Ans. IMM Conference.* N.T.. August: 49-57

Chadwick. J. 1996. McArthur River. *Mining Magazine* 174(3): 138-145.

Curutchet G.. Donati E. and Tedesco P. 1990. Influence of quartz in the bioleaching of covellite. *Bioret overy* 2: 29-35.

Deveci. H. 2002. Effect of solids on viability of acidophilic bacteria. *Minerals Engineering* 15: II8I-1190

Dew D.W.. Lawson E.N. and Broadhurst .l.L. 1997. The BIOX" process for biooxidation of gold bearing ores or concentrates. In *Biontining: Theory. Microbes ami Industrial Processes,* ed. Rawlings D.E. Springer-Verlag. Berlin: 45-79.

Dispirit». A.A. Dugan P.R. and Tuovinen O.H. 1981. Inhibitory effects of particulate materials in growing cultures ol *Thiobacillus ferrooxidans. Biolei Imology anil Bioengineering* 23: 2761-2769.

Gomez C. Blazquez M.L. and Ballester A. 1999. Bioleaching of a Spanish complex sulphide ore-bulk concentrate. *Minerals Engineering* I2(I): 93-106.

Gordon. A.R. 1985. Zinc extraction and refining. In *Scientific and Technological Developments in Extractive Metallurgy.* GK Williams Memorial Volume. The Aus. IMM: 67-86.

Grant. R.M. 1994. Emerging developments in zinc extraction metallurgy. In *Metallurgical Process for the Early 21th Century: Technology and Practice.* Vol II. ed. Sohn H.Y.: 125-144.

Komnitsas C. and Pooley F.D. 1991. Oplimisation of the bacterial oxidation of an arsenical gold sulphide concentrate from Olympias. Greece. *Minerals Engineering* 4(12): 1297-1303.

Logan R.C.. Leung K. and Karelse G.J. 1993. The McArthur River Project. In *World Zinc 93: Prot: Int. Synip. on Zinc.* The Aus. IMM. Hobart: 27-39

Miller P.C.. Rhodes M.K.. Winby R.. Pinches A. and van Sladen P.J. 1999. Commercialisation of bioleaching foi metal extraction. *Minerals and Metallurgical Processing* 16(4): 42-50.

Morin D.. Battaglia F. and Olliver P. 1993. Study of the bioleaching of a cobaltiferous pyritic concentrate. In *Biolivitroinerallurgicul Technologies Vol. 1: Proc. of Int. Biohvdronielalliirgy Synip..* eds. Torma A.E.. Wey J.E. and Lakshmanan V.l. USA: 147-156.

Norris P.R., Burton N.P. and Fouhs N.A.M. 2000. Acidophils in bioreactor mineral processing. *Extrentophiles* 4: 71-76.

Rawlings D.E.. Dew D. and du Plessis C. 2003. Biominerahzation of metal containing ores and concentrates. *Trends in Biotechnology* 21(1): 38-44.

Sand W Gehıke T Jozsa PG and Shıppeıs A 2001
    (Bio)chennstiy ot bacieual leachmg-diiect vs incluect
    hioleaching *Huliomctiillui<;* 59(2-1) 159-175

Shııhaıı Kuinai R Gandhi KS and Nataiaian KA 1991
    Role of cell attachment in leaching ol chalcopyııte mineial
    *by Tliwbcu illin JeittifnuUui'i Applied Mu ıohıtılo^\ Bıo-
    leilimihW* % 278-287

Suzuki I 2001 Mıcıobıal leaching ol metals lioin sulphide
    mineials *Bmiet luwh>x\ Atluıuutı* 19 I I9-H2

Toima A E Waiden C C and Branıoıı R M R 1970 Mıcıo-
    biologic.il Leaching of a zinc sulphide conccnliate *Blu-
    tet lmttīo^\ tintl Bioeiixitieeriiit;* 12 SOI-S 17

TuoMiien OH and Bhatti T M 1999 Miciobiological
    leaching ol uıanıum oies *Mmeials tutti Mekilhtit;ttttil
    Pimesunz* 16(4) 51-60

Characterization of Surface Roughness of Calcite by BET and Surtronic 3[+] Techniques

U. Ulusoy & M. Yekeler
Cumhuriyet University, Department of Mining Engineering, 58140 Sivas, Turkey

C. Hiçyılmaz
Middle East Technical University, Department of Mining Engineering, Ankara, Turkey

ABSTRACT: Experimental investigations to determine the surface roughness of calcite mineral ground in ball, rod and autogenous mills by BET (Brunauer-Emmett-Teller) and Surtronic 3[+] techniques are presented. The surface roughness values of particles determined by the BET technique were stated in terms of the RBET values by calculating from the measured BET surface area values and varied between 15.98 and 19.98. The surface roughness values of particles in pelleted forms determined by Surtronic 3[+] direct measurement technique were also stated in terms of the R_a values and varied between 2.90 and 3.54 um. Considering the surface roughness values of calcite mineral ground in different mills determined by both techniques, the lower roughness values were observed in the autogenously ground particles while rod mill products had higher surface roughness values. Finally, some correlations were made between the calculated surface roughness (RBET) and measured surface roughness (R_a) values, in which the R_a values increase with increasing RBET values. The empirical relationship was found as RBET= 6.24 R_a - 2.16.

I INTRODUCTION

Grinding by different mills is very important for the minerals for further processing in mineral processing operations, In fact, it is essential to liberate and increase the surface area of valuable minerals from the gangue minerals. (Frances et al., 2001).

Mechanical grinding causes considerable changes in surface.

The different types of mills can be classified as regards to the main stresses that act on the particles: compression, shear, attrition, impact and internal forces. It is also difficult to discriminate these stresses on the particles, because at least two of them are obviously simultaneously acting in each machine. However, three modes of breakage are usually defined, which are abrasion, chipping and impact breakage (Redner, 1990).

Specific surface area (area per unit mass or volume) is a useful measure of particle size, characterization and roughness. When a clean solid surface is exposed to a gas (e.g.; NT). the gas molecules are attracted to the surface and form adsorbed layers. Under fixed conditions, the extent of adsorption is proportional to the total surface area of the solid (Hogg, 1980; Allen, 1975).

The BET (Brunauer-Emmett-Teller) method measures all the area, which can be reached by the molecules of the gas being used (often N: at liquid N: temperatures) (Adamson, 1976).

At a small enough scale, however, all real surfaces contain some degree of nonuniformity. Because of this, discrepancies between theoretical predictions and experimental observations are frequently attributed to surface roughness effects (Suresh&Walz, 1996).

In general, roughness is confined to changes in the surface representing movements of the surface larger than the interatomic distances (Jaycock& Parfitt, 1981).

Surface roughness is, most likely, due to fluctuations around a smooth and sharp interface, but may also represent a lower free energy state (Szleiferetal., 1986).

Surface roughness is becoming increasingly important applications in many fields (Bennett, 1992).

Roughness of surfaces is of interest to a wide range of researchers in materials science (Lange et. al., 1993). The roughness of the particles can be estimated by the measurement of BET gas adsorption. Once the surface area is measured, roughness of the surface can be characterized.

$$R_BET=A_BET.d.(D/6) \quad \dots \quad (1)$$

where, ABET is the BET surface area measured, d is the density of solid and D is the particle diameter (Jaycock&Parfitt, 1981).

Surface roughness is known to play an important role in the spreading behavior of liquids and the measurement of the macroscopic contact angle.

The surface roughness measurement method is based on the mechanical sensing of surface topography in combination with electronic amplification of the signal obtained (Rank Precision Industries, 1944). Such measurements represent a highly accurate method (reproducibility within 10 Angstrom of vertical resolution in the latest types of equipment, i.e. Talystep 1 of the Rank-Taylor Hobson Co.) for rapid, non-destructive analysis of the surface topography. The measuring element of the apparatus is essentially the same as the ones found in the pick-up element of present-day gramophones. Vertical displacements, stemming from the sample moving at constant speed along the diamond needle of the sensing element, are amplified electronically. The fact that the actual measuring procedure is fully electronic ensures instant read-out. The main advantage of the method of surface roughness is to be found in the direct mechanical nature of the technique (Deelman, 1977).

The purpose of this study is to determine the surface roughness values of calcite particles as an example mineral to study, using two different methods that are BET gas adsorption and direct measurement by Surtronic 3^+, and also investigate and correlate the validity of these two approaches.

2 MATERIALS AND METHOD

2.1 Materials

The mineral used in the grinding test, surface area measurements and surface roughness measurement tests were calcite from Niğde locations of Turkey. This material was prepared by crushing to -20+30 mesh sieve fractions for ball milling, -4+6 mesh sieve fractions for rod milling and -10+1 cm for autogenous milling. The chemical compositions of calcite mineral is given in Table 1. Figure 2 and 3 show the composition of calcite sample used in the experiments by SEM and XRD techniques, respectively.

Table 1. Chemical composition of calcite mineral used in this study.

CaCO,. <K	SiO,. %	MgO. %	R;0,. %
99.14	0.30	0 11	0.25

After grinding for a certain time, the appropriate amounts of fine mill products were saved for further

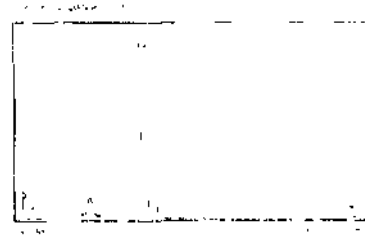tests such as BET surface area measurements and the direct surface roughness measurements.

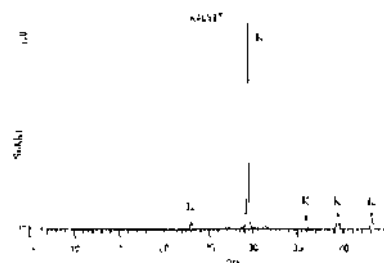Figure 1. Chemical composition of caicite used in the study by SEM

Figure 2. Mineralogical analysis of calcite used in the study by XRD

2.2 Mills

The ball milling experiments were performed in a cylindrical mill of 200 cm internal diameter and 5776 cm' volume, using the mixture of steel balls of 30 mm and 26 mm diameters that weight 5475 g. A loading of 20 % of the mill volume filled by the ball bed, a fractional interstitial filling of the bed voids by the dry powder of 0.5 at 75 % of the critical speed were chosen to run the tests. Feed size of the mineral was 374 g for calcite of -800+600 urn.

Sieving schedules were established which gave complete sieving without excessive abrasion from a sieving kinetics study, a required sample taken by cone and quartering technique was wet sieved first and then dry sieved for 10 minutes in a Ro Tap shaker for screen analysis.

A conventional rod mill has been used, with an internal diameter of 200 mm and volume of 8792

426

cm using a total 22.6 kg rod in different diameters (29. 24 and 19 mm in diameter). Feed size of the mineral for rod milling was -4750+3350 um. The sieving procedures were set for 10 minutes of dry screening following the wet screening on the samples taken by cone and quartering technique.

For dry autogenous grinding, a 420x225 mm laboratory scale autogenous mill with 31156 cm volume and rubber lining was employed. The charge as media consisted of 3.0 kg of -80+50 mm pebbles. The mineral Iced size to grind was -10 000+1000 urn that weights 2.0 kg. Sieving schedules was the same as described in the rod milling case.

2.3 The BET surface area measurements

The surface area of particles ground in ball, rod and autogenous mills was measured by using Micromentics Flowsorb II 2300, which employs BET nitrogen adsorption technique. The surface roughness (RBET) of the calcite particles was calculated from the BET measurements by using equation (1). For each mill products three measurements were made and the RBET values determined by taking the average of the three measured values.

2.4 Direct measurement of surface roughness by Surtronic 3*

In order to determine the surface roughness of particles, a portable stylus-type roughness-measuring instrument, Surtronic 3[+], which has a microprocessor was used (Figure 3). It measures the average roughness (R„) values directly by traversing across the surface of the pellets formed. For each mill products three measurements were made and the R„ values determined by taking the average of those three values.
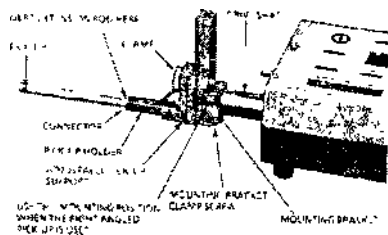

Figme 1 Siirlionic 3* Instrument used in the direct roughness measurements

3 RESULTS AND DISCUSSION

Figure 4 shows the product size distributions of calcite mineral ground dry in ball, rod and autogenous mills. The feed sizes were -800+600um for ball mill, -4750+3350um for rod mill and -80+50 mm of media mineral and -10+1 mm of ore to be ground for autogenous mill. In order to carry out BET surface area measurements and Surtronic 3[+] surface roughness test, the appropriate amounts and size of samples were taken from these grindings; i.e: the grinding time to give 100 % passing at 250 urn was the optimum grinding length to save samples for further tests. These grinding times were 16 minutes for ball and rod mills; while they were 128 minutes for autogenous mill depending on the mineral as whose product size distributions with the grinding times were given in Figure 4 (a) through (c).

Abrasion is the main mechanism of comminution in autogenous mills, while impact crushing predominates in ball and rod mills. Hence, in autogenous grinding liberation and size distribution of the ground product depend on mineralogical properties: a rock with stable grains and weak boundaries gives a steeper size distribution and a better liberation in the autogenous mill than by ball milling (Digre, 1979).

The surface areas of the particles measured by BET nitrogen adsorption technique for these minerals ground in three grinding mills are outlined in Table 2. The calculated surface roughness (RRCT) values using equation (1) are also included in the same Table. Figure 5 shows the bar graphs of the BET surface areas of calcite mineral with the grinding mills employed.

As it is easily seen from Table 2 and Figure 5, the surface roughness (RBET) values are the highest for rod mill product and the lowest for autogenous mill product of calcite mineral. This is due to the breakage characteristics of mineral being ground and the type of mill used for the comminution of the mineral.

The results of the direct measurement of surface roughness (R„) values of calcite mineral by Surtronic 3[+] instrument are outlined in Table 2 and the comparison of the R„ values determined by Surtronic 3[+] technique is shown in Figure 6 for each mill. The surface roughness (R„) values are the highest for rod mill product and the lowest for autogenous mill product of calcite as in the case of BET measurements. This was also attributed to the breakage characteristics of the calcite mineral and grinding actions of the mills employed.
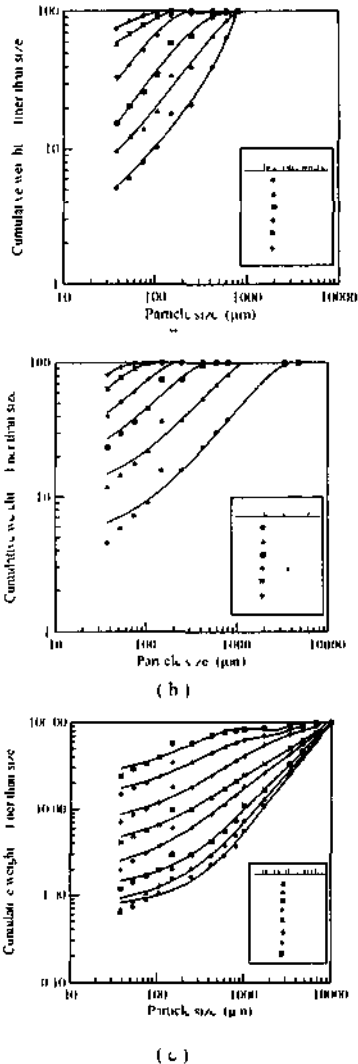
Figuie S The BET suitace roughness (R_BFT) values ot Iht pioducts of calcite giound in ditleient mills

l-iguie 6 The Suilionic V sulfate roughness (R) values of the puxluUs ot talute giouiul in different mills

(c)

Figuie 4 Panicle size distiihution of calcite mineuil ground by (a) ball mill (h) lodimll te) autogtneous mill

Table I Suitace ıoughness values ot calcite mineial calculated from BET nıtıogen adsorption technique and measuied by a Suıtronıc *V* ınstıument

Mill type	ABET (mVgi)	RBET	R, (M»')
Ball	0 27	l7 98	t 24
Rod	010	l9 98	154
Aulogeneous	0 24	l5 98	2 90

The surlace roughness (RBCI) values determined by BET nitrogen adsorption technique weie correlated to the surface roughness values (RJ determined by Surtronic 3[+] technique ol calcite (Table 2) The established coirelation is shown in Figure 7 tor calcite mineial studied based on ball, rod and autogenous mills ıesults It is obviously seen that (RBLT) increases as the R, ıncıeases This means that it the suitace area ot calcite mineial measured by BET nitrogen adsorption technique is known, the surface roughness ot this mineral can be easily estimated or vice-versa

4 CONCLUSIONS

The surface roughness values obtained trom the BET surface aiea measurements were in the ıange ot 15 98-19 98 tor calcite mineial ground by ball, rod and autogenous mills The lower surface roughness (Rutr) value was 15 98 lor autogenous milled product, while the highest value obtained was 19 98 toi tod-milled calcite the surface roughness values, on the othei hand, obtained by Surtronic 3[+] were in the ıange ot 2 90-3 54 urn tor calcite mineral ground by ball, lod and autogenous mills The lower surface

428

roughness (R„) value was 2.90 um for autogenous milled calcite. while the highest value obtained was 3.54 urn for rod-milled product of calcite. In both techniques, the determined surface roughness values show good agreement and lower surface roughness values were obtained by autogenous milling comparing lo steel media charged mills. This is due to the abrasion mechanism that is in effect mostly in autogenous mills.
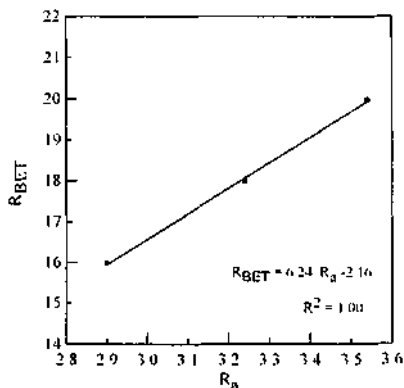

Figure 7. The variation of the RBET and R„ values

It was concluded that autogenous grinding generated particles having lower surface roughness than the other mills employed, i.e. ball and rod mills.

Therefore, the roughness values (RBET) determined by BET techniques of calcite particles increases (Figure 7) as the surface roughness values (R„) determined by a Surtronic 3^+ increases. The empirical relationship found experimentally with a linear relationship is given as RBET= 6.24 R„ - 2.16.

There is a correlation found between the RBET values and R„ values for calcite mineral studied regardless of mill type used. As the RBET values increase, the R„ values increase as well in the form of RBET= a. R„ + b type of relationship, where a and b are constants (Figure 7). The R value of this linear relationship found to be 1.00.

NOMENCLATURE

ABET	'• surface area measured by BET, enr/g
cl	: density of solid, g/cnr'
D	: particle diameter, cm
RBET	'• surface roughness values determined by BET
R„	: average roughness, urn

REFERENCES

Adamson. A.W. 1976. *Plivsical Chemislrv of Surfines:* Thud Edition. Wiley. New York.

Allen. T. 1975. *Purin h Si:e Measurement,* 2nd Edition. Halsted Press,.

Bennet. J. M.. 1992. Recent Developments in Surface Roughness Characterization. *Mens. Sit. Technol.* 3: 119-1127.

Deelman. .l. C. 1997. Surface Roughness Measurements and the Analysis of Pelrofabrics. *Geol. Mu/f.* 114. (6): 459-466.

Digre. M. 1979. Autogenous Grinding in Relation lo Abrasion Conditions and Mineralogical Factois: in M. Digre (ed.): *Autogenous Grinding Seminar.* Trondheim. paper A-1.

Frances. C. Le Bolay. N.. Belaroui. K.. Pons. M.N. 2001. Panicle Morhology of Ground Gibbsile in Different Grinding Environments. *Im. J. Min. Prot:* 61: 41-56.

Hogg. R. 1980. Characterization of Mineral Surfaces, in *P.* Somasundaran (ed.): *Fine Particle Processing.* I, Society of Mining Engineers of AIME. New York.

Jaycock. M. J.. Parti«. G. D. 1981. *Chemtstiv of Interfaces.* Ellis Horwood. Chichester.

Lange. D. A. Jennings. H. M. and Shah. S. P.. 1993. Analysis of Surface Roughness Using Confocal Microscopy. *Jmirnal of Materials Science,* 28: 3879-3884.

Rank Precision Industries. 1944. Report on the Measurement ot Surface Finish by Stylus Method. Rank Precision Industries. Taylor-Hobson Div.. Leicester.

Redner. S. 1990. *Fragmentation. Statistical Model for the Fnu lure of Disordered Media,* Elsevier.

Rideal. D. 1963. *Inlet fat ial Phenomena.* Academic Pi ess.

Suresh. L. and Walz. .1. Y.. 1996. Effect of Surface Roughness on the Interaction Energy Between a Colloidal Sphere and Flat Plaie. *J. Coll. Int. Sc-i..* 183: 199-213.

Szleii'er. I.. Shaul. A. B. and Gelben. W. M.. 1986 Cham Statistics in Micelles and Bilayers: Effects of Surface Roughness and Internal Energy. ./. *Chem. Phvs.* 85. (9): 5345-5358

The Effect of Chemical Treatment on The Production of Active Silica from Rice Husk

H. Kurama
Osmangazi University, Mining Engineering Department, Batı -Meşelik, Eskişehir, Turkey

S. K. Kurama
Anadolu University, Department of Material Science and Engineering, Eskişehir, Turkey

ABSTRACT : In this study the effect of chemical treatment on the production of high purity silica from rice husk was investigated. Rice husk, supplied from Kastomonu region-Turkey, was used as a sources of silica. They were washed with water to remove the contaminants present in them then dried in an oven at 100"C for 24 h. The dried husks were then subjected to the chemical treatment before calcinations in order to increase silica contents of husk ash. In experiments, HCl was used as a leaching reagent for extracting inorganic impurities from the husk and the affect of leaching temperature, reactive concentration, leaching time and solid percent on the purity of silica ash were systematically investigated. The results of leaching test showed that high purity amorphous silica could be produced with a 99.74 %/t grade. The surface properties of both rice hush and husk ashes were analyzed by Scanning Electron Microscope (SEM).

1 INTRODUCTION

Rice husk are the natural sheaths that form on the rice grains during their growth. Removed during the refining of rice, these husks have no commercial interest. When it burns, the silica rich ash (87-97 %) from 13-29 % by weight is produced depending on the variety, climate and geographic location (Amick 1982). The silica in husk is in hydrated amorphous form, either opal or silica gel. Due to the high silica content, rice husk has become a source for preparation of number of silicon compounds such as solar grade silicon (Ikram et al. 1988), silicon carbide (Sharma et al. 1984, Krishnarao et al. 1992, Romero et al. 1996), silicon nitride (Rahman 1994), zeolite and concrete and cements surfactant (Real et al. 1996).

Presently, the word production of rice is approximately 500 million tons a year containing 50-100 million tons of rice husks (Andreoli et al. 2000). In Turkey the annual rice production is about 240000 tons, equivalent to 2.4×10^4 tons of rice husk. These husks are mostly thrown away as waste.

The husk is mainly consisted of 70 - 75 % organic matters such as lignin. cellulose and sugar and remaining silica with small amount of alkali and other trace elements. Utilization of rice husk as a source of silica is based on removal of impurities with a low effort. Many authors (Riveros et al. 1986, Patel et al. 1987, Chakraverty et al. 1988, Krıshnaroa et al. 2001, Delia et al. 2002) have concluded that preliminary simple acid leaching of rice husk before thermal treatment proved to be effective in substantially removing most of the metallic impurities and producing silica ash with a high specific surface area (<250 m7g) and small particle sizes (<5qm). However, except for some studies on the thermal treatment of rice husk, few systematic work has been done to determine the optimum conditions for the acid leaching steps of silica ash production. The objective of the present work is to determine the effect of acid treatment parameters such as percent solid, leaching temperature, and reactive concentration and leaching time on the production of high purity silica ash from rice husk.

2 EXPERIMENTAL

2. / *Material and Methods*

The rice husk sample was supplied from Kastomonu region-Turkey. They were washed with water to remove the contaminants present in them then dried in an oven at 100"C for 24 h. The chemical composition of the sample is shown in Table 1. SiOi was found to be 13.66 %, the carbon and water content is 84%.

There are several leaching agent that can be used in the extraction of inorganic impurities from rice husk such as HCl, HiSOjand HNO,. However using H2SO4 leads to formation of metallic sulphates, some of which are not easily soluble in water. Again HCl

Table 1 Chemical composition ot nee husk

| Elements	Weigh Percent * rice husk
SiO$_2$	13.66
AhO,	0.76
Fe,0,	0.02
CaO	1.08
MfiO	0 56
K,0	0 50
LOI	83 42

nction of

tiealment time

is cheaper and more effective than HNCh, hence the choice of HCl as an extracting agent for leaching test in this study. A known weight (5 and 10 g) of dry husk was reacted with 100 ml of HCl acids solution in a 250 ml glass flaks with mounted magnetic stirrer and toped with reflux condenser in the case of boiling point tests in order to prevent evaporation losses of the solution. The leaching test were performed with 1, 2, 3 M HCl solution at 25"C, 60"C and 90"C, in order to determine the effect of solution concentration and temperature on the product. After leaching tests, the husk was washed with distilled water and then dried. Acid treated husks were then subjected to the thermal treatment at 700"C which was determined as optimum temperature in previous study (Kula et al. 1996), in electric muffle furnace. The samples were thus kept in furnace for 2 hours until complete combustion took place.

Quantitative chemical analyses of ashes were done by X-ray fluorescence (XRF) and standard wet methods. The surface structure and distribution of silica and inorganic impurities were analyzed by using Jeol 5600 1 scanning electron microscope (SEM). SEM was also employed in combination with energy dispersive X-ray analysis (EDX) in order to investigate the chemistry of the un-treated and treated husk ash.

3 RESULTS AND DISCUSSION

3.1 Contacting Time

Figure 1 shows the leaching test results for 1 M HCl acid solution concentration, 10 % solid, (10 g of husk in 100 ml solution) at 25"C after the_calcination process. It clearly indicates that, the dissolution of impurities are continues up to 2 hours. In other words the silica contents of husk ash was increased from 88 % to 97 °k with increasing contacting time up to 2 hours after this point no further change was observed.
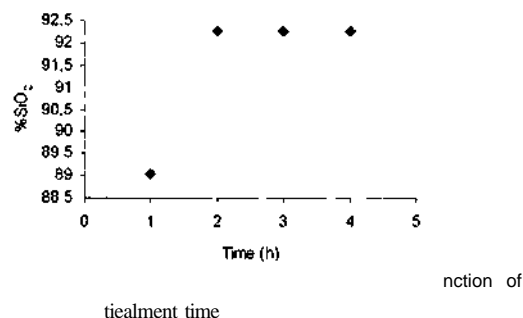
3.2 Effect of Solid Percentage

The effect of solid percentage on the dissolution ot inorganic impurities from rice husk were tested for 5 % 10 % solid with using 1 M HCl acid solution at 25"C for 2 hours contact lime. It was found that the final SiOi content of husk ash increase with the decreasing solid content from 10 to 5 %. The SiO$_2$ content increased from 91.28 to 97.63 %. This can be explained by the better contact of solution with husk at lower solid content due to the low specific density of husk.

3.3 HCl Concentration

The leaching test results for HCl treatment (1-3 M) for 2 hours duration and 5% solid at 25"C are given in Table 2. It was found that, the silica percent of rice husk does not show any linear relationship with molarities of acid used during the treatment. However the silica content of ash is increased from 88.02 to 99.50 % for 2 M HCl concentration.

Table 2. Silica m husk ash loi different acid conccntialion

Treatment	SiO %
Non-treated	88 02
1 M	97.63
2 M	98 49
3 M	97.95

3.4 Effect of leaching Température

The effect of the leaching temperature on the purity of the husk ash was tested with 1, 2 M HCl concentrations at 5% solid and 25, 60, 90"C. It was determined that increasing the leaching temperature from 25 to 60"C is resulted slightly higher product purity. However, further increase of temperature did not caused any positive effect on purity. This can be explained by the saturation of impurities extracted with HCl at 60"C.

Table 3 Effect of acid leaching tempeiature tor the production of amoiphous silica ash

| Temperature	SiO, %	
('C>	1MHCI	2MHC1
25	97.63	99.50
60	98.44	99.74
90	98.44	99.74

The analysis of the impurities and the effect of the chemical treatment on husk ash purity are given in Table 4. This indicates that, inorganic impurities present in husk are effectively removed by leaching with HCl before calcinations.

Table 4 *In* organic Oxides content ol treated *(2 M. 5% solid. 2 hours)* and untieated silica ash

Sample	Impurities %				
	$A1_20,$	$Fe_20,$	K_20	CaO	MgO
Un treated	3.65	0.10	4.60	2.60	0.73
Treated (2.VC)	0.04	0.04	0.17	0.09	0.08
Treated (90"C)	0 04	0.023	0.05	0.04	0.06

3.5 Microscopic studies

Rice husk and all products, both chemically treated (2M HCl, 5% solid at 25"C) and untreated husk ash were examined by scanning electron microscopy (SEM) in order to find out the effect of chemical treatment on silica ash. In Figure 2 the characteristic cob-shaped cellulose skeleton of the outer epidermis of husk and calcined products was clearly visible. It showed that chemical treatment did not cause any deleterious effect on ash structure.
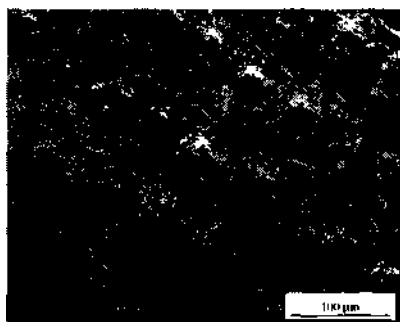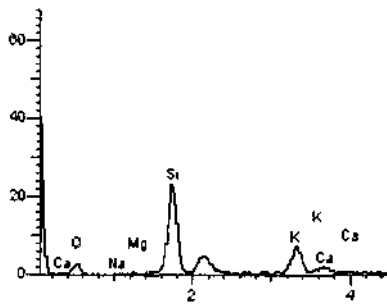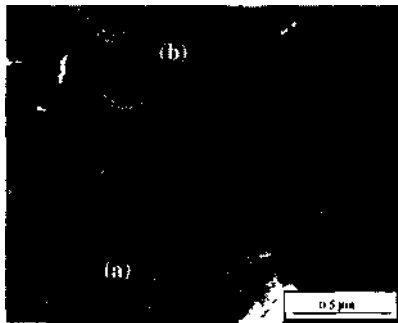

(a)

(b)

(c)

Figure 2. SEM miciogiaphs of silica liom rice husk (a), calci-nated husk (b) and acid treated + calcinated husk (c).
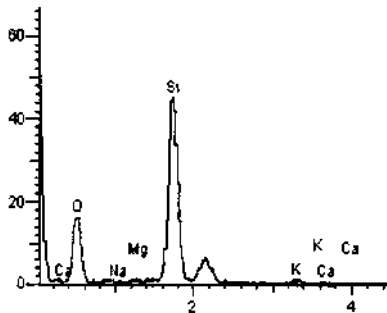
The micrograph of the natural rice husk is shown in Figure 1 a. The organic molecules appeared to be ar-ranged over the skeleton. This caused the slightly smoothening of the protuberances and widening of parallel grooves between the protuberances. Al-though these organic molecules are partly removed from skeleton surface by calcination (Fig. lb), acid treatment before calcinations is led to complete re-moving of the organic part and leaving behind the silica skeleton alone (Fig. 1c).

The silica and inorganic impurities distribution of both calcinated products were analyzed by using EDX and results arc presented in Figure 3, 4. It was detected that, silica is more concentrated in the outer epidermis than inner epidermis for untreated husk ash (Fig. 3). The inorganic impurities, mainly potas-sium was also still present in ash and concentrated in the inner epidermis. Krisnaro et al. (1994) reported thai the black particle in husk ash are due to the car-bon fixed in them. This happens due to surface melting of silica m the presence of K_20 impurity causing the decreasing of the silica purity. But in the case of acid treated husk ash, however the silica

content of outer epidermis is slightly more than the inner epidermis, it can be concluded that, silica is distributed all over the husk ash (Fig. 4). The peak intensity of silica is higher than the untreated one. This can be attributed the complete removal of impurities by acid treatment.
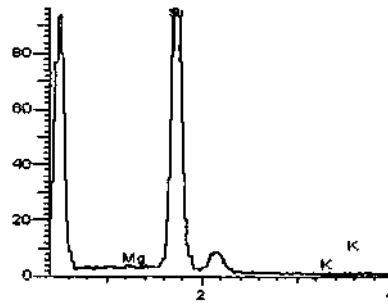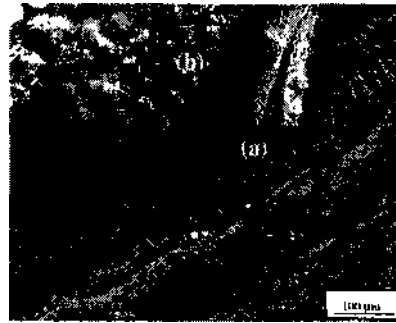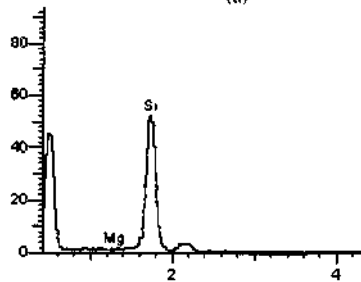

(a)

(b)

Figure 4 The SEM micrographs and EDX diffractogiani!. of acid Heated husk ash; (a) innei epideimis; (b) outer epidermis

(a)

(b)

Figuie 3 The SEM micrographs and EDX diftractogiams of calcinated husk; (a) innei epidermis, (b) outer epidermis

4 CONCLUSIONS

Many interesting material preparation routes are burdened with high material cost. As an example the cost of the preparation of porous silica for the use of commercial products ranges $US 2-10 per kg. (Conradt et al. 1992) For this reason, the production of porous and high-grade silica from rice husk as a competitive raw material is gaining interest. In this

434

study, it was found that purity of silica ash is greatly affected from chemical treatment and treatment parameters. From these experiments, the following conclusions can be drawn;

- The silica content of husk ash can be increased from 88.03% to 99.70% by HCl acid treatment before calcinations process.
- Although the amount of silica obtained from raw rice husk does not follow any linear relationship with the molarity of acid used during treatment, for 2 M HCl concentration the silica content of ash increased to 99.50 %.
- The highest silica content was obtained from 2 M HCl treatment at 60"C. However due to the extra cost of heating solution to 60"C, slightly less pure can also be obtained more cheaply at 25"C.
- The chemical and EDX analyses results showed that acid treatment with 2 M HCl, 5% solid at 25"C nearly complete treatment of impurities from husk ash.
- The cost of the treatment method used in this study is estimated to be around $US 4 / kg. Given that silica production cost in the market ranged ranges between $US 2-10 / kg, the proposed method in this study may be commercially feasible.

REFERENCES

Anne. .I.A. 1982. Purification of Rice Hulls as a Source of Solar Grade Silicon for Solai Cells. *J. Elettroihem. Stic.* 129:864-66.

Andreoli. M.. Luca. G.T. and Miyamaru Seo. E.S.. 2000. riiaractenzation of Rice husk for Chlonnation Reaction. *Material Latten.* 44: 294-98.

Cliakraveity. A.. Mishra, P. and Banerjee. H.D.. 1988. Investigation of Combustion of Raw and Acid-leached Rice Husk for Production of Pure Amorphous White Silica. ./. *Material Stiente* 23: 21 -24.

Conradt. R.. Pimkhaokham. P. and Leela-Adison. U. 1992. Nano-Structured Silica from Rice Husk ./. *tif Non-Crystalline Solids* 145: 75-79.

Delta. V.P.. Kühn. !. and Hotzu, D,, 2002. Rice Husk Ash as an alternate Source for Active Silica Production. *Material Letten,* 57: 818-21.

İkram, N and Akhter. M.. 1988. X ray diffraction Analysis of Silicon Prepared from Rice Husk Ash. *J. Material Stieme* 23: 2379-81.

Krishnarao. R.V and Godhindi. M.M.. 1992. Distribution of Silica in Rice Husk and its Effect on die Formation of Silicon Carbide. *Ceminin International* 18: 243-49.

Krishnarao. R.V.. Subrahmanyam. J. and Kumar. T.J., 2001. Studies on the Formation of Black Particals in Rice Rusk Silica Ash. *J. Eur. Ctram. Stic.* 21: 99-104.

Kula. S.. Ay. N.. Turan. S. and Putiıı. E., 1996. Effect of Active Silica on the Microstructure of Porcelain *IV.Ceramtc Conn/ess Prot eetliiijis Book lEılt. Turan, S., Kara, F. anıl Putıiıı, E.)* 279-86.

Rahman . I.A . 1994. Preparation of S^Na by Corbothenmil Reduction of Digested Rice Husk. *Ceramit s International* 20: 195-99

Real, C. Alcala. M.D. and Cnado. J.M.. 1996. Preparation of Silica from Rice husk. *J. Am. Ceram. Sot.* 79: 2012-16.

Riveros, H. and Garza. C. 1986. Rice Husk as a Source of High Pmity Silica. *J. Crvstal Growth* 75: 126-31

Romero. J.N. and Reinoso F. R..I996 Synthesis of SiC from Rice Husk Catalyzed by Iron. Cobalt or Nickel. *J. Material Scient e* 31:779-84.

Patel. M.. Kaiera. A. and Prasanna.P.. 1987. Effect of Thermal and Chemical Treatments on Carbon and Silica Contents in Rice husk *J. of Material St it-tit e* 22: 2457-2464.

Sharnia, N.K.. Williams. W.S. and Zanguıl. H.D., 1984. Foimation and Structure of Silicon Carbide Whiskeis from Rice Hulls. ./. *Am. Ceram. Sot:* 67: 715-20.

Masonry Units Heat-Insulating from No-Fines Lightweight Concrete (Pumice)

A. Sanışık

Maden Mühendisliği Bölümü. Mühendislik Fakültesi, Afyon Kocatepe Üniversitesi, 03000, Afyon, Türkiye

ABSTRACT: Owners and building proprietors are demanding high-capacity heat-insulating exterior masonry component}, specifically for further energy saving. The thermal conductivity of such materials shall be considerably lower than as specified in DIN 4I08-4. The major variables influencing the thermal conductivity of masonry materials are illustrated by taking blocks made from no-fines lightweight concrete as an example, and notes for an optimised product development are also provided. A description is given for procedures to demonstrate the thermal conductivity of the masonry units by performing measurements on the masonry material and the subsequent calculations that have to be made.

1 INTRODUCTION

It is necessary to make allowance for the influences from the masonry material, the moisture of the material, the ratio of core holes in the block as well as the recess configuration, in the development of masonry units where the thermal conductivity shall be considerably lower than the values given in DIN 4108-4. A further possibility constitutes such units where the core holes arc filled with an insulating material. Legal requirements shall also be observed in the development of these products, and also the thermal conductivity of the units shall be demonstrated by established procedures.

2 PROBLEM DEFINITION

In view of today's policy of predatory cutting price, only those can make money who actively take part in the market by offering exceptional products. It is for this reason that high-end masonry units with extremely low values of A# = 0.10 W/m*K for the thermal conductivity are now available in Germany.

According to DIN 4108-4:1991 -11, a minimum of A# = 0.14 W/m*K is only possible for masonry walls. The German construction supervisory authorities permit however, alternative, more accurate, evidence whereby the benefit of individual masonry units can be shown to their best advantage in terms of the block material and optimisation of the core-hole configuration. The procedure for demonstrating this by conducting measurements on the masonry materials and the subsequent calculation are

described in this article. Explanatory notes on the rules in the Construction Regulations List A - Appendix 2.7 (Bauregelliste, 1998) is also given. The method is principally equivalent to procedures in future European norms and standards. The major variables influencing the thermal conductivity of the masonry materials as well as notes for an optimized product development process, are given by taking units made from no-fines lightweight concrete as an example for this.

3 MASONRY MATERIALS

The starting point for all considerations is the masonry material to be used. The most important influencing variable is the apparent specific gravity of the dry substance here.

This is because the lighter material has the better the heat-insulating characteristics. The apparent specific gravity of the dry material are influenced by the apparent specific gravity of the aggregate and the percentile porosity attributable to the no-fines proportion (particle size distribution). The bulk density of the chosen aggregate mixture describes both influencing variables by a single parameter. The quantity of cementing material also has an influence on the apparent specific gravity of the dry material. The more cement that is used, the higher is the weight and hence the higher the thermal conductivity is.

The apparent specific gravity of dry material is the major, though not the only, influencing variable for describing the thermal conductivity. The differences between the various types of aggregates are minor.

though these are often crucial in determining the product's competitiveness. Thus natural pumice has a lower thermal conductivity than expanded concrete. The differences in the thermal conductivity of cementing materials may not be overlooked here. Cement is not an ideal material from the thermal conductivity point of view, and the thermal conductivity of anhydrous lime is lower. (KS-Yali), Calimax block (Calimax-Warmediimmstein) and aerated-concrete units utilize this favourable property of using anhydrous lime as the cementing material.
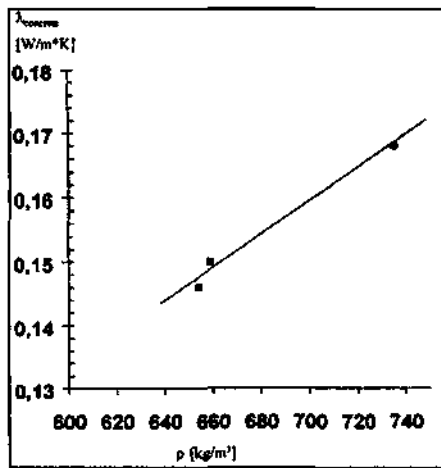

Figure 1. Example of a regression between material density and measured test values of thermal conductivity

The thermal conductivity of the masonry material has to be measured in the two-plate equipment in accordance with DIN 52612-1:1979-09 in order to determine all these characteristics. Three measurements per class of apparent specific gravity make it possible to establish a relationship between the apparent specific gravity of the dry material and the thermal conductivity of a particular masonry material. Then the apparent specific gravity of dry material is determined with a sufficient margin of safety at the upper limit of the apparent specific gravity of the material to be used for the unit, and the initial value for the thermal conductivity can then be read off at this point for calculating the class for the apparent specific gravity (Fig. 1). The Construction Regulations List (Bauregelliste, 1998) requires classification by means of a table for the value that is determined. ISO 10456:1997(E) uses a statistical evaluation technique for the data in order to compensate for scatter by the values that are measured.

Measurements are not necessary in every case. It is also possible in accordance with the Construction Regulations List to use the values given in DIN 4108-4:1991-11, whereby a moisture factor, as de-

scribed in the following section, is already included. Should the recipe, and hence the masonry material, not have undergone any change, then values from W-approvals given earlier can be taken for further use. Additional tables of thermal conductivity values for lightweight concrete made with no-fines of internal porosity are given in prEN 1745:1994, prEN 1520:1997 and prEN 12524:1996.

4 MOISTURE FACTOR

The material in the construction is not as favourable as in the case of the oven-dried samples used for measurements. The moisture that is naturally present in the substance lowers the heat-insulation properties. The influence of this on the thermal conductivity is taken into account by a moisture factor Z. Higher values of the between 20% and 25% are given for a flat-rale increase in the DIN 52612-2:1984-06.

This includes a certain margin of safety as in all norms. More accurate evidence is therefore allowed by the Construction Regulations List. Thermal conductivity measurements are performed to this end on moist samples and a relationship there by established between the moisture content and the thermal conductivity of a particular masonry material. Yet which moisture content in the subsequent construction will then set in Investigations (Schule, 1999) carried out on constructions to this end have shown that the reference moisture content according to DIN 52620:1991-04 corresponds to this value. The sorption moisture is measured and the value for the moisture factor Z is determined in Ihis way for the masonry material in question (Fig. 2).

Characteristic values for the moisture content are also found in prEN 1745:1994, prEN 1520:1997, prEN 12524:1996, ISO 10456:1997(E) as well as in the draft for DIN V 4108-4:1998-10. In addition to this, some of the norms include factors for converting the thermal conductivity for the various moisture content (by mass and by volume) and for the average temperatures of the materials.

5 CORE-HOTE RATIO

The next step is to define the core-hole ratio for the block. The manufacturer wishes this of course to be as high as possible. Selling voids are always the best method to earn money. The thermal conductivity of the block is furthermore lowered by a favorable arrangement for the holes in the core.

Table 1. Thermal conductivity values of recesses lor air pockets, according to DIN EN ISO 6946-1

Thickness, d [mm]	Thermal Conductivity, A [W/(m*K)l	Thermal Resistance, R [(m"*KVw]
5	0.046	0.11
7	0.054	0.13
10	0.067	0.15
15	0.088	0.17
20	0.111	0.18
25	0.139	0.18

Figure 4. Favorable design with small slits

Also to be observed here is a limitation of the core-hole ratio in the various specifications for masonry materials (Sariisik, 2001).

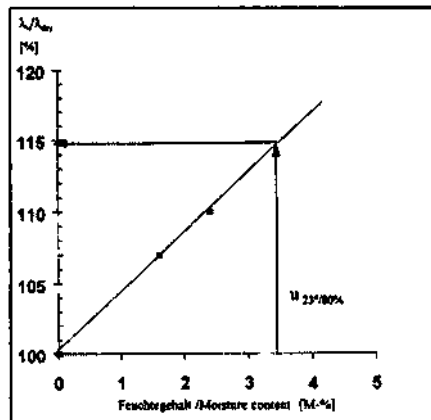Figure 5.Favorable design with regular slits

Figure 2. Example of moisture content vs thermal conductivity

A higher core-hole ratio also means a higher apparent specific gravity of the masonry unit for the same apparent specific gravity of the material used. Savings in the expensive lightweight aggregate materials can thus be made in this way. Increasing the apparent specific gravity does however also lead to an increase in the thermal conductivity of the masonry material (Fig. 1) and hence that of the whole unit as well. The strength of the high-capacity heating-ınsulatıng masonry materials is only low, a high core-hole ratio reduces the load-bearing cross-section, and hence the mechanical strength is lower as well.
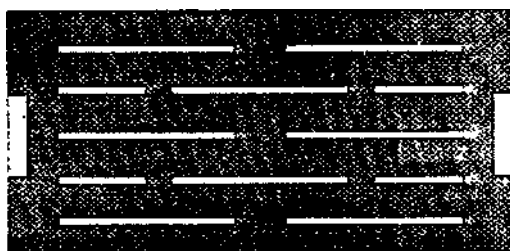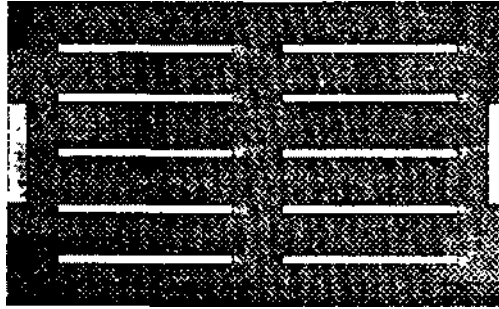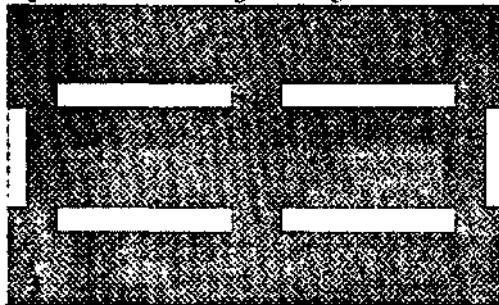

Figure 3. Unfavorable slit design

Table 2. Results of three-dimensional calculations with mortar LM 21

Block Configura-tion as in	Thermal Cond., X R ST of the masonry material	Thermal Cond., X ,-nv of the cavities	Calculated X	U-value include plaster on,both sides
	(W/m*K)	|W/(m*K)]	[W/(m*K)|	[W/(m"*K)l
Figure 3	LAC 0.14	air 0.139	0.145	0.44
Figure 4	LAC 0.14	air 0.067	0.132	0.40
Figure 5	LAC 0.14	air 0.067	0.131	0.40
Figure 4	concrete 2.10	polystyrene 0.04	0.821	1.72
Figure 5	concrete 2.10	polystyrene 0.04	0.759	1.63

6 RECESS SHAPES

The thermal conductivity of a recess in a masonry block depends on the width of the recess. Table 1 illustrates the relationship in that this can be calculated using the equations given in DIN EN ISO 6946:1996-11 as a function of the geometry. The following conclusions can be drawn from the table:

- The more narrow the recesses are, the lower is the thermal conductivity.
- The insulation by 4 recesses each of 5 mm in width is better by a factor of 2.4 than one recess 20 mm in width.
- The insulation by recesses of a width less than 4 mm is even better than using commercial available insulating materials.

The objective in designing block must therefore be an arrangement for as many narrow recesses as possible. The only limitation to this goal is by the rib structure between the recesses. The minimum width for these ribs are given by the engineering in production of charging the mold with appropriate material, and this depends both on the largest-grain size as well as on the plasticity of the mix. (Liapor Super K.) has 10 recesses for a unit width of 30 cm and a rib thickness of 19 mm. This is only possible for technical reasons in manufacturing by using a small largest-grain size and a spherical shape for the aggregate admixed with the expanded concrete. Figure 3 and 4 show the clearly apparent influence of the recess geometry. Both blocks have the same core-hole ratio of 12% here. The results of a three-dimensional heat-flow calculation are shown in Table 2. The thermal conductivity is 9% lower in the case of the more favourable core-hole arrangement of narrow recesses (Sariisik, 2001).

7 ARRANGEMENT OF RECESSES

Figure 5 shows a block having exactly the same core-hole ratio and made of the same masonry material as in Fig. 4. The only difference is that the arrangement of recesses over the cross-section is more regular. The calculations give a reduction in of less than 1%. Such an optimisation thus only realises slight advantages in blocks made of highly heat-insulating masonry materials. The key to the design of the masonry unit is the number and fineness of the recesses.

8 FILLING WITH INSULATING MATERIAL

A different situation is given where the cavities are filled with insulating material. This is because there is difference in thermal conductivity between the masonry material and the insulating material used. The difference is very high here and the influence from a consequential arrangement of the recesses in order to avoid thermal bridges is very significant. Figure 4 and 5 were re-calculated in the same way as before yet the thermal conductivity of polystyrene was taken for the cavities and concrete was used as the masonry material. The results are shown in Table 2. In this case, the thermal conductivity is lowered by some 8% by the more favorable core-hole configuration with a regular arrangement of between recesses and ribs.
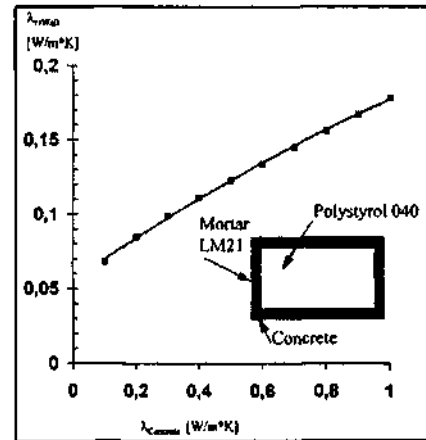

Figure 6. Thermal conductivity of a given block with variation of the material

440

The proportion of insulating material should be chosen to be as large as possible in order to achieve a low thermal conductivity for the whole masonry unit. Thermal bridges are to be avoided and a low thermal conductivity for the masonry material is to be aimed for. Figure 6 shows the values for the thermal conductivity that can be attained using different combinations of materials for a given block configuration (Sariisik, 2001).

9 CALCULATIONS

The thermal conductivity of the masonry unit can be determined once the characteristic of the materials to be used have been established and the configuration for the block has been defined. The influence of the core-hole configuration, the type of mortar used, whether filled or empty mortar pockets, etc., is taken into account in the calculations for the three-dimensional heat flow. The result from the calculations are the thermal conductivity $X,$ for the masonry structure.

A list of possible computing programs for this is included in (Christoph, Z.. Thomas F.,1998). The DIN EN ISO 10211-1:1995-11 also provides notes on the accuracy requirements for the programs and the calculations. Examples of calculations are given in prEN 1745:1994 for reference. These examples cannot be verified because no dimensions for the geometry's are given here.

10 REGULATIONS FROM THE CONSTRUCTION SUPERVISORY AUTHORITIES

The values calculated for A#, the thermal conductivity of the masonry construction, are given with an accuracy to the second decimal place. A classification table based on the principles of statistical techniques is given to this end in the Construction Regulations List, Appendix 2.7. This classification table is the source of much joy or disappointment depending on whether the target value is just reached or slightly exceeded. However it does give greater transparency in the market and enables a clearer differentiation between individual products.

In view of today's policy of predatory cutting price, only those can make money who actively take part in the market by offering exceptional products.

Formal rules have to be observed in order that the values determined by a demonstration of the thermal protection may be used. On the one hand, the values can be listed in a certificate of approval from the German Institute for Construction Engineering (DIBt). For masonry units meeting the particular requirements of each norm, more favourable values can be determined in comparison to the DIN 4108-4 in the calculations for masonry constructions made using walling components as a function of the type of mortar within the scope of the harmonisation procedures given in Appendix 2.7 of the Construction Regulations List A Part I (Bauregellisle, 1998) from the surveillance offices and established by the certifying authorities. It can then be attested in the certificate of compliance that the manufacturer can present in combination with the symbol of compliance (Ü symbol) as a major selling point (Liihr. 1999). At the present time, the established value that has been calculated to published in the Federal Gazette.

REFERENCES

Bauregellisle. A Teil i. 1998. Anhang 2.7. Ausgabe 98/1. Ernst & Sohn Verlag Berlin.

Cahmax-Wàrmedammsteni. Zulassung Nr. Z-17.1-406 und ZI7.1-458. Fraunhofei-lnfoimaiionszentruni Raum und Bau IRB. Stuttgart.

Liapor Super K.Fi'aunhofer-Inl'oimationszentrum Raum und Bau IRB. Stuttgart. . Zulassung Nr. Z-17.1-451 und Z-17.1-501

Lühr. H.-P. 1999. Rechenwerte fur die Wärmeleitfähigkeit von Baustoffen Mauerwerkskalender 1999. Einst & Sohn Verlag Berlin.

Normen/Codes: www.DIN.de oder / or www.cenorm.be

Sariisik, A.. 2001.Evaluating The Pumice(Bims) Stone of lsparla(TR) Region as a Lightweight Building Material . Forschungsprojekles. Institut für Massivbau.Techniche Universität Darmstadt.

Schule,W.&Kiessl." K. 1999 Feuchtetechnische Fragen beim Mauerweiksbau. Mauerwerkskalender 1999 Ernst & Sohn Verlag Berlin.

Yah. KS. Zulassung Nr. Z-17.1-433. Fraunhofei-Informalionszentium Raum und Bau IRB. Stuttgart.

Zürcher. C.& Thomas. F. 1998 Bauphysik (Bau und Energie; Band 2) Teubner Veilag Sluttgait.

The Effect of Fraction of Mill Critical Speed on Kinetic Breakage Parameters of Clinker and Limestone in a Laboratory Ball Mill

V. Deniz, A. Gelir & A. Demir
Mining Engineering Department, University of Süleyman Demirci, Isparla, Türkiye

ABSTRACT: In this study, the effect of fraction of mill critical speed was investigated on the limestone and the clinker samples using Göltaş cement factory (Isparta/Turkey) at batch grinding conditions based on a kinetic model. For this purpose, firstly, six different mono-size fractions were carried out between 0.850 mm and 0.106 mm formed by a V2 sieve series. Then, S, and B_M equations were determined from the size distributions at different grinding times, and the model parameters (S,, a-i.a.y and *fy,)* were compared for five different mill speed (fractional of mill critical speed; 55%, 65%, 75%., 85% and 95%).

The result of tests, the effect of fraction of mill critical speed on the grinding, it was found more different results from two different samples.

I INTRODUCTION

Comminution is extremely energy intensive, consuming 3% to 4% of the electricity generated world-wide, and comprising up to 70% of all energy required in a typical cement plant. Considering these factors, a small gain in comminution efficiency can have a large impact on the operating cost of a plant, while conserving resource as well (Fuerstenau et al., 1999).

During the last decade there have been considerable improvements in comminution efficiency not only due to the development of machines with the ability to enhance energy utilisation, but also due to the optimal design of grinding systems and operating variables that enable more efficient use of existing machines (Öner. 1999).

In the design of grinding circuits in cement plant, the Bond method is widely used to evaluate the performance and determine the power required and mill size for a material. This method is very complex and time consuming. In addition, it is very sensitive to procedural errors. For this reason, different methods have been proposed as alternative to the Bond method by many investigators.

In the recent years, matrix model and kinetic model, which are suggested by investigators, have been used to in the laboratory and in the industrial areas. Kinetic model, which an alternative approach is, consider comminution as a continuous process in which the rate of breakage of particles size is proportional to the mass present in that size.

The analysis of size reduction in tumbling ball mills using the concepts of specific rate of breakage and primary daughter fragment distributions has received considerable attention in years. Austin has reviewed the advantages of this approach and the scale-up of laboratory data to full-scale mills have also been discussed in a number of papers (Austin et al., 1981).

The use of Portland limestone cements has many benefits, both technical and economical. The European Pre-standard prEN 197-1 identifies 2 types of Portland limestone cement containing 6-20% limestone and 21-35% limestone, respectively. It is expected that the future world production and use ot Portland limestone cement will be significantly extended. These materials have different grindabilities and the individual particle size distribution of each component influences the cement hydration and finally its performance (Tsivilis et al., 1999).

Various laboratory studies, pilot plant works and full size plant observations showed that, fraction ol mill critical speed which is operating variables can affect grinding efficiency at a given output fineness.

The normal specific rates of breakage vary with speed'in the same way. However, the maximum in power occurs at different fractions of critical speed from one mill to another, depending on the mill diameter, the type of lifters, the ratio of ball to mill diameter, and the ball and powder filling conditions. The maximum is usually found in the range of 70 to 85%' of critical speed. Within the range of speed near the maximum power draw there are relatively small changes in the normal specific breakage rates

443

with rotational speed. There is no significant variation in B values with rotational speed within this range (Austin et al., 1984).

This change from cascading to cataracting pattern is the cause of the peak of feed size specific rate of breakage S, in Figure 1. In this case, J= 0.5 and U= 1 in dry batch grinding of dolomite (Herbst, and Fuerstenau, 1972). For these conditions, and with the eight 0.25 inch lifter bars on the 10 inch diameter shell, the change occurred at N=0.75. Further, the change to cataracting is accompanied by a reduction in Si and hence cascading is the major action within the mill for the conditions stated.

Austin and Brame (1983) have attempted to quantify the correction to aj in Eq. 1, and hence to S, for mill speed by:

$$a_j \propto (N - 0.1)/\{1 + \exp[15.7(N - 0.94)]\} \qquad (1)$$

This paper presents a comparison of the breakage parameters with fraction of mill critical speed under the standard conditions in a small laboratory ball mill of clinker and limestone samples, which are ground at the condition 70% of critical speed of cement ball mill in Göltaş cement factory (lspart a/Turkey).

2 THEORY

When breakage is occurring in an efficient manner. the breakage of a given size fraction of material usually follows a first - order law (Austin, 1972). Thus, the breakage rate of material that is in the top size interval can be expressed as:

$$\frac{-dw_1}{dt} = S_1 w_1(t) \qquad (2)$$

Assuming that Si does not change with time (that is. a first-order breakage process), this equation integrates to

$$\log(w_1(t)) - \log(w_1(0)) = \frac{-S_1 t}{2.3} \qquad (3)$$

where, W|(t) is the weight fraction of the mill hold-up that is of size 1 at time r and i'/ is the specific rate of breakage. The formula proposed by Austin et al. (1984) for the variation of the specific rate of breakage S, with particle size is

$$S_i = a_r X_i^{\alpha} \qquad (4)$$

where X, is the upper limits of the size interval indexed by /. mm, and ai and a are model

parameters that depend on the properties of the material and the grinding conditions.

On breakage, particles of given size produce a set of primary daughter fragments, which are mixed into the bulk of the powder and then, in turn, have a probability of being refractured. The set of primary daughter fragments from breakage of size j can be represented by b,,, where b_M is the fraction of size j material, which appears in size i on primary fracture, $n > i > j$. It is convenient to represent these values in cumulative form.

$$B_{i,j} = \sum_{k=n}^{i} b_{k,j} \qquad (5)$$

where, B_M is the sum fraction of material less than the upper size of size interval (' resulting from primary breakage of size y material: $b_{,,} = \beta_w - \beta_{,} + ; ,.$ Austin et al. (1981) have shown that the values of B,.| can be estimated from a size analysis of the product from short time grinding of a starting mill charge predominantly in size j (the one-size fraction BI1 method). The equation used is,

$$B_{i,j} = \frac{\log[(1 - P_i(0))]/\log[(1 - P_i(t))]}{\log[(1 - P_{i+1}(0))]/\log[(1 - P_{i+1}(t))]} \qquad n \geq i \geq j+1 \qquad (6)$$

where, P,(t) is the fraction by weight in the mill charge less than size X, at lime (. B,., can be fitted to an empirical function (Austin and Luckie, 1972).

$$B_{i,j} = \phi_j [X_{i-1}/X_j]^{\gamma} + (1-\phi_j)[X_{i-1}/X_j]^{\beta} \qquad n \geq i \rangle j \qquad (7)$$

where

$$\phi_j = \phi_1 [X_j/X_1]^{-\delta} \qquad (8)$$

where, δ, 0, y, and β are model parameters that depend on the properties of the material. It is found thai, B functions are the same for different ball filling ratios, mill diameters, etc. (Austin et al., 1984). If B,,, values are independent of the initial size. i.e. dimensionally normalizable, then S is zero.

3 EXPERIMENTAL STUDIES

.?. / Materiell

Limestone and clinker samples taken from Göltaş cement factory (Isparta/Turkey) were used as the experimental materials. The chemical properties of the limestone and the clinker samples are presented in Table I.

3.2 Grinding Tests

Firstly, Standard Bond Work index tests were made for limestone and clinker samples. The Bond Work

444

index values of limestone and clinker samples were determined as 13.52 kWh/t and 13.69 kWh/t, respectively. The standard set of grinding conditions used is shown in Table 2, for a laboratory mill 6283 cm volume. Six mono-size fractions (-0.850+0.600, -0.600+0.425. - 0.425 +0.300, - 0.300+ 0.212, - 0 212+0.150, -0.150+0.106 mm) were prepared and ground batch wise in a laboratory-scale ball mill for determination of the breakage functions. Each sample was taken out of the mill and dry sieved for product size analysis.

Table I.Chemical composites of clinker and limestone samples using in expeiiments.

Oxides (^{t}/r)	Limestone	Clinker
SiO,	10.60	22.22
A1,0,	1.07	3.61
Fe,0,	0 59	3 30
CaO	48.99	67.44
MgO	1.11	1.80
SO,		1.50
Loss on ignition	38.72	0.11

Table 2.The standard set of grinding conditions.

Mill	Diameter, mm			200		
	Length. mm			200		
	Volume, cm			6283		
Mill Speed	Critical (N$_c$)^a, rpm			101		
	Operational (ϕ_c). %	55	65	75	85	95
Balls	Diameter, mm			25 4		
	Specific gravity			7.8		
	Quality			Alloy Steel		
	Assumed porosity. %			40		
	Ball filling volume fraction (J%)^b			20		
Material	Specific gravity		Clinker: 3.0	Limestone: 2.69		
	Powder filling volume fraction (f$_c$ %)^c			4.2		
	Interstitial filling (U%)^d			52.5		

^{a} Calculated from $N = 42 \ 3/\sqrt{D - d}$ (D.d in metres)

^{b} Calculated from $J = \left(\dfrac{mass \quad of \quad balls \ / \ ball \quad density}{mill \quad volume} \right) \times \dfrac{1 \ 0}{0 \ 6}$

^{c} Calculated from $f = \left(\dfrac{mass \quad of \quad powder \ / \ formal \quad bulk \quad density}{mill \quad volume} \right)$

^{d} Calculated from $U = \dfrac{f}{0 \ 4 \ J}$

4 RESULTS AND DISCUSSION

4.1 Determination of S parameters

The lirst-order plots for the various feed sizes of limestone and clinker samples are given in Figure 2 toi 1. The results indicated that breakage generally the first-order relation and values of S, could be determined from the slope of straight-line of first-order plots (Table 3 to 4). Additional, Figure 12 to 13 shows the values of S, for grinding of the five fraction of mill critical speed studied, as a function of size.

4.2 Determination of B parameters

The values of B were determined from the size distubutions at short grinding times using BII method, and arc shown in Figure 14 to 15. The results of limestone and clinker samples showed a typical normalized behaviour, so that the progeny distribution did not depend on the feed particle size and the parameter 8 was zero. The model parameters are also given in Table 3- 4.
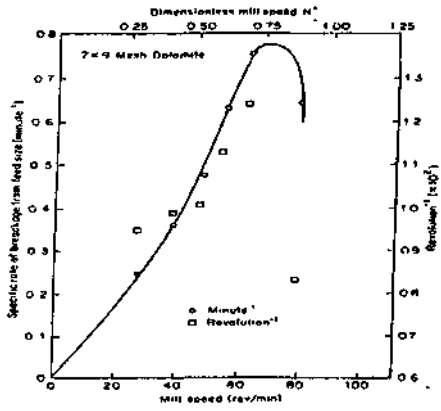
Figuie 1. Variation of specific rate of breakage from feed size versus mill speed (Herbst and Fuerstenau, 1972).
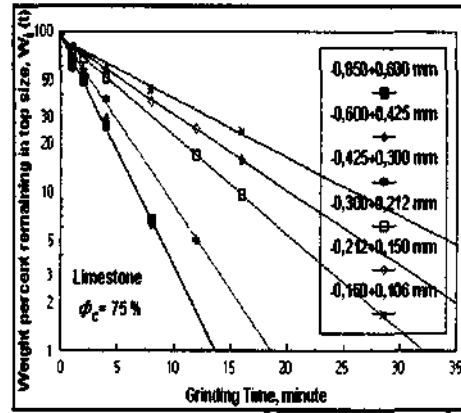

Figuie 2. First-order plots for (^=55% of Limestone.

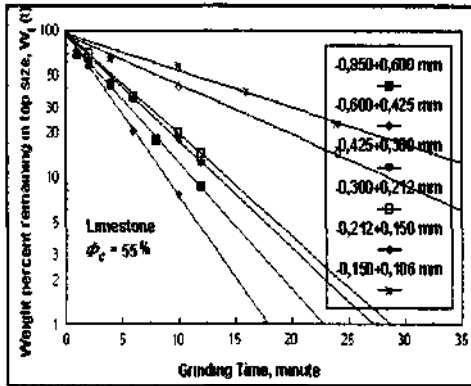Figuie J. First-order plots for «^ =65% of Limestone.

Figure 4. Firsl-order plots for ^ =75%. of Limestone.

Figure 5. First-order plots for ^ =85% of Limestone.

Figure 6. Fust-order plots for ◇ =95%i of Clinker.

446
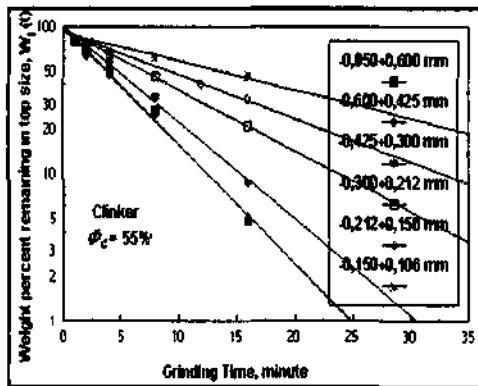
Figure 7 First-order plots for ϕ_c =55% of Clinker
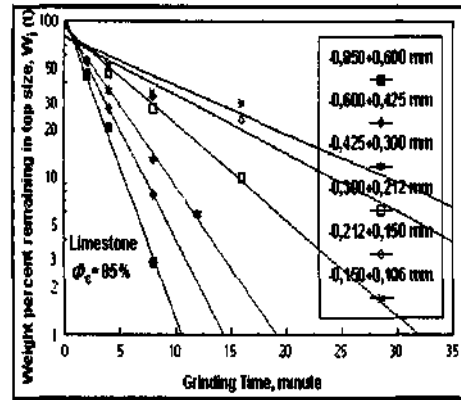

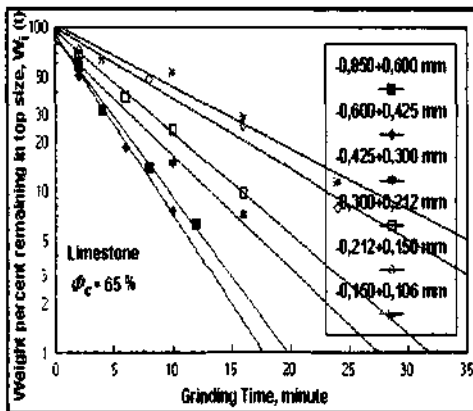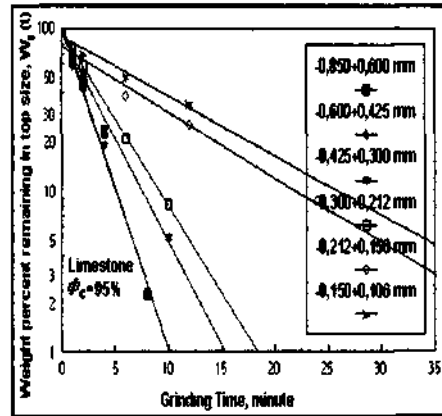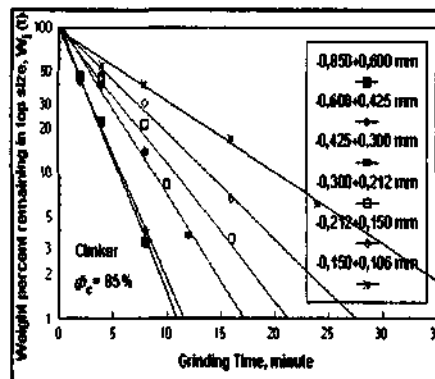Figure 10 First-order plots for ϕ_c =85% of Clinker.
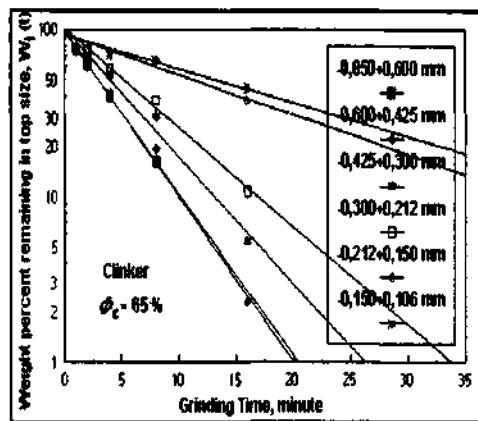
Figure 8. First-order plots for ϕ_c =65% of Clinker.
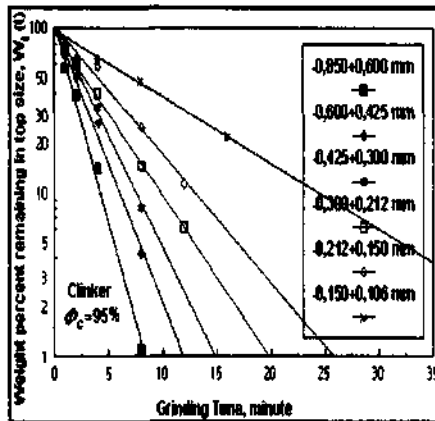
Figure 11. First-order plots for ϕ_c =95% of Clinker.
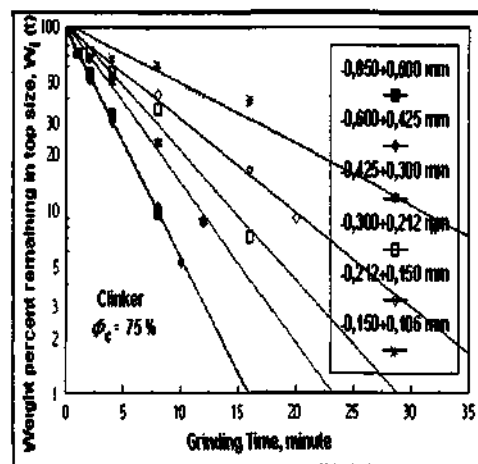
Figure 9. First-order plots for ϕ_c =75% of Clinker.
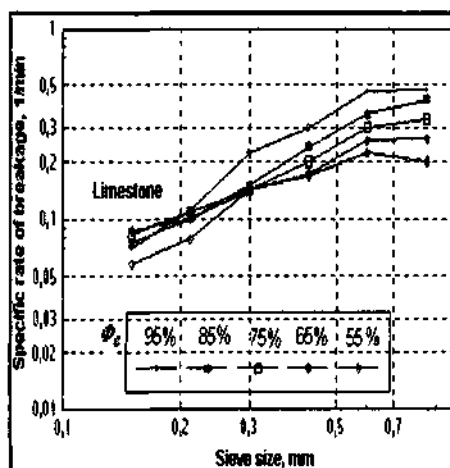
Figure 12 Specific rates of breakage for Limestone

447
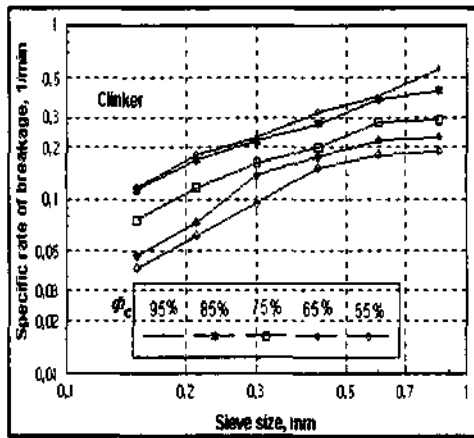
Figure 13. Specific rates of breakage for Clinker.

Figure 16 Variation of specific rate of breakage with fraction of critical mill speed for Limestone.

Figure 14. Cumulative breakage distribution functions for Limestone.

Figure 17. Variation of specific rate of breakage with fraction of critical mill speed for Clinker.
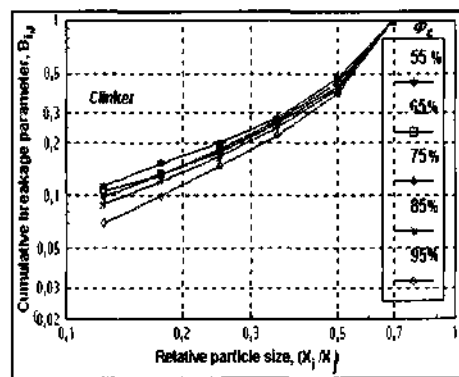
Figure 15 Cumulative breakage distribution functions for Clinker
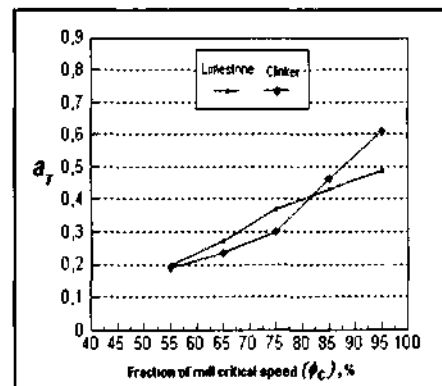
Figure 18 Variation of a_T with fraction of critical mill speed.

448

Table 3. Model parameter values of limestone for fraction ot mill critical speed.

ϕ_c (%)	$\overline{0.300+0.212}$ (mm) Si	α	a_T	ϕ_1	γ
55	0.139	0.831	0.199	0.507	1.315
65	0.141	0.765	0.273	0.510	1.336
75	0.142	0.752	0.371	0.514	1.357
85	0.150	0.833	0.436	0.504	1.432
95	0.220	1.278	0.489	0.497	1.237

Table 4. Model parameter values of clinker for fraction of mill critical speed.

(%)	0.300+0.212 (mm) Si	a	a_T	ϕ_1	Y
55	0 095	1.261	0.191	0.419	0.801
65	0.137	1.314	0.234	0.415	0 809
75	0.162	1.249	0.301	0.413	0.848
85	0.217	1.241	0.462	0.394	0.857
95	0 230	1.272	0.611	0.387	1.081

It can be seen from the data in Table 3-4 that model parameter values with the fraction of mill critical speed is similar to that indicated by the critical speed, with the ϕ_1 values, showing the trend to decrease for both samples, and the y values to increase with the increase in traction of mill critical speed for clinker, but y values to increase with the increase up to 85% of mill critical speed for limestone, later y values to decrease for higher from 85% of mill critical speed. The maximum of y is usually found in 85% of mill critical.
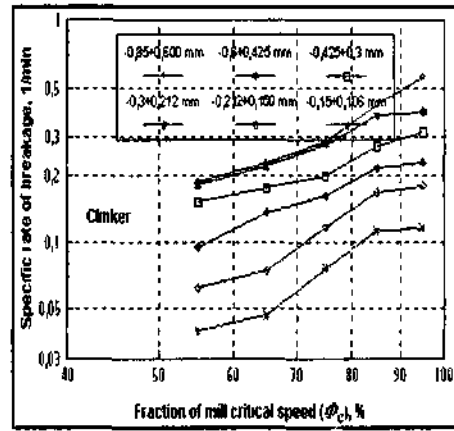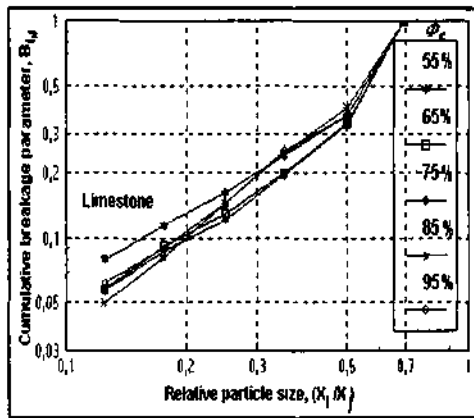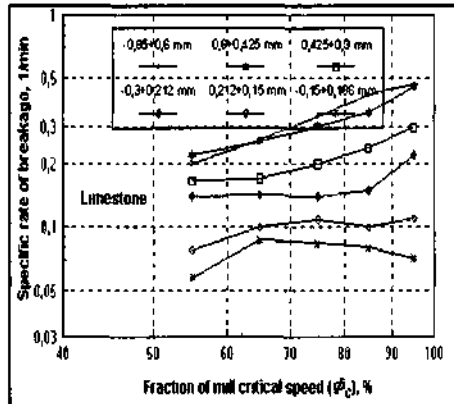
4.3 Variation of specific rale of breakage with fraction of mill critical speed

Herbst and Fuerstenau (1972) demonstrated relationships of specific rate of breakage from feed size versus mill speed. For this same purposes, variation of specific rate of breakage with fraction of mill critical speed for limestone and clinker samples were investigated, and show the graphical represent Figure 16 to 17.

The result of graphical representation, it was found different results than Herbst and Fuerstenau (1972).

4.4 Variation of ar values with fraction of mill critical speed

Austin and Brame (1983) showed variation of aj with mill speed in Eq. 1. For this purpose, variation of UT values with fraction of mill critical speed for both samples were investigated, and show the graphical represent Figure 18. Eq. 9, 10 for clinker and limestone could be determined from Figure 18. The functions of this present work are different from Eq.l.

For Clinker;

$$a_T = 0,0344 \exp(0,003\phi_c) \quad r^2 = 0.98$$

For Limestone;

$$a_T = 0,0225 \exp(0,062\phi_c) \quad r^2 = 0.96 \quad (10)$$

5 CONCLUSIONS

The dry grinding of size intervals of limestone and clinker samples showed that both samples followed the fust-order breakage law with constant normalised primary breakage distributions. In additional, these samples do not depend on the particle size from cumulative breakage distribution function.

Although, limestone and clinker samples have close work index values 13.53 kwh/t and 13.69 kwh/t, respectively, they have demonstrated different characteristics entirely in the selection function and the breakage function model parameters.

The values of the primary daughter fragment distributions and the values of a in S, = ajX^a were difference in the limestone and the clinker. As the amount of S, or aj values increased, the effective breakage increase, and broke as very fast in the undersizc of original particle size. The experimental values show that ax grinding is faster grinding for every two samples as fraction of mill critical speed increase. But, clinker is faster grinding of original particle size than limestone.

Herbst and Fuerstenau (1972) showed that change from cascading to cataracting pattern is the cause of peak of feed size specific rate of breakage S,, the change occurred at $\phi_c=$ 75%. The present study showed that change from cascading to cataracting pattern is occurred at (ϕ_c)=85%.

Austin et al. (1984) demonstrated that variation B values are no significant with rotational speed. The present work is significant variation B values with fraction of mill critical speed.

The B,, values for grinding of clinker are different from the B,, values of limestone, since the ground materials are different from each other. The y value of clinker is lower than that of limestone (y= from 0.801 to 1.081 for clinker, y= from 1.231 to 1.431 for limestone), which emphazing that the grinding of clinker produces more fine material in the fines region than the limestone grinding.

a_T values of clinker samples have decreased with increasing fraction of mill critical speed. However, a_T values of limestone .sample have decreased value up to 75% with increasing fraction of mill critical speed and it researches to peak point and, (a_T), values have decreased for later 75% mill critical speed.

In this study, it has been appeared that, these experimental values for every sample must be seen in order to lower the energy costs in grinding process.

REFERENCES

Austin. L.G.. 1972. A review introduction to the description of grinding as a rate process. *Powder Technology*. Vol. 5. 1-7.

Austin. LG. and Luckie. P.T.. 1972. Methods for determination of breakage distribution parameters. *Powder Technology*. Vol. 5. 215-222.

Austin. L.G. and Bagga. R.. Çelik. M.. 1981. Breakage properties of some materials in a laboratory ball mill. *Powdei Technology*. Vol.28. 235-241

Austin. L.G. and Brame. K.. 1983. A comparison of the Bond method for sizing wet tumbling mills with a size-mass balance simulatipn method. *Powder Teihnoloitv*. Vol. 34. 261-274.

Austin, L.G.. Khmpel. R.R. and Luckie. P.T. (eds.). 1984 Process Engineering of Size Reduction: Ball Milling. *A.I.M.E., S.M.E.,* NewYork, USA.

Fuerslenau. D.W.. Lutch. J.J. and De. A.. 1999. The Effect of ball size on the energy efficiency of hybrid-pressure toll mill/ball mill grinding. *Powder Technology*. Vol.105. 199-204.

Herbst. .I.A. and Fuerslenau. D.W.. 1972. Influence of mill speed and ball loading on the parameters of batch grinding equation. *Trans. SME/AIME*. Vol. 252. 169-176.

Öner. M.. 1999. Ball size rationing affects clinker grinding. *World Cement Research*. February. 101-106.

Tsivilis. S.. Voglis. N. and Photou. J.. 1999. A study on the intergrinding of clinker and limestone. *Mineral Engineering*. Vol. 12. 837-840.

Relationships Between Bond's Grindability (G_{bg}) and Breakage Parameters of Grinding Kinetic on Limestone

V. Deniz
Department of Mining Engineering, Süleyman Demirel University, İsparta, Turkey

ABSTRACT: The grindability of a material is the only factor used to determine the required size of a grinding machine. Although, Bond's grindabilty test is widely used to the estimate power required of an industrial grinding mill. Recently, kinetic model has been mostly used to the design of grinding circuits.

In this study, the relationship between the Bond's grindability (Ghj.) and breakage parameters (S,, a-r, y and ß) were examined. The validity of the obtained relationship parameters of S,, a-r, ß and *y* has been confirmed with correlation coefficients of 0.96, 0.92, 0.90 and 0.78, respectively, through a regression analysis of samples of limestone.

I INTRODUCTION

Grindability data, based on various techniques to measure comminution characteristics, are used to evaluate the crushing and grinding efficiency in mineral processing operations. The importance of achieving improved comminution efficiency, in terms of energy consumption, has been emphasized increasing in the cost of electricity, recently (Horst and Bassarear, 1976).

Many expressions of grindability have been proposed over the years, but two of these have come into prominence because they have become the recognised basis for design of certain types of mill. One of them is the Hardgrove index, associated mainly with vertical spindle mills and the other is Bond's grindability. associated with tumbling mills (PrasherJ987).

Bond's grindability can be empirically related to the energy required for comminution and thus is useful for the design and selection of crushing and grinding equipment (Deniz et al., 1996).

İn the recent years, matrix model and kinetic model, which are suggested by investigators, have been used in the laboratory and in the industrial areas. Kinetic model which an alternative approach is considered comminution as a continuous process in which the rate of breakage of particles size is proportional to the mass present in that size (Deniz and Onur, 2002).

The analysis of size reduction in tumbling ball mills using the concepts of specific rate of breakage and primary daughter fragment distributions have received considerable attention in years. Austin has reviewed the advantages of this approach and the scale-up of laboratory data to full-scale mills have also been discussed in a number of papers summarized by Austin et al. (1984).

This paper presents a comparison of the breakage parameters of six different limestones in a batch laboratory ball mill under standard conditions, and also the relationship between Bond's grindability and breakage parameter values of limestone samples.

2 THEORY

When breakage is occurring in an efficient manner, the breakage of a given size fraction of material usually follows a first - order law (Austin. 1972). Thus, the breakage rate of material that is in the top size interval can be expressed as:

$$\frac{-dw_1}{dt} = S_1 w_1(t) \qquad (!)$$

Assuming that S| does not change with lime (that is. a first-order breakage process), this equation integrates to

$$\log(w_1(t)) - \log(w_1(0)) = \frac{-S_1 t}{2.3} \qquad (2)$$

where, W|(l) is the weight fraction of the mill hold-up that is of size I at time *t* and 5/ is the specific rate of breakage. The formula proposed by Austin et al.

(1984) for the variation of the specific rate of breakage S; with particle size is

$$S_i = a_T X_i^a \qquad (3)$$

where, X, is the upper limits of the size interval indexed by i, mm, and ax and a are model parameters that depend on the properties of the material and the grinding conditions.

On breakage, particles of given size produce a set of primary daughter fragments, which are mixed into the bulk of the powder and then, in turn, have a probability of being refractured. The set of primary daughter fragments from breakage of size j can be represented by b,.,, where b_M is the fraction of size j material, which appears in size /' on primary fracture, $n > i > j$. It is convenient to represent these values in cumulative form.

$$B_{i,j} = \sum_{k=n}^{i} b_{k,j} \qquad (4)$$

where, B,, is the sum fraction of material less than the upper size of size interval i resulting from primary breakage of size / material: />-,= B_u - ß,$_{+/}$., . Austin et al. (1981) have shown that the values of B_M can be estimated from a size analysis of the product from short time grinding of a starling mill charge predominantly in size j (the one-size fraction BI1 method). The equation used is,

$$B_{i,j} = \frac{\log[(1 - P_i(0))]/\log[(1 - P_i(t))]}{\log[(1 - P_{j+1}(0))]/\log[(1 - P_{j+1}(t))]}, \quad n \geq i \geq j+1 \qquad (5)$$

where, P,(t) is the fraction by weight in the mill charge less than size X, at time t. B_u, can be fitted to an empirical function (Austin and Luckie, 1972).

$$B_{i,j} = \phi_j [X_{i-1}/X_j]^\gamma + (1 - \phi_j)[X_{i-1}/X_j]^\beta \qquad n \geq i \rangle j \qquad (6)$$

where

$$\phi_j = \phi_1 [X_j/X_1]^{-\delta} \qquad (7)$$

where $\hat{o}$, $cf>$, y, and β are model parameters that depend on the properties of the material. It is found that, B functions are the same for different ball filling ratios, mill diameters, etc. (Austin et al., 1984). If B,,| values are independent of the initial size, i.e. dimensionally normalizable, then 5 is zero.

3 MATERIALS AND METHOD

3.1 Material

Six limestone samples taken from different regions of Turkey were used as the experimental materials.

452

The chemical properties of the limestone samples arc presented in Table 1.

Table I. Chemical composition of limestone samples using in experiments.

Oxides (%)	GI	G2	G3	Yi	Y2	Y3
C;iO	31.03	39.09	53.56	55.43	57.20	48.99
SiO	0.05	1.65	0.08	0.59	0.05	10.60
AhO,	0.90	1.37	1.27	0.99	0.90	1.07
He.0,	0.00	0.00	0.00	0.00	0.00	0.59
MsO	22.42	13.92	0.75	0.40	0.22	1 II
SO,	0.02	0.03	0.03	0.12	0.02	0.09
NibO	0.07	0.07	0.06	0.05	0.05	0.04
K,0	0.10	0.16	0.09	0.10	0.09	0.08
Loss un ignition	45 24	43.05	43 41	42.05	42.74	38.72

3.2 The test of standard ball mill Bond grindability

The standard Bond grindability test is a closed-cycle dry grinding and screening process, which is carried out until steady state condition is obtained. This test was described as follow (Bond and Maxson, 1943: Yap ct al., 1982; Austin and Brame, 1983; Magdalinovic, 1989):

The material is packed to 700 cc volume using a vibrating table. This is the volumetric weight of the material to be used for grinding tests. For the first grinding cycle, the mill is started with an arbitrarily chosen number of mill revolutions. At the end of each grinding cycle, the entire product is discharged from the mill and is screened on a test sieve (Pi). Standard choice for P, is 106 micron. The oversize fraction is returned to the mill for the second run together with fresh feed to make up the original weight corresponding to 700 cc. The weight of product per unit of mill revolution, called the ore grindability of the cycle, is then calculated and is used to estimate the number of revolutions required for the second run to be equivalent to a circulating load of 250%. The process is continued until a constant value of the grindability is achieved, which is the equilibrium condition. This equilibrium condition may be reached in 6 to 12 grinding cycles. After reaching equilibrium, the grindabilities for the last three cycles are averaged. The average value is taken as the standard Bond grindability.

4 EXPERIMENTS

Firstly, Standard Bond's grindability tests were made *for* six limestone samples. Result of tests. Bond grindability values of limestone samples were appeared 6.14 g/rev, 2.89 g/rev, 2.58 g/rev, 2.48 g/rev, 2.42 g/rev and 1.54 g/rev, respectively. Then, the standard sets of grinding conditions used are shown in Table 2, for a laboratory mill of 6283 cm

volume. Eight mono-size fractions (-1.7+1.18, - 1.18+0.850, - 0.850+0.600,-0.600+0.425, - 0.425 +0.300, - 0.300+ 0.212, - 0.212+0.150, -0.150+0.106 mm) were prepared and ground batch wise in a laboratory-scale ball mill for determination of the specific rate of breakage. Each sample was taken out of the mill and dry sieved product size analysis.

Table 2. The standard set of grinding conditions.

Mill	Diameter	200 mm					
	Length	200 mm					
	Volume	6283 em-^{1}					
Mill Speed	Critical	101 rprn					
	Operational (0 = 75 90	76 rpm					
Balls	Diameter (mm)	25.4 mm					
	Specific gravity	7 8					
	Quality	Alloy Steel					
	Assumed porosity	40 %					
	Ball filling volume fraction (J)	20% (J =0 2)					
Matenal	Powder gravity, g/cm'	G-1 2.78	G-2 2.76	G-3 2.65	Y-1 2.62	Y-2 2.63	Y-3 2.69
	Interstitial filling (U%)	52 5% (U = 0 525)					
	Powder filling volume (f 9f)	4.2 %(f =0.042)					

4.1 Determination of the specific rate of breakage

The first-order plots for various feed sizes of limestone samples are illustrated in Figure 1-6. The results indicated that grinding of all size fractions, six samples could be described by the first-order law. In additional, parameters of specific rate of breakage to supply by first-order plots are present in Table 3. The specific rates of breakage of each mono-size fraction that exhibited first-order grinding kinetic behaviour were determined from the slope of straight-line of first-order plots. Additional, Figure 7 shows the values of S, for grinding of the six different limestone samples, as a function of size.

4.2 Determination of B function

By definition, the values of B were determined from the size distributions at short grinding times. The parameters were determined according to the BII method (Austin et al, 1984), and show the graphical representation on Figure 8. Limestone samples show a typical normalised behaviour, and the progeny distribution does not depend on the particle size, and it followed that the parameter ô was zero. Model parameters supply by cumulative distribution and these parameters are presented in Table 3.

Table 3.Bond's gnndability values and characteristic breakage parameters tor samples of limestone.

Material	Ghe gr/rev	S, (0.212-0.150 mm) (mm")	ar (mm^1)	a	Y	f.	ß
G-1	6.14	1.15	4.01	0.785	0.478	0.51	1.199
G-2	2.89	0.69	2.61	0.988	0.531	0.38	1.509
G-3	2 58	0.67	2.79	1 161	0.722	0.30	1.716
Y-1	2.48	0.63	2.11	1.564	0 368	0.24	1.699
Y-2	2.42	0.53	2.30	1.178	0.897	0.32	1 571
Y-3	1 54	0.50	0.87	0 228	1.218	0.41	1.712

Figure 1. First-order plots for G-1.

Figure 2. First-order plots for G-2.
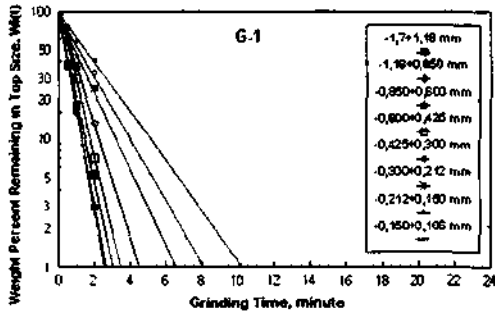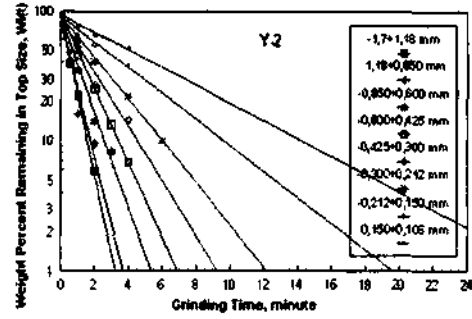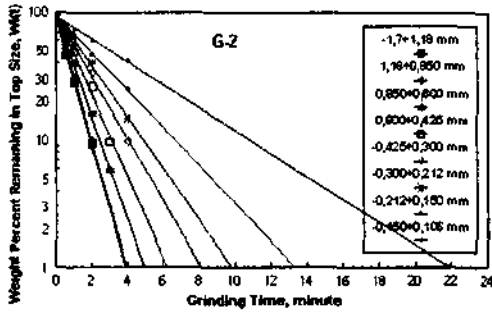

Figure 3 First-order plots for G-3.

Figure 4. First-order plots for Y-1.

Figure. 5. First-order plots for Y-2.
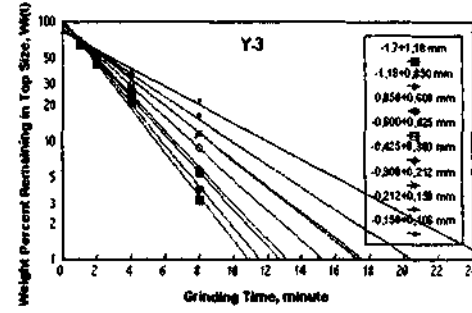
Figure 6. First-order plots for Y-3.
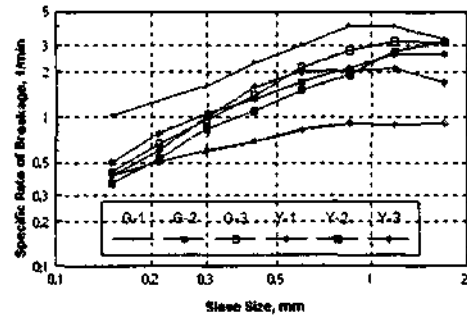
Figure 7. Variation of specific rates of breakage with particle size for samples of limestone.
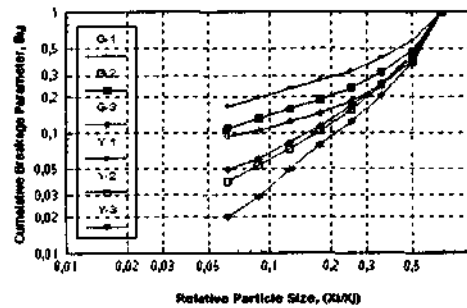
Figure 8. Cumulative breakage distribution functions for limestone.

454

5 VALIDATION OF THE RELATIONSHIPS BETWEEN BOND'S GRINDABILITY AND BREAKAGE PARAMETERS

5./ Variation of specific rate of breakagefS,) with Bond's grindability values(Gi,t)

For the same purposes, variation of specific rate of breakage (S,) with Bond's grindabilty (Gh$_S$) for six limestone samples was investigated, and it is shown in Figure 9. The values of S, seem to satisfy a linear with Gb$_S$ with a correlation coefficient 0.96 that can be expressed as follows:

$$S_i = 0.192 + 0.178 G_{b_g} \qquad (8)$$
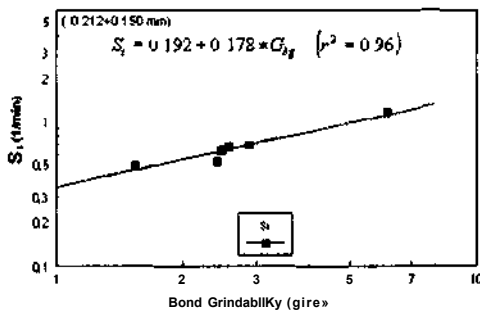
Figure 9. Variation of S, with Gb$_S$.

5.2. Variation of first-order breakage constant (ar) with Bond's grindability values (Gi,$_K$)

The values reported in Table 3 have been plotted in Fig, 10 referring to relation for different G$_{bs}$. The values of aj seem to satisfy a logarithmic with Gb$_F$ with a correlation coefficient 0.92 that can be expressed as follows:

$$a_T = 0.254 + 2.177 \ln(G_{b_g}) \qquad (9)$$
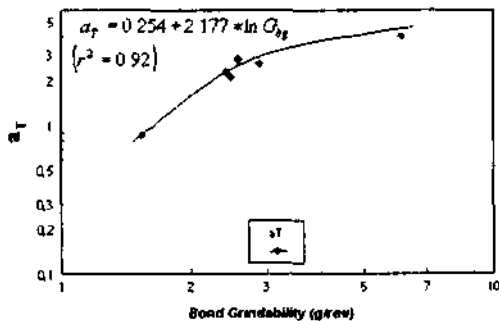
Figure 10. Variation of a$_T$ with G$_{b_g}$.

5J Varation of primary cumulative breakage constant (ß) with Bond's grindability values (G$_h$)

For the same purposes, variation of primary cumulative breakage constant (/}) with Bond's grindabilty (Gi,$_t$,) for six limestone samples was investigated, and it is shown in Figure II. The values of ß seem to satisfy a logarithmic with Gh$_F$ with a correlation coefficient 0.90 that can be expressed as follows:

$$\beta = 1.99 e^{-0.0821 G_{b_g}} \qquad (10)$$
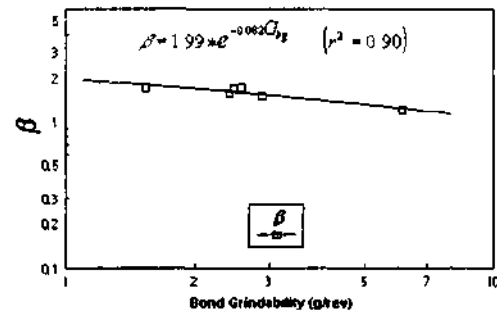
Figure 11. Variation of ß with Gi,$_s$.

5.4 Variation of primary cumulative breakage constant (y) with Bond's t>rindabilit\' values (GiJ

The values reported in Table 3 have been plotted in Fig. 10 referring to relation for different Gt,$_f$. The values of y seem to satisfy a power with Gb$_S$ with a correlation coefficient 0.78 that can be expressed as follows:

$$\gamma = 1.426 (G_{b_g})^{-0.669} \qquad (11)$$
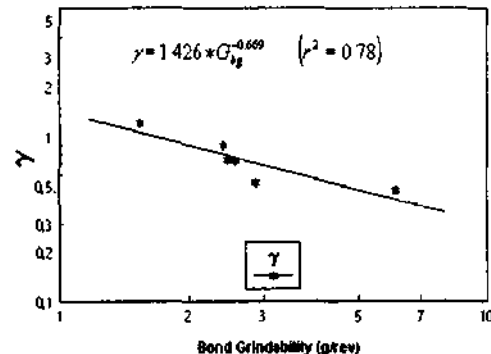
Figure 12. Variation of y with Gh$_E$.

6 CONCLUSIONS

The dry grinding of size intervals of limestone samples showed that these samples followed the first-order breakage law with constant normalised primary breakage distribution function.

The values of the primary daughter fragment distributions and the values of a in $S^\alpha \text{or} X''$ are different in the samples of limestone. As the amount of S, or c_i- values increase, the effective breakage increases, and breaks as very fast in the undersize of original particle size. The experimental values show that grinding is faster grinding for samples as fraction of bond grindability values (Gh_c) increase. Thus, G1 is faster grinding of original particle size than other samples of limestone.

The y value, which is the fineness factor, is lower for GI than other sample of limestone, indicating that more fines are produced in limestone grinding. Similarity, the Bond's grindability value (Gh_g) for G1, which is the easy grindability, is higher than other samples of limestone.

As a result of comparison for four breakage parameters, a high correlation coefficient is obtained. These four relationships may be used to provide an estimate of Bond's grindability for limestone.

REFERENCES

Austin. L.G.. 1972. A review introduction lo the description of grinding as a rate process. *Ponder Teclmologx:* Vol.5. 1-7.

Austin. L.G and Luckie. P.T.. 1972. Methods for determination of breakage distribution parameters. *Powder TeclmoloRW* Vol. 5.215-222.

Austin. L.G. and Bagga. R. Çelik. M.. I981. Breakage pıopeılıes of some materials in a laboratory ball mill. *PmulerTetlmology.* Vol. 28. 235-241.

Austin. L.G. and Brame. K.. 1983. A comparison of the Bond method tor sizing wet tumbling mills with a size-mass balance simulation method. *Powder Technology.* Vol.34. 261-274.

Austin. L.G.. Klimpel. R.R. and Luckie. P.T.. 1984. *Process Engineering oj Size Redm lion: Ball Milling.* SME-AIME. NewYork. USA.

Bond. F.C. and Maxson. W.L.. 194.3. Standard grindability tests and calculations. *Tram. SME- MME.* Vol. 15.3. 362-372.

Deniz. V. Balta, G and Yamık, A. 1996 The mterielalionships between Bond grindability of coals and impact strength index (İSI), poinl load mdex(ls) and Friability index *(FD).Changing Slopes in Mineial Processing* Kemal et all Edltors). *A.A. Bılkeınıı.* Roterdam. Netherlands. 15-19.

Deniz. V. and Onur. T.. 2002 Investigation of the breakage kinetic of pumice samples as dependent on powder filling in a ball mill. *Int. Journal of Mineral Proi essing.* Vol 67. 71-78.

Horst. W.E. and Bassarear. J.H.. 1976. Use of simplified ore grindability technique to evaluate plant perfoimance. *Trans.SME- AIME.* Vol. 260. 348-351.

Magdalinovic. N.. 1989. A procedure for lapid determination of the Bond woik index. *Inl. Journal of Mineral Processing. Val 21.* 125-132.

Prasher. C.L.. 1987. *Crushing and Grinding Process Handbook.* John Wiley & Sons. Chichestei. England.

Yap, R.F.. Sepulude. J.L. and Jauregui. R.. 1982. Determination of the Bond work index using an ordinary laboratory batch ball mill.. *Design and Installation of Comminution Cin nils.* A.L. Miliar (Co-Editor). Soc. Mm. Eng. *AIME.* USA. 176 -203.

Feldspar Beneficiation from Manisa Alaşehir Pegmatites

S. Saklar, C. Oktay. M. Karadeniz & S. Gürsu
General Directorate of Mineral Research and Exploration (MTA), Turkey

ABSTRACT: Feldspar beneficiation on the samples from Manisa-Alaşehir pegmatites were investigated. Chemical analysis showed that the total alkali content of the samples was around 7-8% as the contents of Fe_2O_3 and TiO_2 were 0.4 and 0.5% respectively. The impurities of the ore were substantially reduced to 0.15% for Fe_2O_3 and 0.03% for TiO_2 with magnetic separation. Flotation was also applied to the samples and impurities were reduced to below 0.1% for both. It was seen from the mineralogical determinations that titanium found in the samples is mainly related to phlogopite which is a Ti-bearing biotite mineral. Therefore, removing of the mica minerals from the ore with magnetic separation cause an effective decrease in titanium content. Firing button tests were also carried out on the concentrates at 1250"C and satisfactory results were obtained.

1 INTRODUCTION

Feldspars are important raw materials for ceramic and glass industries and chemical compositions; especially alkali contents determine their quality and price (Bayraktar and Çakır. 2002). The main problem in these ores from the point of mineral processing is iron and titanium bearing minerals which decrease the worth of the ores. All beneficiation studies for feldspar ores based on the separation of these undesired impurities (Bayraktar et al, 2000).

Feldspar beneficiation studies from the various ore deposits have attracted increasing interest during the last a few decades in Turkey. Therefore, kinds of feldspar rocks such as pegmatites, granites, syenites have been investigated in detail by means of mineral processing methods. In general, using rare earth magnetic separators alone is enough to separate iron-bearing minerals usually with satisfactory results. On the other hand, for removing titanium bearing minerals such as rutile and sphene, the ore is subjected to flotation, because of the ore mineralogy (Bayraktar, et al. 1998: Çelik, et al., 2001).

In these study, a pegmatitic rock from Manisa-Alaşehir region was investigated. It was found that most of the iron and titanium bearing minerals in the ore were substantially decreased with only by magnetic separation because of the ore mineralogy.

Flotation was also applied to the ore to obtain best concentrate for the industrial requirements.

2 MATERIAL AND METHODS

2. / *Mineralogy-Petrography*

Sample used in experimental studies was leucocratic granular textured coarse-grained pegmatitic rock from Manisa-Alaşehir region. It is composed of a group of fairly large euhedral-subhedral phenocrysts of orthoclase and microcline displaying cross-hatched twinning with 2.97-5.45 mm and 0.93-1.40 mm grain size respectively. The matrix mainly consists of fine-grained alkali feldspar (orthoclase and microcline), plagioclase, quartz, muscovite (0.024-0.4 mm grain size) and biotite (phlogopite) minerals with 0.020-0.600 mm grain size including accessory minerals such as garnet, chlorite, apatite, zircon, rutile thai has been slightly changed into leucoxene, rarely limonite and pyrite.
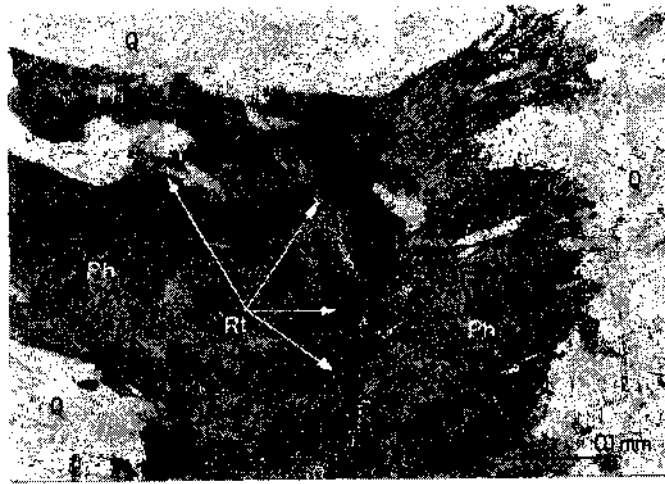
Figure I. Photomicrograph Showing Ti Rich Biotite (Phlogopite) and Rutile Needles Formed within the Phlogopite. Plane Polarized Nicol. Q-Quartz, Ph-Phlogopite and Rt-Rutile

Because of the low grade metamorphism of the pegmatitic rock, Ti bearing biotite (phlogopite) were rarely formed fine grained rutile needles with 20-24 |jm grain size and were slightly altered to chlorite minerals. Also, due to the same reason, micro folds and foliation planes improved weakly. In other words, biotites contain micro-rutile particles in its structure as inclusions (Fig 1).

Chemical composition of the sample determined by X-Ray Fluorescence (XRF) analysis is given in Table 1.

Table 1. Chemical Analysis of the Sample.

Compound	%
S i a	66.03
AI2O3	16.83
MnO	0.08
P2O,	0.21
MgO	1.10
Na,0	3.19
K;0	4.49
Fe,Oj	4.00
TİO.	0.48
CaO	1.98
L.O.I.	1.00

2.2 Method

The ore sample was crushed from 10-15 cm to 1 cm by a combination of jaw and cone crushers and its size was reduced down to -2 mm by a roll crusher.

Magnetic separation sample was prepared by screening in -600+75 urn size range. For the flotation test, a sample was ground down to its liberation size of-230 urn in a ceramic mill.

Magnetic separation tests were performed by using a rare earth permanent magnetic separator (permroll). Test samples were passed from permroll in two stages at the same conditions to achieve better separation of impurities.

In order to decrease the iron content of the ore to desired level, flotation was also applied to the samples. Experiments were performed as mica and oxide flotation separately. Amine type collector (tallow amine acetate) was used for mica. For oxide mineral flotation, petroleum sulphonate (cyanamid-R825) and Na-oleate were used separately. Before flotation experiments, slime (-25pm) was removed by a four-step décantation and its total amount was around 17-20 % in weight. Optimum flotation conditions were given below (Oktay and Saklar, 2002):

Mica flotation:

Pulp density (conditioning)	70 % by weight
Pulp density (flotation)	30 % by weight
Collector type and dosage	Armac T, 450 g/t
Conditioning time	3 min
pH	2.8
Frother type and dosage	MIBC, 40 g/t

Oxide flotation:

Pulp density (conditioning)	70 % by weight
Pulp density (flotation)	30 % by weight
Collector type I and dosage	Na-oleate, 500 g/t
Collector type2 and dosage	R825, 500 g/t
Conditioning time	5 min
PH	5
Frother type and dosage	MIBC, 70 g/t for only Na-oleate

3 RESULTS

Chemical composition of non-magnetic feldspar-quartz concentrate obtained with a permroll magnetic separator with 80% recovery by weight is given in Table-3 column A. The impurities of the ore were notably reduced to 0.15% for FciOi and 0.03% for TiOi. Firing button tests results of the concentrate at 1250"C confirmed the result of chemical analysis which gave white-light cream color.

Flotation test results were also satisfactory for R825 and Na-oleate presented in Table-3 column B and C respectively. Recovery values arc almost the same for these collectors; in mica and oxide notations are 20-21%, and 5-6% in weight, respectively. The recovery of best flotation concentrates obtained with Na-oleate was 70.96% as it was 69.01%. with R825. The firing button tests of concentrates were also similar in white-light cream colors but buttons of Na-oleate slightly better white color than R825's. It is known that range of titanium + iron level corresponds to color difference in firing buttons (Bayraktar et al.. 1997).

The results obtained showed that magnetic separation or flotation can be applied to the ore. But, magnetic separation seems to be more applicable for this ore because of its simplicity and low operating costs.

An interesting point for Manisa-Alaşehir pegmatitic rock was easiness of decreasing its TiOi content from 0.48% to 0.03% only by magnetic separation. Therefore, removing of the biotites from the ore with magnetic separation cause an effective decrease in titanium content.

Table 3. Chemical Analysis of the Magnetic Separation and Flotation Concentrates.

Compound	A (Permroll) %	B (Na-oleate) %	C (R825) %
SiO-	74.54	7.3.52	75.72
AHO,	14.5.3	13.69	14.13
MnO	0.01	0.01	0.01
P,Os	0.18	0.08	0.07
MgO	0.08	0.0.3	0.0.3
NmO	3.51	3.59	3.36
K,0	3.45	3.49	3.50
Fe,O,	0.15	0.05	0.08
TiO.	0.03	0.02	0.02
CaO	1.97	1.79	1.68
L.O.I.	0.85	2.90	0.55

4 CONCLUSIONS

1. It was shown that main titanium bearing mineral of the ore is Ti including biotite (phlogopite), which contains rutile needles as inclusion.

2. Quality feldspar concentrate from the Manisa-Alaşehir pegmatites can be obtained by magnetic separation or flotation methods. The impurities of the ore were reduced for $T\backslash0->$ from 0.48% down to 0.03%' and for Fe_2O, from 4.0%. down to 0.15% by magnetic separation only.

3. It was found that Fe_2O, and TiO contents of the ore were reduced to 0.05% and 0.02% respectively with amine and Na-oleate flotation, which is slightly belter than amine and R825.

4. Firing buttons of the magnetic separation and flotation concentrates at 1250 °C gives satisfactory results and they confirmed the results of chemical analysis.

REFERENCES

Bayraktar. I. Gulsoy. O Y.. Ekınekvi. Z . Can. M . Orhan. E C 2000. *Mom Ceninin Raw Materials (Feldspar. Quail: and Kanlın) Pnxessini;,* Kaleinaden. Haziran-Temmuz. p.8-12.

Bayraktar. I. and Çakır. U., 2002. Quality Feldspar Production at Çine Akınaden. *Industrial Minerals,* May. p.56-59.

Bayraktar. İ. Ersnyın, S, Gülsoy, Ö Y., 1997 Upgrading Titanium Bearing Na-Fcldspar By Flotation Using Sulphonatos. Succinamate and Soaps of Vegetable Oils. *Minerals Engineeriiif;.* Vol:I. No:12. p. 1363-1374

Bayraktar, I.. Ersaym. S, Gülsoy. ÖY, 1998 Magnetic Separation and Flotation of Albite Ore. *Innovations in Mineral and Coal Pıoces\ıın;,* Atak. S.. Öııal. G.. Çelik. M.S.IEds.). p.315-318.

Çelik, M S . Pehlivanoglu. B . Aslanbaş, A , Asmatulu, R . 2001. Flotation of Colored Impurities from Feldspar Ores. *Minerals and Metallurgical Processing.* Vol: 18. No.2. p. 101-105.

Oktay, C . Saklar, S . 2002 Manisa-Alaşehır-Azıtepe Feldıspat Cevherinin Zenginleştirme Çalışmaları. *MTA Raporu.*

Bacterial Leaching of Pyrite

F. Göktepe
Balıkesir University, Balıkesir Technical College, Balıkesir, Turkey

F.D. Pooley
Cardiff University, School of Engineering, United Kingdom

ABSTRACT: The ability of bacteria to catalyse the oxidation of sulphide minerals is well known. Pyrite is the most common of the naturally occurring sulphide minerals and is present as an accessory mineral in practically all commercial sulphide ore deposits. This paper presents the results of the bacterial leaching of pyrite with different particle size and pulp density. Pyrite leaching was performed in flask and the laboratory scale stirred reactor using a 1.7 litre capacity for different size fractions. The pyrite leaching was found to have increased as particle size decreased. Fe oxidation rate also found to be depending on the pulp density for the coarser particle size. At 1 % pulp density 45 % Fe oxidation was obtained in 48 hours whereas with 0.5 % pulp density 35 % Fe oxidation was obtained for -63+56 micron size fractions for the same time interval. The experiments revealed that the rate of bacterial oxidation of pyrite was depend on particle size and slightly rapid oxidation obtained in flask comparing the reactor.

1 INTRODUCTION

The ability of certain microorganisms to catalyse the oxidation of sulphide minerals has attracted much attention in recent years in minerals engineering. Bacterial oxidation of sulphide minerals is an attractive method for the production of metals from ores or concentrates as it is flexible, does not require high operating temperatures or pressures, it is self-generating in terms of solvent in the form of acid ferric sulphate solution. It involves reactanls which cannot be produced by simple chemical means alone, being a less energy intensive and an environmentally attractive process (Pooley, 1987).

Pyrite can be considered to be the most important sulphide mineral substrate as far as leaching with bacteria is concerned, and it is also the most common contaminant of complex sulphide ores and the tailings produced from their beneficiation. Materials containing pyrite in excess are therefore ideal substrates and feedstock for conventional bacterial leaching treatment as it contains equal quantities of ferrous iron and sulphur required for energy sources (Pooley, 1998). The iron oxidising bacterium *Thiobacillus ferroroxidans* was isolated from an acid mine waters in 1947. They were soon associated with the dissolution of metals from ores. Since then, extensive efforts have been concentrated in this direction in an attempt to gain belter understanding of pyrite bioleaching. The removal of pyritic sulphur from coal has also been investigated and the commercial feasibility of removing sulphur from coal has been realised using bacteria.

Bacterial leaching also has been shown to offer alternative routes to the production of many metals such as copper, zinc and nickel containing sulphides (Pooley 1987, Göktepe et al. 1998, Smith et al. 1993, Brierly, 1978). It offers process options for low grade, especially extraction of copper and uranium metals from low grade ore or mine waste, small deposits and problematic ores that would be uneconomic to treat using conventional process technology. One of the most rapidly developing areas in hydrometallurgy is the application of bacterial leaching as a pre-treatment step for the extraction of gold from refractory ores and concentrates, offering potentially significant advantages over the conventional oxidative pre-treatment alternatives (Komnitsas and Pooley, 1989). Bacterial leaching has been shown in numerous dump and heap leaching situations to be an economic process for the treatment of various commercial sulphide ores.

The aim of this paper is to provide an overview of the pyrite bioleaching considering particle size related to the research carried out for pyrite removal from coal by bacterial leaching.

2 THE MECHANISIM OF SULPHIDE MINERAL OXIDATION BY BACTERIA

Thiohacillns jcrrooxidans and *Thiohacillus thiooxklans* are live in inorganic matter (autotrophic) and utilise oxygen for growth (aerobic) bacteria and require an acid environment between pH 1.5-5. These organisms exhibit different temperature optima for different strains and substrates but optimum is often considered 30-35° C. The organisms are slow-growing and division time is variable with conditions (Poolcy, 1998).

The exact role of bacteria in bacterial oxidation of sulphide minerals is complex. The bioleaching is due to a catalytic effect of the organisms. Two main mechanisms for bacterially assisted oxidation of insoluble sulphide minerals have been proposed, which often referred to as the direct and indirect mechanisms. Both direct leaching (bacteria attached to the sulphide minerals) and indirect leaching (Fe^{+2} oxidised to Fe^{4+} by the bacteria followed by metal leaching by the Fe^{+}) take place. In the presence of water, oxygen and sulphuric acid pyrite slowly autooxidises, due to the formation of reaction product layers such as sulphur on the surface of pyrite particles that resulting in diffusion controlled reactions, according to equations 1 and 2 :

$$2FeS_2 + 7O_2 + 2H_2O \rightarrow 2FeSO_4 + 2H_2SO_4 \quad (1)$$

$$2FeS_2 + 2 H_2SO_4 + O_2 \rightarrow 2FeSO_4 + 2H_2O + 4S \quad (2)$$
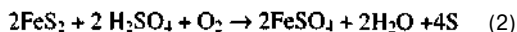
The fundamental reaction for indirect leaching then involves the microbial oxidation of ferrous iron to ferric sulphate and elemental sulphur to sulphuric-acid as shown in equations 3 and 4 respectively. *Thiohacillus ferrooxidans* are able to oxidise ferrous iron at a rate 500.000 times as fast as would occur in their absence (Brierly, 1978).

$$4FeSO_4 + 2H_2SO_4 + O_2 \xrightarrow{\text{bacteria}} 2Fe_2(SO_4)_3 + H_2O \quad (3)$$
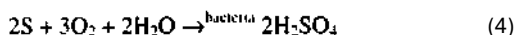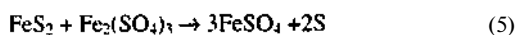
$$2S + 3O_2 + 2H_2O \xrightarrow{\text{bacteria}} 2H_2SO_4 \quad (4)$$

The ferric sulphate formed during the indirect mechanism reacts with pyrite according to equation 5

$$FeS_2 + Fe_2(SO_4)_3 \rightarrow 3FeSO_4 + 2S \quad (5)$$

The ferrous sulphate and sulphur which are formed in equation 5 are again oxidised by bacteria to ferric sulphate and sulphuric acid as shown in equation 3 and 4. The overall reaction equation for direct oxidation of the ferrous sulphate ions of pyrite ıs represented by equation 6

$$2FeS + 15/2 O: + H<) \xrightarrow{\text{hjucr,J}} Fe_2(S0_4)_3 + H_2S0_4 \quad (6)$$
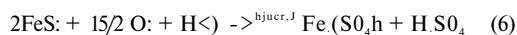
The direct attack on the sulphide mineral with ferrous iron as the oxidant as shown in equation 6 proceeds rapidly and is chemically controlled. The reaction products such as elemental sulphur do not form on the pyrite surface since they are oxidised by the bacteria (Pooley, 1998).

3 MATERIALS AND METHODS

3.1 Materials

Pure pyrite sample was used in the bacterial leaching experiments and was crushed and ground to below 63 micron in the tema mill. Then sample was separated to size fractions by using the Cyclosizer and after 15-20 minutes processing, sample from each cyclone were collected into separate beakers, filtered, dried and weighed. Bacterial leaching was applied for each cyclone fractions.

3.2 Microorganisms

A culture of iron oxidising *Thiohacillus Ferrooxidans* which have been grown on a variety of sulphide concentrates over years in the Cardiff University, Division of Materials and Minerals Engineering Department were used throughout the study.

3.3 Methods

The bacterial leaching experiments performed in this study employed by shake flasks and pachuca air-stirred reactors techniques.

Shake flask tests consists of culturing the bacteria with the pyrite samples in 250 ml Erlenmeyer flasks containing 100 ml of suspension in an thermostated gyratory shaker at 220 rpm maintained at 35 ˚C. Nutrient chemicals, "9 K" salts medium, to promote bacterial growth (0.01 gr/l Calcium Nitrate, 0.1 gr/l Potassium Chloride, 3gr/l Ammonium Sulphate, 0.5g/l Magnessium Sulphate) was used throughout the tests. The desired quantity of the mineral size fraction followed by addition an innoculum of bacteria harvested from a stock reactor where they had been grown on pyrite to provide an initial concentration of approximately 1x10" cells/ml. 100 ml of bacterial ferric sulphate stock solution and 9K medium was dispensed into an Erlenmeyer flask and flasks were stoppered and incubated in the gyratory shakers at the required temperatures. Correction for evaporation was made prior to sampling by the addition of acidified water (pH 1.8).

Pachuca air stirred reactors of 1.7 litre capacity, which was sparged with air, was also used to compare their efficiency with the results of shake flask leach tests under similar conditions. The reaction vessel was maintained at a temperature of 30-33°C by means of warm water socket. The

leaching tests were initiated by charging the 1.7 litre reactor by an inoculums bacterial stock leach solution and sample plus "9K" nutrient chemicals to promote bacterial growth. Water lost due to evaporation was replaced by the addition of acidified water (pH 1.8) to the predetermined mark before sampling.

Throughout the experimental programme bacterial oxidation of the pyrite with respect to time was monitored by measuring the iron concentrations and Eh/pH values of the leach solutions at specific time intervals. The Eh/pH of the medium was measured using a Corning Eh/pH meter. Periodically representative 1 ml .sample of leach suspensions were removed from the shake flasks and pachuca reactors. To determine iron oxidation sample was diluted which necessary for metal analysis on the A.A.S (Perkin Elmer Atomic Adsorption Spectrometer).

4 RESULTS AND DISCUSSIONS

Bacterial leaching processes are affected by numerous variables. Variations in the mineralogical structure of the mineral may significantly alter the oxidation response of sulphide minerals. Also there are a number of critical variables which effect the reactions, these include particle size, pulp density, iron content of ferric liqueur solutions, bacteria amount and time of process,

Ferric iron plays an important role in bacterial leaching and its content in leaching liqueur has effect on oxidation rate. The influence of initial ferric iron on bacterial oxidation of sulphides is complex. In the literature it has been reported that $Fe^+7Fe^+\sim$ couple is the major intermediate electron acceptor/donor system for pyrite oxidation in the bacterial leaching (Başaran et. al. 1987).

Also surface area is important in bacterial attachment, since increased surface exposure provides greater area for attachment (Brierly, 1978). The rate of bacterial and chemical oxidation of sulphides can be enhanced by increasing the total surface area exposed to leach solutions. This can be achieved by decreasing the size of particle which increases the specific surface area and increasing the pulp density which places more particle mass of fixed specific surface area into a unit volume. It appears that a low specific surface area metal extraction is limited by the availability of solid surface for bacterial activity.

The significance of particle size and distribution has been investigated using sized fractions of pyrite and a series of tests were conducted. Figures 1 and 2 illustrate graphically rate at which pyrite can be leached for 0.5% and 1 % pulp density for different particle sizes. At the beginning the Eh/pH of the solutions were 686 mV/ pH 1.28 and 716 mV /pH 1.26 respectively. Eh/pH was varied between 650-

720 mV/1.20-0.96 trough all experimental study. Fe content of the stock bacterial ferric liqueur solution was about 12g/l. Leaching rates have been found to be proportional to the pyrite particle size. As shown in Figure I leaching rate almost doubled especially with the fine particle fractions and as particle get coarser slower leaching was occurred. More rapid metal dissolution occurred -20+10 micron and -10 micron size fractions due to the higher available mineral surface area. Reducing the particle size from 63 micron to less than 32 micron almost doubled the rate of bacterial leaching. Figure 2 shows the I % pyrite leaching with the same particles fractions with the similar experimental conditions. With particle size below 10 micron in 50 hours 90% Fe oxidation occurred while for -63+56 micron size fraction about 42% Fe oxidation occurred for the same time interval. As expected leaching is very depend on particle size, metal extraction decreased with increasing particle size. When the results were compared between Figures 1 and 2, it is shown that for -20+10 and -10 micron size fractions leach rate was two times faster in 0.5% pulp density while the other fractions revealed not very much differences probably very small increase in pulp density. It has been shown that the highest rate of oxidation occurs at a particle size below 20 micron.

As Figure 3 shows, leaching in the reactor with 1% pulp density slower leach rate was observed comparing the shake flask with the similar experimental conditions. Within 60 hours about 40% Fc oxidised for -56+45 micron fraction while 65% oxidation was obtained in shake flasks for the same
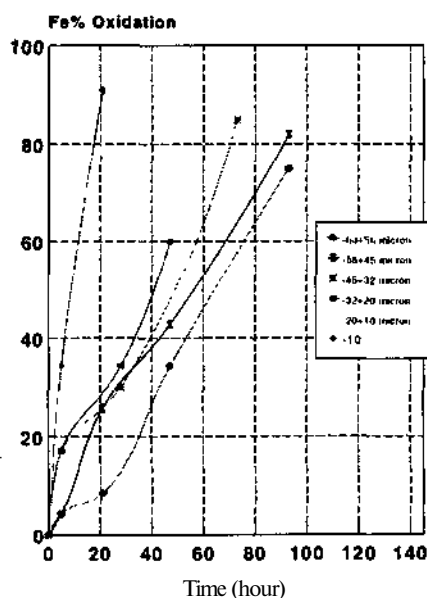
Figure l. 0.5 % pyrite bacterial leaching in Ihe flask

traction These figures show that within 2 days 80% and 55% pyute can be leached respectively in flask and leactoi

Fe% Oxidation

Figure 1 1% pyite bacteiial leaching in the leactor

Fe% Oxidation

Figure 2 1% pyite bacteiial leaching in the flask

It has been shown a relationship between the leach late and surface area where high surface area was maintained decreasing the particle suitace Investigation have revealed that pyrite leaching was veiy depend on particle size even very nariow paiticlc tractions Expected etlect ot pulp density was not observed tor the tine particle tractions in the used low pulp density Bacterial leaching ot pyrite in the leactor showed slightly slower leaching rate

It is pioven that oxidation ot pyrite by the presence ot *Tliiobacillus feiooxulans* is greatly accelerated by the suitace atea

REFERENCES

Başaran A and Tuovmene O H 1987 hon pyite oxidation by Tliiobacillus Feirooxidans Sulphm intermediate', soluble end pioducls and changes in biomass *Cool Puparatiim* Vol *S* pp 19 ≪ِ

BiieilyC 1978 Bacteiial Leaching *CRC Cnlitul Rı\ıı\\,\ in Muiiibioli)i(* Novemhei pp 207 262

Goktepe F & Pooley F D 1998 Recoveiy oi coppei fioin a sulphide tailings by bacteiial leaching *liuunatiom in Minimi and Coal PwiiHiiit;* Pioctulings ot the 7" international Mıneial Piocessmg Symposium Istanbul/Turkey (eds) S Atak G Onal & M S Çelik

Komnitsas C and Pooley F D 1989 Mıntıal charactenstics and tieatment ot letiattoiy gold oies *Minimis I-ni(iuuuma* 2 449 4V7

Pooley F D 1987 Mıneial Itachıng with batteiia *Em ilanım Mal BiaUtlnnili>i;* Chaptei 1 114 114 Eds Foistei and Wase Ellis Hoiwood Publisheis

Pooley F D 1998 The lole ot hiohydiometalkugy in mıneial piocessıng *lnno\ation\ tu Minemi ami Coal Proiiwmx* Puxeedings of the 7" international Mineral Piocessmg Svmposium Istanbul/1 urkey (eds) S Atak G Onal & M S Çehk

Smith RW and Mısra M 1991 Recent developments in the Bıoprocessıng of Mineials *Minimi Pmcusmi; anil C\tiaili\iMitalluiji* fti/i≫ Vol 12 pp 17 60

The Effect of Reagent Addition Points and Aeration on the Flotation Performance of Sulphide Minerals

A. Asian
Karadeniz Technical University, Mining Engineering Department, Trabzon, Turkey

Z. Ekmekçi & İ. Bayraktar
Hacettepe University, Mining Engineering Department, Ankara, Turkey

B. Aksanı
Çayeli Bakır İsletmeleri A.S. Rize, Turkey

ABSTRACT: Several different reagents have been used in flotation process all around the world. Flotation response of minerals could be changed not only by the type of reagents used in the plant but by the addition points of these reagents also. Therefore, it is important to determine the most appropriate reagent addition points in the flotation plant in order to obtain the best metallurgical results. In this study, flotation tests were performed in order to determine the effects of reagent addition points and aeration on the flotation behaviour of sulphide minerals. Collector and lime were added together or separately before grinding or after grinding at the flotation tests. Moreover, flotation pulp was aerated in two tests in order to determine the effect of aeration. It was found that the pulp potential changed significantly as the collector and/or lime addition points were changed. Also, the flotation behaviour of ehalcopyrite, pyrite and sphalerite was affected by the changes in the reagent addition points and aeration. Not only the copper grade and recovery of Cu rougher concentrate were affected but also chalcopyrite-sphalerite and chalcopyrite-pyrite selectivity was considerably affected. It was concluded that both reagent addition points and aeration affected the flotation behaviour of sulphide minerals in different ways. Hence, the selection of reagent addition points in a flotation plant was very important that it affects the recovery and the selectivity in the flotation of sulphide minerals. The subject has to be studied in detail in order to obtain the best results in the plant.

1 INTRODUCTION

Froth flotation has been used in the mineral processing industry since the mid-1800's with many of its broad-based applications to mineral recovery extensively developed between 1900 and 1925. Today, at least 100 different minerals, including almost all of the world's copper, lead, zinc, nickel, silver, molybdenum, manganese, chromium, are processed using froth flotation. In 1997, the estimated worldwide mineral production, using froth flotation, was two billion tons.

The mineral industry requires the use of a wide variety of both inorganic and organic chemical reagents for its operation. The reagents most commonly used in mineral processing range from chemicals used in froth flotation, grinding aids, flocculants, dewatenng agents, dispersants, solvent extraction and leaching chemicals to binding agents in pelletizing plants. However, flotation reagents predominate over any other mineral industry chemicals because the flotation process has become the single most important method for the separation of minerals from ores (Fuerstenau and Urbina, 1987).

Both inorganic and organic compounds are used extensively in flotation processing. Inorganic chemicals are added to regulate pH, to control the surface charge on minerals, to complex ions, to prevent collector adsorption and to regulate flocculation and dispersion. Organic reagents are added mainly to control wettability and the frothing behaviour of the system. The selective adsorption of collectors is directly responsible for making mineral surfaces hydrophobic. More recently, organic compounds are being utilized as depressants (Bogusz et al., 1997; Bulatovic, 1999; Drzymala et al., 2002).

Huge amounts of these reagents are used in flotation plants all over the world. Therefore, it is very important to use the appropriate reagents conveniently in the plant in order to minimize the consumption and hence the cost of the process.

Aeration of pulps at complex sulphide ores also affects the flotation behaviour of sulphide minerals as well as selectivity (Kylmowsky and Salman, 1.970). Therefore, aeration tanks are used at many flotation plants after grinding in order to improve the selectivity between sulphide minerals (Konigsmann, 1973).

It was reported that aeration improved the flotation of sphalerite while depressing pyrite (Ek, 1985; Bulatovic and Wyslouzil, 1985). Hout and Duhamet (1990) showed that both grade and recovery of

sphalerite concentrate were increased as the aeration was extended. The beneficial effect of aeration on sphalerite flotation resulted as the activation by copper sulphate advanced by aeration. It was also found that dissolved oxygen concentration of flotation pulps affects considerably the adsorption rale of xanthate on both pyrite and chalcopyrite (Kuopanporatti et al., 1997). Similarly, it was observed in a study performed by using Küre copper ore that the oxidation state of pyrite and chalcopyrite surfaces and the stability of oxidation products on the surface of these minerals changed by the extended aeration and the recovery and selectivity of flotation affected significantly (Ekmekçi and Hassoy, 1999). It can be concluded that the flotation behaviour of sulphide minerals can be controlled by adjusting dissolved oxygen content of the flotation pulp (Berglund and Forrsberg, 1988).

In this study, the effects of reagent addition points and aeration on the flotation behaviour of sulphide minerals in a complex sulphide ore were studied in detail. Flotation test were performed by adding reagents at different stages and by applying aeration after grinding. Consequently, the flotation behaviour of chalcopyrite, sphalerite and pyrite at Cu rougher flotation was assessed on the basis of recovery and grade as well as flotation rate. Besides, chalcopyrite-sphalerite and chalcopyrite-pyrite selectivity were calculated.

2 EXPERIMENTAL

2. / Material

In this study, a complex sulphide ore obtained from the Çayeli Bakır İşletmeleri A.Ş.. Turkey was used. It is the plant feed of CBİ Cu/Zn flotation plant and consists of mainly chalcopyrite, sphalerite and pyrite. The average feed grade of the ore is 4.5 % Cu and 4.2 % Zn.

The reagents used in the flotation tests were lime (CaO) as pH regulator, di-isobutyl dithiophosphinate (Aerophine 3418A) as collector and methyl iso-butyl carbinol (MIBC) as frother. All of these reagents were obtained from the CBİ Cu/Zn flotation plant and prepared freshly before each test.

2.2 Flotation tests

The ore was ground in a rod mill to 70 % passing 36 microns. The pulp was directly transferred to the 2 It. flotation cell after grinding and flotation test was performed for ten minutes with a Humboldt Wedag flotation machine. Six separate concentrates were collected at 15 sec, 30 sec, I min., 2 min., 5 min. and 10 min. intervals. The pulp pH was adjusted to nearly 11.8 before flotation at all the tests.

The chemical analysis of the products was done using atomic absorption spectrophotometer for Cu, Zn and Fe. The redox potential, dissolved oxygen concentration and pH were recorded continuously throughout the flotation tests. The parameters kept constant during flotation tests were given in the Table I.

Table I. Flotation Test Parameters

Parameter	Property
Flotation Machine	Humboldt Wedac
Cell Volume	2000 ml (plexiglass)
Sample Weight	- 1000 g
Pulp Density	36 %(v/v)
Grinding Time	55 min.
Impeller Rale	1250 rpm
Reagents	Lime (added as solid) Aerophine 3418A(1%) MIBC (added pure)

The reagents were added at the different stages of the tests. Furthermore, the pulp was aerated at some of the tests for 20 min. before flotation.

Also, a flotation test was conducted with the pulp sample taken from the secondary cyclone overflow which was pumped to the feed box of Cu rougher tlotation circuit in the plant. In this test, no reagent was added because lime and collector were added together into the mill.

The flotation test conditions were summarized in the Table 2.

Table 2. Flotation Test Conditions

Test No	Test Conditions
1	Test with the pulp sample taken from the secondary cyclone overflow. No reagent was added.
2	Lime and collector were added after grinding.
3	Lime was added into the mill and collector was added after grinding.
4	Both lime and collector were added into the mill.
5	Lime was added after grinding. Then pulp was aerated and collector was added after aeration.
6	Lime was added into the mill. Collector was added after the aeration.

3 RESULTS AND DISCUSSION

Flotation tests were evaluated from the point of view of the flotation behaviour and flotation rate of chalcopyrite, sphalerite and pyrite. Also, a selectivity index was used in order to determine the selectivity between chalcopyrite-sphalerite and chalcopyrite-pyrite.

3.1 Chalcopyrite

The effect of reagent addition points and aeration on the flotation behaviour of chalcopynte was shown in Figure I.

It can be seen that the best metallurgical results were achieved when the pulp was aerated before flotation (Tests 5 and 6). On the other hand, both Cu grade and recovery were considerably low when no reagent was added into the mill (Test 2). It is noteworthy that aeration affects the flotation behaviour of chalcopynte significantly by improving the metallurgical results (Fig. I).

It has been shown that the flotation of chalcopynte improved at high pulp potentials (Trahar, 1984; Richardson and Walker, 1985; Tolley et al., 1996; Yuan et al., 1996). Therefore, as the pulp potential increased to more oxidizing potentials by aeration, the oxidation of collector on chalcopyrite surfaces enhanced which then resulted to an increase at copper recovery.

Moreover, it can be said that the surfaces of pyrite particles were coated with hydrophilic metal hydroxides by aeration which hindered the interaction of pyrite surface with the collector in the pulp. Hence, the copper grade of Cu rougher concentrate was higher when the pulp was aerated before flotation. There are many plants around the world using aeration tanks before flotation in order to depress pyrite by oxidizing the surfaces (Berglund and Forrsberg, 1988; Ekmekçi and Hassoy, 1999).
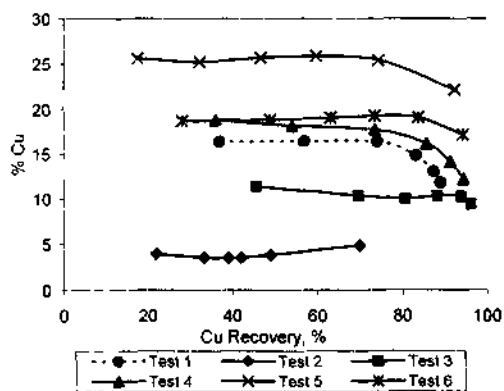
Figure I. Flotation behaviour of chalcopyrite in different test conditions

Although the overall recovery and grade was highest when the pulp was aerated before flotation, the flotation rate of chalcopyrite was rather slow at the beginning of the flotation (Fig. 2). Aeration may caused the formation of metal hydroxides on the surface of chalcopynte (Senior and Trahar, 199I) which makes the formation of metal xanthates on the

chalcopyrite surface difficult resulting slow flotation rates at the beginning.
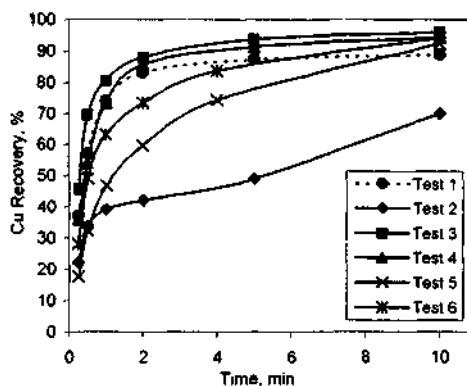
Figure 2. Flotation rate of chalcopyrite in different test conditions
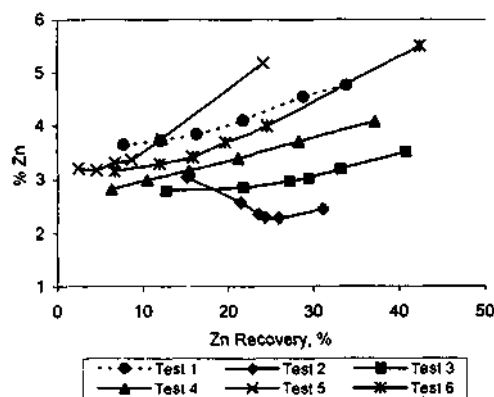
Figure 3. Flolution behaviour of sphalerite in different test conditions

As seen from Figure 3, the flotation behaviour of sphalerite was quite different from chalcopyrite. The zinc recoveries were around 35-40% at all tests except the test in which no reagent was added into the mill and pulp was aerated before flotation (Test 5). The highest zinc grade and recovery were obtained when the lime was added into the mill and pulp was aerated before flotation (Test 6). The zinc grades of concentrate was not changed at all tests and remained same as the zinc grade of feed (Fig. 3).

The flotation rate of sphalerite was faster when lime was added into the mill (Test 3) and also when no reagent was added into the mill (Test 2). When both lime and collector were added into the mill (Test 4), the flotation rate of sphalerite was nearly

467

same as the test performed with the pulp taken from the flotation feed (Test I) (Fig. 4).
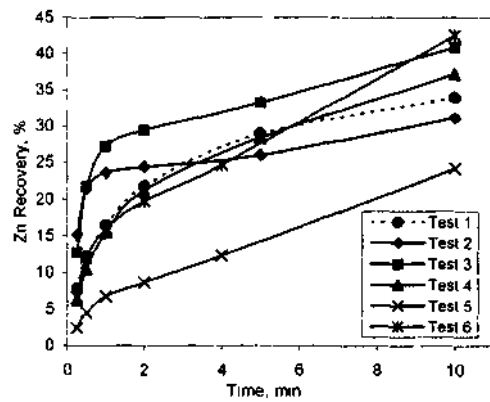
Figure 4 Flotation rate of sphalerite in different test conditions

It was observed that the flotation of sphalerite improved at more anodic potentials (Berglung and Forssberg, 1988: Labonte et al., 1990rBerglund, 1991; Boulton et al., 2001), so the zinc recovery increased when the pulp was aerated. But the effect was more pronounced when lime was added into the mill (Test 6). It can be said that copper hydroxides precipitated on sphalerite surfaces acted as a source of copper ion and increased the activation ol sphalerite (Wang et al., 1989a. b) when lime was added into the mill. Besides, as the pulp was aerated, more copper ions dissolved from chalcopyrite which caused inadvertent activation of sphalerite (Yuan el al,, 1996).

3.2 Pvrite

The recovery of pyrite at the Cu rougher flotation increased when lime was added into the mill (Test 3) and also when no reagent was added into the mill (Test 2). It is noticeable that the amount of pyrite reported to the concentrate was lowest at the Test 5 where no reagent was added into the mill and the pulp was aerated before flotation (Fig. 5). It can be seen that when both lime and collector were added into the mill (Test 4), the results were same as the test performed with pulp taken from the flotation feed (Test 1). Here, it must be considered that lime and collector were added into the mill and the pulp was pumped directly to the feed box of Cu rougher circuit in the plant.
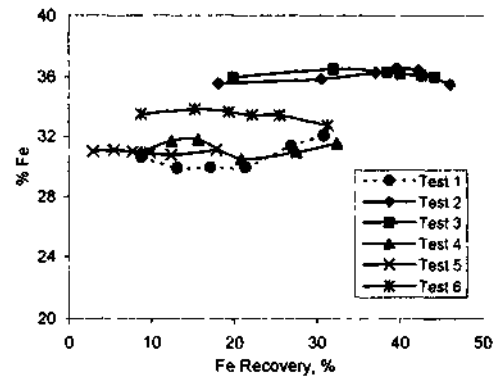
Figure 5. Flotation behaviour of pyrite in diltèrent test conditions

Similarly, the flotation rate of pyrite was faster when lime was added into the mill (Test 3) and when no reagent was added into the mill (Test 2) (Fig. 6). The flotation rate of pyrite was very slow when no reagent was added into the mill and pulp was aerated before flotation (Test 5).
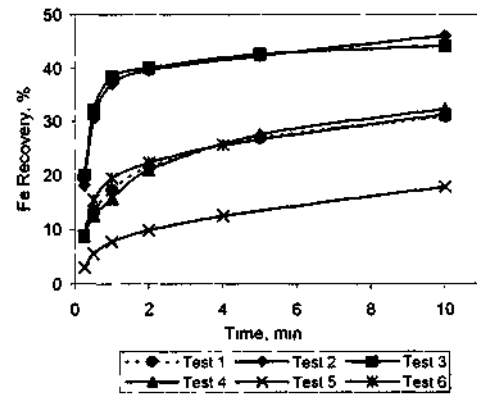
Figure 6 Flotation rate of pynte in different test conditions

It is obvious that the flotation of pyrite retarded when the pulp was aerated. Pyrite is one of the more easily oxidized sulphide mineral while chalcopyrite and sphalerite oxidation is rather slow (Hayes et al., 1987; Buckley et al., 1989). It is well known that oxygen promotes not only the anodic dissolution of minerals but also the formation of metal hydroxides in solution that, with time, will eventually precipitate on the mineral surfaces (Shen et al. 1998). The formation of metal hydroxides which are highly hydrophilic on pyrite surfaces hindered the interaction

468

of collector with the surfaces (Shannon and Trahar, 1986).

3.3 Selectivity between minerais

Selectivity index between chalcopyrite-sphalerite and chalcopyrite-pyrite were calculated using Eq. (I) (Broadbent. et al.. 2000).

$$SI = \frac{100 - R_{P_v}}{100 - R_{Cp}} \times \frac{G_{P_v}}{G_{Cp}} \qquad (1)$$

Here ;

$Rt'n$: Recovery of valuable mineral
Rp_v : Recovery of gang mineral
Gci : Feed grade of valuable mineral
Gp_v : Feed grade of gang mineral

It is helpful to use this selectivity index because variations in the feed grade at the flotation tests can be eliminated. So, more accurate comments can be done about the results.
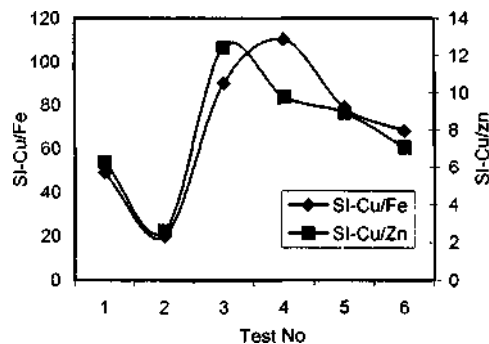
Figure 7. Selectivity index between minerals in Cu rougher flotation

It can be seen that the selectivity between chalcopyrite and sphalerite was most favourable at Test 3 where lime was added into the mill (Test 3) while best selectivity between chalcopyrite-pyrite was achieved when both lime and collector were added into the mill (Test 4) (Fig. 7).

4 CONCLUSIONS

As a result of this study, following conclusions can be drawn;
- The flotation behaviour of chalcopyrite, pyrite and sphalerite was affected by the changes in the reagent addition points and aeration.
- Aeration increased the pulp potential to more anodic values where chalcopyrite dotation enhanced.
- Sphalerite flotation improved when lime was added into the mill and pulp was aerated before flotation.
- The amount of pyrite reported to the Cu rougher concentrate decreased when pulp was aerated before flotation.
- Reagent addition points and aeration also affected the selectivity between sulphide minerals significantly.

Consequently, the results indicated that the selection of reagent addition points in a dotation plant is so important that it affects the metallurgical results of the flotation process as well as the selectivity among the sulphide minerals. Thus, the subject has to be studied comprehensively in order to obtain the best metallurgy in the plant.

REFERENCES

Berglund. G. and Forrsberg, K.S.E. 1988. Redox and oxygen influence on the flotation behaviour of sulphide ores. *Pnu. Int. Svm. Electrochem. in Mineral ami Metal Process.* II (Ed. P.E. Richardson and R. Woods). Electrochem. Soc. vol. 88-21. 183-197.

Bogusz. E.. Buenne. S.R . Butler. E., Rao. S.R. and Finch. .I.A.. 1997. Metal ions and dextrin adsorption on pyrite. *Min. Eiiiiiin.* 10.4.441-445.

Boullon. A.. Fornasiero. D. and Ralston. J. 2001. Depression of iron sulphide flotation in zinc roughers. *Mm. Enclin.* 14. 9. 1067-1079.

Broadbent. Q.. Yan. D. and Dunne. R. 2000. Selective flotation of chalcopyrite and pyrite and the effect of ore type. *Proc. 21" Int. Mm. Process. Congress* (Ed. P. Massacci.) B8h-I52-I59. Roma. July.

Buckley. A.N.. Woods. R. and Woulerlood. H.J. 1989. An XPS investigation of the .surface of natural sphalerites under flotation-related conditions. *Int. J. Min. Process.* 26. 29-49.

Bulatovic. S.M. 1999. Use of organic polymers in the flotation of polymelallic oies: A review. *Min. Eni;ni>.* 12, 4. 341-354.

Bulatovic. S.M. and Wyslouz.il. D.M. 1985. Selection of reagent scheme to treat massive sulphide ores. *Complet Sıllliclt's. Pnicessin.i: of Ows. Concentrates anil Bv-Prodmt* (ed. A.D. Zunke'l. R S. Booiman. A.E. Morris and R.J. Wesely). Metallurgical Society. 101-141.

Drzymala. J.. Kapusmyak. J. and Tomasik. P. 2002. Removal of lead minerals from copper indus»ial flotation concentrales by xanthate flotation in the presence of dextrin. *Int. J. Min. Pi o,ess.* 1621. 1-9.

Ek. CS. 1985. Selective flotation of different complex pyritic ores. *Complex' Sulfides. Pratesstnx of Ores, Concentrates and Bv-Piodiuts* (ed. A.D. Zunkel. R.S. Boorman. A.E. Morris and R.J. Wesely). Metallurgical Society, 83-101.

Ekmekçi. Z. and Hassoy. H 1999 Palp oksijen içeriği ve elektrokimyasal potansiyelinin süiftırlü cevherlerin flotasvon seçimliliğine etkileri *Türkiye 16. Madeınilik Konares.*. 375-382.

Fuerstenau. D.W. and Urbina. R.H. 1987. Flotation Fundamentals. *Réticents in Mineral Teclıuolt>ı>y* (ed. P. Soinasundaran and B.M. Moudgil). New York and Basel: Marcel Dekker. Inc.

Hayes, RA.. Price. D.M.. Ralston. J. and Smith. R.W. 1987. Collectorless flotation of sulphide minerals. *Miner. Protei*. Exlr. Mehdi Review,* 2, 203-234.

Houot. R. and Duhamet. D. 1990. Importance of oxygenation of pulps in the flotation of sulphide ores. *Int. J. Min. Process.*. 29. 77-87

Konigsmann. K.V. 1973. Aeration in plant practice. *5'" Annual Meeting of CMP*. CIM. 300-315.

Kyhnowsky. I.B. and Salman. T. 1970. The role of oxygen in xanthale flotation of galena, pyrite and chalcopyrite. *CIM Bull.*. 63. 698. 683-688.

Kuopanporatti, H.. Suorsa. T. and Pöllanen. E. 1997. Effects of oxygen on kinetics of conditioning in sulphide ore flotation. *Min. En,ng.*. 10. 11. 1193-1205.

Senior. CD. and Traliar. W.J. 1991. The influence of metal hydroxides and collector on the flotation of chalcopyrite. *Im J Min. Process.,* 33, 321-341.

Shen. W.Z.. Foniasieio, D. and Ralston. J. 1998. Effects of collectors, conditioning pH and gases in the separation of sphalerite from pyrite. *Min. Eııgıug.,* 11.2. 145-158.

Richardson. P.E. and Walker. G.W. 1985. The flotation of chalcocite. bornite. chalcopyrite and pyrite in an electrochemical cell. *Prm: 15'" IMPC*. Cannes. Fiance. 198-210.

Shannon. I..K. and Trahar. W.J. 1986. The role of collector in sulphide ore flotation. *Advances in Min. Prm*. (Ed. By P. Somasundaran). SME, 408-425.

Tolley. W.. Koltyar. D. and Wangoner, R.V. 1996. Fundamental electrochemical studies of sulphide mineral flotation. *Min. Eiiftii!!*- 9. 603-637.

Traliar. W.J. 1984. The influence of pulp potential in sulphide flotation. *Principles of Mineral Flotation* (Ed. By M.H. Jones and .IT. Woodcock), Aus. IMM. vol. 40. 117-135.

Wang. X.H., Forssberg. K.S.E. and Bolin. N.J. 1989a. Effects of oxygen on Cu(ll) adsorption by sphalerite in acidic to neutral media. *Scan. J. Metall.* 18. 243-250.

Wang. X.H.. Forssberg, K.S.E. and Bolin. N.J. 1989b. The aqeous and surface chemistry of activation in the flotation of sulphide minerals- A review. Part I: An electrochemical model. *Miner. Process. Extr. Metall. Review*. 4, 135-165.

Yuan. X. M.. Pals.son. B.I. and Forsberg. K.S.E. 1996. Flotation of a complex sulphide ore I. Cu/Zn selectivity control by adjusting pulp potential with different gases. *Int. J. Min. ' " Prot ess.* 46. 155-179.

470

Bioleaching of a Complex Sulphide Ore by Mesophilic and Extremely Thermophilic Bacteria: Statistical Analysis of Data Using Ergun's Test

H. Deveci
Department of Mining Engineering, Karadeniz Technical University, 61080, Trabzon, Turkey

M.A.Jordan & N.Powell
Camborne School of Mines (University of Exeter), Redruth, Cornwall, TRI 5 3SE, UK

ABSTRACT: This study investigates the effects of bacterial strain, salinity and pH on the bioleaching of a complex ore using mesophilic and extremely thermophilic bacteria with the statistical analysis of the results using Ergun's test. The results showed that the ore was readily amenable to the selective extraction of zinc and the extreme thermophiles as confirmed by the statistical analysis displayed .superior kinetics of dissolution of zinc compared with the mesophiles. The bioleaching performance of the extreme thermophiles was found to improve in response to the increase in acidity (pH 2.0 to 1.0) while the activity of the mesophiles was adversely affected by decreasing the pH. The statistical analysis indicated that the effect of pH was insignificant in the range of pH 1.0-1.6 for the extreme thermophiles and pH I.6-2.0 for the mesophiles. The salinity was shown to have a suppressing effect on the mesophiles. However, the extreme thermophiles appear to be halophilic in character as they could operate efficiently under the saline conditions (1-4% CI").

I INTRODUCTION

Bioleaching processes have gained importance in recent years for the extraction of metals particularly from the difficult-to-treat and low grade ores or concentrates (Rawlings et al. 2003). Bioleaching is essentially a dissolution process with the involvement of acidophilic bacteria which have the ability to oxidise ferrous iron (I) and/or elemental (2) or reduced sulphur compounds to derive the energy required for their growth and other metabolic functions (Ingledew 1982. Suzuki 2001). The reaction products, ferric iron and/or acid attack the sulphide minerals such as sphalerite (3 & 4) resulting in their dissolution (Sandetal. 2001).

$$2Fe^{2+} + 1/2O_2 + 2H^+ \xrightarrow{\text{bacteria}} 2Fe^{3+} + H_2O \qquad (1)$$

$$S^0 + 3/2O_2 + H_2O \xrightarrow{\text{bacteria}} H_2SO_4 \qquad (2)$$

$$ZnS + 2Fe^{3+} \rightarrow Zn^{2+} + 2Fe^{2+} + S^0 \qquad (3)$$

$$ZnS + 2H^+ \rightarrow Zn^{2+} + H_2S \qquad \mathbf{(4)}$$
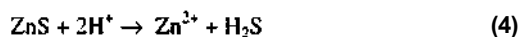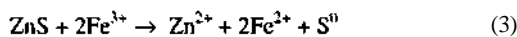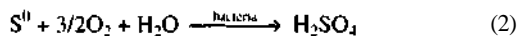
Mesophilic bacteria e.g. *T. ferrooxidans, L. ferrooxidans and T. thiooxidans* operating at <40°C are the most commonly used microorganisms for the bioleaching of sulphide minerals (Bosecker 1997). Thermophilic bacteria with their ability to thrive at high temperatures up to 85°C have great potential for use in bioleaching processes probably due to the improvement expected in the kinetics of metal dissolution particularly from the recalcitrant minerals such as chalcopyrite (Norris ct al. 2000, d~Hugues et al. 2002, Rawlings et al. 2003).

The rate and extent of oxidation of sulphide minerals within bioleaching processes are closely controlled by the oxidative activity (growth) of bacteria. There are many factors including pH and the toxicity of anions (e.g. CI") and cations that may affect the growth and hence the optimum leaching performance of a bacterial culture (Bosecker 1997, Dew et al. 1997, Deveci 2002). The level of salinity of process water to be used may be of great importance for the application of bioleaching processes in the areas where the availability of chloride-free process water may he limited (Budden & Spencer 1991, Weston et al. 1994).

The accurate interpretation of batch leaching data on which the development of a process is based is of vital significance for the determination or optimisation of process conditions. Despite the general availability of a variety of statistical techniques, the

time-dependent nature of biolcaching data (i.e. metal concentration varying with time) restricts the use of many conventional statistical methods for the analysis of experimental data (Jordan el al. 1997). Powell & Jordan (1997) demonstrated a corrective technique based on Ergun's test (Ergun 1956) for the eradication of time dependency of leaching data.

Within this study, the potential amenability of a complex sulphide ore to the selective extraction of zinc using mesophilic and extremely thermophilic bacteria was evaluated. The effects of pH and salinity (Cf ions) on the bioleaching performance of the selected cultures were investigated. Statistical assessment of the experimental results using Ergun\s test to (i) eradicate the time-dependency and to (ii) examine the differences between the varying experimental conditions (i.e. pH, bacterial strain and chloride concentration) for significance was undertaken.

2 EXPERIMENTAL

2. / Mineral Sample

A complex sulphide ore sample originated from the McArthur River deposit. Northern Territory of Australia was used in this study. The ore sample were found to contain sphalerite (ZnS), galena (PbS) and pyrite (FeS_.) as the major sulphide phases with a chemical composition of 16.2% Zn, 5.6% Pb and 7.95% Fe. The crushed ore sample as received was ground to -300 (jm (d_{NO}=-25() pin) prior to use in the experiments.

2.2 Bacteria and growth media

The mesophilic cultures, SJ2 *(T. ferrooxidans)* and the mixed culture designated WJM (Jordan 1993), and the extremely thermophilic cultures, *Sulfolobus (S. metallicus)* and DSM 1651 *(Acidiantts brierleyi)* were used in the bioleaching experiments. The growth of mesophiles (30°C) and extreme thermophiles (70°C) on the ore (1% w/v) were carried out on orbital shakers using an enriched salt solution containing $MgSO_4.7rLO$ (0.4 g/1), $(NH_4),SO4$ (0.2 g/1), $K_.HPO_4.3H_.0$ (0.1 g/1) and KCl (0.1 g/1) as the growth media.

2.3 Bioleaching experiments

Bioleaching experiments were carried out in 250 ml Erlenmeyer flasks with a working volume of 100 ml. A \% w/v ore in enriched salt solution (90 ml) was prepared in a flask which was then auloclavcd prior to the inoculation with a 10 ml (10% v/v) aliquot of an appropriate culture previously grown. In the chloride experiments the calculated amounts of chlo-

ride (as NaCl) were added to the flasks to produce 1%. 2% and 4% CI' in the final volume of solution.

The oxidation of the ore was monitored by the daily removal of 1 ml samples. These samples were used to determine the metal concentration (Zn, Fe and Pb) by AAS and the pH. If exceeded, the pH was adjusted to the predetermined level by the addition of 18 M $H_.SO_4$. The mean values of replicate (duplicate or triplicate) experiments were presented in the results.

2.4 Statistical methodology for the analysis of data

Ergun's test in conjunction with Moving Regression Analysis was adopted as the statistical methodology for the analysis of the bioleaching data. The maximum rate of metal dissolution (max. gradient) was initially determined from the bioleaching profiles using Moving Regression Analysis (Deveci 1997) in which the linear regression lines were fitted to the selected number of data points (e.g. five data points) starting from the first data set (i.e. 1—»5) and then the second (i.e. 2—»6) and so forth. The largest gradient with a statistically acceptable correlation coefficient was assigned as an estimate of the maximum rate of metal dissolution.

Having determined the maximum gradients for each bioleaching profile, Ergun's test was applied to eradicate the time-dependent nature of the rates of metal extraction (gradients) and to test for the differences between these for the varying pH values, the type/strain of bacteria and the chloride concentrations. The details of statistical analysis procedure used herein and the outlines of the mathematical methodology for Ergun's lest can be found elsewhere (Powell & Jordan 1997).

3 RESULTS AND DISCUSSION

3.1 Bioleaching tests using mesophiles

Figure 1 illustrates the bioleaching of the ore using WJM and SJ2 cultures at pH 1.4 and 1.6. Compared with the acid leach as indicated by the control, the contribution of the mesophilic bacteria to the dissolution of zinc was substantial with an enhancement of > 12-fold in the rate and of >8-tbld in the recovery. Over 95% of zinc was dissolved in the presence of both cultures at the both pH levels.

An increase in the pH from 1.4 to 1.6 had a positive effect on the bioleaching performance of both cultures with an increase in the dissolution rate of zinc observed for WJM culture in particular (Fig. 1). These findings suggested that the optimum pH for both cultures may well be above pH 1.6 as, in fact, further tests using WJM culture showed that the dissolution of zinc further improved with increasing the pH to 2.0 (Fig. 2).
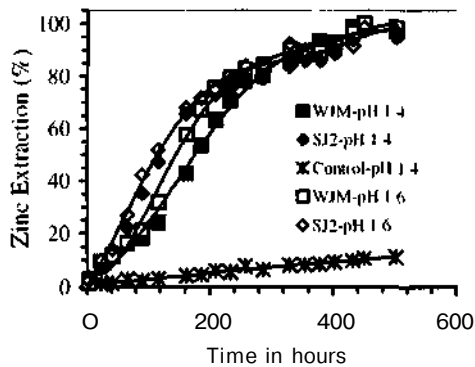
Figme 1   Exrraclinn üt zinc liom the ore using me.sophilic bactei ia at 3()°C & pH 1.4 & 1.6

Figure 3. Effect of added chlonde (0-4% CD on the extraction of zinc fiom the oie (19c w/v) usin« WJM cultuie at 30°C & pH I 4

Figure 2. Hftect of pH (1.2-2 0) on the extt action of zinc from the ore (1% w/v) using WJM culture at WC

This was consistent with the optimum pH range of 2.0-2.5 for me.sophilic bacteria (Bosecker 1997). However, the potential for the precipitation of iron would increase with decreasing acidity and could become significant at high pHs as the pulp density increases leading to the increase in the availability of precipitate forming ions such as ferric iron. Considering the extensive dissolution of zinc occurred at pH 1.2 and 1.4 (Figs. 1-2) both cultures can be adapted to operate efficiently at low pHs as demonstrated by Porro et al. (1989).

The addition of chloride (1-4% CI") appeared to severely inhibit the activity of WJM culture (at pH 1.4 and 30°C) with a marked decrease in the dissolution rate and extent of zinc as shown in Figure 3. Leong et al. (1993) also noted the detrimental effect of chloride (up to 8 g/l CD on the bioleaching of a copper ore using mixed cultures of *Thiobacilli.* These in-

vestigators also reported that adaptation of bacteria to chloride levels of up lo 5 g/l was possible ameliorating the deleterious effect of chloride on the dissolution process.   In a recent study Deveci (2002) observed that the extent of the adverse effect of chlonde depended on the bacterial strain and the concentrations of chloride with the possibility of adaptation of mesophiles up to -8-10 g/l CI". Weston et al. (1994) argued thai the deleterious effect of salt was not due to the chloride present but rather due lo the coexisting ions such as sodium leading to the formation of jarosite precipitates since they observed no apparent effect of salinity at 1-2 g/l CI" *on* the bacterial oxidation rate when operating at lower pHs (1.1-1.3). Dew et al. (1997) suggested that high concentrations of chloride in solution could damage the membrane of the bacteria.

3.2 Bioleaching lests using extreme thermophiles

Figure 4 shows the bioleaching of the ore using the extremely thermophilic strains *Sulfolohus* and DSM 1651 *(Acidianus Brierleyi)* at pH 1.2 and 1.4. Compared with the mesophiles (Figs. 1-2) the extreme thermophiles were able to dissolve >99% of the zincpresent in the ore over a relatively short incubation period of 260 hours.

Although the zinc extraction was practically complete at the end of incubation period, both the extreme thermophiles consistently exhibited a better performance for the dissolution of zinc at a pH of 1.2. This was consistent with the data presented in Figure 5 showing the effect of pH (1.0 to 2.0) on the bioleaching activity of DSM 1651 culture.

It was observed (Fig.5) that the rate and extent of dissolution of zinc increased with decreasing the pH in contrast to the mesophiles which did not illustrate

473
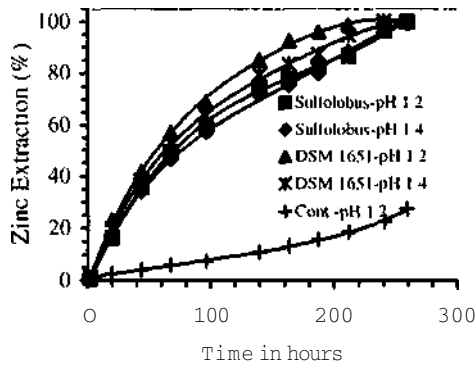
Figure 4 Extinction of zinc from the ore using extremely thermophilic bacteria at 70°C & pH 1 2 & 1 4
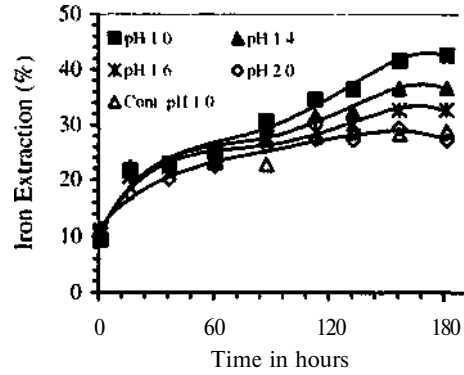
Figure 6. Effect of pH (1 0-2.0) on the extraction of iron from the ore (1 % w/v) using DSM 1651 culture at 70°C
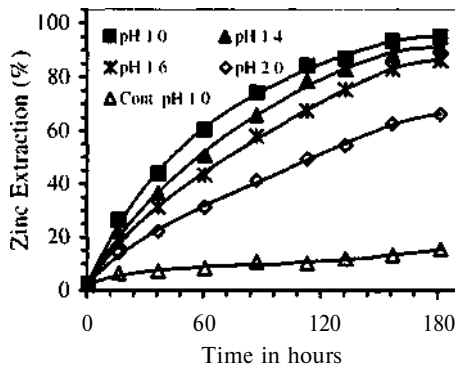
Figure 5. Effect of pH (1.0-2 0) on the extraction of zinc from the ore d * w/v) using DSM 1651 culture at 70°C

both minerals with sphalerite having a lower rest potential and hence being electrochemically more active than pyrite under the oxidising conditions (Natarajan 1990).

Figures 7-8 show the effect of salinity (0-4% Cl'') on the extraction of zinc by both the extreme thermophiles at pH 1.2. The response of both cultures to the saline environment was similar in character with an identical pattern for metal extraction under the same experimental conditions. In contrast to the suppressing effect on the mesophiles, the addition of chloride appeared to produce a positive effect on the extraction of zinc by the extreme thermophiles particularly following an initial period of -50 h. To illustrate, over 98%) of zinc was extracted by DSM 1651 culture at 1-4% Cl' compared with 85% Zn recovery in the absence of added chloride.

such a trend in response to the decrease in pH (Fig. 2). A limited zinc extraction of only 66% at a dissolution rate of 6.8 mg/l/h occurred at pH 2.0 compared with 95% Zn recovery (at 12.7 mg/l/h) recorded at pH 1.0. Jordan (1993) had shown that the dissolution rate of zinc and copper from a complex concentrate by the extreme thermophile *Sulfolobus* increased with decreasing the pH in the range of 2.0-1.2 in agreement with the current findings.

The enhancement in the bioleaching performance of DSM 1651 culture with increasing acidity was also evident from the bioleaching profiles obtained for iron (Fig. 6). The limited extraction of iron (i.e. 43% at pH 1.0) compared with extensive extraction of zinc (i.e. 95%) may be an indication of preferential/selective oxidation of sphalerite over pyrite. This is consistent with the electrochemical properties of
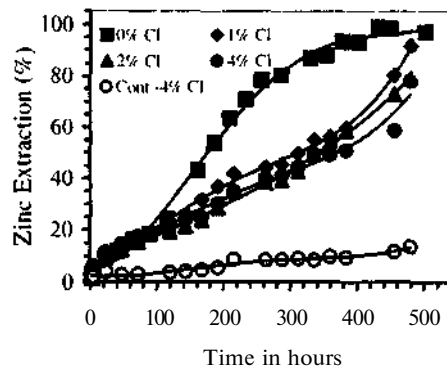

Figure 7. Effect of added chloride (0-4% Cl) on the extraction of zinc from the ore (1% w/v) using *Sulfolobus* culture at 70°C & pH 1 2

474
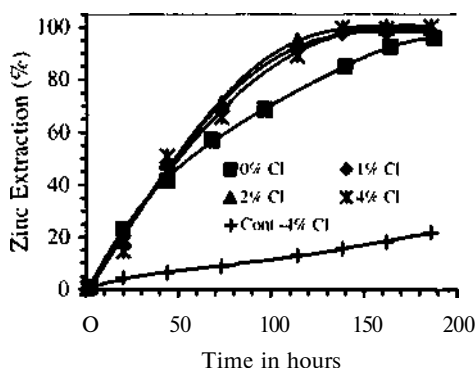
Figure 8 Effect of added chloride (0-4% Cl") on the extinction of zinc from the ore (\'h w/v) using DSM I65I culture at 70°C&pH 1.2
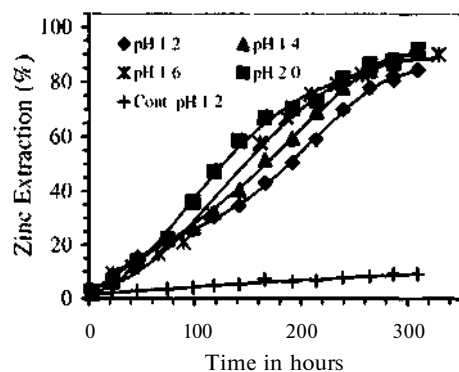
These findings were consistent with the published data for the extreme thermophiles (Deveci 2002) where it was reported that the addition of chloride up to -30-50 g/l Cl" improved the metal extraction by the extreme thermophiles with the apparent adverse effect at -80 g/l Cl". It may be inferred that the extreme thermophiles are halophilic in nature with their ability to tolerate extremely saline environments.

It is of prime importance to note that the formation of jarosite-type precipitates in particular could present problems in the extremely thermophilic systems operating at high temperatures (70°C) presumably due to the availability of counter ions such as Na^+ present in saline environments. Such precipitates could adversely affect the metal extraction via the formation of a passivating layer on the un reacted minerals surface (Weston et al. 1994). In this respect, the ability of the extreme thermophiles to operate at low pHs (Fig. 5) could become important from the overall process point of view to minimise the formation of potentially deleterious precipitates. It should be noted that the decrease in pH would probably alleviate the formation of jarosite-type precipitates (Dutrizac 1983).

With respect to the behaviour of lead within the experiments where no chloride was added, the solubilisation of lead was minimal with over 98% of lead having reported to the residues most likely in the form of either insoluble lead sulphate or undissolved galena irrespective of the type (and strain) of bacteria and pH. This rellects the selective extraction of zinc from the complex ore within the bioleaching process. However, the dissolution of lead, most likely via lead-chloro comp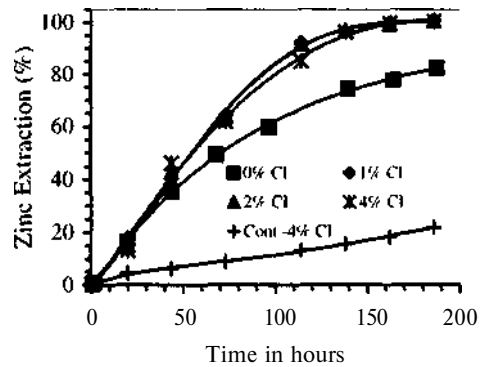lexes was promoted with the addition and/or increasing the concentration of chloride in solution. To illustrate, the extraction of lead increased from 4 to 69% with increasing the

level of Cl" from 1 to 4% during the bioleaching of the ore using *Siilfolohus* culture at 70°C.

3.3 Statistical Analysis of the Results

Statistical tests for the significance of the differences in the maximum dissolution rates of zinc under the experimental conditions were carried out in respect of the methodology previously outlined i.e. Ergun's test-essentially One-way Analysis of Variance (ANOVA) for gradients. This postulates the equality of the maximum gradients (dissolution rates) as a Null Hypothesis. The outcomes of the statistical analysis of the various tests are summarised in Table 1 where the significance of the differences is indicated either at 5% ("significant") or 1% ("highly significant") or 0.1% ("extremely significant") levels.

Initially the contribution of the mesophilic and extremely thermophilic cultures of bacteria to the dissolution of zinc was tested as indicated by the "control versus bacteria"" in Table I. It was assumed that the (maximum) dissolution rate of zinc occurred in the control was equal to that in the bioleaching (i.e. Null Hypothesis). This hypothesis was rejected in that the differences in the rates were clearly "extremely significant"'. In other words, the dissolution rate of zinc was substantially enhanced in the presence of all the cultures. Since this initial assumption was rejected, subsequent tests were performed for differences between the dissolution rates produced at different conditions in an attempt to compare the performances of strains (and groups) of bacteria, to determine the optimum pH (i.e. the pH effect) for the cultures concerned, and to examine the effect of chloride on the bacterial cultures.

Ergun's lest did not detect any significant difference between the maximum rates of dissolution of zinc produced by the mesophiles (WJM and SJ2) at pH 1.6 and the extreme thermophiles *(Sulfolobus* and DSM 1651) al pH 1.2 and 1.4. However, the differences in the performance of WJM and SJ2 cultures at pH 1.4 appeared to be statistically significant probably as an indication of the better acid tolerance of SJ2 culture.

Statistical analysis of the pH data for WJM and DSM 1651 cultures suggests that the pH in the range of 1.0-2.0 is an important parameter affecting the dissolulion process. Notwithstanding this, the differences recorded in the dissolution rates of zinc were found to be statistically insignificant in the pH ranges of 1.6-2.0 and 1.0-1.6 for WJM and DSM 1651 cultures respectively (Table 1). These may be regarded as the optimum pH range for the process using these cultures.

In a similar manner, Ergun's test was applied to evaluate the effect of chloride on the dissolution of zinc by the mesophilc WJM and the extreme thermophile *Sulfolobus* and DSM I65I cultures. These tests affirmed the inhibitory effect of chloride on the

Table 1 The summary of the statistical analysis of the experimental icsults using hrgun's test ("a" represents the level of significanee and the test results are presented as "significant" at 5%. "highly significant" ât 1⁄2> and "extremely significant" at 0.1% levels)

Statistical Test	F value	F critic (ıı)	Significance
Mesophiles			
Control vs bacteria (WJM and S.I2) at pH 1.4	32.27	16.39(0.1%)	Extremely significant
pH U v s p H 1.6 (SJ2)	0.76	5.99 (5%)	Not significant
WJM vs SJ2 at pH 1.6	0.06	5.99 (5%)	Not significant
W I M v s S J 2 a t p H 1.4	6.38	5.99%(5%)	Significant
pH effect on WJM (pH 1.2-2.0)	9.71	5.95(1%)	Highly significant
pH 1.2 vs pH 2.0 (WJM)	20.98	13.75(1%.)	Highly significant
pH U v s p H 2.0 (WJM)	14.00	13.75(1%)	Highly significant
pH 1.6vspH2.()(WJM)	0.35	5.99 (5%)	Not significant
pH U v s p H 16 (WJM)	8.95	5.99(5%)	Significant
CI clfect on WJM (0% vs 1% CI")	13.39	5.99(5%)	Significant
IV, CI" vs 23-CI" vs 4% CI"	1.68	5.99 (5%)	Not significant
Extreme thermophiles			
Control vs bacteria (Sulfolobus and DSM 1651) at pH 1.4	30.15	16.39(0.1%)	Extremely significant
pH 1 2vspH 1.4 (Sulfolobus)	0.51	5.99 (5%)	Not significant
Sulfolobus vs DSM 1651 at pH 1.2	0.23	5.99(5%)	Not significant
pH effect on DSM 1651 (pH I.0-2.0)	5.33	4.89(1%)	Highly significant
pH 1.0 vs pH 1.2 (DSM 1651)	0.04	5.99 (5%)	Not significant
pH I.OvspH 14 (DSM 1651)	0.78	5.99 (5%)	Not significant
pH I.OvspH 1.6(DSM 1651)	3.13	5.99 (5%)	Not significant
pH 1 0vspH2.0(DSM 1651)	13.65	5.99 (5%)	Significant
pH 1.6 vs pH 2.0 (DSM 1651)	10.81	5.99 (5%)	Significant
CI" effect on Sulfolobus (0% vs 4% CD	1.06	5.99(5%)	Not significant
CI" effect on DSM 1651 (0% vs 4% CD	0.51	5.99(5%.)	Not significant
Comparison of mesophiles with extreme thermophiles			
WJM (at pH 2.0) vs DSM 1651 (at pH 1.0)	9.46	5.99(5%)	Significant

dissolution of zinc by WJM culture and the ability of both the extreme thermophiles to oxidise the ore efficiently under the saline conditions. Finally, the "best" performed cultures of mesophiles (WJM at pH 2.0) and extreme thermophiles (DSM 1651 at pH 1.0) were compared with the results indicating that the extreme thermophiles have superior capacity for the bioleaching of the ore.

4 CONCLUSIONS

The bioleaching tests performed within the current study have shown that the complex sulphide ore is readily amenable to the selective bacterial extraction of zinc with lead present in the ore remaining in the residues during the bioleaching process.

The pH appears to exert a significant effect on the dissolution process controlling the oxidative activity of the mesophiles and extreme thermophiles. The bioleaching performance of the mesophiles tends to decrease with increasing acidity from pH 2.0 to 1.2. The extreme thermophiles however have greater tolerance for acidity than the mesophiles as the extraction of zinc was observed to improve with decreasing the pH in the range of 1.0-2.0. Statistical analysis of the pH data allowed the determination of the optimum pH range to be pH 1.0-1.6 for the extreme thermophiles and pH 1.6-2.0 for the

mesophiles since the differences in the dissolution rates of

zinc produced by the respective cultures within these ranges of pH were found to be statistically insignificant.

The quality of process water with particular reference to salinity appears to be of practical importance for the mesophiles since the addition of chloride (I-4% CI') was shown to have a detrimental effect on the bioleaching activity of the mesophilic WJM culture. These findings were consistent with the results of the statistical analysis of the data. However, the extreme thermophiles were found to consistently perform well under the saline conditions tested indicating the halophilic nature of these microorganisms.

The statistical analysis of the experimental result also affirmed that the extreme thermophiles exhibit superior kinetics for the dissolution of zinc from the ore compared with the mesophiles. The statistical methodology adopted herein has proved a useful tool for the accurate interpretation of the batch experimental results and it can be used for the optimisation (or estimation) of process parameters.

REFERENCES

Bosecker. K. 1997. Bioleaching: Metal solubilization by microorganisms. *FEMS Microbiology Reviews* 20: 591-604.

Budden. J.R. and Spencer. P.A. 1991. The effect of temperature and water quality on bacterial oxidation- The advantages of a moderately theunophilic culture over conventional Thiobacillus cultures. In *Randal Gold Fanım.* Caııns: 271-274.

Deveci. H. 1997 Investigation of the selective dissolution of metals fiom a complex sulphide ore using acidic ferric .sulphate solutions and acidophilic bacteria. *MSc Thesis.* Camborne School of Mines. University of Exeter.

Deveci. H. 2002 Effect of salinity on the oxidative activity of acidophilic bacteria during bioleaching of a complex Zn/Pb sulphide ore. *European Journal of Mineral Processing and Environmental Protcilion* 2 (31: 141-150.

Dew D.W.. Lawson E.N. and Broadlnirsl J.L. 1997. The BIOX'" process for biooxidation of gold beating ores or concentrates. In *Bitiminin/;: Theory, Microbes anil Industrial Processes,* ed. Rawlings D.E. Springer-Verlag. Berlin: 45-79.

Dulnzac. J.E. 1981. Factors affecting alkali jarosite precipitation *Metallurgieal Titmsaitions* I4B: 531-539.

d'Hugues P. Foucher S.. Gallc-Cavalloni P and Morin D.. 2002. Continuous bioleaching of chalcopynte using a novel extiemelv thermophilic mixed cultuie. *International Jinirmil of Mineral Processing* 66: 107-119.

Ergun. S. 1956. Application of the principle of least squares to families of straight lines. *Industrial and Engineering Chemistry* 48: 2063-2068.

Ingledew, W.J. 1982. *Thiobacillus ferrooxtdans:* The bioenergetics of an acidophilic chemolithotroph. *Bioihim'ua et Bıoplnsica Acta* 683: 89-117.

Jordan. M.A. 1993 The oxidation of base metal sulphides and mechanisms and preferential release of ferrous Iron. *PhD Thesis.* Camborne School of Mines. University of Exeter.

Joidan M.A.. Powell N.. Phillips C.V. and Chin CK. 1997. Experimental data analysis: A guide to the selection of simple statistical tests. *Minerals Engineering* 10 (3)- 275-286.

Leong B.J.Y.. Dreisinger D.B., Lo M.. Bramon R.M.R. Hackl R.P. Gormerly L.S. and Crombie D.R. 1993. The nuciobiological leaching of a sulphidic copper ore in a strongly saline medium I: Shake flask and column studies. In *Bio-lıvılromelallırgİLal Technologies Vol. I: Prot, of Int. Btolivdromi'lallurgv Svmp..* ed. A.E. Torma. .I.E. Wey and V.l. Lakshmanan. USA- 117-126.

Natarajan. K.A 1990. Electrochemical aspects of bioleaching of base metal sulphides. In *Microbial Mineral Retoverx.* eds. H.L. Ehrlich and C.L. Brierley. McGraw-Hill: 79-106

Nords P.R.. Burton N.P. and Foulis N.A.M. 2000. Acidophilus in bioreactor mineral processing. *E\tremophiles* 4: 71-76.

Porro S.. Boiardi J.L. and Tedesco P.H. 1989. Bioleaching improvement at pH 1.4 using selected strains of *Thiobacillus ferrooxidans.* Biorecovery 1: 145-154.

Powell. N. and Joidan. M.A. 1997. Batch leaching data analysis: Eradication of lime dependency prior to statistical analysis. *Minerals Engineering* 10 (8): 859-870.

Rawlings D.E.. Dew D. and du Plessıs C. 2003. Biommerahzation of metal containing ores and concentrates. *Trends in Biota hnologx* 21 (1): 38-44.

Sand W.. Gehrke T.. Jozsa P.G. and Shippers A. 2001. (Bio)chemislry of bacterial leaching-direct vs. indirect bioleaching. *rlvdrometalltirgy* 59(2-3): 159-175

Suzuki. I. 2001. Microbial leaching of metals from sulphide minerals. *Biotechnology Advances* 19: 119-132.

Weston T.. Perkins .l. Ritchie 1. and Marais H. 1994. Concentrate biooxidation in a hypersaline environment foi Knowna Belle. In *Bioinine'M. Int. Conference and Workshop Applications of Biotechnology to the Minerals Industry.* Australian Mineral Foundation, Penh. W.A.

The Flotation of Murgul - Çakmakkaya Copper Mine and The Determination of the Results of Locked Cycle Flotation Tests

V.Çakın Önen & H.Özşen
Mining Engineering Department, Selçuk University, Konya

ABSTRACT: In this work, locked cycle flotation test results have been determined by simulation method as a result of Murgul-Çakmakkaya copper ore flotation by using discontinuous laboratory test data. Thus locked cycle flotation periods and necessary total cell volumes has been determined without applying locked cycle tests which are very difficult to perform, long timing and sometimes impossible.

1 INTRODUCTION

Before plant setup stage, locked cycle flotation tests and pilot plant studies must be carried out. Discontinuous flotation tests done in laboratory does not represent the continuous test results completely. By these tests, parameter optimization has been supplied and necessary preliminary information has been obtained about métallurgie performance of enriching operation.

Locked cycle flotation tests are long lasting flotation tests that give cleaner tailings and scavenger concentrates which are obtained in the preceding circulation. They are collected in required places tor floating again (Nishimura at all, 1989, Yalçın, 1992).

These tests are lime consuming. It is necessary for a simple cycle to be balanced. 5 or even generally 6 circulations. And also cycle can't be balanced or tests can not be finished because of heavy load (Nishimura at all, 1989, Çilek, 1995).

To annihilate these disadvantages of locked cycle flotation, some studies show that locked cycle flotation test results can be pre-determined from discontinuous test results. For tis purpose various mathematical models have been developed which can simulate flotation tests (Nishimura at all, 1989, Yalçın, 1992, Reuter at all. 1992. Deng at all. 1996. Çilek, 2000).

Due to these mathematical models by connecting classic flotation data and plant conditions, optimum conditions are obtained. Therefore, disadvantages of locked cycle flotation tests are removed and at the same time faults in setting up the plant are minimized.

2 METHOD

In this work distribution coefficient (D) obtained from discontinuous laboratory test data is given was used in all cycles (close flotation, cleaner and scavenger flotation) in applied simulation method. Distribution coefficients in flotation cycle are calculated by rating solid amount, water amount and grade value to the same properties of the feed.

Then feed is distributed to inferior cycles related to the distribution coefficients calculated specially for grade, weight and water amount and these conditions continue until arriving to balance point.

Accepting that distribution coefficients in the cycles does not change until chemical conditions differ in these conditions; weight and grade values are calculated by created mathematical equations (Yalçın. 1992).

3 EXPERIMENTAL

Murgul-Çakmakkaya copper ore have been used in this experimental research. Run of mine ore has 3.7 % chalcopyrite and 10.6 % pyrite minerals. Elemental analysis of the ore gave the result of 1.27 % Cu, 6.12 % Fe and 78.95 SiO_2. Free grain size for pyrite and chalcopyrite from gangue is 74 urn, and pyrite from chalcopyrite is 43 urn.

Table 1. Collective flotation test results.

Products	Rougher			Scavenger			Cleaner		
	%Weight	%Grade	% Solid	%Weight	%Grade	%Solid	%Weight	%<Gradc	%Solid
Concentrate	17.77	6.00	25.01	11.24	1.27	12.56	58.45	9.52	12.04
Tailing	82.23	0.25	31.34	88.76	0.12	38.67	41.55	1.04	8.07
Feed	100.00	1.27	30.00	100.00	0.25	31.34	100.00	6.00	25.01
Flotation period		2 min.			4 min.			2 min.	

Table 2 Selective stage rougher and cleaner cycle flotation test results.

Products	Rougher			Cleaner		
	%Weight	%Cu	%Solid	%Weight	^{r}/rCu	%Solid
Concentrate	55.62	12.14	12.21	22.91	24.44	8.67
Tailing	44.38	6.236	21.00	77.09	8.484	10.48
Feed	100.00	9.52	15.00	100.00	12.14	12.21
Flotation period		10 min.			2 min.	

Table 3 Selective stage scavenger 1 and scavenger 2 flotation test results.

Products	Scavenger 1			Scavenger 2		
	%Weight	%Cu	%Solid	%Weight	9iCu	%Solid
Concentrate	53.81	8.03	15.58	48.66	7.26	14.30
Tailing	46.19	4.146	19.02	51.34	1.195	15.70
Feed	100.00	6.236	21.00	100.00	4.146	19.02
Flotation period		5 min.			5 min.	

4   EVALUATION OF LABORATORY TEST RESULTS BY SIMULTANEOUS METHOD

4.1   Determining mathematical equations for collective stage
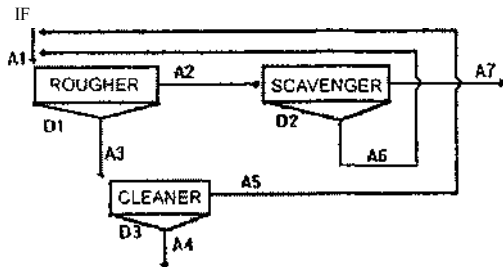
Figure 1 Locked cycle flow chart for collective flotation.

Initially: IF=Ai
$A_:=A|D|$
$A,=A,(I-Di)$
$A_4=Ai(l-Di)(l-Di$

$A,=A,D,=A|D_1(l-D,)$
Afi=A:(1-D2)=A|D,(l-D_2)
$A_7=A:D2=\hat{A}|D|D;$

Balanced: $A_1=1F+A_s+A_r,$
$A|=IF+A,D_3(I-D,)+A,D|(1-D_2)$
$IF=A,[1-D,(1-D,)-D,(1-D:)]$

$$A_1=\frac{IF}{[1-D_3(1-D_1)-D_1(1-D_2)]}$$

4.2   Determining mathematical equations for selective stage
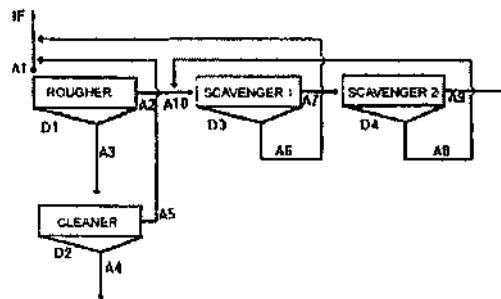
Figure 2 Selective stage locked cycle flow chart.

Initially: $A_1 = IF$
             $A_2 = A_j D$,
             $A_3 = A_1(1-D_1)$
             $A_4 = A_3(I-D_2) = A_1(1-D_1)(1-D_2)$
             $A_5 = A_1 D := A_1 D_2(1-D_1)$
             $A_6 = A_2(I-D_1) = A_1 D_2(I-D_1)$
             $A_7 = A_2 D_i = A_1 D_1 D_3$
             $A_8 = A_7(I-D_4) = A_1 D_1 D_3(1-D_4)$
             $A_9 = A_7 D_4 = A_1 D_1 D_3 D_4$

Balanced: $A_1 = IF + A_5 + A_7$,
             $A_2 = A_1 + A_8$
             $A_3 = A_7(I-D_4)$
             $A_7 = A_1 (>D_1$
             $A_8 = A_1 n D_1(I-D_4)$
             $A_1 = FA_1 D_1 + AH, D_1(1-D_4)$

$$A_{10} = \frac{A_1 D_1}{[1-D_3(1-D_4)]}$$

$$A_A = A_1 . K_1 - D_0$$

$$A_1 = \frac{A_1 D_1(1-D_3)}{1-D_3(1-D_4)} + A_1 D_2(1-D_1) + IF$$

$$A_1 = \frac{IF}{1-[D_1(1-D_3)/1-D_3(1-D_4)]-D_2(1-D_1)}$$

4.3 Calculating locked cule flotation results by simulation method

"IF" value used in the equations below for three different concepts, is used as *i\ first feed amount* for weight balance calculations: secondly it is used as a *first feed unit* for grade balance calculations and thirdly it is used as a *water content in first feed,* for watei balance calculations.

So "IF'" is accepted as below;
For collective stage weight balance calculations.
IF= 474 t/h
For collective stage grade balance calculations;
IF= 127 t/h
For collective stage water balance calculations;

IF= 1106 t/h
For selective stage weight balance calculations;
IF= 59.09 t/h
For selective stage grade balance calculations:
IF= 952 t/h
For selective stage water balance calculations;
IF= 33.84 t/h

Then as explained in Part 2 distribution coefficients are calculated related to laboratory test data obtained. So;

Weight balance distribution coefficients;
In collective stage
Forroughei cyctcrD_1=0.822
For scavenger cycle D_2=0.888
For cleaner cycle D_i=0.416

In selective stage
For rougher cycle D_1=0.4438
For cleaner cycle D_2=0.7709
For scavenger 1 cycle D_i=0.4619
For scavenger 2 cycle D_4=0.5134

Grade balance distribution coefficients;
In collective stage
For rougher cycle D_1=0.1618
For scavenger cycle D_2=0.426
For cleaner cycle D_i=0.072

In selective stage
For rougher cycle D_1=0.2907
For cleaner cycle D_2=0.5387
For scavenger I cycle D_v=0.3071
For scavenger 2 cycle D_4=0.1480

Water balance distribution coefficients;
In collective stage
For rougher cycle D_i=0.772
For scavenger cycle D_2=0.642
For cleaner cycle D_i=0 526

In selective stage
For rougher cycle D_1=0.295
For cleaner cycle D_2=0.731
For scavenger 1 cycle D_i=0.402
For scavenger 2 cycle D_4=0.486

Table 4 Collective stage locked cycle flotation test results calculated by simulation method.

Flow branch	Weight		Grade %	Pulp solid/ liquid rate	Water How m'/h	Pulp flow m-Vh	Pulp density gr/cm
	ton/h	%					
Al	568.48	119.92	1.25	23.70	1830.82	2020.31	1.19
A2	467.29	98.57	0.25	24.85	1413.39	1569.15	1.20
A3	101.19	21.35	5.90	19.51	417.42	451.15	1.15
A6	62.33	11.04	1.25	9.37	505.99	523.43	1.07
A7	414.95	87.53	0.12	31.37	907.39	1045.70	1.26
A4	59.09	12.47	9.36	22.99	197.86	217.55	1.18
A5	42.09	8.88	1.02	16.08	219.56	233.59	1.12

Table 5 Selective stage flotation results calcidated by simulation method.

Flow branch	Weight		Grade %	Pulp solid/ liquid rate	Water How mVh	Pulp flow mVh	Pulp density gr/cm
	ton/h	%					
Al	224.42	379.79	7.26	14.97	1274.61	1349.42	1.11
A2	99.60	168.55	4.76	20.94	376.01	409.21	1.16
A3	124.82	211.24	9.26	12.19	898.60	940.21	1.09
A6	69.15	117.03	6.43	19.25	290.12	313.17	1.15
A7	59.36	100.45	3.32	23.33	195.03	214.81	1.19
A8	28.87	48.88	5.81	22.36	100.25	109.87	1.18
A9	30.47	51.57	0.96	24.32	94.78	104.93	1.20
A4	28.60	48.40	18.64	10.58	241.72	251.25	1.08
A5	96.22	162.84	6.47	12.77	656.88	688.95	1.09

5 CALCULATING LOCKED CYCLE FLOTATION PERIODS AND REQUIRED CELL VOLUMES

For determining flotation periods in actual plant size applications, periods used in laboratory discontinuous flotation tests and yield values obtained from laboratory tests are utilized. Flotation periods necessary for continuous system determined from laboratory tests can be found from the equations below;

$$R_I = 1 - e^{-kt_I}$$
$$R_E = kt_E/(1+kt_E)$$
$$R_L = R_E$$

Necessary flotation periods obtained from the equations above;

Collective stage
Rougher cycle flotation period=5.75 min
Cleaner cycle tlotation period=9.74 min
Scavenger cycle tlotation period=6.36 min

Selective stage;
Rougher cycle tlotation penod= 19.75 min
Cleaner cycle tlotation period=2.761 min
Scavenger 1 cycle flotation period=9.54 min
Scavenger 2 cycle tlotation period= 14.94 min

Cell volumes for every cycle related to tlotation periods and pulp How volumes:

Collective stage;
For rougher cycle= 193.61 m^3
For scavenger cycle= 166.32 m
For cleaner cycle=73.23 rtr

Selective stage;
For rougher cycle=444.18 m^3
For scavenger I cycle=8(). 14 m
For scavenger 2 cycle=53.49 m^1
For cleaner cycle=43.27 m

6 RESULTS

- When grade values; obtained from calculations and discontinuous flotation test results are compared it is seen that all concentrate grades go down in value in the end of locked cycle tlotation tests.
- It is observed that tlotation periods obtained from calculations and the periods applied in the values in the plant arc coincide to each other. However calculated cell volume is bigger than actual size plant's cell volume this situation is the result of studying on the test situation which have low solid rate and higher cycling load amount.

482

- Bulk concentrate obtained from collective flotation is 9.36 % Cu and it has an amount of 59 t/h. In the light of these data collective stage yield has been calculated 91.83%. In the ore dressing plant bulk concentrate amount is 45 t/h, grade 9.5 % and collective stage yield is 90.19%.

- Il is determined that grade of Cu concentrate is 18.64 % Cu and as an amount of 28.6 t/h with a yield 90 % as a result of calculations. On the other hand Cu concentrate produced in the site plant is 20 t/h, and it has a grade of 20 % Cu. Cu preparation yield in site plant is then 87 %. One stage cleaner process has been done while three stages is being done in site plant.

- As a result, this research study can be explained that using mathematical method in locked cycle flotation tests as presented here, not only determines problems that might be appeared in process but also process analysis can be evaluated without demolishing site plants working conditions. Therefore it is possible to compare alternative flow sheets with the actual applied flotation cycle in progress.

REFERENCES

Çakın Önen V . 1996. *Miirgnl Çakınakkaya Bakır Cevherinin Flolusyomı* ve *Tesis Tasarımı*. SDU. Fen Bilimleri Enstitüsü. Yüksek Lisans Tezi.

Çilek. EC. ve Yamık. A, 1995 Flotasyonda Kapalı Devre Oluşturma ve Ölçek Büyütme. *Madencilikle' Bılgısavar Uygulamaları Sempozyumu Bildiriler Kitabı,* Umir

Çilek. E.C. 2<K)0. Simulation of Locked Cycle Flotation Tests. *Yerbilimleri Geımnıul Dergisi*. 36: 197-206. ISSN 1019-1003.

Nıshımura S, Hirosue. H. Snobu, K, and Jınnal. K. 1989 Analytical Evaluation of Locked Cycle Flotation Tests. *Iiiternaliiiiiiil Journal of Mineral Proi esxiiig*. 27:39-50.

Reuter. M.A., and Devemer. J.S.J., 1992. The Simulation and Identification of Flotation Processes by Use of a Knowledge Based Model. *International Journal of Mineral Pronssme*. 35.13-49

Yalçın. M 1992 Kapalı Devre Flotasyon Deney Sonuçlarının Önceden Tahmininde Kullanılan Eşitliklerin Analitik Çözümleri. *Maileni ilik* 31 Sayı 3

Solution of Ore Blending Problem by Stochastic Approach

M. Kumral

Department of Mining Engineering, Inonn University Malatya, Turkey

ABSTRACT: Ore flows from production faces, seams or orebodics may have different qualitative features. Therefore, the grade fluctuations may lead to quality variations in the finished product. One available option to deal with this problem is to blend ores coming from different sources. For this reason the blending rates should be determined from each face, seam or orebody to provide a mix that effectively achieves implicit blending. In this paper, the problem is expressed as a minimisation problem of the total material cost of the finished product such a way as to satisfy the blending requirements. Using information of the random variables that characterise the mineral contents of each ore source, chance constraints are straightforwardly converted into deterministic constraints. Then the problem is solved by the simulated annealing (SA) algorithm to find so-called best result. The variability of each variable in each flow was quantified by semi-variograms. Each flow was simulated to reproduce the characteristics, or behaviour, of the phenomenon as observed in the available data. The expected value of each variable in each flow was calculated by averaging of the simulated values. The technique is demonstrated on a case study compared with the result obtained by Zoutendijk's Method.

I INTRODUCTION

Mineral blending facility is used in various industrial operations. For instance, ore processing and metallurgical plants for ore concentration, coke ovens, blast furnaces, coal washery, copper and bauxite, pyrite-fed sulphuric acid, cement, fertiliser, palletising and glass production plants.

Regardless of the extent to which an acceptable production and homogenisation schedule is accomplished, the stockpiling may not satisfy contractual constraints or plant requirements. In the stockpiling operation raw material is added having a high- or a low-grade in a given proportion to meet the specifications (Gy. 1999). In this case the blending (proportioning) rates should be determined.

The linear programming (LP) has often been recommended as the best and the most widely applied method for blending goals (Gershon, 1988; Bott D.L. and Badiozamani K.. 1982; Gunn and Rutherford, 1990). For example, in order to meet Fe and SiO: specifications in an iron-steel plant, the blending problem can be defined as a minimisation problem in the deterministic manner:

$$Min \quad \sum_{i=1}^{n} p_i x_i$$

subject to:

$$F_L^* \le \sum_{i=1}^{n} F_i x_i \le F_U^*$$

$$S_L^* \le \sum_{i=1}^{n} S_i x_i \le S_U^*$$

$$\sum_{i=1}^{n} x_i = 1$$

$$x_i \ge 0 \quad \forall_i$$

where:

x_i	is the blending ratio for ore type i
p_i	is the unit price of ore type i
F_i	is the Fe content of ore type i
S_i	is the SiO: content of ore type i
F_L and F_U	are the lower and upper limits for acceptable Fc content
S_L and S_U	arc the lower and upper limits for acceptable SiO: content
	is the number of ore types or sources

However, The LP has important drawbacks:

I. The LP uses only a single goal in the objective function whereas there may be two or more objective functions in some applications. This kind of problem can be solved after extensive

modification of the LP, which is quite time-consuming (Lyu *et. ai,* 1995).

2. As the number of constraints increases, the convergence becomes increasingly difficult to achieve whereas a realistic case involves many constraints.

3. The LP might require unrealistically small amounts of some ores or leave "small heaps" of ore in the inventory which would just be a nuisance (Candler, 1991). In other words, the LP may yield extreme solutions, which cannot be used in practice. In order to avoid this problem, the modifications that incorporate additional constraints in the LP can be used (Lai and Chen, 1996).

4. The LP yields optimal results for the formulated problem but not for the real world problem because the LP takes no account of the random nature of ore variables. Traditional LP can be operated on the basis of deterministic values.

These drawbacks of LP induce to seek alternative approaches.

2 STOCHASTIC APPROACH

In the work described here an integration of Chance-Constrained Programming (CCP) (Chaînes and Cooper, 1963) and the simulated annealing (SA) (Laarhoven and Aarts, 1987; Eglese, 1990; 1992; Dowsland, 1993; Ansari and Hou, 1997) is used.

The CCP comprises 'chance constraints', which incorporate a strict measure of the probability with which the constraints must be met. For example, the chance constraints of the Fe content in an ore blend fed to an iron-steel operation may be specified as:

$$P\left[F_L^{\tau} \le \sum_{i=1}^{n} F_i x_i\right] \ge \alpha_F \qquad (3)$$

where:

v_i	is the blending ratio for ore type i
F_i	is the Fe content of ore type i
F_L	is the lower limit for Fe content
n	is the number of ore types or sources
a_F	is the reliability or risk level for the constraint on Fe grade
P	is probability

The constraints require the specification of both the target qualities and the specified probability of meeting the target quality. F_L* *and ar* are

deterministic values. On the other hand, F, is random variable.

Assume the random vector of Fe content for each different ore source:

$$F = (Fi.i=l......n \qquad (4)$$

The expected value, $E(F)$, and «variance matrix of F, $VAR(F)$, are:

$$E(F) = \{E(F_i), i=1, ..., n)\} = \tilde{m}^T \qquad (5)$$

$$VAR(F) = V_F = COV(F_i, FJ) \qquad (6)$$

The *Fe* content of ore blend is a random variable, *ly*

$$r_F = \sum_{i=1}^{n} F_i x_i \qquad (7)$$

The content has an expected value and a standard deviation, which depend upon the values assigned to the non-random decision variables x:

$$\mu_{r_F} = \tilde{m}^T x \qquad (8)$$
$$\sigma_{r_F} = (x^T V_F x)^{0.5} \qquad (9)$$

where x is the column vector and $.t^T$ is its transpose. The expected value and variability of each variable in each ore flow should be quantified. This aspect is discussed in the next section.

After the mean and variance are determined for each ore source, the distribution of the random variable, */•/-.* should be specified for the reliability level. If the F,'s are normally distributed, the variate */>•* also exhibits normal distribution. The following variate is obtained:

$$Z(\alpha) = \frac{r_F - \mu_{r_F}}{\sigma_{r_F}} \qquad (10)$$

$$F_Z\{Z(\alpha)\} = \alpha \qquad (11)$$

where $F-A-)$ is the cumulative normal distribution function. Integrating the above two equations yields

$$\Pr[r_F \le (\mu_i + Z(\alpha)\sigma_i)] = \alpha \qquad (12)$$

and the deterministic equivalent is expressed as:

$$F_L^{'} \le \sum_{i=1}^{n} \mu_F x_i + F_z^{-1}(\alpha_F)(x^T V_F x)^{0.5} \qquad (13)$$

486

The similar equivalents can be derived for other variables if any. The grade components of the ore sources do not necessarily follow normal distributions. Sengupta (1972) summarises how non-normal distributions can be used in CCP but the solutions become significantly more complex. Liu (1999) indicated that complex CCP models could be solved by modern heuristic methods such as neural network, genetic algorithms or simulated annealing.

2.1 Estimation of means and variances used in stochastic programming

The variance of the grades of samples within some specified volume is equal to the mean value of the semi-variogram of the samples within the specified volume. The variability of the grades over time in the ore stream determined by the sequencing model can be estimated from the semi-variogram model:

$$\gamma(h) = \frac{1}{2N(h)} \sum_{(i,j)|h_{ij}=h} (v_i - v_j)^2 \qquad (14)$$

where h us separation vector, N is the number of data pans separated by h and i".v are data values over the $N(h)$. The dispersion variance may thus be regarded as a type of variogram calculation in which pairs of values are accepted in the averaging procedure as long as the separation vector h_v is within the ore stream, S:

$$\sigma^2(o/D) = \frac{1}{2N(S)} \sum_{(i,j)|h_{ij} \in S} (v_i - v_j)^2 \qquad (15)$$

where $s'(o/D)h$ the variance of the average value of the attribute (e.g. grade) of sampling sizes within the total deliverable tonnage. Although this could be estimated from a set of sample data, it is usually derived from a semi-variogram model:

$$\overline{\sigma}^2(o/D) \approx \overline{\gamma}(S) \qquad (16)$$

where the right-hand side refers to the semi-variogram model $\gamma(S)$ averaged over all possible vectors within S. In practice, the ore stream is subdivided into n discrete time intervals and the average semi-variogram values can be calculated by approximation of the exhaustive average of the semi-variogram by an average of the $n\sim$ semi-variogram values at the n discrete time intervals:

$$\overline{\sigma}^2(o/D) \approx \frac{1}{n^2} \sum_{i=1}^{n} \sum_{j=1}^{n} \overline{\gamma}(h_{ij}) \qquad (17)$$

Sequential Gaussian simulation can be used to reproduce the characteristics, or behaviour, of the phenomenon as observed in the available data. Global means are calculated by averaging of the simulated values.

3 SIMULATED ANNEALING

Simulated annealing is a stochastic method for solving large objective combinatorial minimisation problems. The method is based on the principle of stochastic relaxation. Simulated annealing was developed by Kirkpatrick et. al. (1983) in the mid-80's. The method has an analogy in thermodynamics, specifically with the way that liquids freeze and crystallise or metal cools and anneals.

Suppose that a cost function in many variables is to be minimised. A simple and iterative local search could be performed to find the minimum cost. During the local search process, an initial solution is given and then a new solution is selected at random. If the cost of the new solution is lower than that of the current solution, the current solution is replaced by the new solution. Unfortunately, a local search may get stuck at local minima. Let $/: X \longrightarrow R$ be a function to be minimised over X, where X is a finite, but very large set. A neighbourhood $N(x)$ c X is associated with each element $x \in X$. Iterations can be defined by first selecting a starting point and then repetitively selecting y e $N(\)$ and comparing successive values. Simulated annealing allows the choice of v to be governed by the following stochastic rule:

$$p_y(T) = min\{1, e^{-(f(y)-f(x))/T}\} \qquad (18)$$

where;

p_y	is the acceptance probability
T	is a parameter known as temperature
A	is the current solution
y	is the new solution
$\Delta f = (f(y) - f(x))$	

As T approaches zero, improving choices accepted and the method reduces to a pure local search. For very large values of T all y solutions chosen in the neighbourhood are accepted. Any $T > 0$ allows the iteration to escape from a local minimum sooner or later. Figure I. illustrates the basic simulated annealing algorithm.

Some decisions must be made prior to implementing simulated annealing. These decisions may be classified into two groups; the first relates to the choice of a cooling schedule (generic decisions) and the second relates to problem-specific decisions. Both decisions affect the speed of the algorithm. Kirkpatrick et al. (1983) remarked that convergence to a global optimum required more iterations than an exhaustive search.

Figure 1 Basit simulated annealing algoithm

i and *j*	are sequence indices
k	is the temperatuie index
T_k	is the tempeiature
l	is the iteration number
L_k	is the allowable length ot the kth Markov Chain
CS and *NS*	are the cunent and new proposed sequence, iespectively
Rem [0,1]	is a landom numbei generated between 0 and I by the i andern numbei generatoi

4 PROBLEM DESCRIPTION

The pioblem tianstormed to deteiministic equivalents is given as below

$$Miu \sum_{i=1}^{m} p_i x_i \qquad (19)$$

subject to

$$\sum_{i=1}^{n} \mu_{F} x_i + F^{-1}(\sigma_F)(\sum_{i=1}^{n} \sigma_i^2 x_i^2)^{0.5} \geq F_U$$

$$\sum_{i=1}^{n} \mu_s x_i \geq S_U$$

$$\sum_{i=1}^{m} x_i = 1 \qquad (20)$$

$$x_i \geq 0 \quad \forall_i$$

Note that this formulation includes non-linear toi m in some constraints

488

5 CASE STUDY

In order to demonstrate the technique, the results obtained by one of Zoutendijk's methods of feasible directions (Van de Panne and Popp, 1963) were compared with the CCP based on the SA.

Zoutendijk's method is one of available techniques for solving convex programming problems. The method is iterative and uses a feasible vector as an initial solution. The procedure iterates the non-linear problem at initial feasible solution into linear case. As non-linear functions are complicated, finding a solution is very difficult. Therefore, the technique is not practical.

The problem was cattle feed blending with probabilistic protein constraint as a minimisation problem. Same problem is often encountered in mineral industries. Therefore, one can conceive as mineral blending problem rather than cattle feed blending problem. Costs, standard deviations, protein and fat contents of raw materials to be hlended were given in Table I.

Table I. Input data

	Prolein Comeni	Fal Content	Cosl	Standard Deviation
Bailey	12.(1	2.3	24.55	0.53
Oats	11.9	5.5	26.75	0.44
Sesame Flakes	41 8	11.1	39.00	4.50
Guiundnut meal	52.1	1.3	40.50	0.79

Specified reliability level is 95% (if l-e is 0.95, q> is -1.645 from table of normal curve area). Protein commit of blend must be more than 21% and fat content of blend must be more than 5%

Minimization problem was expressed as:

$$f(x) = \sum_{t=1}^{4} c_t x_t \qquad (21)$$

subject lo:

$$12x_1 + 11.9x_2 + 41.8x_3 + 52.1x_4 - 1.645(0.53^2 x_1^2 + 0.44^2 x_2^2 + 4.50^2 x_3^2 + 0.79^2 x_4^2)^{1/2} \geq 21$$

$$2.3x_1 + 5.6x_2 + 11.1x_3 + 1.3x_4 \geq 5$$

$$x_1 + x_2 + x_3 + x_4 = 1 \qquad (22)$$
$$x_1, x_2, x_3, x_4 \geq 0$$

The minimisation problem defined above is submitted lo the SA algorithm. The computer program was written in FORTRAN 90 by the author. The required annealing parameters were specified as follows:

Initial temperature. The acceptance ratio must be almost 1 at the initial temperature and it should drop rapidly from I. In this research $T_{m,mi} = 0.1$
Temperature decrement. $T_{J+} = a7''j$ is used as the decrement function, where a is almost I. In this research *a* is accepted as 0.95.
Stopping Criterion. The procedure is terminated when the cosl of the solution obtained in the last trial of the Markov chain remains unchanged for three consecutive temperatures.
Number of iterations in each temperature. 100 000 iterations are implemented in each temperature.
Limit of successful moves in each temperature. If 10 000 iterations are successful in any temperature, temperature is directly decreased.
Required reliability level for each temperature. Specified reliability level is 95%.

Table 2. shows results obtained from Zoutendijk's Method and CCP based on SA As seen the results, the CCP based on SA yielded very similar results to Zoutendijk's Method.

Table 2. Results compared with a traditional method

	v;	\,	ıı	w	,/fvi
Zoulendijk s Method	0.6359	0.0000	0.3127	0.0515	29.892
CCP based on SA	0.6284	0.0088	0.3096	0.0532	29.891

6 CONCLUSIONS

The CCP based on the SA can be easily implemented to solve the mineral blending problem. The method is flexible to changing structure of objective function and constraints. The computer running time is approximately 50 minutes. Moreover, the program can easily be incorporated into multi-objective case. The technique is able to deal with random nature of the blending problem. The performance of method was, to a large extent, depends upon selection of cooling schedule of SA. For a further research the problem can expressed as a dynamic (multi-period) approach.

REFERENCES

Ansan. N. &. Hou. N. (1997). *Computational Intelligence For Optimization.* 225 p.. Kluwer Academic Pub.

Bott D.L. *&* Budiozamam K.. (1982), Optimal Blending of Coal to Meeting Quality Compliance Standard;,. *17. APCOM (Application of Computer* ami Operation* Research in the M'meial Industries) Symposium I'roceeilintjs,* pp.15 - 23.

C.UKİleı W (1991) Owl Blending Willi Acceptance Sampling CiMii/HftcM *ımıl Opuiitmiial* fiı *samlı* Vol 7 pp 591 596

Charlies A At Cnopei WW (1%1) Deteinmiislic Kjuivalents loi Optimising and Satisfying Undei Chance Constiaints *Optimums Reseaiili* Vol I l/l pp 18 19

Dowsland K (1991) Simulated Annealing *MIHICIII Heuiistit Itilmitptis foi Conibiiiatoiial Piohkms* Ed C Reeves pp 20-61 Oxtoid

Eglese RW (1990) Simulated Annealing A Tool foi Opeıatıonal Reseaich *Cuioptan Journal of Opcialuiiial Ristauh* Vol 46 pp 271-281

Geishon M (1988) Computerised Appioaches to Coal Blending *Mining Eni>iiicirinn* Vol 40 12 pp 1121-1124

Gunn EA & Rutlieiloid P (1990) Inlegiating ot Annual and Opetatioanl Planning in a Coal Mining Emeipuses *22APCOM (Appluation uf Computus anıl Opıalıoıs Rtsiaiih in the Mmtial liulusliics) Ssuiposiuin Piottcdtıuts* pp 95 106 Geimany

Gy P (1999) Optnni/ing the Opeıatıonal Stıategy ot a Mine Metalluigy or Quany Cemuit Woik Complex *Camuhan Metalim e« al Quartals* Vol 18 No 1 pp 157 161

Kııkpatııck S Gelait C D & Vecchı MP (1981) Optimization By Simulated Annealing *Si unie* Vol 220 pp 671 680

Lai 1 & Chen C (1996) A Cost Minimization Model for Coal Impoit Stıategy *Ena xs Polin* Vol 24 No 12 pp 1111 1117

Laaihoven P I M & Aaits E H L (1987) *Smiiiltilul Annealing Timin anıl Applications* Reıdel Doıdecht

Liu B (1999) *Umirtain Pioxiaiiiiiiiiii;* Wiley 248 p

Lyu J Gunesakaian C Y Chen Y & Kao C (1995) A Go il Piogiammiiig Foi the Coal Blending Pioblem *Coinputa millEitittnieiin\>* Vol 28 No4 pp 861 868

Sengupta JK (1972) Stochastic Ptogramming Method and Applications 111 p

Van de Panne C & Popp W (1961) Miiiumum Cost Cattle heed Undei Piobahihstic Piotein Consliaint Management Science Vol 9 pp 405-410

490

Statistical Design and Optimization of Leaching Tests for Iron Removal from Pyrophyllite Ore

T.Şahin, M.Kumral & M.Erdemoğlu
Department of Mining Engineering, İnönü University, 44069 Malatya, Turkey

ABSTRACT: As an impurity in pyrophyllite deposits, iron affects ceramics quality. Therefore, it should be removed before the end use. In this study, it was aimed to compare and estimate the effects of different factors on the removal of iron from ore by statistically designed experiments and to find optimum experimental parameters in such a way that the iron removal will be maximised. Effect of each factor was determined by Yates Method. Which effects had significance on the recovery was determined by the analysis of variance. After insignificant effects were removed, adequacy of new model was tested. Based on these effects, the multiple regression equation was derived as a function of four parameters. These were organic acid concentration, sulphuric acid concentration, time and temperature. Given that the objective was to maximise the iron removal which was response variable, the regression model was accepted as an optimisation problem and solved by the steepest ascend (SA). The results showed that the method combining the multiple regression analysis and the SA could be used to find optimum experimental parameters qualitatively and quantitatively.

1 INTRODUCTION

The presence of iron in many industrial minerals such as quartz sand, kaolin, talk and pyrophyllite can prevent their use mainly in the ceramic industry. The red to yellow pigmentation in many clay deposits are mainly due to the associated oxides, hydroxides and hydrated oxides of Fe(III) such as hematite, maghemite, goctite, lepidocrocite, etc (Ambikadevi and Lalithambika, 2000). These oxides and hydroxides can present either as coatings on particles or as discrete fines in the clay body.

The iron content of clays can be reduced by a number physical, physicoehemical and chemical methods. The appropriate method for the removal of iron from a clay ore depends on the mineralogical forms and the distribution of iron in the particular ore. Chemical methods involve leaching of the ore with organic and inorganic acids. The most commonly used organic acids are oxalic, citric, ascorbic, acetic, fu marie and tartaric (Panias et al., 1996), and inorganic acids are hydrochloric, hydrofluoric, sulfuric and perchloric (Ubaldini et al, 1996). Of the above organic acids, oxalic, citric and ascorbic are the most used carboxilic acids, due to their effectiveness as solvent reagents (Panias et al, 1996).

The present work aims to study the main factors that are involved in the removal of iron from pyrophyllite ore by leaching with various organic-acids. Consecutive series of the tests were performed, in each of which all the factors were simultaneously varied according to rules of statistical design of experiments in order to determine the main effects and the interactions among the investigated factors.

2 MATERIAL AND METHOD

2.1 *Mineral sample*

Pyrophyllite used for leaching studies was obtained from the Piitiirge-Malatya region of Turkey. The chemical composition of the original pyrophyllite sample is given in Table 1. Depending on the XRD analysis, it consists of mainly pyrophyllite and quartz with small quantities of kaolinite, muscovite and feldspar. The sample was crushed by jaw and impact crusher and was ground in a ceramic ball mill to produce desired particle size fractions. The sample with a particle size of less than 0.150 mm was chosen to carry out the leaching experiments.

2.2 *Experimental procedure*

Prior to leaching experiments, the sample was subjected to dry magnetic separation to remove the iron particles contaminated during the crushing.

Batch-leaching experiments were conducted in 250-mL mechanically agitated spherical glass reactor submerged in a thermostatically controlled water bath. Analytical grade oxalic, tannic, citric and sulphuric acids were used to prepare desired leach solutions. After the given time was consumed agitation was stopped and pulp was filtered to remove the solid phase. Total iron was determined in aqueous phase using Philips PU9100X model flame atomic absorption spectrometer and the degree of iron removal (i.e. % of iron removed) was calculated using the iron content of pyrophyllite sample

Table I. The chemical analysis of original pyrophyllite sample as determined by XRF

Ma|or consument	wt %
A1;0,	31 98
SiO,	61.76
He,C)ₜ	0.21
CaO	0.18
MgO	0.26
Na.O	0.07
K*0	0.14
MnO	-
Loss on ignition at 1000° C	3.24

Table 2. Design variatvles and levels

No	Variable	Low	Base	High
X,	Oxalic acid (M)	0.2	0.3	0.4
	Tannic acul (nig/L)	200	300	400
	Citric acul (M)	0.3	0.4	0.5
X;	Temperature (" C)	30	40	50
Xs	Leaching time (nun.)	10	20	30
Xj	HJSOJ concemiation (N)	0.2	0.3	0.4

Table 3. Parameters studied in coded scale and percentage of removal for each acid

	X|	X:	X,	$\mathbf{X_4}$	Iron Removal. Y (%)		
					Oxalic Acid L.	Tannic Acut L.	Citric Acid L.
1	-	-	-	-	27.95	25.85	16.34
-)	+	-	.	-	31.58	29.12	18.56
3	-	+	-	-	32.73	30.79	17.59
4	+	+	-	-	30.53	32.11	17.98
5	-	-	+	-	30.84	30.98	19.10
6	+	-	+	-	31.76	31.52	18.06
7	-	+	+	-	31.53	30.34	19.67
8	+	+	+	.	31.19	31.75	20.29
9		-	-	+	27.60	29.43	15.44
10	+	-	-	+	28.76	29 39	16.79
II	-	+	-	+	29.53	31.52	17.79
12	+	+	-	+	30.76	31.34	17.48
n	-	-	+	+	30.68	25.85	17.21
14	+	-	+	+	28.77	25.58	15.67
15	-	+	+	+	31.30	30.96	22.91
16	+	+	+	+	^ 1.69	30.61	20.79
17	0	0	0	0	25.83	26.75	17.35
18	0	0	0	0	24.52	27.87	18.46
19	0	0	0	0	23.75	27.14	18.22
20	0	0	0	0	25.25	28.12	17.93
21	0	0	0	0	24.90	2X.53	16.62
22	0	0	0	0	25 40	27.29	17.36

3 STATISTICAL DESIGN

The leaching experiments have been conducted on the basis of the design variables. The variables and level of 2^4 factorial design are given in Table 2.

In each experiment set the variables arc one of organic acids (Oxalic, tannic and citric), the temperature, the leaching duration and the H2SO4 concentration. The higher level of variables is designated as "+'" and the lower level is designated as "-". Matrix in four variables varies at these two levels (Table 3). Hence, three factorial experiment sets arc obtained separately.

The regression model equation can be written as:

$$Y = bn + b,X, + b_2X_2 + h,X, + b_4X_4 + b_{t2}X,X_2 + bi.<XiX.< + b_NXiX_4 + h_{2<}X_2Xj + b_{24}X_2X_4 + b.»X.<X_4 + bi_2<XiX->Xt + bn_4X/X-'X_4 + bn_4XiX<X_4 + b_2<_4X->X<X_4 + b,_{2M}X,X_2X<X_4 \qquad (1)$$

where; Y is the percentage of iron removal, b is model coefficients and X's are coded factors.

The analysis of variance in the 2^4 experiments can be applied easily once the effects totals have been calculated. A systematic method for estimating the effects and performing the analysis of variance was proposed by Yates. (Chatfield. 1978; Morgan, 1997). Yates's method has been used to estimate the effects. For the leaching with each acid type, the coefficient values were computed and incorporated in Eq. (1). Then the analysis of variance has been performed and obtained which effects are significant. Adequacies of the models have been tested at %90 confidence level by the Fischer test and the obtained models have been given as follows:

For oxalic acid leaching:

$$Y = 30.45 + ().71X2 + 0.52Xr - 0.56X_4 + 0.5VXiX?X_4 \quad (2)$$

For tannic acid leaching:

$$Y = 29.H2 + l.36X_2 - 0.96X.,X_4 + 0.90X_2X.<X_4 \quad (3)$$

For citric acid leaching:
$$Y = I8.23 + U)8X_2 + 0MX., + 0.62X_2X., + 0.65X_2X_4 \quad (4)$$

As the acid type has changed, different variables are effective. In the oxalic acid leaching, the temperature and the time have a positive effect while the sulphuric acid concentration has a negative effect. In the tannic acid leaching, the concentration of organic acid and the temperature have a positive effect while the sulphuric acid concentration has a negative effect. In the citric acid leaching, the temperature and the time have a positive effect. The interactions exist in all acid types.

4 OPTIMISATION

Each equation is an unconstrained optimisation problem to be maximised. The steepest ascend method was used to find the optimal parameters. Ascend methods are the general name of direct methods, gradients methods and Hessian methods.

The methods are first to select an initial solution that is the most likely place where optimal solution exists. Then they find a new point from the initial solution by analysing the behaviour of the objective function. This process is repeated until stopping criterion is satisfied. The steepest ascend is a useful method for moving towards the optimum in as few experimental performs as possible (Winston, 1991, Radrin, 1998, Liu. 1999).

In the oxalic, tannic and citric acid leaching the step sizes are determined on the basis of the coefficients in the Eq. 2, 3 and 4, respectively (Table 4, Table 6 and Table 8). Optimum parameters found according to the determined increments for each leaching type is given in Table 5, 7 and 9.

Table 4. Determined step size for each variable in the oxalic acid leaching

	Oxalic acid concentration (M)	Temperature (C°)	Leaching time (minute)	H2SO4 concentration (N)
Coefficient (b)	0.18	0.71	0.52	0.56
Step size (Z)	0.1	10	10	0.1
b x Z	0.018	7.1	5.2	0.056
Normal steps	0.1	39.44	28.88	0.31

Table 5. Optimum parameters for oxalic acid leaching.

Oxalic acid concentration (M)	Temperature (C°)	Leaching time (minute)	H2SO4 concentration (N)	Y (Iron removal) (%)
0.3	40	20	0.3	30.45
0.4	79.44	48.88	0.61	45.46
0.5	118.88	77.76	0.92	93.60

Table 6. Determined step size for each variable in the tannic acid leaching

	Tannic acid concentration (mg/L)	Temperature (C°)	Leaching time (minute)	H2SO4 concentration (N)
Coefficient (b)	0.36	1.36	0.12	0.49
Step size (Z)	100	10	10	0.1
b x Z	36	13.6	1.2	0.049
Normal steps	100	37.8	3.34	0.14

Table 7. Optimum parameters for tannic acid leaching.

Oxalic acid concentration (M)	Temperature (C°)	Leaching time (minute)	H2SO4 concentration (N)	Y (Iron removal) (%)
300	40	20	0.3	29.82
400	77.8	23.34	0.44	40.87
500	115.6	26.7	0.58	84.28

Table 8. Determined step size for each variable in the citric acid leaching

	Temperature (C°)	Leaching time (minute)	H2SO4 concentration (N)
Coefficient (b)	1.08	0.98	0.22
Step size (Z)	10	10	0.1
b x Z	10.8	9.8	0.022
Normal steps	10	9.08	0.02

Table 9. Optimum parameters for citric acid leaching.

Temperature (C°)	Leaching time (minute)	H2SO4 concentration (N)	Y (Iron removal) (%)
40	20	0.30	18.23
50	29.08	0.32	20.45
60	38.16	0.34	24.90
70	47.24	0.36	29.97
80	56.32	0.38	37.19
90	65.40	0.40	45.40
100	74.48	0.42	55.00
110	83.56	0.44	65.92
120	92.64	0.46	78.41
130	101.76	0.48	92.13

5 CONCLUSIONS AND PROPOSALS

This research focuses on statistical design and optimisation of leaching experiments to remove iron from pyrophyllite ore. When the acid types are compared, the oxalic and tannic acids remove almost same iron percentage. However, the iron removal with citric acid is quite low. The most important variable is temperature for all acid types. The second important factor is leaching duration. $HiSO^{\wedge}$ concentration is only significant with interactions. If complex regression models are selected for modelling, the steepest ascend had important drawbacks. In this case, modern heuristic methods such as the genetic algorithms and the simulated annealing techniques can be used easily. These

resulls may yield a background tor pilot applications.

REFERENCES

Ambıkadevı, V.R.. Lalithambika. M.. (2000). Effect of organic acids on feme iron lemoval from iron-stained kaolimte. *Applied Clav Scıeııı e.* 16:1.1.1-145

Cliatflekl. C. (1978). *Statistics for Technology: A course in Applied Statistics,* 170 p.. Chapman and Hall Pub.

Liu. B.. (1999). *Uncertain Programming.* Wiley. 248 p.

Morgan. E.. (1997). *Chenmnielrics: Experimental Design.* 275 p.. John Wiley and Sons.

Panias. D.. Taxiarchou. M.. Paspaliaris. I.. Kontopoulos, A.. (1996), Mechanisms of dissolution of iron oxides in aqueous oxalic acid solutions. *Hvdrometallurgy.* 42:257-265.

Radii» R.L.. (1998). *Oplimiuilion in Operations Research.* Prentice-Hall International. 919 p.

Ubaldini. S.. Piga. L. Fornari, P.. Massidda. R,, (1996). Removal of iron from quartz sands : a study by column leaching using a complete factorial design. *Hvdrometallurgy.* 40:169-379.

Winston, W.L.. (1991), *Operations Research Applications and Algorithms.* PWS-KENT. p. 1262

494

Determination of Leaching Conditions of Sphalerite Concentrate in Acidic Ferric Chloride Solution

A. Aras, S. Aydoğan & A. Özkan
Selçuk University, Department oj Mining Engineering, Konya, Turkey

M. Canbazoğlu
Cumhuriyet University, Department oj Mining Engineering, Sivas, Turkey

ÖZET: Bu çalışmada sfalerit (ZnS) konsantresinin FeClj/HCl çözeltisinde liçing şartlarının belirlenmesi araştırmaları yapılmıştır. Araştırmalarda karıştırma hızının, ferrik iyonları derişiminin (O-I.O M), katı/sıvı oranının (5/500-100/500 g/ınl). liç sıcaklığının (40-90 °C) ve tane boyutunun Zn çözünmesine etkisi incelenmiştir. Elde edilen sonuçlara göre Zn çözünme veriminin; katı/sıvı oranı ve tane boyutu ile ters orantılı, sıcaklık ve ferrik iyonları derişimi ile doğru orantılı olarak arttığı ve karıştırma hızından bağımsız olduğu belirlenmiştir. 8. saatin sonunda 80 °C sıcaklık. 10/500 g/ınl katı/sıvı oranında ve 1.0 M Fe*[rı] derişiminde %82'lere varan verimle Zn kazanımı sağlanmıştır.

ABSTRACT: In this study, the determination of leaching conditions of sphalerite concentrate (ZnS) in FcCli/HCI solution was investigated. Effects of stirring speed, Fe[u] ion concentration (0-1.0 M), solid/liquid ratio (5-500-100/500 g/ml), leaching temperature (40-90 °C) and particle size on dissolution of Zn were determined in the experimental study. According to the results obtained, the Zn extraction varied inversely with solid/liquid ratio and particle size, and directly proportional with temperature and Fe[ıı+] ion concentration, and independent from stirring speed. At the end of leaching time of 8 hours, the Zn extraction increased to approximately 82[x]/r at the temperature of 80 °C, the solid/liquid ratio of 10/500 g/ml and the concentration of 1.0 M Fe * ion.

1 INTRODUCTION

Sphalerite (ZnS) generally associated with other sulphidic minerals ($CuFeS_2$, PbS, FeS etc.) form complex sulphide ores. About 6 million tones/year of world's zinc production is produced via treatment of concentrates recovered using notation method from sulphide ores containing sphalerite. Zinc is frequently produced by roasting + leaching + electrowinning methods from concentrates. SO_2 gas formed during the roasting process causes some environmental problems (Wills 1984; Çopur, 2001).

Environmental problems and requirement of use of small and complex mineral sources lead to development of new alternative methods. Leaching of sulphidic ores bearing zinc has been important at the last 40 years. Advantages such as elimination of roasting step and high zinc extraction increased the importance of hydrometallurgical processes. In this scope, leaching studies were performed by sulphuric-acid (H_2SO_4)f (Demopoulos and Baldwin, 1999: Parker, 1961), nitric acid (HNO_3) (Çopur, 2001) hydrochloric acid (HCl) (Mizoguchi and Habashi, 1981: Majima et al.. 1981: Canbazoğlu and Özkol. 1980). ferric ions (Fe^{3+}) in the acidic medium (Dutrizac and MacDonald, 1974, 1978; Bobeck and Su, 1985; Warren et al., 1987; Rath et al., 1988; Palencia and Durtizac, 1991) and ammonia (NH_3) solutions (Rao et al., 1992; Ghosh et al., 2002)

It is possible to dissolve some sulphidic minerals using only acid. For example, sulphidic minerals decompose according to Equation (1) under the only (non-oxidative) acidic conditions;

$$MS + 2H^+ \rightarrow M^{2+} + H_2S \qquad (1)$$

Equation (1) is true for CuS, PbS, CdS, ZnS, NiS, CoS and FcS, however, this reaction does not occur placed for $CuFeS_2$ and FeS_2 under the same leaching conditions (Majima and Awakaura, 1979). Majima and Awakaura (1979) expressed the solubility of base-metal sulphides under non-oxidative leach conditions as a function of hydrogen ion concentration or pH (Fig. 1). From Equation (1) the solubility product K can be written;

$$K = (aM^+ . P_{H2S})/(aH^+)^2$$

Thus

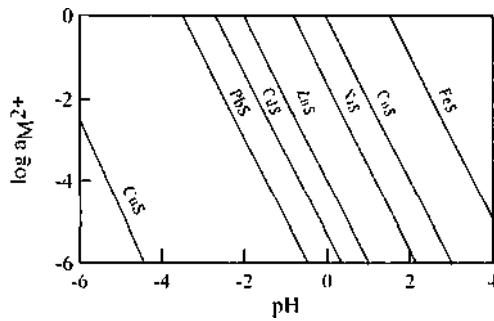$$pH = 1/2 (\log K \cdot \log aM^{2+} - \log P_{H2S})$$

Figure I. Effect of pH on acid decomposition of base-metal sulphides (Majima and Awakura. 1979)

Use of oxidative factors in the acidic medium is commonly investigated for dissolution of sulphides. Ions used as oxidative agents are kupric and ferric ions. Ferric ion is one ot the most importirnl in the the oxidative agents. Potential of $Fc\sim7Fc\sim^+$ couple can be given by Nernst equation;

$$E = E° - 0.0591 \log \frac{a_{Fe^{3+}}}{a_{Fe^{2+}}} \qquad (2)$$

where E°: Half-cell standard potential, R: Gas constant, F: Faraday constant, z: Number of exchanging electrons, a: activity of ions in solution phase. According to Equation (2), even if Fe^+ amount is million fraction of $Fe\sim^+$, potential of $Fe\,7Fe\sim^+$ couple is 0.416 V. This potential value can oxidize all of the base metals and also Zn (Çakır. 1976). However, it is not possible to keep iron, form of ferric ions in solution at normal conditions. In order to prevent this situation, the solution must be strongly acidified. Ferric sulphate $(Fe2(SO_4)0$ and ferric chloride (FeCIO may be used as source of $Fe^{'1+}$. In this situation, possible dissolution reaction equations of ZnS are given in Equation (3) and (4) (Dutrizac and MacDonald, 1974, 1978).

ZnS + 2FeCl,   -> ZnCI-, +2FcCl, + S°   (3)
ZnS + FcMSOah -> $ZnSO_4$ + $2FeSÖ_4$ + S°   (4)
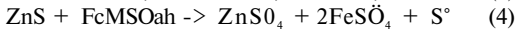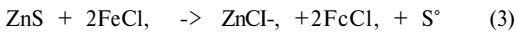
It was reported that ferric chloride has more advantage than ferric sulphate (Dutrizac and MacDonald, 1974, 1978).

2 MATERIAL AND METHODS

2.1 Material

The sphalerite concentrate (ZnS) recovered by notation from Sivas-Koyulhisar $CuFeS_2$-PbS-ZnS complex ore was used in the experimental study. The concentrate used were sieved to -212+106, -106+75, -75+45, -45+38 and -38 urn panicle size fractions. First, wet sieving was made and   the

materials were dried, and then dry sieving was performed using the same screens. The chemical analysis of each fractions are given in Table 1.

Table I. Chemical analysis of each fraction of sphalerite concentrate

Particle Size (um)	Element (%)		
	Zn	Cu	Pb
-212+106	57.87	-	0.03
-106+75	59.97	-	-
-75 +45	61.73	0.85	0.04
-45 +38	57.70	0.53	0.75
-38	39.53	1.43	5.00
Total	48.76	0.90	2.71

2.2 Experimental procedure

In order to provide the Zn dissolution from ZnS concentrate, Fe^{3+} ion leaching in acidic medium was performed. FeCl, was used as source of Fe^+. Experiments were carried out in a glass vessel put in the hot water bath whose temperature can be adjusted in the range of 0-100°C with ±0.2°C accuracy. Stirring process was provided via a mechanical stirrer with teflon shaft whose stirring speed can be adjustable between the 0-2000 rpm.

500 ml of $Fe^{'1+}$ solution was used for each parameters. To prevent of hydrolysis of Fe ions, pH value of the solution was kept constant (pH=1.0) by adding HCl.

The experiments were carried continuously. In the experiments to investigate the effect of temperature, a denser system was used to prevent evaporation. In order to determine the dissolution recovery of Zn, 2 ml of sample solution was taken from leach solution at the end of leaching experiment. After, 2 ml of original solution was added to leach solution. Zn analysis was determined by a Vista AX CCD model ICP-AES apparatus.

In the experimental studies, the effects of stirring speed, Fe^u ion concentration, solid/liquid ratio, temperature and particle size on the dissolution of Zn were investigated.

3 RESULTS AND DISCUSSION

3.1 Effect of stirring speed

The effect of stirring speed on the dissolution of Zn was performed at different stirring speeds and leaching times. The results from these experiments are shown in Fisiurc 2.
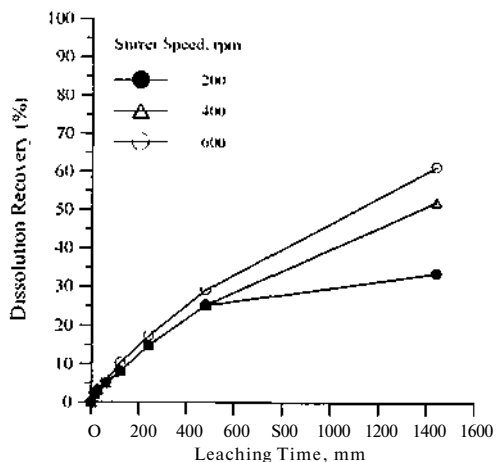
Figure 2 Effect of stirring speed on the dissolution of Zn (Temperature: 50 'C, Fe^+ concentration- 0.25 M. solid/liquid ratio. 10 g/500 ml. particle size: -75+45 pin)

As seen from Figure 2, the dissolution recovery of Zn was not changed in the range of 0-480 minutes for stirring speed values of 200 and 400 rpm. At the stirring speed of 600 rpm, the dissolution recovery of Zn reached to 60% at the end of leaching lime of 1440 minutes. Therefore, stirring speed value of 600 rpm was selected for investigation of the effect of other parameters.

3.2 Effect of Fe * ion concentration

The effect of Fe^+ ion concentration was investigated using solutions of 0, 0.1, 0.25, 0.5 and 1.0 M Fe^+ concentration. HCl (pH=1.0) was the only one used in non-ferrous medium. The results of those are given in Figure 3.
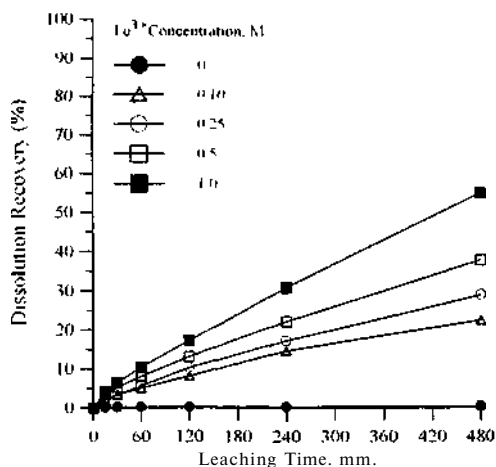

Figure 3 Effect of Fe * ion concentration on the dissolution of Xn (Temperature 50 C. stirring speed' 600 rpm. solid/liquid ratio 10 g/500 nil. panicle size: -75+45 urn)

From Figure 3;

i) The dissolution recovery of Zn increased with increasing Fe^+ ion concentration. At the end of leaching lime of 480 minutes, the dissolution recoveries of Zn for without Fe^u ions and 0.1 M Fe^{3+} ion concentration reached to 0.5% and 22,13%), respectively. In addition, this recovery value increased to -55% for 1.0 M concentration of Fe^{3+} ion.

ii) The dissolution recoveries at the beginning of leaching increased as directly proportional with increasing Fe^+ ion concentration.

iii) For the experiments performed using only HCl, the dissolution recovery of Zn was very slow according to ferric medium. This result is consistent with that of Majima and Awakura (1979).

The highest dissolution recovery of Zn was obtained with 1.0 M concentration of Fe^+ ion. Therefore, this concentration value was used for further investigations.

3.3 Effect of solid/liquid ratio

The effect of solid/liquid ratio were investigated at solid/liquid ratio values of 5/500, 10/500, "20/500, 50/500 and 100/500 g/ml. The obtained results arc shown in Figure 4.
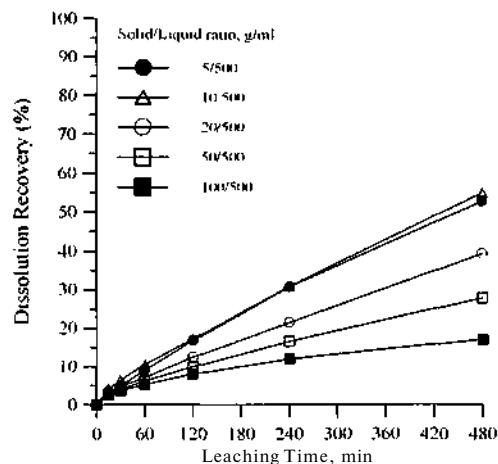

Figure 4. Effect of solid/liquid ratio on the dissolution of Zn (Temperature. 50 "C. staring speed- 600 rpm. Fe^+ ion concentration- I 0 M. panicle size -75+45 urn)

As seen from Figure 4, there was not any important variation on the dissolution recovery of Zn for the solid/liquid ratio values of 5/500 and 10/500 g/ml. Solid/liquid ratio value of 10 g/500 ml was used for investigation of effects of other parameters.

3.4 Effect of temperature

Figure 5 shows the effect of leaching temperature on the dissolution recovery of Zn. It is possible to reach

497

following conclusions from the Figure 5:

i) As leaching temperature increases, the dissolution recovery of Zn increases.

ii) Although the dissolution recovery of Zn increased with increasing temperature at the first 15 minutes of leaching time, the dissolution recovery of Zn remained at almost same values for the temperatures of 80 and 90 °C. For these temperature values, the dissolution recovery increased to -90% at the end of leaching time of 480 minutes.

3.5 Effect of panicle size

The experiments for determination of the effect of particle size on the dissolution of Zn were performed at 80 °C. -212+106,-106 +75. -75 +45, -45 +38 and -38 urn particle size fractions and original concentrate (not sieved to fractions) were used in the leaching studies as shown in Figure 6.

As seen from Figure 6;

i) The dissolution recovery of Zn generally increased with decreasing particle size. At the end of leaching time of 120 minutes, while the dissolution recovery of Zn was 85% for -38 urn particle size, this ratio remained at -52% for -45+38 |im particle size fraction.

ii) The dissolution recoveries obtained for -212+106 and -106+75 urn particle size fractions were very close to each other. In addition, these recovery values gave similar results for the size fraction of -75 +45 and -45 +38 um.

iii) At the end of leaching time of 480 minutes, the dissolution recovery of Zn for original concentrate (-212 urn) was reached to -82%..
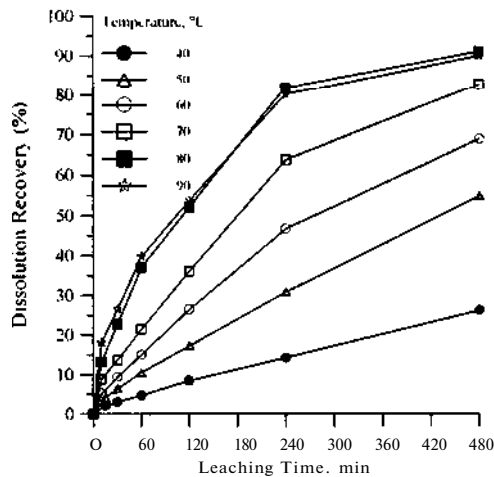

Figure 6. Effect of particle size on the dissolution of Zn (Leaching temperature' SO T. sniring speed 600 rpm. Fe¹'* ion concentration- I 0 M. solid/liquid mho- 10 g/500 ml)

4 CONCLUSIONS

The following conclusions can be drawn from the ferric chloride leaching tests on the concentrates recovered by the flotation method from Sivas-Koyulhisar Cu-Pb-Zn ore.

The dissolution of Zn was not affected by the stirring speed in the range of 200-400 rpm. At the stirring speed of 600 rpm. an increase on the Zn dissolution was observed. On the other hand, the Zn dissolution recovery varied proportionally with ferric ion concentration and temperature, however this recovery varied as inversely proportionally with solid/liquid ratio and particle size.

The optimum leaching conditions were determined as: stirring speed of 600 rpm, Fe^+ concentration of 1.0 M, solid/liquid ratio of 10/500 g/ml and leaching temperature of 80 °C. At the end of leaching time of 480 minutes under the above conditions, the Zn dissolution recoveries increased to 85%.. 89% and 92% for -75+45 urn, -45+38 urn and -38 (am particle size, respectively. Moreover, the Zn dissolution recovery reached to 82%' value for original concentrate (-212 urn).

Figure 5. Effect of temperature on the dissolution of Zn (Stirring speed- 600 rpm. Fe¹⁺ ion concentration: 1.0 M. solid/liquid ratio- 10 s/500 ml. particle size: -75+45 um)
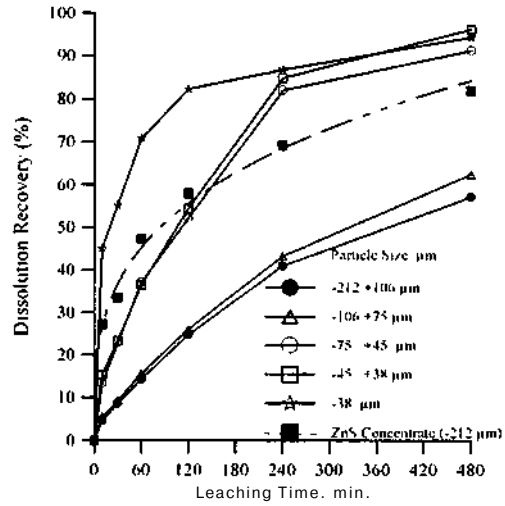
REFERENCES

Bobeck. G.E., and Su. H., 1985. The kinetics of dissolution of sphalerite in ferric chloiide solutions. *Melul. Trimx.* 16B:413-424

Canbazoğlıı. M. and Ûzkol, S.. 1980 Leaching of Çayeli complex sulphide ore by HCl+MgG: solution: recovery of Pb. Zn and CuFeS; concentrates. *Coinple.\ Sulphide Ores Gmfemit e,* The Institution of Mining and Metallurgy. Rome. Italy. 7-11.

498

Çakır. A F . 1976 Harşıt Köprübaşı Kompleks Cu-Pb-Zn-Sb-Ag-Cd Cevher Konsantresinin Fenik Klorür Çözeltisinde Lıçı. I T U Maden Fakültesi

Çopur. M. 2001. Solubility of ZnS concentrate comainin pyıite and chulcopynte in HNO₍ solutions. *Chem. Binchem. Ena. Q-* l-">⟩(4⟩: 181-184.

Demopoulos, G.P. and Baldwin. S.A.. 1999. Stoichiometric and kinetic aspects on the pressure leaching of zinc concentrates. *In Mishit. B. (Eil.). TMS Animal Meeting.* San Diego. 567-583

Dutrizac. .I.E. and MacDonald. R.J.C. 1974. Ferric ion as a leaching medium. *Minerals Sı İ. Eiinnn-* 6. no 2. 59-100

Dutrizac. J.E. and MacDonald. R J.C. 1978. The dissolution of sphalette in ferric chloride solutions. *Metall. Trans..* 9B:543-55I

Ghosh. M.K.. Das. R.P. and Biswas. A.K. 2002. Oxidative ammonia leaching of sphalerite I : Noncatalytic kinetics. *Int. J. Miner Process.* 66:241-254.

Majima. H. and Awakaura. Y.. 1979. Non-oxidative leaching of base metal sulphide ores. *In XIII International Mineral PriKessmu Congress.* Warsaw, preprints of papers volume I Laskowski J. Ed. (Warsaw: Polish Scientific Publishers. 19791.665-689.

Majima. H.. Awakaura. Y.. Misaki. N.. 1981. A kinetic study on nonoxidative dissolution of sphalerite m aqueous hydrochloric acid .solution. *Metall. Trans.* 12B. 645-649.

Mizoguchi. T. and Habashi. F. 1981. The aqueous oxidation of complex sulfide concentrates in hydrochloric acid. *Int. J. Miner process.* 8:177-193.

Parker. E.G.. 1961. Oxidative pressure leaching of zinc concentrate. *CIM Bull.* 74 (51:145-150

Palencia Perez, 1. and Dutrizac. .I.E.. 1991. The effect of the iron content of sphalerite on its rate of dissolution in ferric sulphate and ferric chloride media. *Hvtlrmnetalhtrxv* 26. 211-232.

Rao. K.S.. Anand. S.. Das. R.P. and Ray. H.S. 1992. Kinetics of ammonia leaching of multimetal sulphides. *Miner. Process. E\tr. Metal.* Rev. 10:11-27.

Rath. P.C.. Paramguru. R.K. and Jena. P.K. 1988. Kinetics of dissolution of sulphide minerals in ferric chloride solution. I: dissolution of galena, sphalerite and chalcopyrite. *Trans. Instil Min. Metal.* Sect. C. 97:150-158

Sarveswara Rao. K. and Ray, H.S. 1998. A new look at characterisation and oxidative ammonia leaching behaviour of multimetal sulphides. *Miner. Ena.* 11(11). 1011-1024

Warren. G.W., Kim. S.H. and Henein H. 1987. The effect of chloride ion on the ferric chloride leaching of galena concentrale. *Metall. Trans..* l8B:59-69

Wills. B.A.. 1984. The separation by flotation of copper-lead-zinc sulphides. *Min. Man..* 36-41

Sorption of Nonionic Organic Contaminants by Organo-Zeolite

B.Ersoy & E.Sabah
Afyon Koctılepe University, Engineering Faculty, Afyon, Turkey

U.Mart & M.S.Çelik.
Istanbul Technical University, Mining Faculty, Istanbul, Turkey

ABSTRACT: Adsorption mechanisms of non ionic organic contaminants (NOCs), aniline and nitrobenzene, which are present in wastewater or underground water were investigated with nalural-zeolitc and organo-zeolite (OZ) in both batch and continuous systems. Adsorption capacities of aniline and nitrobenzene onto natural zeolite surface is very low or almost zero for the case of aniline but when the zeolite surface was modified by hexadeeyltrimelhylammonium (HDTMA) its adsorption capacity increased significantly. Partitioning mechanism is responsible for the adsorption of NOCs onto OZ. The effectiveness of partitioning mechanism is directly associated with hydrophobic properties of the NOCs. The adsorption of nitrobenzene on OZ is found to be higher than that of aniline.

I GENERAL INSTRUCTIONS

A natural zeolite mineral, clinoptilolite has three basic properties: ion exchange, adsorption and molecular sieve. These properties are exploited in a wide spectrum such as abatement of air, water and soil pollution (Ames. 1960:1962: Breck, 1974: Mumpton, 1978: Blanchard, 1984;Hlavay el al., 1983; Sirkecioglu et al., 1995). Organo-zeolitc (OZ) or modified zeolite is the modified form of natural zeolite in which zeolite surface is covered with cationic surfactants like HDTMA. OZ is also used for adsorbing non ionic organic contaminants (NOCs) in water e.a., benzene, napthalene. toluene, (Neel, 1992; Li and Bowman, 1998; Li ct al., 2000; Hutlenloch ct al., 2001), inorganic anionic contaminants such as Chromate, selenate (Haggerty and Bowman,1994; Sullivan et al.,1998), various anionic dye molecules (Özdemir et al.. 2002). In addition to modi lied zeolite minerals, a number of modified clay and modified earth minerals have been also used in the adsorption of NOCs (Lee el al., 1989: Smith et al.. 1990; Gitipour al., 1997). The literature results indicate that adsorption capacity of natural zeolite, clay and earth minerals for NOCs is nil or very low, but become remarkable upon modifying them by typical quaternary amines.

Aniline and nitrobenzene, which are aromatic NOCs, are usually generated from petrochemical plants, coal conversion plants and leaks from underground storage tanks (Gitipour et al., 1997). They have harmful effects on the health of human and other lives. The maximum treshold values for aniline and nitrobenzene in water are 2 and 1 ppm, respectively (Budavari, 1989; Lewis and Nowstand, 1991). In the present paper, the adsorption mechanism of aniline and nitrobenzene onto HDTMA-lreated clinoptilolite (OZ) is investigated in both batch and continuous (column) systems with the aim of identifying the mode and extent of their uptake.

2 MATERIALS AND METHODS

The natural adsorbent zeolitic tuff from the Gördes region of Turkey (hereafter will be referred to as zeolite) assaying about 92 percent clinoptilolite was used. The detailed properties of clinoptilolite are given elsewhere (Ersoy and Çelik, 2003). For the modification of zeolite surface, HDTMABr [CH.,(CH$_2$),,N(CH.,).. Br, 99% purity, Sigma] was used. Aniline [C$_f$,H,NH$_2$, 99% purity, Panreae] and nitrobenzene [C$_6$H-;NO:, 99% purity, Merck] were used as NOCs with some properties given in Table 1.

2.1 Preparation of organo-zeolitc for batch tests

Zeolite sample was ground in a ball mill for 1.5 hours and passed through a 100 urn sieve and then used in the preparation of organo-zeolite (OZ) for batch adsorption tests. A sample of 50 g zeolite was placed in a 2 L beaker and 1 L of HDTMABr solution of 2x10$^{'2}$ M was added into the beaker. The pulp was conditioned on a magnetic stirrer for 2 h at 400 rpin at room temperature. The solid material

was rinsed off twice with distilled water after solid-liquid separation by centrifugation (Hetiich Universal 16A Centrifuge). The sample was centrifuged again, and dried in an oven at 100 "C for 2 h. The dry sample was ground in an agate mortar for one minute to produce an organo-zeolite sample of minus 100 um in size.

Table I Some properties of nonionic organic contaminants

Nonionic organic contaminants	Solubility in water at 25 ^{0}C (g /L)	Partitioning coefficient in octanol-water (K_{ow})	Molecular Structure
Anilit	3.6	7.9	NH$_2$
Nitrobenzene	1.9	70.8	

2.2 Adsorption tests in hatch system

First, stock solutions of 1500 mg/L of aniline and nitrobenzene were prepared with distilled water. Aniline and nitrobenzene solutions of 10 mL at different concentrations in the range of 100-1500 mg/ L were removed from their stock solutions and transferred into 50 mL centrifuge tubes containing 0.5 g ol OZ or natural zeolite. They were conditioned on a shaking-table for 2 h at 400 rpm in order to reach an equilibrium, followed by centrifugation at 5500 rpm. The supernatants were analysed by UV-Spectrophotometer (UV-1208 Shimadzu). The adsorbed amount was calculated from the difference between initial and equilibrium concentrations of NOCs in solution.

2.3 Column Tests

In the column tests, zeolite crushed to 1-2 mm particle size was washed with tap water and dried at 100 "C for 4 h. A sample of 300 g dry zeolite was taken and placed into a fiberglas column of 3 cm in diameter and 100 cm in length. The 70 mg/L of HDTMABr solution prepared in distilled water was fed into the column from the top by a peristaltic pump at an average flow rate of 64 mL/min at its natural pH of 7.5-8.5 at room temperature. Samples were collected from the effluent at the bottom of the column at every 0.5 h in the first 2 hours and then in one hour intervals through 25 hours. The samples were analysed for HDTMA using the two phase titration method (Ersoy and Çelik, 2003). The HDTMA-treated zeolite (OZ) was then used for the capture of NOCs.

Aniline or nitrobenzene solution of 30 mg/L NOC was placed into the feeding tank and fed from the top of the column containing the OZ at an average flow rate of 64 mL/min at its natural pH at room temperature. Samples taken from the effluent were analysed by UV-spectropholometer. The breakthrough curves for NOCs/OZ system were constructed by plotting the number of bed volumes (BV) passing through the column versus C/C_0.

$$V = f .t /V \qquad (1)$$

Where f is the flowrate of feed solution (mL/min or mVmin), t is the appearance time (min), V is the fixed bed volume including the voids (m) and C and C,, are the column influent and column effluent concentrations of the substance (mg/L).

3 RESULTS AND DISCUSSION

3.1 Adsorption

Figure 1 shows the adsorption curves of aniline and nitrobenzene, with both natural zeolite (NZ) and organo-zeolite. The adsorption capacity of NZ with aniline remains nil at all equilibrium concentrations, while that of OZ increases almost linearly with nitrobenzene concentration. At 500 mg/L of equilib-

rium aniline concentration the adsorption density reaches 4.5 mg per gram of OZ and at 1000 mg/L it reaches 8 mg per gram of OZ. For nitrobenzene, the adsorption capacity of natural zeolite at 100 mg/L is I mg/g and reaches 2.5 mg/g at 300 mg/L above which it remains constant at this capacity. However, the adsorption capacity of nitrobenzene on OZ rises sharply to high levels of adsorption density with
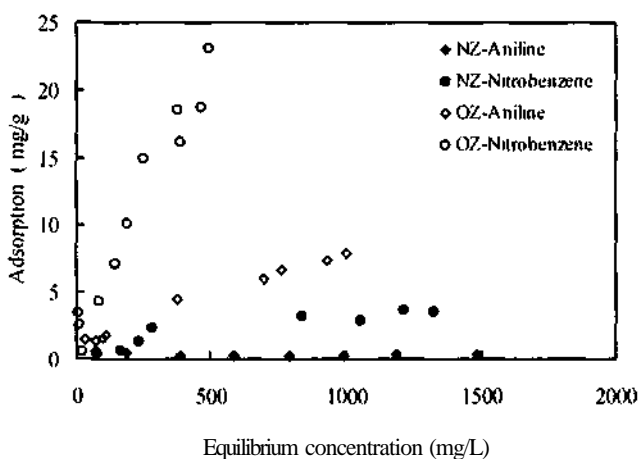

Figure I Adsorption of NOCs. aniline and niirnbenzene. by natural- and organo-zuolite.

increasing the equilibrium concentration of nitrobenzene. It is interesting to note that the adsorption curves of OZ exhibits a linear character indicative of partitioning (non-competitive) adsorption mechanism of NOCs, as will be explained later. Also, it is also evident that the uptake of nitrobenzene on OZ is higher than that of aniline. It is assumed that, this results from the hydrophilic character of NZ surface due to the release of such cations as Ca^{2+}, K^+, Na^+, Mg^{2+} and their subsequent adsorption on its surface or in its crystal .structure. Because, these cations have high hydration energy (Atkins, 1994; Sheng and Boyd, 1998) they adsorb water molecules in aqueous solution. These water molecules bonded to natural zeolite surface prevent the adsorption of hydrophobic NOCs onto the zeolite surface. But nitrobenzene molecules which have more hydrophobic character than aniline (Solubility in water: 19 g L^{-1} for nitrobenzene, 3.6 g L^{-1} for aniline, Table 1) can interact with hydrophobic siloxane (Si-O-Si) groups on the zeolite surface and thus lead to little adsorption of zeolite. It is known from the literature that aromatic NOCs of hydrophobic structure can adsorb onto natural clay minerals by means of their siloxane groups (Jaynes and Boyd, 1991; Stevens et al., 1996).

The linear character of aniline and nitrobenzene adsorption on OZ (see Fig. 1) is in line with the lit-

erature reports on aniline adsorption onto HDTMA-treated zeolite (Li et al., 2000) and this indicates that the adsorption of NOCs occurs through partitioning mechanism. It is reported in the literature that partitioning mechanism operates on the basis of interaction of various NOCs with clay minerals (Li and Bowman, 1998; Hultenloch et al., 2001 ;Lee et al., 1989; Smith et al., 1990; Zhu et al., I997;2000; Jaynes and Vance, 1999; Bowman et al., 2000). The hydrophobic interactions between the NOC and HDTMA molecules of long hydrocarbon chain are controlled mostly by Van der Walls forces. The adsorption mechanism of NOCs onto organo-clays with organic cations of large HC chain is characterized by partitioning mechanism, while that with organic cations of small HC chain (or small aromatic organic cations) is driven by competitive sorption mechanism (Lee et al., 1989; Smith et al., 1990).

Partitioning mechanism is defined as the tendency or preference of a surfactant (or compound) between two different phases (i.e., water and organic) and this preference can be characterised by a term "partitioning coefficient or distribution coefficient" (Perry and Green, 1984; Standal et al., 1999). That is, the weight of fraction of solute in the organic phase (C,,,.s) divided by the weight of fraction of solute in the water phase at equilibrium is called the partitioning coefficient (K) which is dependent

503

on pH. salinity, and ionic strength in the water phase (Standal et al., 1999). As seen in Figure I, there is a steady increase rather than a sharp increase in the uptake of NOCs onto OZ; this is a typical indicator of partitioning (non competitive) sorption mechanism. However, the sorption of nitrobenzene is larger than that of aniline due to the differences in their solubility and partitioning coefficient values given in Table 1. The octanol-walcr partitioning .coefficieni (K_{im}) of nitrobenzene is 70.8 while that of aniline is 7.9 (Zhu et al., 1997; 2000). Also the solubility of nitrobenzene is 1.9 g/L and that of aniline is 3.6 g/L in water at 25 "C. Both the solubility

and partitioning coefficient values indicate that the aniline is more conducive to remain in the water phase instead of organic (HDTMA) phase than nitrobenzene. Therefore, aniline adsorption onto OZ is lower than nitrobenzene.

3.2 Column Teils

In order to see the ability of NOCs to adsorb onto HDTMA-treated zeolite in a continuous (dynamic) system, column tests were performed. It must be noted that the HDTMA-treated zeolite (or organo zeolite)   was
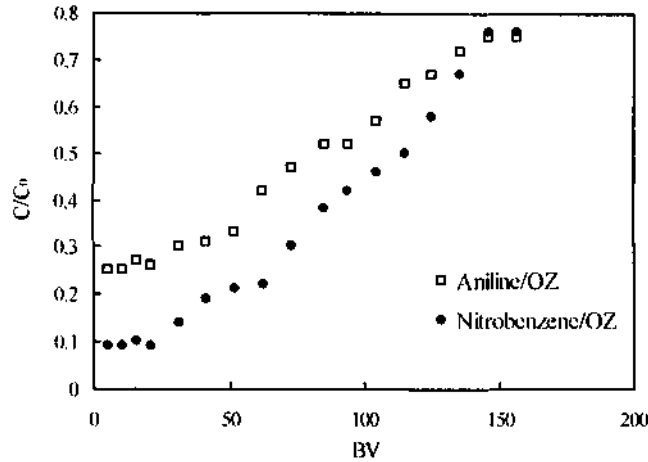

Figure 2 Breakthrough curves for nitrobenzene/OZ and anilinc/OZ systems

prepared by means of passing the HDTMA solution through a fixed bed of natural zeolite column for 27 hours. That is, the OZ (1-2 mm in size) used in the column tests is not the same as the one (-0.1 mm in size) used in the batch tests.

As shown in Figure 2, the breakthrough curves in the column tesis have been constructed for NOCs/HDTMA-lreated zeolite. Unlike batch systems there is no static equilibrium of sorption process and the position of equilibrium m always changes (Harland, 1994). The shape of the breakthrough curve, also the mass transfer of a substance, depends *on* factors such as flow rate, particle diameter of solid phase, feed concentration of the substance in solution, solution pH and température (Ames, I960; Harland. 1994).

Although there are a number of column studies in the literature relevant to the removal of ionic contaminants such as heavy metals, ammonium, radioactive metals from water by zeolite (Ames, I960; Hlavay et al., 1983: Zhao et al., 1998; Mier et al., 2001), only one has been found on the NOCs adsorption onto sorbents modified by surfactants (or organic compounds). This is polyoxyethylatcd nonylphenols adsorption on HDTMA-lreated soil

materials (Hayworth and Burris, 1997) who demonstrated that a NOC surfactant can be removed from water by a surfactant-enhanced sorbent zone. It is clear that the results obtained about the NOC adsorption on OZ is not as good as expected because the break points for both aniline and nitrobenzene occur rather sharp (Figure 2). For both aniline and nitrobenzene, the C/Q, values at 20.9 BV are 0.25 and 0.1, respectively. After the 15 hours (156 BV) of operation the effluent concentrations of aniline and nitrobenzene reach 22.13 and 22.87 mg/L, respectively. Aniline and nitrobenzene adsorption capacity of OZ were calculated approximately using equation (2) as suggested by Ames (1960).

$$r = V_b x C_{(1}/W_b \qquad (2)$$

In which V_h is the volume of effluent solution corresponding to the BV value at "C/C,, = 0.5" point (L), W,, is the weight of the zeolite bed (g) in the column and C(, is the influent concentration of substance (mg/L).

But it must be noted that for influent concentration (C,,) of aniline and nitrobenzene respectively, 22.35 (this value was determined by subtraction of 0.25 C,, from C,,, C,, is 30 mg/L) and 27.17 mg/L

504

(this value was determined by subtraction of 0.10 C,, from e«, Co is 30 mg/L) were used instead of the original feed concentration of NOCs, 30 mg/L . Subsequently, the approximate adsorption capacity of OZ bed for aniline and nitrobenzene were determined as 2.15 and 3.83 mg per gram of OZ, respectively. As seen, the effective amount of nitrobenzene adsorption onto OZ is higher than the aniline according to the differences in the effectiveness of their partitioning mechanism explained above.

İl ıs clear that the differences between (he results obtained from the column tests and those from batch experiments are very significant. That is, under the experimental conditions, the adsorption of NOCs per gram of OZ in a continuous system is much lower than that in the batch system. It is assumed that the main reason for this is that the modification of zeolite surface by HDTMA in column is not made properly. In other words, the required amount of HDTMA to adsorb NOCs in the organic phase at the zeolite surface is not sufficient. In addition, dynamic equilibrium conditions in the column system and static equilibrium conditions in the batch system can affect the adsorption of NOCs onto OZ.

4 CONCLUSIONS

Adsorption capacity of natural zeolite is nil for aniline and 2.5 mg/g for nitrobenzene. When zeolite surface was modified by organic cation (HDTMA), its adsorption capacity for aniline and nitrobenzene reached 4.5 and 23 mg/g at 500 mg/L of NOC equilibrium concentration, respectively

The column studies reveal that the adsorption of aniline and nitrobenzene onto OZ under the present study was determined as 2.15 and 3.87 mg per gram of OZ.

Partitioning mechanism is responsible for NOC adsorption onto organo-zeolitc but the effectiveness of this mechanism largely depends on the hydrophobic properties of NOC molecules (i.e., its solubility in water, partitioning coefficient in oclanol-water phases) and also the manner in which sorption tests (batch or continuous test methods) are conducted.

REFERENCES

Ames t. L I960. The catuin sieve properties of clinoplilolite. *Am.Min.* 45. 689-700

Ames L.L. 1962 Elfecl of hase cation on the cesium kinetics otchnopttlohte. *Am. Min.Al.* 1310-1316.

Atkins A 1994. *Phvsiial ı heniisrrv* (fifth edition). Oxford Unıveısıty Pi ess. pp.55-90

Blanchaid G. 1984. Maunaye M. and Martın G.. Removal hem j metals from waters by means ol natural zeolites. *Wal. Res..* 18.110.12. 1501-1507.

Bowman R.S.. Sullivan E.J. and Li 7,. 2000. Uptake of cations, anions, and nonpolar organic molecules by suilactant-modificd clinoplilohle-rich luff. In: *Natural Zeolites Foi Third Millenium.* ColellaC. And Mumpton F.A. (eels.) De Frede Edılore. Napoli, pp 287-297.

Breck D. W. 1974. *Zeolite Molecular Sieves.* John Wiley. New York. pp. I-19.

Budavan S. (editor) 1989 *The Merck liulex,* Merck co. Inc.. USA

Ersoy. B. and Çelik. M.S. 2003. effect of hydrocaibon chain lenglli on adsorption of canonic surfactants onto clinoptilohte. *Claws ami Clav Min..* 51.2. 173-181.

Gitıpour S.. Bowers M.T. Bodocsi A. 1997. The use of modilied bentonite for removal of aromatic organics from contaminated soil .*1. Colloid ami Inlnfaie Ai..196.* 191-198.

Haggerty G.M. and Bowman R.S. 1994. Sorption of eliminate and other inorganic anions by oigano-zeolite *Environ. Sei* 7V<7m»/.28.452-458.

Harland CF.. 1994. *Ion Enhance Theory ami Practise* (second edition). The Royal Society of Chemisliy. Cambridge, pp. I-18.

Hayworth J.S and Burns D.R. 1997. Noniomc surfactant-enhanced solubilization and recovery of organic contaminants ft om within cntionic surfaclanl-enhanced sorbent zones. 1. experiments. *Environ. Sti. Teihnol.* 31. 1277-1283.

Hlavay J.. Vigh G.. Olusu V. and Inczedy, J. 1983. Ammonia and iron removal from drinking watei with clinoplilolite tuff. *Zehntes. T..* 188-190(1.

Huttenlocli P.. Roehl K. A. and Czurda K. 2001. Sorption of nonpolar aromatic contaminants by chlorosilane surface modified natural materials. *Environ. Set. Techno!..* 35. 4260-4264.

Jaynes W.F. and Boyd S.A. l99I.Hydrophobicity of siloxane sui faces m smectites as revealed by aromatic hydrocarbon adsorption from waler. *C7«v.v and Clav Minerals.* 39, 428-4.36

Jaynes W.F. and Vance G.F. 1999.Sorption of benzene, toluene, elhylbenzene. and xylene (BTEX) compounds by hectorne clays exchanged with aromatic organic cations. *Clavs and Clav Minerals.* 47. 358-365.

I.ee J.F.. Cram J.R. and Boyd S.A. 1989.Enhanced retention of organic contaminants by soil exchanged with organic cations. *Environ. Sı ı Tcclinol.23.*1365-1372.

l-ewi.s R.,l. and Nowstand R. (ed.s) 1991. *Hazaiilom Cliemital Desk Reference,* New Yoik.

Li Z... Burt T. and Bowman R.S. 2000. Sorption of lomzable organic solutes by suil'actant-modified zeolite. *Environ. Sei. Tecilimi.,* 34. 3756-.3760.

Li Z. and Bowman R.S. 1998 Sorption of perchloroethylene by surfactant-modified zeolite as controlled by suifactant •loading. *Environ. S, i.* 7V<7ı»o/,32.2278-2282.

Mier M.C.. Callejas R.L.. Gehr R.. Cisneros B.E.J, and Alvarez P.I..I 2001. Heavy metal removal with mcxican chnoptilohle multi-component ionic exchange. *Wat Res..* 35. 373-378.

Mumpton FA. 1995. Natural zeolites: a new industrial mineral commodity. In: *Natural Zeolites : iOnurence.Properties and Use).* Sand L.B. and Mumpton F.A. (eds). pp. l-27.

Pergamon Press.Oxford (1978) Sirkecıoğlıı A. Altav Y. anıl Erdem-Şenatalar A . Adsorption of H;S and SO: on Bigadiç Clinoplilolile. *SV/>. Sd. and Teılı..M):* 2447-2762.

Neel D. l992.Quantificalion of BTX sorption to siirface-alleied zeolites. Hydrology Open File Report No:H92-2. New Mexico Institute Of Mining and Technology.

Özdemir O. Bentli 1, Ersoy B . and Sabah fi. 2002 Utilization of poıous minerals in the abatement of dyes in textile wastewaters. In: *liileriintiimal Confèrente Environmental Ptohlems Of The Mediterranean Region.* Gokcekus H.(ed.).I2-I5 April. Neu Nicosia- Northern Cyprus.

Perry R.H and Green D.W. (eds.) 1984. Perry's Chemical Kngineers'Handbook. McGraw-Hill Inc. NewYork.

Sheng G and Boyd S.A 1998. Relation of water and neutral organic compounds in the uuerlayers of mixed Ca/tnmethylphenylammoniiim-smectites. *Claws and Clav Mineral*. Ab.* 10-17.

Smith .1 A. Jaft'e P.R. and Chiou C.T. 1990. Effect ot ten quaternary ammonium cations on tetrachloromethane sorption to clay fiom water. *Enviion. Sei. Teclmol..* 24. 1167-1172.

Stevens J.J.. Anderson S..I. and Boyd S.A 1996. FTIR study of competitive water-arene sorption on tetramethylammoniuni- and triinelhylammonium-montmonllonites. *Claxs and Clav Minerals.* 44. 88-95.

Standai S.H.. Blokhus A.M.. Haavik J.. Skauge A. and Barth T. 1999. Partition coefficients and interfacial activity for polar components in oil/water model systems. *J.Colloid andlnterfmeSci..* 212. .13-41.

Sullivan K.J.. Hunter D.B. and Bowman R.S. 1998. Fourier transform rainan spectroscopy of sorbed HDTMA and the mechanism of Chromate soıption to surfactant-modified clinoptilolite. *Environ. Si i. Teclmol..* 32 :1948-1955.

Zhao D.. Cleare K.. Oliver C. Ingram C. Cook D.. Szostak R. and Kevan L. 1998. Characteristics of the synthetic heulandue-clmoptilolite family of zeolites . *Mk rnporous and Mexoporous Materials.* 2 1. 371 -379.

Zhu L.. Li Y. and Zhang J.. 1997. Sorption of organobentoniles to some organic pollutants in water. Environ. *Sei. Techiiol..* 31.1407-1410.

Zhu L. Chen B. and Slien X. 2000. Sorption of phenol, p-mlrophenol. and am h ne to dual-cation organobentonites from water. *Em iron. Sei. Teclmol..* 34. 468-475.

506

Briquetting of Washed Coal Fines of Merzifon-Yeni Çeltek Coal Enterprise

G. Özbayoğlu, Ü. Atalay & C. Hiçyılmaz
Mining Engineering Department, Middle East Technical University, 06531 Ankara, Turkey

ABSTRACT: In this study, the influences of some of the most important parameters on the strength of briquettes were studied. The preliminary laboratory studies showed that lime and molasses were the optimum binder combination considering not only the mechanical properties of briquettes but also the operational cost and their availability. Briquetting pressure, amount of milk of lime and molasses, blending time of briquetting charge and drving time were the parameters tested through the research.The best results were obtained with 84.21 kg / cm' briquetting pressure, 5.8% molasses, 5.8% milk of lime, and drying at 50°C for 3 days. The briquettes produced with these values of parameters had more than 67 kg crushing load.The pilot plant scale briquettes production were done at the Mineral Research and Exploration Institute (MTA). A Flowsheet was designed for 10-15 tph capacity briquetting plant.

I INTRODUCTION

Modern coal mining with mine mechanization and advanced coal cleaning techniques generate appreciable amount of fine coal materials that must be processed and handled.

Furthermore, due to the very strict environmental regulations the fine coal production will increase in future, since finer grinding will be required to liberate finely disseminated ash and sulfur impurities from coal. In addition, low quality coals with high moisture content also show a tendency to disintegrate when they are dried. The loading, transportation and unloading processes contribute to the formation of fines. All these fines not only cause serious handling problems such as losses with wind in transportation, spontaneous combustion & freezing but also cause incomplete burning in the furnace. Therefore, the fine coals arc agglomerated to minimize these problems.

Briquetting is the most appreciable and universally accepted method to prevent these serious problems. Briquetting is made practically in every country in which coal is mined. Investigations are being carried out in these countries to check the suitability of domestic coals for briquetting.

The aim of this study is briquetting of -3.36+0.5 mm (-6+28 mesh) washed coal fines of Merzifon-Yeni Çeltek Coal Enterprise. Although the company has no marketing problems with +3.36 mm product, -3.36 mm product can not be sold easily due to its fine size and high sulfur content. The research focused on both to enlarge the size and to reduce the sulfur emission by laboratory and pilot plant test works (Özbayoğlu et. al.. 2002).

2 MATERIALS AND METHODS

Almost 0.5 ton of -3.36 +0.5 mm washed coal sample was used through out the research which was produced by Merzifon-Ycni Çeltek Coal Enterprises. The proximate and particle size analysis of sample are given in Table I and 2 respectively.

Table I. Proximate analysis of -3.36+0.5 mm washed coal fines.

Analysis	Original	Air Dried
Moisture *(7t)*	8.33	–
Inherent Moisture	2.59	2.83
Ash C7r)	25.96	28.32
Volatile Matter *(%)*	.11.91	34.81
Fixed Carbon *CX)*	33.80	36.87
Total Sulfur *(%)*	2.03	2.21
Combustible Sulfur ('*)	1.74	1.90
Pyrıtıc Sulfur (%)	0 54	0.59
Lower Calorific Value (kcal/kg)	4461	4921
Upper Calorific Value (kcal/kj>)	4714	5142

The laboratory scale briquettes were made in cylindrical shape mould having 55 mm in diameter. They were pressesed with an external pressures varying from 63.15 to 105.26 kg/cm². Tinius Olsen Stan-

dard Super L-typc hydraulic press having 200 tons capacity was used throughout the research. The briquettes were dried at 50°C in an oven.

Table 2. Size Analysis of -3.36+0.S mm washed coal fines

Size (mm)	Weight C/r)	Cum. Weisiln <%)	Pyrilie Sulfur C3Î)	Pyrilie Sulfur Dısıιibulum (%)
- U6+1 68	37.40	37.40	0 89	56.60
-1 68+0 595	41.W	78.70	0 49	34.4
-0.595+0 5	21.30	100.00	0.25	9.0
Totril	100.00		0.588	

In pilot-scale briquctting tests. SKB trade name roll press having 630 mm roll diameter & 100 mm roll width was used. The rotational speed of rolls were 2 rpm. The produced briquettes have 45 mm length, 31 mm width and 25 mm thickness.

2. / Quality Control of Briquettes

The quality control of briquettes was done by means of compressive strength, tumbling and drop tests. The compressive strength tests were performed by compressing the briquette between two movable plates. The amount of load applied to the briquette, just before the initial crack occurs, was recorded as crushing load (kg) of the briquette. The crushing load in radial direction can be used to express the induced tensile strength of a cylindrical briquette (Ataman, 1982).

$$\sigma = \frac{2P}{DL}$$

where, CT = Tensile Strength (kg/cm")
P = Crushing Load (kg)
D = Diameter of briquette (cm)
L = Length of briquette (cm)

Since "D" and "L" are constant, the crushing load was used to compare the quality of briquettes instead of tensile strength.

It is required to obtain 80 kg crushing load for first class coal briquettes and 60 kg crushing load for 2"'i class coal briquettes (TS I2055. 1996)

Tumbling tests were performed at 20◁▷x30 cm drum containing 4 lifters of 2 cm wide. 500 grams of briquette sample were placed into the drum and rotated two minutes with 30 rpm. The tested material was then screened through 3 mm and percentage of screen oversize material was expressed as Tumbling Index. Tumbling index is 75% for l" class coal briquettes and 65% for 2"J class coal briquettes (TS 12055,1996)

The drop test was carried out to assess the ability of the briquettes to withstand the falls at the transfer points during handling and transportation. The briquettes were allowed to drop from 120 cm height on a concrete platform. The number of drops, before the initiation of any crack was the measure of this test.

The waler resistance test were not necessary since the briquettes will be marketed in nylon bags.

3 RESULTS AND DISCUSSIONS

.?. / Laboratory Briquetting Tests

In the laboratory hriquetting tests, the effects of amount of milk of lime & molasses, briquetting pressure, blending time for briquette charge and drying time of briquettes at 50°C were tested.

Preliminary briquetting showed that the coal briquettes produced without binder have not sufficient crushing load. 7.5 to 10 kg crushing loads were obtained from the coal briquettes that made with its original moisture (= 10%) under 126.31 to 168.42 kg/cm" briquetting pressure.

Coal briquettes produced with lime (CaO) have not also sufficient resistance to crushing load. Figure I shows the effect of lime on crushing load of briquettes.
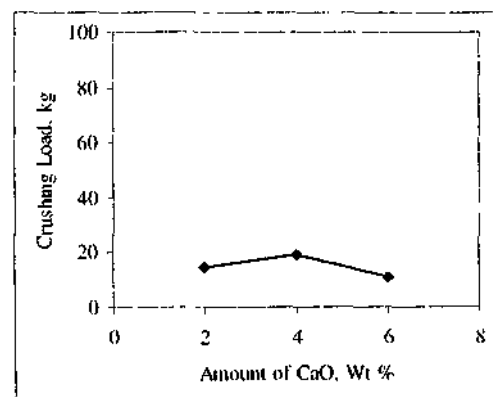

Figure I. The effect of lime on crushing load of briquettes (8/◇ water: 84.21 kg/em'" briquetting pressure; drying at 50°C for 2 days).

Preliminary tests showed that briquctting only with its original moisture and lime is not sufficient to produce marketable coal briquettes. Therefore it was decided to use binder at the following tests. Molasses is one of the famous and versatile binder considering its availability, cheapness and effectiveness in binding. So, molasses was selected as the binder for the following tests.

In order to investigate the effect of briquetting pressure to crushing load of briquettes, briquetting pressure was varied from 63.15 kg/cm" to 105.26 kg/cnr with 5.8% milk of lime and 5.8% molasses. The briquettes were dried at 50°C for 3 days. The re-

508

suits which are shown in Figure 2 indicated that all briquettes have satisfied the crushing load requirement.
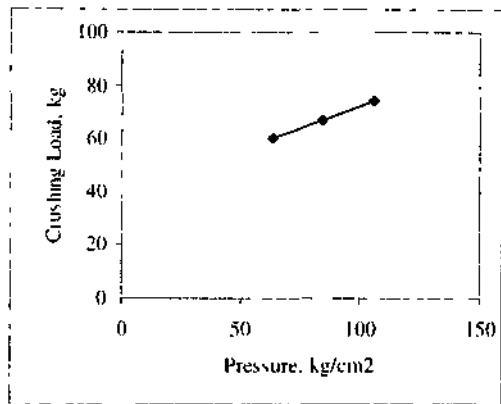

Figure 2 Effect ot briquetting pressuie on crushing load ot briquettes.

Milk of lime and molasses are an important combination in the briquetting of coal industry. Due to the exothermic reaction between the binding agents, briquettes became hardened without external heating. In this set of experiment, amount of molasses was changed when the milk of lime was 5.8%, briqueuing pressure 84.21 kg/cm" and drying at 50°C for 3 days. The results were given in Figure 3.
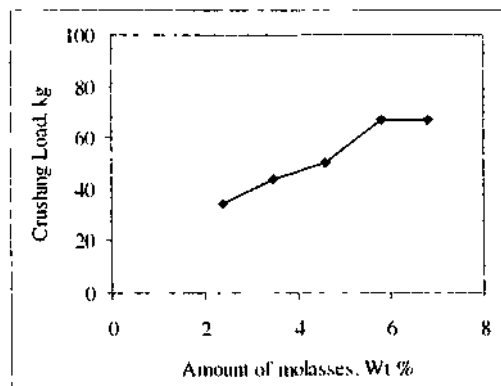

Figure 3 Ettect of amount of molasses on ciushing load ol bnquettes.

As it is seen from Figure 3 amount of molasses has positive elfect on crushing load of briquettes. However high amount of molasses do not only increase the cost of briquettes but also increase moisture which has negative effect on crushing load. So it was determined that 5.8% molasses was the optimum amount.

The effect of milk of lime was investigated herealter. The results of series of experiments can be observed in Figure 4. which shows the positive effect of milk of lime on crushing load of briquettes. High amount of milk of lime will also decrease the $S0_2$ cmmission to atmosphere by the formation of $CaSO_4$ as the result of reaction of sulfur with lime. However high amount of milk of lime will also increase the content of inorganics in coal briquettes which will be resulted as ash after combustion of it. Therefore 5.8% milk of lime was accepted as optimum value which satisfy the specifications of TS 12055.
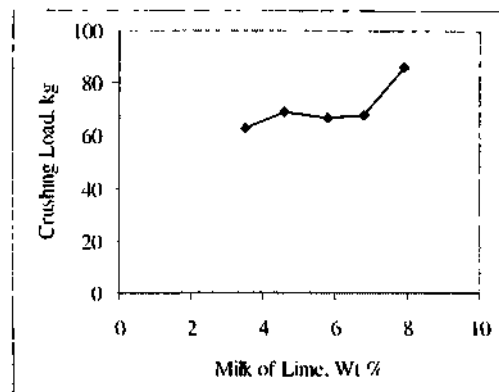

Figure 4. Effect of amount of milk of lime on crushing load ol briquettes (5.8'/ molasses; 84.2lkg/cm2 briquetting pressure; drying at 50"C for 3 days).

Blending tunc is not only important to obtain an homogeneous mixture but also important from the view of reaction kinetics of lime and molasses. It was tested with a set of experiments changing from 3 lo 12 minutes. The results are shown in Figure 5 which can be concluded as "more blending time, more crushing load".
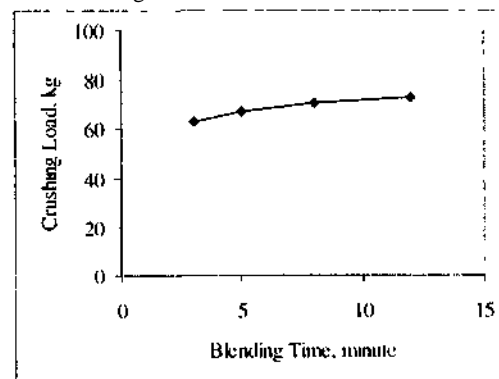

Figure 5 Effect of blending time on crushing load of briquettes (5.8% molasses. 5 8% milk of lime; 84.21 kg/crrr briquetting piessure. drying at 50"C foi 3 days! .

Finally effect of drying time on crushing load of briquettes was tested. The briquettes produced at optimum conditions (5.8% molasses, 5.8% milk of lime.

509

H4.2I kg/cm" briquetting pressure) were dried at 50°C for different periods. As shown from Figure 6, drying time has positive effect on crushing load of briquettes.
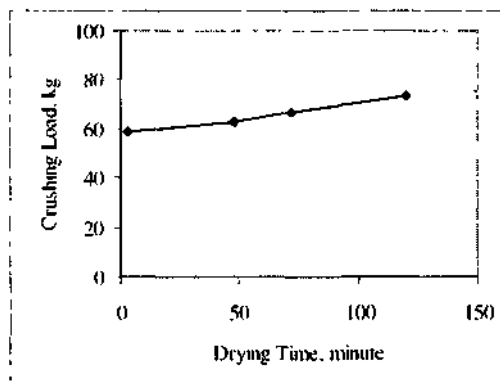

Figure 6. Effect of drying time on crushing load of briquettes

J. 2 Pilot Scale Briquetting Tests

In the pilot-scale operation, coal, milk of lime and molasses were mixed in an automatic cement mixer. The mixture was fed to the roll press where briquettes were produced. Optimum conditions found during laboratory investigations were applied for the preparation of briquette charge (i.e. 5.8% molasses, 5.8% milk of lime and original moisture of coal drying at 50°C for 3 days).

However briquetting pressure could not be adjusted since the roll press used was not operating well. Moreover, feeding mechanism was out of order and moulds on the rolls was not matching each other. Feeding was tried to be done manually.

All these improper conditions prevented the production of briquettes continuously and in desired shape. The average crushing load of briquettes were found as 32 kg. However droping test and tumbling test gave satisfied results where briquettes crushed after 6 drops and pieces of briquettes were all coarser than 3 mm in drop test. Tumbling index was $92^t/r$.

Finally a flowsheet was developed for the briquetting plant with 10-15 tph capacity. Since the moisture of coal was around 10-11 %, thermal drying was not projected in flowsheet. Figure 7 and Table 3 shows the developed flowsheet for Yeniçeltek briquetting plant.

4 CONCLUSIONS

1. Laboratory briquetting tests demonstrated that Merzifon-Yeni Çellek washed coal fines (-3.36+0.5 mm) can be successfully briquetted with binders of milk of lime and molasses. The briquettes are all satisfy the specifications of TS 12055 standards.
2. Milk of lime and molasses amount, briquetting pressure, blending lime and drying time at 50°C have all positive effect on crushing load of briquettes.
3. Although pilot plant briquetting resulted low crushing load due to improper conditions drop and tumbling tests were all satisfactory.
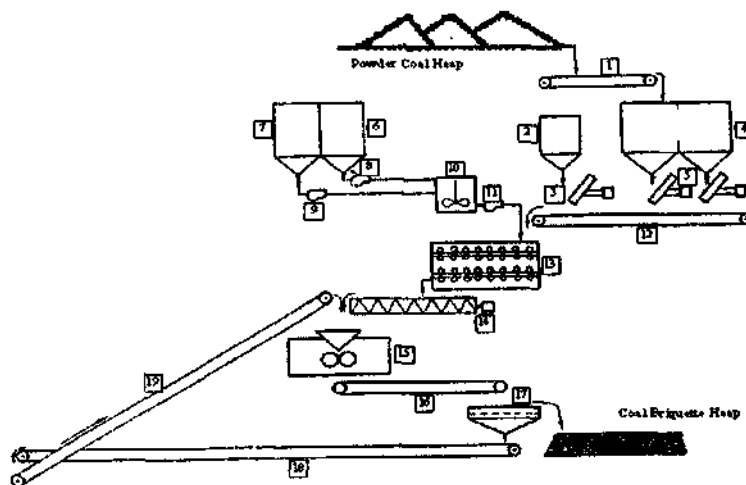

Figure 7. Flowsheet of Yeniçeltek Coal Briquetting Plant (for coal containing 10% moisture).

510

Table 3. List of equipment in the plant.

Unit Number	Naine of Equipment
1	Banı Konvevör
2	Lime Bin
.1	Vibrating Feeder
4	Dry Powder Coal Bins
S	Vibrating Feeders
6	Melas Tankı
7	Su Tankı
X	Melas Pompası
9	Water Pump
10	Isıtmalı Karıştırma Tankı
II	Pump
12	Bant Konvevör
13	İki Şaftlı Karıştırıcı
14	Screw Conveyor
1?	Briqueiting Machine (Feeder Included)
16	Bant Konveydr
17	Vibrating Screen
IX	Bant Konvevör
19	Bant Konvevör

REFERENCES

Ataman T.. (1982). Intioduction to Rock Mechanics. Middle East Technical University. Faculty of Engineering Publication. No: 69. (Turkish), pp. 18-20. Ankara.

Ozbayoğlu, G.. Atalay. Ü.. Hıçyılmaz. C . 2002. Briquetling of washed fine coals of Merzifon Yeni Çeltek Co.. METU. Applied Research No: 02.03.05.2.00.02. 20 pages (Turkish). Ankara.

TS I2055. (1996). Coal Biiquettes-For Household Heating. 19 pages.

Utilisation of Granite Sawing Mud and Borax Tailings as A Ceramic Material

M.S.Başpınar
Technical Education Faculty. . Afyon. Turkey

A.Kartal, A.Evcin & S.Anasız
Ceramic Engineering Department. Kocatepe University. Afyon, Turkey

ÖZET: Bu çalışmanın temel amacı: granit kesimi esnasında işlem atığı olarak ortaya çıkan granit kesim çamurunu karakterize etmek, sintcrlenme davranışını belirleyerek seramik amaçlı kullanılabilirliğini incelemektir. Bu amaçla yine bir işlem atığı olan boraks zenginleştirme tesisi atıkları (DSM elek üstü atığı) farklı oranlarda granit atığına ilave edilerek, farklı sıcaklıklarda sinterleine deneyleri yapılmıştır. Deneyler sonunda, granitin teorik yoğunluğuna yaklaşan yoğunlukta hatasız malzemeler üretilmiştir. H25°C'de pişirilen numunelerin iyi bir şekilde sinterlendiği. su emme oranlarının %3'iin altında, eğme mukavemetlerinin 27 MPa üstünde olduğu tespit edilmiştir.

ABSTRACT: The main objective of this study is to characterize the granite sawing mud and investigate the possible usage as a ceramic material. For (his puipose, different amounts ol" Borax concentrator plant tailings (DSM sieve disposal) were added to the granite mud and sintering study was conducted at different temperatures. As a result, defect free dense materials were produced at nearly theoretical density of natural granite. It was observed that, samples were succesfully sintered at I I25°C. Water absorption was found to be less than 3% and fiexural strength was higher than 27 MPa.

I INTRODUCTION

Granite is a natural slone which contains Quartz and Feldspar as main mineral phases and illite, mica, muskovite, ilmenite, apatite, biotite as accessory phases. Due to its good hardness and low water absorbtion. it is used for covering floors and walls of the buildings. Cutting of granite generates important amount of waste material. However, this waste material not only contains granite fines but also contains metallic iron and lime which arc used for cutting process of granite. Resulting cutting residue is called as sawing mud which is filter pressed and dischaiged from the cutting system. There are only a few studies about the utilisation of the granite sawing mud. Most of these studies are related with the vitrification of the granite mud with other industrial wastes in order to immobilize the ha/ardous components in these wastes (Pelino, 2000 and Pisciclla, 2001). Fritting and crystallization of glass-ceramic glaze was studied (Romero, 2002). Granite sawing mud was used in porcelanized stoneware composition as a replacement of feldspar (Hernandez, 2001). Injection molding of granite powders were studied for production of wear parts

such as thread-guide (Felix, 2001). Granite fine from the quary was used in self-compacting concrete applications as a filler material (Ho, 2002). Granite sludges were used in brick and floor tile type ceramic formulations (Ferreira, 2002) However, there is still very limitted knowledge about the utilization of granite sawing mud.

Every year almost 150.000 tons of boron containing fine clay tailings are produced in Etibor Kırka Borax Company's Concentrator Plant in Turkey (Ediz, 2002). Évaluation of this clay and carbonate containing boron tailings are classified into three group; (i) utilization in ceramic and construction industry. (ıi) recovery of the boron from tailings and (iii) enviromentally safe disposal of tailings (Bentli, 2002).

The main objective of the research is investigated the properties of granite mud and the sintering behaviour of the samples which are produced from granite mud and borax tailings.

2 MATERIAL AND METHOD

In order to know the properties of the materials, characterization study was conducted on the as

received granite mud. Chemical and mineralogical structure of granite mud was determined. Three series of samples were prepared with adding 0 %, 5 % and 10 % boron tailing to the granite mud. The dried granite mud and the boron tailings were wet mixed in porcelain ball mill and homogenized for 6 hours. After drying, powder mixture was sieved from 250 (im for granulation. Prismatic samples, which have 55 xlO x 8 mm (length, height, width) in size, were shaped at 40 bar pressing pressure with 10% water content. Shaped samples were dried at laboratory conditions for 1 day. then oven dried at 105°C. Then, dried samples were fired at 1100"C, I125"C, 1150 and I175"C temperatures for 30 minutes.

The fired samples were tested for the determination of bulk density, water absorbtion and appereant porosity by water absorption test. Firing shrinkage amounts of the samples were measured. Flexural strength of the fired samples was measured with 40 mm span length. Table 1. shows the chemical analysis of borax tailing and granite mud. Mineralogical composition of the borax tailings are given below (Emrullahoğlu. 2002):

Dolomite	CaMg (CO,h
Montmorillonite	NaCaMgFeSiAIOOH-nH$_2$0
Calsite	CaCO,
Ortochlase	KAIShOs
Sanidin	(Na,K)AlSi,Os
Sodyum Borate	Na$_2$B$_4$0$_7$

Table I. Chemical analysis of Borax tailing (Ediz. 2002) and granite mud.

Oxide	Borax tailing	Granite mud
SiO	15,83	62,44
Al-.0,	1,06	13,69
CaO	20,66	3,16
MgO	19,84	032
K,0	0,63	3,99
Na.O	2,58	3,29
Fe^Ch	0.24	12,51
B^Ch	3,99	—
L.O.I	34,75	0,1

Particle size distribution is given in Table 2.

Table 2. Particle size distribution of granite mud.

Particle size	wt/(
< l63 м m	100 %
<22um	75%
< 7 uni	50 %
< 2 um	25 %

According to the XRD analysis (Fig. I) it was found that: granite sawing mud contains quartz, chlinochlore, muskovite, ortochlase, albite and kalsite as a main mineral phases.
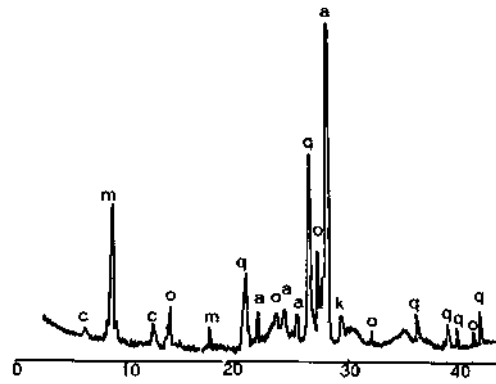

Figure 1. Mineral structure of the granite sawing dust. (c:chlinochlore, m:muskovite, o:ortochlase, q:quartz. a:albite. k:kalsite).

3 RESULTS AND DISCUSSION

Samples which were produced with only the granite mud (G) could be fired without any problem up to 1175°C. However, melting and deformation were observed when borax tailing were added to the granite mud and fired at 1175°C. Decrease in the flexural strengths was observed after 1125°C for the granite mud samples (Fig 2.). 5% borax tailings containing samples (G+5%BA) were fired without any problem up to II50°C but sudden melting behavior was observed at I175°C. 10 % borax tailings containing samples (G+10%BA) were showed a sudden decrease in strength at 1125°C as similar to samples without tailing addition. According to these results, it was concluded that I125°C temperature is the optimal firing temperature for these samples. Because, technical properties of the samples were decreased at sintering temperatures higher than 1125^, such as flexural strength. At higher temperatures bloating of the samples starts and controlling the firing becomes difficult. Increase in the fluxing oxide content with the addition of borax tailings is the main reason for

the bloatings.

514
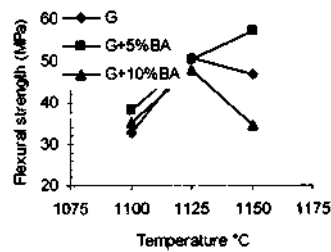
Figure 2. Change in the flexural strengths with firing temperature.

Firing shrinkage Al (%), water absoption (wa %), apperant porosity (Ap.p. %) and bulk density ($D_{h,,}$n) of the samples which were fired at I I25°C are given in Table 3.

Firing shrinkage, flexural strength and bulk density values depend on the amount of the boron tailing addition. They were higher at 5% tailings addition level, but decreased with 10% tailing. Water absorption values were substantially lowered upon tailings addition (Table 3).

Table 3. Some properties of the samples which were fired at 1125"C. (wa: water absorbtion. Ap.p.: apurant porosity. Dhuii; bulk density)

	G	G+5%BA	G+109ÎBA
C/t) Firing Shrinkage	9,1	9,6	9,0
wa°/c	0.98	0,1	0,08
Ap.p. %	2.4	0,21	0.18
Dlnilk (gr/cm)	2,35	2,39	2,31

Low level of boron tailing addition possitively affect the sintering behaviour, but after a certain level properties detoriate. High amount of glassy phase formed in samples which contained 10% boron tailings and surface was closed. As a result, the gas which remains in the sample caused bloating. By this way, firing shrinkage and flexural strength were reduced. In other word, this makes it possible to choose the optimum firing temperature depending on the addition ratio. This effect can be seen clearly in Table 3. Sample G+10%BA has lower water absorption than the other groups but has also lower bulk density.

A metallic iron impurity which originated from the cutting process is found to have no negative effect on the properties. But, combined effect of fine granite powders and magnetic effect of metallic iron impurities creates agglomeration of the powders. This makes the processing steps difficult. Structural heterogenity was observed between the metallic iron and ceramic matrix interphase according to the mierostruclural investigations. This was mainly due to the different thermal expansion coefficients of the metallic iron and matrix material.

4 CONCLUSIONS

In this study, effect of different amount of boron tailing addition on the properties of granite sawing mud was determined under different firing temperatures. Granite sawing mud was easily shaped by pressing with the addition of boron tailing (DSM sieve disposal). 5 ʿk addition was found to be optimal to help the pressing and supply enough flux material for the enhance densificalion. Further

addition caused bloating of the samples. Properties were negatively affected at higher firing temperatures. It was determined that, samples can be succesfully sintered al II25°C. Water absorption was found to be less than 3% and flexural strength was higher than 27 MPa.

Samples which contain boron tailing additions were sintered without any problem at a relatively low firing temperature of 1125°C. Choosing the correct amount of the additon has great importance, otherwise bloating of the samples was observed and especially strength values were adversely affected. As a result of this study, it is assumed that, addition of these materials to the tile formulations will cause an improvement on the properties. Dark color formation after sintering due to the impurities which comes from the accessory minerals of granite and effect of metallic iron impurities on the glaze quality should be taken into consideration. As a result, granite sawing mud can be considered as a potential candidate material for the tile industry and the next investigations will be focused on this direction.

REFERENCES

Benth. I., Özdemir. O . Çelik. M S.. Edız, N., Boron, 2002. Tailings and Evaluation Strategies. *Prut: ı>\ the l" Im. BORON S\mn..* p.250-258.

Edız. N . Yurdakul, H . Issı, A . 2002. Investigation on the Usability of Etibor Kırka Borax Sieve Disposal for Fill Material of Wall Square. *Prut: of lite I" Int. BORON Sxmp..* p.246-249.

Emrullahoglu. O F.. Emmllahoğlu, C B . 2002. Effect of Etibor Kırka Borax Tailing Addition on the Properties of Floor Tile Body. *Proc. tit the I" Int. BORONSvmp.,* p.213-218.

Felix. C. Blazdel. F.. Nogueıra. Q., 2001. Production of Complex Parts by Low-Pressure Injection Molding of Granite Powders. /" *mn^ressti Brasileirti tie Ennenlutria tie Ftibretictw.* 2-4 April 2001. Parana- Brasil, p.201-209.

Feueira. F.. Torres. C. Silva. S.. Labrincha, A.. 2003. Recycling of Granne Sludges in Brick Type and Flooi Tile Type Ceramic. *Fuiiimlutinns. Eumcertmi News,* no. 14. . p. I-10.

Hernandez. C. Rincon. .1.. 2001. New Porcelanized Stoneware Materials Obtained by Recycling MSW Incinerate» Fly Ash and Grainle Sawing Residues *Cemime International.* • vol:27. p 713-720.

Ho. S . Sheinn. M.. Tanı. T, 2002. The Use of Quarry Dust Foi SCC Applications. *Cement ami Cnirele Research,* vol.32, p 505-51 I

Pelıno. M., 2000. Recycling of Zmc-Hydromelallurgy Wasies in Glass and Glass Ceramic Materials. *Wane Management.* vol .20.. p.56l-56H.

Pisciella. P.. Cnsucci. S.. Karamanov. A.. Pelıno, M., 2001. •Chemical Durability of Glasses Obtained by Vinification of Industrial Wastes. *Waste Management.* vol.21.. p. l-9.

Romero. M.. Rincon. J.. Acosia. A.. 2002. Effect of Iron Oxide Coulent on the Crystallizaton of a Diopside Glass-Ceramic Glaze. *Journal til Eitrtipetm Ceramit Saiiely.* vol.22 . p.883-X90.

The Effect of Circulating Load and Test Sieve Size on The Bond Work Index Based on Natural Amorphous Silica

V. Deniz. N. Sütçü & Y. Umucu
Department of Mining Engineering Süleyman Deınirel University, İsparta, Turkey

ABSTRACT: Bond work index is being widely used to estimate power required to grind materials. Because grindability is so widely used in mill design the assumption is often made that the method is valid without a sufficiently critical examination of the associated uncertainties, which can lead to large contingency factors in design. Too large an energy contingency factor can lead to a drive motor having to be operated at such a fraction of maximum load that a considerable efficiency penalty is invoked. Hence the problems of grindability inaccuracies are important.

In this study, the effect of circulating load (CL) and test sieve size (P,), which are inaccuracies of Bond grindability, on the Bond ball mill grindability (G_{hg}) and work index (W,) are investigated based on four samples of natural amorphous silica.

In the experimental studies, the relationships between the Bond work index with circulating load and test sieve size were examined.

I INTRODUCTION

Currently, silica fume is widely used as a supplementary cementing material to enhance the strength and durability of concrete. Concrete containing silica fume has yielded higher compressive strengths, increased sulfate and acid resistance, and decreased chloride permeability in many applications. Amorphous silica possessed many physical and chemical properties similar to those of silica fume (Anderson et al. 2000).

Diatomaceous rocks are sedimentary rocks of biogenic origin with high natural amorphous silica (NAS) content. The amorphous silica is mainly in the form of diatom frustules, and secondarily in the form of sponge spicules, silicone-flagcllate skeletons and/or radiolarian cells. Beside its amorphous silica contenl, diatomite rocks may also contain carbonate and clay minerals, quartz, feldspars and volcanic glass (Fragoulis et al. 2002).

Amorphous silica is widely used as filtering agent, special fillers, absorbents, insulation product and a supplementary cementing material etc. In these industries, ultra fine grinding of amorphous silica is needed.

In the design of grinding circuits in a mineral processing plant, the Bond method is widely used for a particular material in dimensioning mills, power needs and the evaluation of performance. Its use as an industrial standard is very common as a result of providing satisfactory result in the all-industrial applications. Despite having many advantages, this method has some drawbacks such as its tiring and long test time as well as it needs a special mill. Due to these difficulties, recently a number of easier and faster methods are developed to determine Bond work index (Berry&Bruce 1966, Smith&Lee 1968. Karra I981, Yap et al 1982, Armstrong 1986: Magdalinovic 1989, Deniz et al 1996. Deniz&Özdağ 2003).

Austin&Brame (1983) and Austin et al.(1984) have summarized the problems with the Bond grindability as circulating load, effects of test sieve size, classifier effectiveness, the optimum mixture of ball size in the charge, variation of the residence time distribution of particles with mill geometry and slurry density, lifter design, slurry rheology(wet milling), it is assumed that specific energy is not a function of ball load contrary to known fact, only the 80% passing size is considered, no account is taken

of over-filling or under-filling of the mill, cause of inefficiency in grinding are not explored.

Smith and Lee (1968) and Tuziin (2001) are investigated variation of test work index with test sieve size for some materials. They showed that the Bond work index increased as the finer sieve size. Magdalinovic (1989) showed that Bond work index is not a validation with test sieve size for 100 to 500 micron of P,,

Armstrong (1986) investigated variation of the Bond work index with different circulating loads for puritic ore, calculated Bond work index is higher with different circulating loads, the Bond work index is higher with lower circulating loads.

The purpose of this study to determine the effects of circulating load (CL) and test sieve size (P;) on the Bond ball mill grindability (G_{ht},) and work index (W,) with natural amorphous silica.

2 MATERIAL AND METHOD

As a base for this study, four natural amorphous silica samples were used for test. The chemical properties of samples are presented in Table 1. Firstly, weigh out 25 kg samples taken from a representative composite of feed to be analyzed. Stages crush the feed so that 100% passes a 3.36 mm screen. Cone and quarter the feed, using a riffle splitter, to recover a representative 600 g head sample. The crude feeds were split into representative smaller batches, which were oven dried at 105 °C. The air-pyenometer densities of four natural amorphous silica were 2.35, 2.28, 2.27 and 2.27 g/cm , respectively. The bulk densities of samples were 0.77, 0.65, 0.72 and 0.74 g/cm^3. Secondly, Standard Bond grindability tests were done for three different test sieve size (150, 106 and 63 microns) and four different-circulating load (100%. 250%. 400% and 550%), and work indexes (W,) were calculated.

2.1. The test of standard ball mill Bond grindability

The standard Bond grindability test is a closed-cycle dry grinding in a standard ball mill (30.5x30.5 cm) and screening process, which is carried out until steady state condition is obtained. This test was described as follow (Bond&Maxson 1943, Yap et al. 1982, Ausiin&Brame 1983, Magdalinovic 1989).

The material is packed to 700 cc volume using a vibrating table. This is the volumetric weight of the material to be used for grinding tests. For the first grinding cycle, the mill is started with an arbitrarily

chosen number of mill revolutions. At the end of each grinding cycle, (he entire product is discharged from the mill and is screened on a test sieve (P,). Standard choice for P, is 106 micron. The oversize fraction is returned to the mill for the second run together with fresh feed to make up the original weight corresponding to 700 cc. The weight of product per unit of mill revolution, called the ore grindability of the cycle, is then calculated and used to estimate the number of revolutions required for the second run to be equivalent to a circulating load of 250%. The process is continued until a constant value of the grindability is achieved, which is the equilibrium condition. This equilibrium condition may be reached in 6 to 12 grinding cycles. After reaching equilibrium, the grindabilitics for the last three cycles are averaged. The average value is taken as the standard Bond grindability ($G_{h!:}$).

The products of the total final three cycles are combined to form the equilibrium rest product. Sieve analysis is carried out on the material and the results are plotted, to find the 80% passing size of the product (P,).

Table I. Chemical composition of amorphous silica samples used in experiments

Oxides (%)	1	II	1ll	IV
SiO,	92.22	87.75	92.41	91.27
Al.O,	0.04	0.10	0.00	0.32
TiO,	0.14	0.12	0.09	0.12
Fe$_2$0,	0.40	0.02	0.00	0.02
CaO	0.57	0.25	0.02	0.60
Na.O	0.05	0.10	0.01	0.11
K,0	0.07	0.03	0.03	0.10
SO,	0.61	0.21	0.08	0.18
Loss on ignition	4.40	5.21	4.77	5.40

3 EXPERIMENTS

3.1 Bond grindability test

The samples taken, are crushed in a laboratory scale jaw crusher and standard Bond grindability test is performed. Work index values (W,) are calculated from equation below.

$$W_i = 1.1 * \frac{44.5}{P_i^{0.23} * G_{bg}^{0.82} * \left[\left(10 / \sqrt{P_{80}}\right) - \left(10 / \sqrt{F_{80}}\right)\right]} \quad (1)$$

W, : work index, (kWh/t)

P, : sieve size at which the test is performed ((.tm)

Ghj. : Bond's standard ball mill grindability, (g/rev)

Pxn . FK»: sieve opening which 80% of the product and feed passes, respectively (<im).

For each samples, G_{hs}, and W, values are given in Table 2.

Table 2. The values of G_{hf} and Wi for samples of Natural Amorphous Silica

No.	P, (μm)	CL %	I		II		III		IV	
			G_{hg} g/rev	W, kWh/t	G_{hg} g/rev	W, kWh/t	G_{hg} g/rev	W, kWh/t	G_{hg} g/rev	W, kWh/t
No.	P 150 (Um)	G 100 %	2.091	11.11	2.066	11.41	1.627	12.99	1.895	11.89
2	150	250	2.911	8.94	3.297	8.05	2.272	10.78	2.055	10.83
3	150	400	3.047	8.52	3.720	7.05	2.386	10.28	2.450	10.07
4	150	550	3.247	8.12	4.036	6.51	2.639	9.61	2.737	9.19
5	106	100	1.454	13.77	1.307	14.62	1.239	14.95	1.349	14.30
6	106	250	1.958	11.44	1.858	11.94	1.739	12.67	1.584	13.16
7	106	400	2.095	11.18	2.709	9.25	1.823	12.16	1.759	12.42
8	106	550	2.195	10.75	3.143	8.24	1.951	11.53	1.927	11.77
9	63	100	0.755	18.11	0.679	19.16	0.652	19.45	0.688	19.07
10	63	250	1.216	14.62	1.095	15.88	1.051	15.88	1.I10	15.48
11	63	400	1.360	13.40	1.567	11.93	1.405	13.11	1.282	14.66
12	63	550	1.516	12.25	1.807	10.50	1.505	12.37	1.476	12.38

3.2. Correlation found from the test results

3.2.1. Effect of circulating load on Bond's work index

Figures 1-3 shown variation in the Bond work index with circulating load. It has been found thai the calculated work index is increased with lower circulating loads for each test sieve size. Otherwise, effect on the Bond work index is mostly for the finer test sieve size (63 micron).
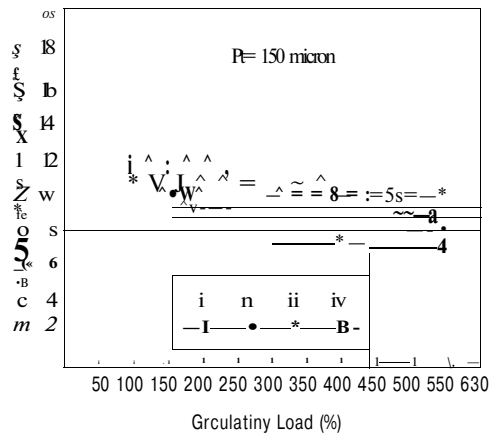

Figure I. Variation of Bond work index with circulating load lbrP,= 150 micron

Figure 2 Variation of Bond work index with circulating load for P = 106 micron

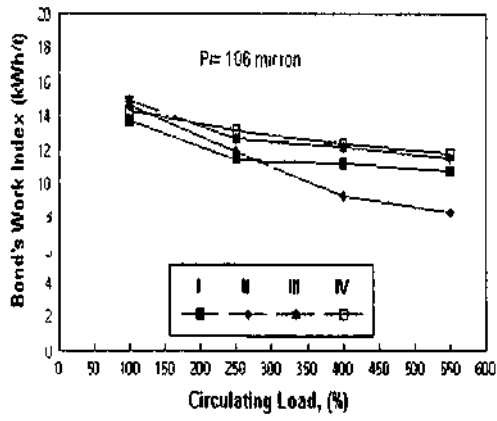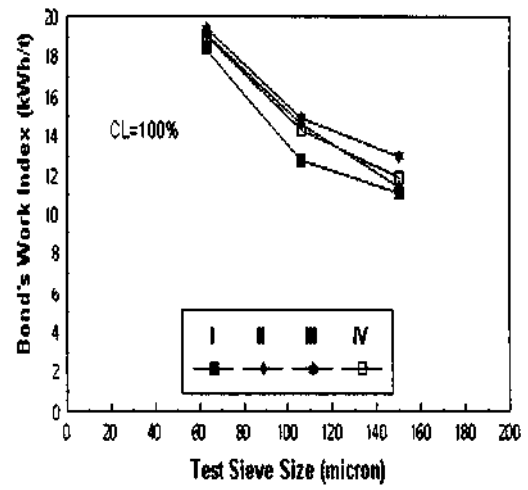Figure 1 Variation of Bond work index with circulating load for Pi=6^ micron

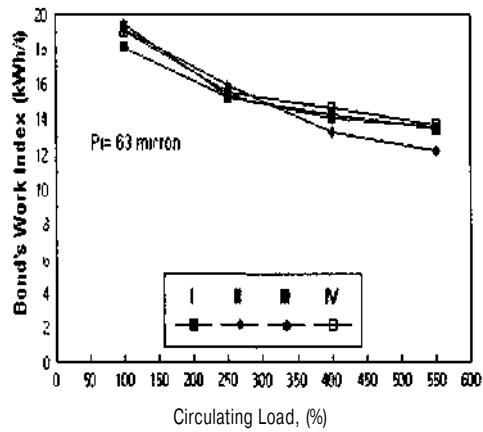Figure 4 Variation of Bond work index with the test sieve size for CL= 100%
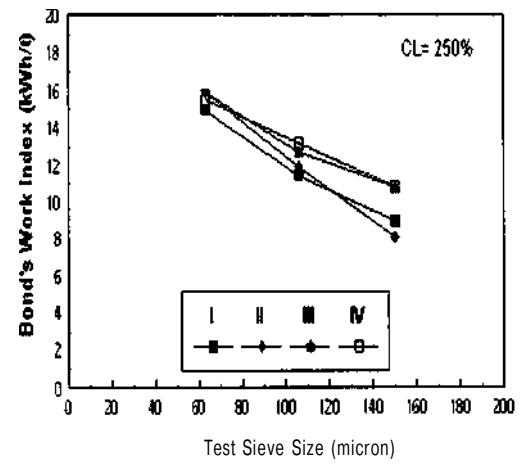

Figure 5 Variation of Bond work index with the test sieve size for CL= 250%

3 22 Effect of diffeient test sieve size on Bond's woik index

Figures 4-7 shown variation in the Bond woik index with test sieve size As test results, The Bond woik index mueased as the liner sieve size was used Espesiuilly, Bond woik index more mueased in 63 mm on as the emulating load was 100%
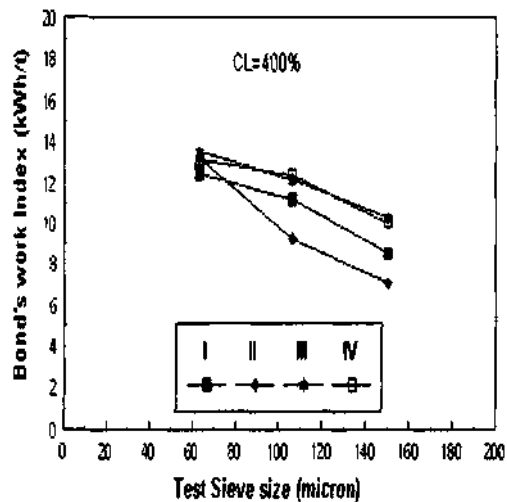
520

Figure 6. Variation of Bond work index with (he test sieve size for CL= 400%
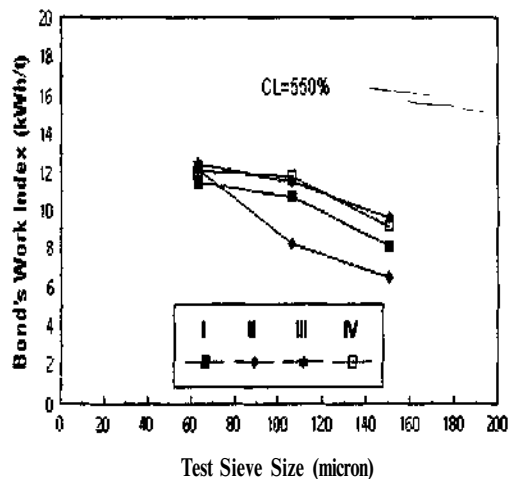

Figure 7. Variation of Bond work index with the lest sieve size for CL= 550'/

4 CONCLUSIONS

The present investigations have shown that a relationship could be established between the Bond's work index with circulating loads and lest sieve size.

The conclusions from the test can be summarized as follows.

1) The Bond's work index values increased as test sieve si/.e decreased.

2) The Bond's work index values increased as circulating load decreased.

3) Bond work index is changed with the change in ihe test sieve size and circulating load. This must be taken inlo account when energy consumption is calculated according to the Bond formula.

4) Bond work index is changed with the change in materials properties. Contents SiOi of sample II is lower than other samples. Hence, Bond work index value of sample II is lover than other samples

5) In grinding of amorphous silica, unit energy cost extra increased as circulating load decreased from 250%. However, unit energy cost decreased as circulating most suitable circulating load for amorphous silica used experiments is 250%.

6) III trail nc grinding, although, unit energy cost is possibility decreased with circulating load increased (higher 250%). However, mill capacity is decreased.

REFERENCES

Andeison. D.. Roy. A.. Seals. R.K.. Carlledge. F.K.. Akliler H and Jones S.C..2002. A preliminary assessment of the use of an amorphous silica residual as a supplementary cemenlary cementing material. *Cement and Concrete Research.* Vol. 30. 473-445.

Armstrong. D.G..I986. An alternative gnndability test: An improvement of (lie Bond procedure. *Int. ./. nf Mm. Praιcssιι;.* Vol. 16. I"7-208.

Austin. L.G. and Brame. K ,1983. A comparison of the Bond method for sizing wet tumbling ball mills with a .size-mass balance simulation model. *Powder Tei hnoloex.* Vol. 34. 261-274.

Austin. L.G.. Klimpel. R.R. and Luckie. P.T..I984. Process Engineering of Size Reduction: Ball Milling. *SME-AIME.* NewYoik. USA.

Beiiy. T.F. and Bruce. R.W.1%6. A simple method ot determining the grindabihty of ores. *Can. Min. J.* Vol. 87. 63-65.

Bond. F.C. and Maxson. W.L,. 1943. Standard gnndability tests and calculations. *Trans. Sac. Min. Eng. AIME.* Vol. 153.362-372.

Deniz V Balta Ci and Yanık A 19% rııc ınlcııclatıonshıps between Bond gıındahıhls ot loals and impact stıengtlı index (ISI) point load index (Is) and Pliability index (F|>) *Cinimi/uf; S<»/JM m Minimi Pitnewint;* Kemal et al (hdilois) A A Balkema Roteidam Nelheilands li-19

Dem/ V and Odag H 2003 A new approach Bond gıındabılıty and woik index Dynamic elastic paıameteıs *Muuıuh k/ıvifietıııiK* (ınpıess)

hagoulıs D Stamatakıs M Papageoıgıou D Pentelenyj L and Csıık G 2002 Dıatomaccous eaıth as a cement additive A cast study ol deposits lıom Ninth eastein Hungaiv and Milos Island Gieece */KU limrnatwmil* Vol Si 8ll Hi

Kana V K I9SI Simulation ot Bond gıındabılıty tests *CIM Bull* Vol 74 I9S-199

King M S 1983 Static and dynamic elastic pıoptıtıes ot locks from the Canadian Shield *lut J Rink Mali Mm* Sil Ä<«i«iiir/i *Aim,* Vol 20 217-24S

Magdahnovic N 1989 Calculation ot energy requited foi gnnding in a Ball mill *hit I of Mm Pun twin/;* Vol 2'> 41-46

Magdalmmic N 1989 A pioceduie toi lapid determination ot the Bond Woik Index *lui I of Mm Pimi-umn* Vol 27 I2VI12

Smith RW and I ee KH 1968 A companson ot data tiom Bond type simulated closed eiicuit and batch type gıındabılıty tests 7*;«;» *Sin Mm bıiif AIME* Vol 241 91 99

Tu/un MA 2001 Wet Bond Mill Test *Mimnih lımımcıııiK* Vol 14 169 171

Yap R F" Sepulude II and lauiegui K 1982 Deteinnnation ot the Bond Woik Index using an ordinary laboıatoıy batch ball mill *DL* we« *ami lıtsttılltıtıum nj ı nmmmuliim ı mints* LG Austin (Fditoi) SMK AIME NewYoik 176-201

Modern Condition of Hard-to-Processing Ores in The Republic of Kazakhstan

Yu.P. Yeryomin & O.R. Kim
Complex Processing of Mineral Raw Materials National Center of the Republic of Kazakhstan, RSE. Almaty. The Republic of Kazakhstan

A.A. Niyazov
SSE "Kazmekhanobr". Almaty, The Republic of Kazakhstan

M.Zh. Zhanasov
NOVA-Tradiiifi & Commerce AG, Almaty, The Republic of Kazakhstan

ABSTRACT: Kazakhstan takes up one of the leading places in the world by reserves of useful minerals. Problems of processing of hard-to-processing ores arise all over the world. Today in Kazakhstan easy-to-processing ores are practically mined as a result of intensive exploitation of mineral resources. The main extracting ores are hard-to-processing ores which are characterised by low content of useful components, increasing of a part of oxidized forms, high content of soluble minerals, increasing of a part of line- and emulsive patching ores. In the paper results of technological-mineralogical investigations of deposits and their parts are presented.

1 INTRODUCTION

Specific nature of processing of hard-to-processing ores of Kazakhstan is in a fact that for full extraction of useful component a thorough study of composition, character of mineral associations of minerals, crystals' size, in-depth technological-mineralogical study is necessary. Especial attention must be paid to investigations of technological compatibility of ores from different parts of a deposit.

There are 37 preparation plants in Kazakhstan, and practically all of them are faces with the problem of hard-to-processing ores processing, especially preparation plants of the Eastern Kazakhstan where complex mixed ores are processed.

For complex and rational using of mineral resources it is necessary to create optimal technology of processing of mineral raw materials which will take into account not only problems of processing stage but also problems of mining operations when forming ore-flows which arc transported to preparation plants.

2 DETAILS OF THE STUDY

Mineral processing is the final stage of mineral raw materials working. Products are received when ore processing comes to metallurgical treatment, where they are smelted or are dissolved. The main purpose of processing is receiving of market product complying with standards of metallurgical stage.

The main result of purposeful technological-mineralogical studying of ores from different parts.

zones and levels of any deposit is forming of a map of washability for its parts. Systematic technological-mineralogical sampling will allow bringing to light such parts of deposits and such types of ores, which may be effectively processed by modern methods and also the others, which need modernization of existing or creating new technologies. In-depth technological-mineralogical analysis of all zones and parts of deposits will at the same time allow bringing to light to the reasons of bad washability of particular ores and define the most effective, priority directions of investigations.

As an example studying Akzhal deposit may be considered. Ore ledge of Akzhal deposit is divided into more than 60 separate fragments ore bodies or parts. In previous works, ores of Akzhal deposit are subdivided into two types: mixed and sulphide.

Mixed ores include up to 70% minerals of zones of oxidation and on the whole are located at a depth of 20-30 m. These are hard-to-processing varieties of ores, and now they are worked out in a high degree, but losses of lead and zinc during processing, which add up to 10% and 16.5% correspondingly, arc evidence of their ingress into a process today.

Sulphide ores are the main at the deposit. 5 genetic varieties may be separated out of these ores, but their technological-mineralogical characteristic properties and distinctions are not studied. They are distinguished from each other by varieties of sphalerite and differences in aggregating rock minerals: in the first case it is thin growing together with carbonates, in the second case it is close growing together with calcite and in the third case - emulsive patching by chalcopyrite. All these varieties are

523

hard-lo-process. There are more favorable ores to process, where large-crystal sphalerite and large-sized galena are predominated, but there is secondary covellile and it negatively effects on selection of lead and zinc.

At the deposit different structural-textural ores are fixed:

Table I Content of elements in ores, ore tailings and concentrates

Product name	Content, mas. %						
	Zn	Pb	Cd	Ag г/т	S	SiO$_2$	CaO
1. Ore sample	3.3	0.13	0.02		2.13	5.03	40.4
2. Ore sample	4.0	0.15	0.032		2.8	8.6	38.3
3. Ore sample	5.06	0.18	0.038		3.57	8.6	35.2
4. Ore tailings	0.26	0.015	0.002		0.62	4.97	45.1
5. Ore tailings	0.26	0.014	0.002		0.73	8.3	41.9
6. Ore tailings	0.25	0.023	0.002		0.59	6.6	44.0
7. Pb – concentrate	4.9	59.9		380			
8. Pb – concentrate	4.7	56.9		350			
9. Pb – concentrate	4.3	67.9		324			
10. Zn – concentrate	51.7	1.05	0.41	48			
11. Zn – concentrate	50.6	0.68	0.42	49.5			
12. Zn – concentrate	53.9	0.86	0.41	62			

massivc - continuos aggregates of sphalerite, galena and other sulphides;

banded - alternating of stripes of sphalerite, galena and carbonates;

patched - patches of sulphides in limestone;

brecciated - fragments of limestone cemented by sulphides and calcite;

emulsive - structures of disintegration of solid solutions.

In Table 1 data are presented of content of elements in ores, ore tailings, and concentrates. They also are evidences of differences in washability of processed ores; variations are substantial both in contents of extracting metals (zinc, lead, cadmium, silver) and also in contents of elements and compounds, characterizing share of sulphide varieties (sulphur) and in quality of influencing rocks - CaO, Si(X

All these ores need particular technological-mineralogical studying which will allow systemizing them by washability and separating into technologically compatible groups.

Forming of ore-Hows, arriving to preparation plant, is carried out today without taking account of washability and technological-mineralogical properties of ores of different parts of the deposit. Ore extracting is carried out with due account of ease of carrying out of stripping operations of this or those parts of the main ledge of the deposit. Mining is carried out by method of complete extraction and ore arrives to preparation plant in arbitrarily mixed condition.

For a more detailed study the open cast was divided into 6 typical parts, distinguishing from each other by technological-mineralogical properties of ores, where representing samples were taken.

Mineralogical studying of the first testing samples showed, that useful minerals are; sphalerite, galena is present in insignificant quantities and in insulated grains - pyrite and chalcopyrile. The most typical textures are non-uniform-patched, rarer veinlet-palched and banded and very rarely densely patched. Dimension of sphalerite grains arc from thousandth parts of mm up to 3-5 mm, grains of 0.1-0.3 mm prevail: dimensions of galena grains - from thousandth parts of mm up to 0.1 mm. Limestones, which are in different degree marblcizcd, cataclastized. quartzed and harytized, present enclosing rocks, rare marble and diabasic porphyrite are present. Calcite, dolomite, quartz, baryte, feldspar, seriate, dark-colour minerals (in the decreasing order) pyroxene, amphibole, epidote, chlorite and garnet present rock-forming minerals.

All samples have characteristic technological-mineralogical distinctions and include different enclosing rocks and minerals, which effect on technological process and quality of producing concentrate.

Ores of different sorts from different zones by washability are mixed, and ore mixture is arrived to preparation plant. This negatively influences on final indexes of the process. That is why today results are not limiting for these types of ores. Upgrading the quality of concentrate and final indexes is possible when detail and in-depth studying of effect of every type of ore in their mixture.

Interconnection of such functioning subsystems as open cast and preparation plant will allow studying them as an integrated system with required qual-

ity characteristics, ensuring technological compatibility of ores, arriving to processing. Influence of technological-mineralogical factor on processing must be taken into account al a stage of timely work with geological reserves.

For increasing of fullness of useful components extraction, it is necessary to systematize ores by washability, and this requires forming technological-mineralogical map of washability of ores from different parts and levels within limits of open-pit field. Such map using will allow stabilizing homogeneity of mineral raw materials, when forming of ore-flows, arriving to preparation plant, regulating their movement and substantially increasing technical-economic indexes of preparation plants.

3 CONCLUSION

High priority of these investigations is based on a fact that at preparation plants ore quality is taken into account mainly by metal content, and this is not enough for representation of true ores washability. Ore-flows forming on this base cause substantial metal losses during processing.

High technological-mineralogical distinction ol ores from different parts is typical for Ak/hal deposit. Advance study and systcmization of ores, forming of technological-mineralogical map of washability will allow forming of ore-flows, ensuring optimization of schemes of ores from different parts of deposit, which are compatible by technological properties, stabilization of homogeneity of mineral raw materials arriving to preparation plant. This will allow increasing the technological indexes of metals extraction into concentrate by 3-5%, improving quality of concentrate and increasing complex utilization of mineral raw materials.

Controlled Stabilization of Nanoparticulate Suspensions

G. B. Başım
Engelhard Corporation Research and Technical Center, Gordon, GA, USA

I. U. Vakeralski. P. K. Singh & B. M. Moudgil
Department of Materials Science & Engineering and engineering Research Center for Particle Science & Technology, Gainesville, FL, USA

ABSTRACT: Stabilization of nanoparticulate systems in extreme processing environments requires new approaches. The increase in the total surface area of the nanoparticulate systems with the decrease in the particle size results in ineffective application of the conventional stabilization techniques, such as electrostatic stabilization and polymeric dispersion. In this investigation, self-assembled surfactant structures were utilized to stabilize nanosize silica suspensions at extreme environments of pH, ionic strength and reactive additives of the chemical mechanical polishing (CMP) process. The strong repulsive force barriers provided by the cationic surfactant stabilized the silica CMP slurries under high pH and ionic strength conditions. In addition, it was observed that stabilization must be achieved by controlling not only the particle-particle interactions but also the particle-substrate interactions, to meet CMP performance criteria. The knowledge base created in this investigation can be extended to the future stabilization requirements of the paint and paper production and mineral processing applications.

1 INTRODUCTION

Several emerging technologies such as chemical mechanical polishing (CMP), high speed coatings, inks, nanocomposites, and biomedical applications are increasingly relying on nanoparticulate dispersions to achieve optimum performance. Many of these technologies operate under extreme conditions such as high salt (CMP, biofluids in medical applications), high pressure (CMP. high speed coatings), and in the presence of complex additives (CMP, nanocomposites, bio applications).

Traditionally used dispersing methods such as electrostatic repulsion and steric stabilization using polymers may not perform adequately under severe processing conditions. Electrostatic repulsion is effective in stabilizing homogeneous, low ionic strength suspensions, where pH can be controlled in order to provide sufficient surface charge. The repulsive energy due to electrostatics decreases proportionally with particle size, and hence a greater surface potential is needed to disperse nanoparticles than relatively larger particles. This effect, coupled with the severe environment may be great enough that pH adjustment, or addition of inorganic dispersant such as sodium silicate, may not lead to suspension stability. In case of polymeric dispersants, polymer layers increase the effective volume fraction, and hence prevent the use of

nanoparticles in concentrated suspensions. Additionally, many polymeric dispersants are polyacrylate based and may perform poorly under extremes of pH and ionic strength. These limitations have motivated the search for alternative dispersants to stabilize suspensions in extreme environments and maintain fluidity in concentrated suspensions. Surfactants can provide a feasible alternative for stabilization of ultrafine particles under extreme conditions. The barrier to aggregation in presence of surfactant aggregates, measured using atomic force microscopy (AFM) was found to be several orders of magnitude higher as compared to barrier expected from electrostatic interactions alone. The onset of this barrier was correlated to dispersion of nanoparticles under extreme conditions. The results indicated that the strength of the barrier increased with increasing compactness of the adsorbed self-assembled surfactant structure at the solid-liquid interface (Adler et al., 2000).

' CMP process is a specific example in which stabilization has to be achieved under extreme chemical and dynamic environments. This process is widely used to achieve multi level metallization in microelectronic device manufacturing. Figure 1 schematically represents the CMP process. In CMP, the main objective is to planarize the metal or dielectric layers

deposited on the wafer surfaces by using slurries containing submicrometer size particles and chemicals. An effective polishing requires an optimal material removal rate with minimal surface deformation. Therefore, it is important to control the particle-substrate interactions that are responsible for the material removal and the particle-particle interactions, which control the slurry stability and consequently the defect density.
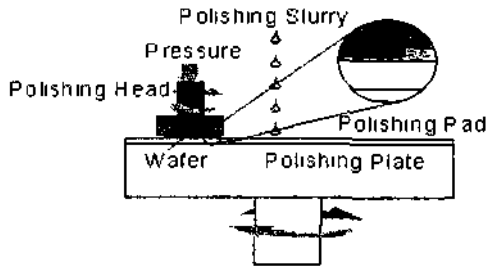

Figure 1. Schematic representation of CMP process.

It is suggested that a perfectly planarized surface with minimal deformation can be achieved by using monosized particulates (Cook, 1990). In practical applications, however, there may be oversize particles in the slurries in the form of larger size particles (hard agglomerates), or the agglomerates of the primary slurry particles (soft agglomerates). The polishing tests conducted in the presence of hard agglomerates (at parts per million concentration) verified a significant degradation in the polishing performance (Basim et al., 2000). The Atomic Force Microscopy (AFM) analysis showed increasing surface roughness and deformation (scratches and pit formations) on the wafer surfaces with significant variation in the material removal rate response. CMP slurries are filtered before polishing to remove hard agglomerates. Nevertheless, even after filtration significant defect counts have been observed on the polished surfaces (Ewasiuk et al., 1999). These are attributed to the possibility of particulate agglomeration during the polishing operations due to the local variations in the particle concentration, ionic strength or pH. Systematic analysis conducted in the presence of soft agglomerates showed significant surface deformations and variation in the material removal rates leading to the conclusion that the CMP slurries must remain stable to obtain optimal polishing performance (Basim & Moudgil, 2002).

The self-assembled structures of $C_{12}TAB$ (cetyl trimethyl ammonium bromide), a cationic surfactant, have been shown to provide stability to silica suspensions at high ionic strengths and extreme pH by introducing a strong repulsive force barrier (Singh et al., 2000). In the present study, this concept was utilized to stabilize the CMP slurry at high pH and salt concentration and under the applied pressure. It was observed that not only the particle-particle interactions but also the particle-substrate interactions must be taken into consideration in stabilizing the CMP slurries.

2 MATERIALS & METHODS

The baseline polishing slurries were prepared from 0.2Dm monosize sol-gel silica powder obtained from Geltech Corporation. Slurry pH was adjusted to 10.5 and the solids concentration was kept at 12wt.%. To stabilize the baseline slurry, dry silica powder was ultrasonicated in deionized water while maintaining the pH at 10.5 with NaOH addition. Preparation of the slurries from a dry powder was necessary to enable the control of system chemistry. To simulate the extreme CMP slurry environment, 0.6 M NaCl salt was added into the baseline slurry, which resulted in coagulation of the abrasive particles. Under these conditions, C_nTAB (n=8, 10, 12) surfactants were added into the suspension. Particle size analyses of the slurries were conducted using Coulter LS 230 instrument utilizing light scattering technique with small volume module. The background water used to run the size analysis was prepared to have the same chemical composition as the modified slurries.

Polishing tests were performed on p-type silicon wafers on which a 2.0Dm thick SiO_2 layer had been deposited by PECVD (supplied by Silicon Quest International). The 8-inch wafers were cut to square samples of 1.0 in. x 1.0 in. and Struers Rotopol 31 tabletop polisher was used for polishing with IC 1000/Suba IV stacked pads supplied by Rodel Inc. A grid-abrade diamond pad conditioner was utilized to abrade the pad before conducting each polishing test. The downforce was set to 7.0 psi (492 gr/cm^2) and the rotation speed was kept at 150 rpm both for the pad and the wafer. Slurry flow rate was 100 ml/min and polishing tests were conducted with 50ml slurries for 30 seconds. The thickness of the oxide film on the wafers was measured via spectroscopic ellipsometry method before and after polishing to calculate the material removal rate. Atomic Force Microscopy (AFM) technique was selected for the surface characterization of the polished wafers. For all the selected conditions, a minimum of four polishing tests were conducted and five 100m xlODm size images were taken on each polished wafer to

528

evaluate the surface roughness and maximum surface deformation responses.

To measure the interparticle forces and the particle-substrate friction in the presence of surfactants, a silica particle was attached to the AFM tip. The details of the force and friction measurements with the AFM technique were discussed elsewhere in detail (Basim et al., 2003).

3 RESULTS & DISCUSSION

To stabilize the silica slurry in the presence of 0.6M Nad at pH 10.5, C_{12}TAB surfactant was used at 1, 8 and 32 mM concentrations according to the previous findings reported (Adler et al., Singh et al., 2000). The baseline polishing slurry contained 12wt%, O.20m monosize silica particles at pH 10.5. Addition of 0.6 M NaCl destabilized the particles by screening the surface charge. As a result, the mean particle size of the slurry increased to 4.30m. When ImM $C|_2$TAB was added into the coagulated slurry, the mean particle size was measured to be 4.8Dm. At 8mM $C|_2$TAB concentration, a jump was observed in the repulsive force barrier due to the formation of the self-assembled surfactant aggregates. The increase in the repulsive force barrier initiated the stabilization of the particles and the mean size of the slurry began to decrease (1.6Dm) with the addition of 8mM C_{12}TAB. Finally, at 32mM $C|_2$TAB concentration, the high ionic strength polishing slurry was completely stable (mean particle size- 0.2 Dm) since a strong enough repulsive force barrier was reached for the particle-particle interactions.

Polishing experiments were conducted with the stable slurry to evaluate the CMP performance. Initially, surface quality response was analyzed in terms of surface roughness and maximum surface deformation by imaging the polished wafer surfaces using AFM technique. Slurries containing 0.6M NaCl resulted in 4.8nm surface roughness and 70nm deep pitting (maximum surface deformation) as compared to 0.85nm and 35nm obtained with the baseline slurry. The poor surface quality in the presence of salt was due to the coagulation of the slurry (Basim & Moudgil, 2002). Since the ImM and 8mM $C_{,2}$TAB concentrations were not able to stabilize the slurries completely, surface qualities were also observed to be poor at these concentrations. However, when complete stabilization was reached with the addition of 32mM $C_{,2}$TAB at high ionic strength, surface roughness reduced to 1.5nm and the maximum surface deformation was recorded to be only 2()nm. Figures 2-a and b illustrate the surface images of the wafers polished with the 0.6M NaCl containing unstable slurry and slurry stabilized by addition of 32mM

$C_{,2}$TAB in the presence of 0.6M NaCl.

To evaluate the overall polishing performance, material removal rate responses of the slurries were also measured simultaneously. Addition of 0.6M NaCl resulted in 7600 A/min material removal rate as compared to the 4300 Å/min with the baseline pH 10.5 slurry. The increase in the material removal rate in the presence of salt is suggested to be due to the increased pad-particle-substrate interactions as a result of the screening of negative charges in the system. This phenomenon was reported to enhance the frictional forces by conducting in-situ friction force measurements (Mahajan et al., 1999). The increase in the friction forces is believed to result in enhanced material removal. When ImM $C_{,2}$TAB was added to the high ionic strength slurry, the material removal rate decreased to 5500A/ min but still remained higher than the baseline result of 4300 A/min. On the other hand, at 8mM and 32mM $C|_2$TAB concentrations a removal rate of only 70 A/min was obtained. Two reasons can be suggested for the negligible material removal in the presence of 8 and 32mM C_{12}TAB. First, it is known that the presence of surfactants in the system results in lubrication between the abrasive and the surface to be polished and therefore decreases the frictional force (Klein et al., 1994). Therefore, the addition of $C|_2$TAB in the polishing slurries at relatively high concentrations may be resulting in negligible material removal by reducing the frictional forces required for polishing. Second alternative is that, the high repulsive force barrier induced by the C_{12}TAB self-aggregated structures may be preventing the particle-surface interaction and therefore resulting in a very low material removal rate. The concentration of $C|_2$TAB, where negligible material removal rate response was obtained coincides with the observation of the jump in the maximum repulsive force barrier as described previously (Adler et al., Singh et al., 2000).
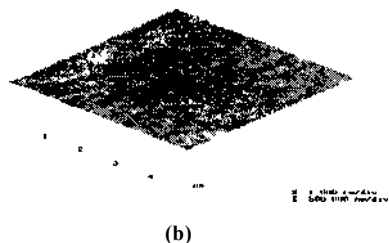

(a)

(b)
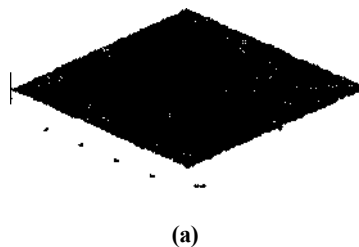
Figure 2. Atomic Force Microscopy images of the wafers polished with (a) 0.6M NaCl containing unstable slurry and (b) Ü.6M NaCl + 32mM C,₂TAB containing stable slurry.

In order to distinguish the effect of lubrication and the repulsive force barrier on material removal response, it was planned to alter the magnitude of the repulsive force barrier. Accordingly, the force barriers of different chain lengths of the CTAB surfactant were measured by AFM above the critical micelle concentration (CMC), where they form the self-assembled structures. The repulsive force barriers created on a 0.2Dm particle by C12TAB, C_{10}TAB and C_8TAB surfactants at 32, 68 and 140mM concentrations in the presence of 0.6M NaCl at pH 9 were 0, 2.2 and 6 nN respectively (Basim et al., 2003). This finding indicates that decreasing the chain length of the surfactant leads to a smaller repulsive barrier. In agreement with the measured force barrier values, none of the slurries prepared by the C_8TAB surfactant, which gave the minimum repulsive barrier, (at ImM, 35mM and 140mM concentrations) were stable. Therefore, the maximum surface deformation values were higher than desired (50-60nm). On the other hand, the surface roughness values were reasonable (-0.9 nm), which may be attributed to the decreased frictional forces due to the lubrication introduced by the surfactant molecules (Xiao et al., 1996). Most importantly, all the C_STAB containing slurries yielded high material removal rates (6000-7000 A/min). Finally, when C_{10}TAB surfactant was added into the unstable slurry, stability was reached at 68mM concentration but the material removal rate was only 500 A/min. It was observed that the stability responses obtained as a function of surfactant chain length strongly correlated with the measured force barrier values. However, to evaluate the impact of the repulsive force barrier on particle-substrate interactions, or in other words the material removal response, it was necessary to know the force applied on a single abrasive particle during polishing. This value was calculated to be 750+150 nN for a 0.2Dm size

particle by determining the pad-substrate contact area at the applied head pressure and the particle concentration at the area of contact of the pad (Basim et al., 2003). Since the measured force barriers for all the CTAB surfactants were much less than this value, the pressure applied per particle is expected to easily overcome the repulsion introduced by the self-assembled CTAB aggregates. Hence, it was more likely that the lubrication effects introduced by the surfactants controlled the material removal by varying the frictional forces between the abrasive particles and the substrate.

In order to understand the surfactant lubrication effect on material removal rate at particle-wafer interaction level, AFM friction force measurements were conducted. A silica particle attached to the cantilever tip was made to raster on the silica wafer surface in the presence of surfactants to simulate the single particle-wafer interaction. The preliminary analysis showed a significant decrease in the friction coefficient of the particle-substrate interaction in the presence of the C_{12}TAB surfactant. Figure 3 illustrates the AFM friction force measurements in the absence and presence of C,₂TAB and 0.6 M NaCl. The measurement of the lateral friction force as a function of the normal load was conducted from which friction coefficient was calculated based on the Amonton's law. It can be seen that for baseline solution, frictional forces increased with an increase in normal forces. On the other hand, with the C12TAB addition, the frictional interactions were minimal.
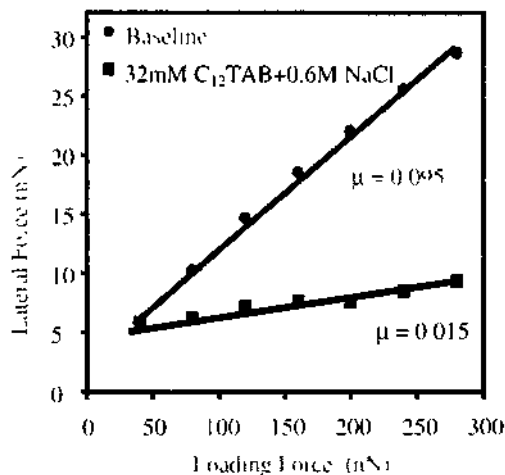

Figure 3. Atomic Force Microscopy friction coefficient measurements with baseline pH 9 solution and 0.6M NaCl + 32mM C,₂TAB solution.

When the friction measurements were conducted on the baseline (pH=10.5) and surfactant mediated solutions in the absence of NaCl (140, 68 and 32 mM, C_STAB, $C_{10}TAB$ and $C_{12}TAB$), it was observed that all the surfactant mediated slurries resulted in minimal friction. Indeed, when polishing experiments were conducted at the corresponding surfactant concentrations in the absence of NaCl, the material removal rate values were observed to be negligible for all the chain lengths (61, 53 and 56 A/min for C_STAB, Cn,TAB and Cj_2TAB, respectively). This result indicated that at any chain length, CTAB surfactant was able to form a lubrication layer in the absence of salt. Consequently, minimal particle-surface interactions occurred in these systems resulting in negligible material removal. It is also important to note that all the slurries were stable without salt addition.

The polishing results in the presence of 0.6 M NaCl, however, showed an increase in the material removal with decreasing chain length of the surfactant (66, 650 and 6167 A/min for $C_{12}TAB$, $C_{10}TAB$ and C_STAB, respectively). When AFM friction force measurements were conducted in the presence of salt, an interesting behavior was observed. It was observed that CsTAB and $C_{10}TAB$ mediated solutions started to exhibit higher friction values above 750 nN. This type of a behavior was also observed on the mica surfaces modified with 2, 5, 7 and 17 chain lengths alkylsilanes (Xiao et al., 1996). It appears that the lubricating surfactant layer is desorbed/destroyed beyond a certain loading force. In the absence of salt, all the surfactants, regardless of the chain length, seems to form a compact adhesion layer due to the electrostatic interaction between the negatively charged silica surface and positively charged surfactant head group. However, the addition of salt appears to screen the electrostatic interactions thereby resulting in weaker adhesion of the adsorbed surfactant layer and possibly desorption of this layer above a certain applied load (Chen et al., 1992). The impact of salt molecules was less effective on the longer chain length surfactants, perhaps due to their ability to form more densely packed and well-ordered layers (Xiao et al., 1996). As the length of the hydrocarbon chain increases, the lateral interactions between the hydrocarbon chains become more pronounced resulting in formation of more compact layers. In addition, the driving force for the surfactant adsorption on the substrate surface also increases with the increased chain length, resulting in denser surfactant layer (Clear & Nealey, 1999).

Thus, it is possible that NaCl addition does not affect the lubrication layers created by $C_{12}TAB$ mediated slurries to the same extent as surfactants with shorter chain lengths. Accordingly, C^TAB yielded negligible material removal of 66 A/min, whereas the shorter chain length $C_{10}TAB$ surfactant, resulted in material removal of 650 À/min indicating that the silica particles were able to engage with the silica wafer surface up to some extent due to the removal of the surfactant. Finally, QTAB mediated slurries also showed an increase in the frictional forces at single particle-surface interaction level, suggesting that they as well should polish the silica surface. However, the significantly high removal rate for the C_NTAB mediated slurries (5167 A/min) should he attributed not only to the easier removal of the loosely packed 8-carbon chain surfactant layer from the wafer surface under applied load, but also to the coagulation of the particulates in the absence of a repulsive force barrier for QTAB at 0.6 M salt concentration resulting in more mechanical interactions.

4 CONCLUSIONS

Robust dispersion of the CMP slurries in extreme ionic strength and high pH environments is a must for optimal polishing performance, which requires the introduction of high enough repulsive forces between the slurry particulates. However, in this study, it was observed that to design optimally performing CMP slurries, the control of particle-particle interactions is not sufficient as it has been in other applications. To enable an optimal material removal rate, it is also necessary to achieve sufficient particle-substrate interactions. In summary, the stability of the CMP slurries must be tailored by controlling both the lateral (particle-particle) and normal (particle-wafer surface) interactions and this can be achieved by utilizing self-assembled surfactant structures and manipulating the frictional interactions by changing the surfactant chain length and slurry ionic strength.

REFERENCES

.1. .1. Adler, P.K. Singh, A. Patist. Y.I. Rabinovieh, D.O. Shah and B.M. Moudgil., Langmuir, 16, 7255-7262 (2000).

(i. B. Basim, J.J. Adler, U. Mahajan. K.K. Singh and B.M. Moudgil, J. Elcctrochem. Soc, 147,3523 (2000).

G. B. Basini, B. M. Moudgil, *Journal of Colloid and Interface Science,* 256, No 1,137 (2002).

G. B. Basini. 1.1). Vakarclski, B. M. Moudgil. Stabilization of Chemical Mechanical Polishing Slurries In Controlling Interaction Forces, *Journal of Colloid and Interface Science* (In press, 2003).

S.C. Clear. P.F. Nealcy. *Journal of Colloid Interfce Sei.* 213.238(1999).

Y.I.. Chen, C. Frank, J. Israelachvili, Journal of *Colloid Interfce Sei.* 153, 244 (1992).

L. M. Cook, J. *Non-Cryst. Solids,* 120.152 (1990).

R. EH asiuk, S. Hong, V. *Desai in Chemical Mechanical Polishing in IC Device Manufacturing III,* edited by Y.A. Arimoto, R.L. Opila, J.R. Simpson, K.B. Silodanım, I. Ali, Y. Homina, (Elcctrochem. Soc. Proc. PV 99-37,1999) pp. 408.

VI Mahajan, M. Bielman and R.K. Singh, *Elcctrochem. Solid-State Utt.,* 2,46 (1999).

./. Klein, E. Kumachcva, I). Mahalu, D. Perahia and L. J. Fetters, Nature, 370, 634, (1994).

P. K. Singh, .1.). Adler, Y.I. Rabiiunich and B.M. Moudgil, Langmuir, 17,468-473 (2000).

X. Xiao, J. Hu, D.H. Charych and M. Sahnenin, Langmuir, 12, 235 (1996).

A Simpler and More Cost Effective Solid-Liquid Separation for the Mining Industry

P. Costelloe
Pnewnapress® Filler Corporation, Richmond, California, USA

Q._Kilavuz
Kilavuz Limited, Mersin, Türkiye

ABSTRACT: This paper discusses new solid-liquid separation technology introduced by Pncumaprcss® Filter Corporation that addresses may of the limitations of conventional filler technology. The operating principle of this technology is outlined and a process How diagram provided. Two case studies of mineral applications are provided to demonstrate the effectiveness of this technology.

I INTRODUCTION

Cost effective solid-liquid separation technology is essential to the economical production of solids or filtrate in the chemical, food processing and mining industries. To achieve this, the plant engineer faces a wide selection of filter technology. The chosen technology should achieve the desired solids and filtrate properties, provide reliable operation as well as offer low installation, operating, and maintenance costs. Unfortunately, a great deal of the technology available today does not satisfy all of these requirements and a misguided decision may result in significant operating difficulties, high operating and maintenance costs, and a poor return on investment. This paper introduces a new technology that addresses these requirements and provides case studies from several applications where this technology has been successfully implemented.

2 CONVENTIONAL FILTER TECHNOLOGY

The most widely used conventional filter technology includes liker presses, vacuum fillers, centrifuges, low-pressure automatic pressure filters and high-pressure or mechanical expression automatic pressure filters. Conventional filter presses sutler Irom unavoidable labor costs and solids build-up removal problems that may result in leakage and damage. Despite attempts at automating filter presses, there remains the need for a great amount of operator intervention and large volumes of wash water to clean the filter media. Vacuum filters often produce high cake moistures, high solids content in filtered liquid and require large amounts of floor space and peripheral equipment. Centrifugal separation often requires high maintenance and expensive installation for the rotating equipment, inefficient washing or dewalering of solids, extensive structural and foundation support, large amounts of surrounding equipment, and large areas of floor space. Low-pressure coolant type automatic pressure filters have been limited in capacity and pressure differential for acceptable throughput and performance. High pressure or mechanical expression automatic pressure fillers arc very complex mechanically, have a multitude of expensive components and require intensive maintenance. Together, these limitations result in unscheduled downtime and loss of production.

3 NEW FILTER TECHNOLOGY

In order to address the limitations of conventional filter technology as outlined above, Pneumapress® Filter Corporation introduced a new series of high-pressure automatic pressure filters (APF's). The focus lor the design of the new high-pressure APF was to develop very effective filtration technology using mechanically simple and robust equipment available in a wide range of capacities. These filters are available cither as a Single Module Filter with only one filter chamber (figure 1.0) or as Multi Module Filter with multiple chambers (figure 2.0). A filter overview with operating sequence, process How diagram, process parameters and case studies are discussed in this paper to illustrate the filters effectiveness and simplicity.
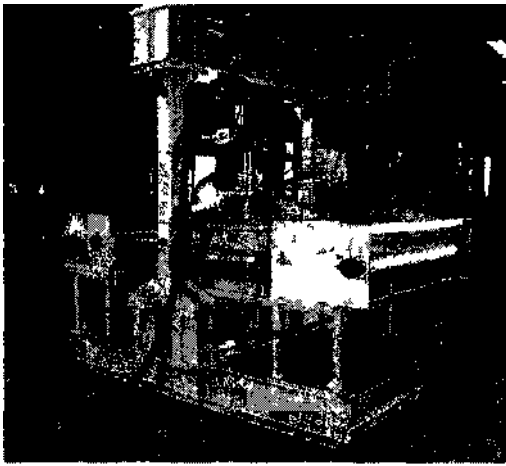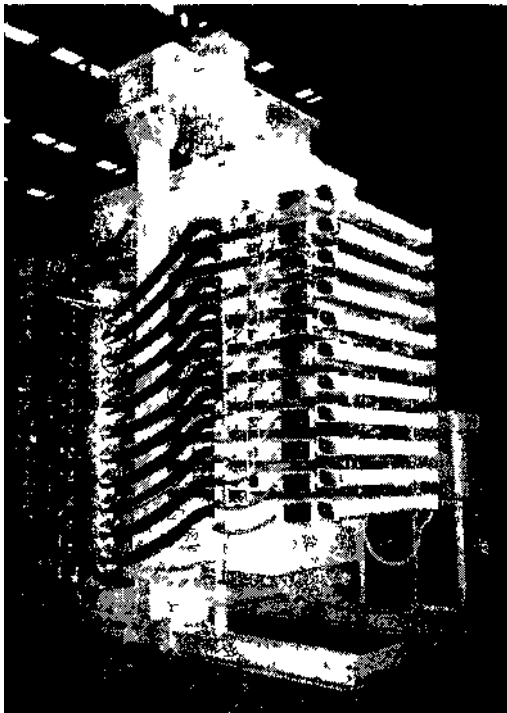
Figure 1 Single Module Filter

Figure 2 Multi Module filter

4 FILTER OVERVIEW

A very simple mechanical structure is used to support the filter. The structure consists of two columns an upper and lower support beam and two base beams. These components are illustrated in figures

534

10 2 0 and 5 0 Within the support structure are the filter plate(s) and a single hydraulic cylinder. The hydraulic cylinder is used to open and close the filter plate(s) and keep the plate(s) closed when the filtration process is in progress. Each filter plate consists or an upper *un* lower chamber with two layers of filler media between the chambers. Each filter plate has its own individual filter belt, belt drive system and belt wash system. Piping to feed the filter is typically supplied as shown in figure 5 0 and the ti I tot is controlled using a PLC. Filter cakes are discharged into a cake removal system such as a mixing box conveyor or tote box as shown it Figure 7 0 A process flow diagram is shown in Figure 6 0

5 FILTER OPERATION

The filter cycle consists of a sequence or filtering steps that incorporate certain filtration principles to optimize the production of solids and filtrate

The sequence of filtering steps in a typical Pncumapress® filter application where slurry must be effectively washed and dewatered to produce substantially dry solids is described below. These steps are illustrated in Figures 3 0 to 3 3

Step 1 - (die) Plate Close

In Step 1, the upper chamber closes on a double layer of filter media or filter belt that is supported by a grid on the lower chamber
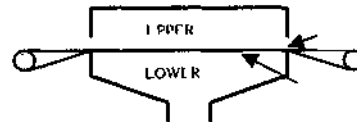

Step 2 - Slurry Fill/Cake Wash

In Step 2, slurry is pumped into the upper chamber of the filter plate (Figure 3 1). A filter cake begins to form on the filter belt as the solids are retained on the filter belt and the clean filtrate passes into the lower chamber of the filter plate and out of the filter. The slurry fill period or duration may be controlled using time slurry pressure, weight or a flow monitoring system. The optimum slurry fill time or slurry inlet pressure set point may be the fill time or pressure set point that produces the most solids or filtrate per cycle without a decrease in cake dryness or loss of wash liquid effectiveness. Increased cake size and a double layer of woven filter media provide a more tortuous path for the slurry, thus improving filtrate clarity and minimizing product loss. After slurry fill is completed cakewash water may be introduced and controlled in the same manner as the slurry fill
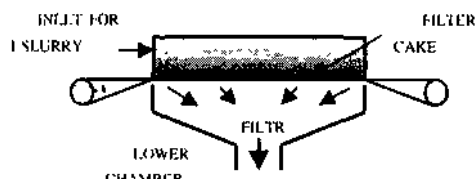
Step 4 - Gas Squeeze

In Step 4, compressed air or gas is introduced into the filter chamber to force liquid from the solids and to squeeze and dry the solids retained on the filter media (figure 3.3). As the air or gas enters the filter chamber it displaces the slurry and de-waters the solids that have formed on the filter media. No diaphragm or other squeeze mechanisms are used within the (liter chamber to dewater and dry the filter cake - the air or gas does all the de-watering and drying. A sufficient supply of compressed air used at optimum pressure differential results in decreased air use and very fast and effective dewatering.
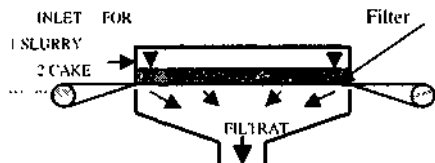

Step 5 - Plates Open

In Step 5, the filter plate opens and the newly formed dry filter cake is retained on the filter belt.

Step 6 - Cake Discharge

In Step 6. the final step of the filtration cycle, the filter bell advances and the dry filter cake is discharged into a mixing box, lole box or onto a conveyor belt (figure 3.3 and 7.0). As the filter belt advances, it is scraped and washed and a clean section of filter belt moves into the filter chambers in preparation for the next filter cycle. No operator intervention is required at any time during the filter cycle -
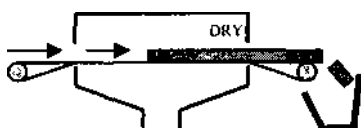
the filler cycle is fully automatic.

After the filter cake is discharged, the filtration cycle is automatically repeated. Typical cycle times vary from less than one minute to several minutes, depending on the application. The operating principle of a single-module filter with one filter plate is virtually identical to that of a multi-module filter with a number of filter plates.

5 PROCESS FLOW DIAGRAM

A typical process How diagram for the installation of a Pneumapress® single or multi-module filter is illustrated in figure 6.0. As illustrated in the process How diagram, ihe installation of the filter is very simple and does not require complex peripheral equipment.

6 PNEUMAPRESS® ADVANTAGES

The Pneumapress® single and multi-module filters differ from conventional fillers in several ways. These key differences greatly enhance the effectiveness of the Pneumapress® filter by providing many operational advantages. Some of these advantages arc discussed below:

Low Installation Costs

Minimal structural installation requirements, minimal floor space requirements, simple assembly, few process connections and minimal peripheral equipment results in low installation costs.

Low Maintenance Costs

Because of the mechanical simplicity of the filler and the selection of components to ensure local availability for the end user, maintenance costs are minimized.

Mechanical Simplicity

Each Pneumapress® filter is designed and constructed with the objective of minimizing the number of components required. The filter uses a fraction of the mechanical components used on other filter equipment.

Operational Simplicity

Each filler is extremely simple to operate. The filter is completely automatic and no operator intervention is required at any time during the filter cycle. The filter may be operated from a control panel next to the filter or from a remote control point using a DCS or other control system.

Reliability

Because of the mechanical simplicity of the filter and the low maintenance required, filter reliability and minimum downtime is ensured.

High Performance

Very high throughput per unit of filter area is achievable because of the fast filtration cycles.

Highly Effective Cake Washing

The design of the filter chamber optimizes molecular contact between the cake wash and the filter cake. This ensures consistent cake wash results with a minimum use of wash waster.

Isolatable Filter Plates

The heavy-duty design and construction of the filter plates allows the individual filter plates of a multi-module filter to be isolated during production. This design also eliminates the risk of damage to the filter plates that results when process malfunctions create internal pressure differences within the filter.

7 CASE STUDIES

7.1 Case Study No. I: Removal of precipitated silica from a clarifier underflow

In the Imperial Valley of California a geothermal power generation facility uses a dual flash, crystallizer-clarifier process to control solids precipitated as the geothermal stream cools. Precipitated silica solids must be continuously removed from the system to maintain effective operation. The solids are removed at the clarifier underflows from a 224°F stream containing approximately 33% solids by weight and approximately 30% dissolved salts.

Among equipment previously utilized to de-water underflow sludge were plate & frame filter presses, cavity filter presses, centrifuges, sludge drying beds, vacuum trucks, horizontal plate filters (low pressure APF's) and high-pressure mechanical expression filters (high pressure APF's).

In the past, horizontal plate filters (low pressure APF's) and expression or squeeze filters (high-pressure APF's) have been the most attractive equipment to dewater geothermal sludge. Benefits of utilizing horizontal plate filtration include uniform distribution of filtered solids and a large filter area. However, the hot corrosive geothermal slurry limits the choice of materials utilized in the filters. Elastomer products such as gaskets, diaphragms, and chamber seals became consumables requiring a significant amount of manpower for disassembly of the filter and removal and replacement of the consumable parts at regular intervals. Problems such as joint leakage, separation of components, and crushing of horizontal divider plates occurred with the low pressure APF. Elastomer diaphragms used to squeeze the hot brine slurry through woven filter media with the high pressure (mechanical squeeze) APF's failed at regular intervals and therefore required frequent replacement. Also, the diaphragm filters require a separate skid, reservoir and piping equipment for diaphragm filling and retraction.

A factor limiting production with the expression (mechanical squeeze) high pressure APF's is the operating cycle and configuration of the filter chamber. Due to the chamber configuration of the high pressure expression APF and non-uniform resistance to flow through the cake, effective cake washing to remove solubles required a large amount of wash water both increasing cycle time and water use. Another factor limiting production is the time involved to fill and retract diaphragms and inflatable seals (when used). A typical expression filter produced a filter cake every 8 to 12 minutes when the filter was in good working order. The Pneumapress® filter, which used shorter cycle times (2 to 4 minutes) combined with more effective solids and filtrate production, substantially outperformed the expression filter with much less filter area - see Figure 4.0.

The limitations in production with the low pressure APF and expression high pressure APF were overcome with the Pneumapress® filter by eliminating diaphragms and expression mechanical equipment, inflatable chamber seals, and diaphragm fill and retract equipment. The problem of crushing filter plate components was overcome by using more suitable filter components and incorporating design parameters better adapted to service the filtering application. To accommodate the severe operating environment of the hot corrosive geothermal slurry and maintain structural integrity, welted filter components were fabricated from a corrosion resistant alloy using fabrication techniques that remove internal residual stresses from the structure, eliminate deformation while in service and prevent sensitization of the filter components. Furthermore, the filter structure is designed to provide effective distribution of the internal pressure and resulting forces, thus enabling the filter to withstand high operating pressures. The Pneumapress® Filter is also designed to accommodate unrestricted flow through an optimum chamber configuration to maximize particle contact in the filter chamber for effective washing of slurry solids. Another benefit of the Pneumapress® Filter is the introduction of technology to eliminate leakage of slurry and filtrate during filter operation without the use of consumables such as gaskets, o-rings or inflatable seals.

Eliminating specialized equipment, eliminating consumable components and adapting appropriate fabrication techniques using corrosion resistant alloys have enhanced the reliability of the Pneu-

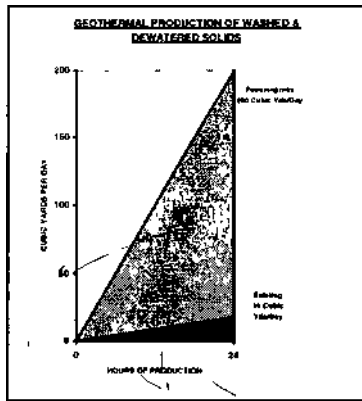mapress® Filter and reduced the cost of operating the Geolhermal Plant.

Figure 4 0 Geothernia1(Piocluction

Figuie 5.0 Single Plate Filler Showing Piping Layout

7.2 Ca.sc• Study No. 2: Dewatering oj Gxpsum A Iphci-lieiiuhydrate Slurry

Calcium sulphate hemihydrate is processed in two forms, alpha-hemihydrate /ind beta hemi-hydralc. TĨe~lIIpTra^emihydrate4s-rHV>d4iccd by the decomposition ot gypsum in water at «Jevated temperature and pressure. It is used in specialty applications such as medical plasters and sclfleveling compounds.

Aflei the conversion process fiom calcium sulphate to alpha-hemihydrate, the alpha-hemihydrate slurry must be de-watered and dried. Conventional technology used in this process included centrifuges -or pressure filtration followed by conveying to a drying system.

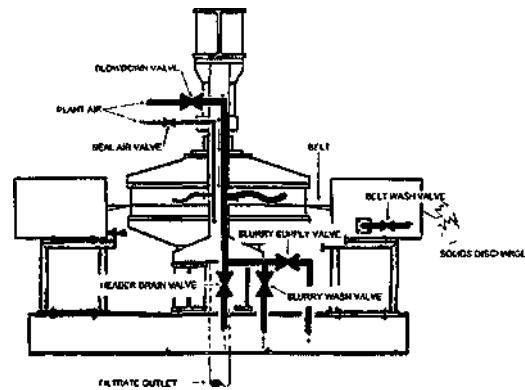A Pneumaprcss® filler using propriety filtration technology developed specifically for alpha-

hemihydrate was installed to replace the conventional dewatcring technology. The installation of the Pneumaprcss® enabled the plant to dewater and dry the gypsum to 98..W solids in a single step, eliminating the dryer, and improving the crystalline structure. This was significantly dryer than previously obtained using conventional technology.

Along with eliminating the operating costs of the dryer the overall process was greatly simplified. The de-watering process itself was simplified, the conveying system to the dryer was eliminated, the dryer was eliminated and the bag house associated with the dryer was eliminated.
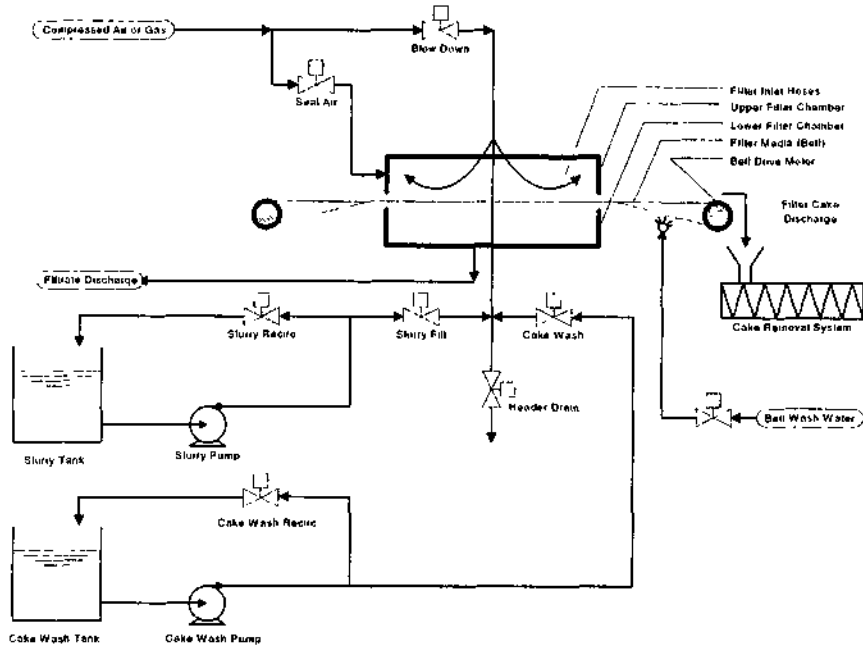
PNEUMAPRESS Process Flow Diagram

Figure 6.0 Process Flow Diagram

Filter Process Parameters

Typical Pneumapress® filler operating parameters arc provided hclow.
Actual operating parameters vary with each product being filtered.

Individual Filler Plate Area	Plaies are manufactured in 1.3 ft. 3 ft². 8 ft². 12 ll². 19 ft². 30 It² (.12m². 28m². .74m². 1.Urn². 1.76m¹. 2.78m²)
Number of filter plaies per filler	Fillers are available with 1 to 24 plates
Total tilter area pel liltei	Filteis aie available in sues of 1.3 ft" to 720ft² (,12m² 1o67 nr)
Sluu y capacity	Filters are available to process from 1 to 10.000 gpm (.22 m'/hrto2.271mVhi)
Solids capacity	Filters may pioduce 1 to 250,000 lbs/hr of de-watered solids (.45kg/hr to ll.3.000kg/hr)
Opciating pressure	Filters are available to operate at up to 360 PSI (25 Bar)
Updating temperauue	Filters are available to opeiate at up to 400"F (204"C)
Filtei cycle tune	Cycle times vary from 30sec to 5mms
Matenals of constiuction	Carbon Steel. Stainless Steel and many specialized materials
Flool space requiicments	Smallest models require 30ft"- largest 150ft² (2.8m² to 14m²)

538

Figuie 7 0 Filter dike Discluige

8 OPERATING BENEFITS AND SUMMARY

Because the Pneumapress® filters are simple, versatile, and almost free of consumable items, they can be suited to many applications, including specialized applications such as processing corrosive and/or high temperature streams. The filters produce dry and uniform solids, high quality filtrate and are simple to operate and maintain. Very dry (up to 98.5% solids) can he produced, which can reduce or eliminate dryer requirements. Containment of toxic gases or volatile materials can be controlled with the simple design. Steam or non-reactive gas may be used to displace liquids from solids to prevent oxidation or avoid reactive mixtures during separation.

Versatility of the filler also means adaptability to rapid advances in filter media technology. Technical advances in nitration media at Pneumapress® arc used lo produce dry cake, effective cake washing, clean filtrate and high filter media cycle life. The filter is adaptable to the most efficient filter media suited for each application.

The result of using the Pneumapress® filter to displace existing equipment simplifies operations, reduces floor space requirements, simplifies CIP and greatly increases efficiency in separating solids and filtrate.

The impact of the single and multi-module Pneumapress® filters in reducing operating and production costs will motivate many cost conscience companies, who want lo retain competitive operations for the future, to utilize a Pneumapress® filter.

Technique of Definition of Costs on Separate Kinds Mining Chemical Products by Their Complex Processing

M.Zh. Bitimbaev. Zh.A. Aldongarov. N. Zhalgassuly. B.A. Moldagulova
The Kunayev's Institute of Mining, Almaty, the Republic of Kazakhstan

ABSTRACT: In a process of complex processing of coal several kinds of products arc produced. And it is difficult to determine costs for separate kinds of the production, because costs proceed simultaneously for all products. In the paper worked out method is presented of determination of costs on separate kinds of production, when complex processing of coal in conditions of market economy. It consists of several operations. The offered method needs no corrections of costs by quality of producing products, physic-chemical parameters etc.. as the prices are taken by analogous quality or are re-counted in correspondence with heating value.

I INTRODUCTION

The most full analysis of all methods of determination of costs on separate kinds of coal-chemical products when complex processing of coals was carried out by authors (Lipovitch et al. 1988)

It is known that methods of distribution of total costs between received products of coal processing may be divided in two groups:
1. Method of subtraction of costs on accompanying production and using waste from total costs.
2. Method of division of costs between producing kinds of production on the basis of physical and cost criteria.

Method of subtraction of costs is based on two operations:

a) estimation of costs on kinds of products by selling price or production cost of analogous products, which is produced by using of traditional methods of production;

b) subtraction of these costs from total costs on the main and accompanying production and industrial waste.

In correspondence with branch instructions the main kinds of production are coke, semi-coke (special coke), synthetic gas and synthetic liquid fuel (SG and SLF). Other production, receiving when complex processing of coal (residual oil, coal tar, paraffin and so on) are classified as accompanying products. Mineral raw materials, which remain after receiving of the main and accompanying products when complex processing of coal, are industrial waste.

Essence of method of proportional division of costs includes *a* sequence of the following operations:

definition of the main indexes of products' quality and directions of their using;
definition of share of industrial products or coefficients, which are determined on the basis of different data (planned prices, duration of production cycle, labour costs, value of useful components, which went from original mineral raw materials to products):
- distribution of total costs proportionally with share or coefficients.

Disadvantage of the method of subtraction of costs is impossibility of determination of costs of every kind of the main production.

Disadvantage of the method of division of costs is a fact that not always share of producing different kinds of production characterizes costs and price, and also their quality and direction of using. Besides, when complex producing of products it is difficult determining planned prices if we don't know costs for separate kinds of products - it is vicious circle.

Common disadvantage of these methods is their difficultly and impossibility to take account of world tendencies in changing of demand for the products and distinction in their world costs, when producing, in individual costs for separate product (Volkov 1995).

2 DESCRIPTION OF THE METHOD

When creating of more precise method of determination of economic indexes of separate kinds of products when complex processing of coal we lake account of the following requirements:

• simplicity of a method:

• achievement of the main objective - determination of individual costs for separate products when their complex producing:

• taking account of world tendencies in improvement of technology of producing of these products:

• taking account of real natural and social conditions of competitive producing of these products.

On the basis of these requirements the method of coefficients, which are calculated on the base of world prices for products, is offered for determination of costs for separate kinds of products when their complex producing. And for determination of today's costs prices of the last year are being taken as a base for calculation; for determination of tendencies of producing and demand for production prices of several years are taking into account (separate or average).

Worked out by us method of determination of costs for separate kinds of products when their complex producing, includes the following operations:

market prices are determined of all kinds of products when complex their producing (P|, P, P V

total price is calculated of a complex of products, that is:

$$\sum_{r-1}^{n} P_r \qquad (I)$$

- price coefficients are calculated of all kinds of products in a complex by a formula:

$$K_j = \frac{P_i}{\sum_{j=1}^{n} P_j} \qquad (2)$$

price coefficients are verified and corrected by a formula:

$$\sum_{i=1}^{n} K_i = I \qquad (3)$$

total costs are determined of all complex products - C;

- separate (individual) costs of all kinds of products are determined by a way of multiplying total costs by price coefficients: C, = CK,:

costs of separate kinds of products are venlied and corrected by a formula:

$$\sum_{i-1}^{n} C_i = C \qquad (4)$$

The offered method needs no verifying and correction of costs by quality of producing products, so as prices are taken by an analogous quality (Kolosov 1987).

In a case, when $C < (0.8 + 0.9)1\ R$, this produclion will be profitable and a recoupment period will be quite enough for creditors, investors and businessmen. If costs of all complex products C will be equal or more than total price of all complex products I P_i, it is necessary to look for ways of decreasing of costs of their producing or not carry out complex producing of products, waiting for decreasing prices for these products at the world market.

3 CONCLUSIONS

Worked out method of determination economic indexes of separate kinds of products when complex processing of coal includes some step-by-step operations: determination of market prices, calculation of price coefficients, determination of total costs of all complex of producing products, corrections of separate stages. The offered method conforms to modern requirements of market economy.

REFERENCES

Kolosov A.V. 1987.Ecological-economic principles of development of mining production. Moscow: Nedra. p. 261

Lipovilcli V.G. & Kolobin G A. & Konetchits I.V. 19X8. *Clinnislrv tmtl totil pmte.\.imx*. Moscow. Chemistry, p. 336.

Volkov V.N.. 1995. Geology and saving of resources of coals (deposits of thick coal seams). Leningrad: Nedra. p. 216.